Study of Algal Biofilm to Enhance Biomass and Lipid Accumulation

Thesis submitted

in partial fulfillment of the requirements

for the degree of

Doctor of Philosophy

by

Nongmaithem Debeni Devi

(166151002)

School of Energy Science and Engineering

Indian Institute of Technology Guwahati

Guwahati-781039

Assam, India

May 2023

School of Energy Science and Engineering

Indian Institute of Technology Guwahati

STATEMENT

I, hereby declare that the information contained in this thesis, "**Study of algal biofilm growth to enhance biomass and lipid accumulation**," is the outcome of research I conducted at the School of Energy Science and Engineering, Indian Institute of Technology Guwahati, Guwahati, India, under the supervision of Prof. Vaibhav V. Goud.

Wherever the study presented is based on the results of other researchers, appropriate acknowledgments have been provided following the standard procedure for publishing scientific observations.

N. Debeni Devi

Nongmaithem Debeni Devi

15th May 2023

(166151002)

School of Energy Science and Engineering

Indian Institute of Technology Guwahati

CERTIFICATE

This is to certify that the work done for the doctor of philosophy thesis by Ms. Nongmaithem Debeni Devi (Roll No. 166151002), entitled " **Study of algal biofilm to enhance biomass and lipid accumulation**," was completed under the supervision of Prof. Vaibhav V. Goud and has not been submitted elsewhere for a degree.

Prof. Vaibhav V. Goud

Professor

Department of Chemical Engineering

Indian Institute of Technology Guwahati

Guwahati - 781039, Assam, India.

Date: 15-05-2023

ACKNOWLEDGMENT

It gives me great pleasure to thank everyone who contributed to the success of my thesis. I'm extremely thankful to my supervisor, Dr. Vaibhav V. Goud, for providing me the chance to join his research team. I will always be grateful to you for your perseverance, encouragement, and support during my Ph.D. path.

I am thankful to my doctoral committee members Dr. Mahuya De, Dr. Animes Golder, and Dr. Lalit Mohan Pandey for their valuable suggestions and guidance during my progress seminar reviews that have led to the successful completion of my Ph.D. thesis.

I would also like to acknowledge my internship Mentor Dr. Bo Hu. Your faith in me inspired me to believe in myself, allowing me to mature and develop a scientific temperament.

I would also like to extend my sincere thanks to Dr. Latha Rangan, Department of Biosciences and Bioengineering for allowing me to use the facilities of the laboratory.

I am delighted to express my appreciation. to Dr. Kaustubha Mohanty, Dr. V. S Moholkar, and Dr. Pranab Goswami former Heads of School of Energy Science and Engineering, IIT Guwahati, for providing me support and necessary facilities.

I would like to thank the faculty and present/former staff of the School of Energy Science and Engineering, IIT Guwahati Dr. Pankaj Kalita, Dr. Lepakshi Barbora, Mr. Dhiren Huzuri, Mr. Debarshi Baruah, Mr. Paragjyoti Sharma, Mr. Nayan for their endless help and support.

I also want to express my gratitude to my teacher, Dr. Mayank Pandey, M.Sc. thesis supervisor at Kumaun University, Uttarakhand for his inspiration and motivation.

I earnestly thank my seniors, juniors, interns, and labmates—Dr. Garima Srivastava, Dr. Mood Mohan, Dr. Robinson, Dr. Dipsikha Kalita, Dr. Atanu Kumar Paul, Mr. Chitta Ranjan Barik, Dr. Chandan Mukherjee, Dr. Dipesh Kumar, Dr. Sutapa Das,

Mr. Sukumar Purohit, Mr. Abebe Moges, Mr. Pravin G. Suryawanshi, Mr. Sajan Babhare, Ms. Swayam Rampal, Ms. Kakali Borah, Ms. Pushpita Das, Mr. Vikas Kumar, Mr. Rahul Tiwari, Mr. Ravichandra C. Patil, Mr. Omkar Desai, Mr. Shubham Jain, Mr. Rupesh Kumar, Ms. Sumee Sharma, Ms. Angana Chaudhuri, Mr. Dalvir Singh, Mr. Mangal Singh, Mr. Abhishek Srivastava, Mr. Shekhar Chauhan, Ms. Khusbu Kumari, Mr. Debarshi Dev—for fostering a conducive research atmosphere. I am grateful for all of their assistance, advice, and affection.

I would like to thank Dr. Xiao Sun, Dr. Lingkan Ding, Dr. Noah Storm, Dr. Fatima Heidari, and Mr. Lief from the Dr. Bo Hu Bioprocessing Group, University of Minnesota, the USA for their constant support and help during my internship.

The most priceless time of my life spent with my loved ones at IITG, will be cherished warmly in my heart. Thank you so much, Mr. Gaurav Bhatt, Ms. Menan Leichombam, Dr. Monica Naorem, Sophia Leimapokpam, Mrs. Abita, Ms. Aruna Soibam, and Dr. Shweta, Dr. Senjuti, Dr. Manish Kumar. Without you, I would not consider my IITG life to be so lovely. Mr. Neelesh Nandan, Mr. Jiban Barman, Mrs. Meena Kandpal, Mrs. Prathistha Shah, Ms. Komal Bandari, Ms. Megha Kori, and Mrs. Diksha Bisht for your "true friend never apart maybe in distance but never in heart".

Then, I would like to thank the funding agencies that provided me with the financial support to conduct my research. I am grateful to the Ministry of Education, Government of India, Indo-US Science and Technology Forum, Department of Biotechnology (Govt. of India), and Department of Bioproducts and Biosystems Engineering, University of Minnesota, USA.

I would like to give my special thanks to the team members of the group "IITG-Manipuri Group" which make me like a home away from home during my stay at IITG.

I would like to remember my parents and siblings for their never-ending love, support, and patience. It is their numerous personal sacrifices that have enabled me to reach this juncture in life. Simple thanks are not enough to convey my deep respect and gratitude toward my family. I am also grateful to my paternal and maternal relatives,

Bhatt's family, and Uniyal's family for their encouragement and prompt assistance during my education and all the difficult moments.

Also, I would like to express my gratitude to my late grandparents, Mama Sumo and Kaka who always believed in my ability to be successful in the academic arena. You've left, yet your faith in me has made this journey possible.

Thanks to the Lord, the Almighty, for showering Her/His/Its grace on me at every step.

Nongmaithem Debeni Devi

Dedicated to my family

Table of Contents

Abstract

Microalgal biomass for the production of biodiesel is emerging at the forefront in the relevant research realm. They are considered the most versatile biomass due to certain characteristics such as (1) the ability to convert carbondioxide (CO_2) into biomass through transesterification, (2) short life-cycle, (3) high growth rate, and (4) micro-algae cultivation that does not compete for fertile fields with food crops. Biodiesel production can be improved by increasing biomass and lipid yield (LY), as well as optimizing downstream processing. Studies have shown various approaches to increase microalgae biomass and lipid production. High biomass productivity (BP) and LY depends on the potential of strains and cultivation strategy. The goal of this thesis is to investigate the potential of microalgae species that are native to North-Eastern, India for biodiesel production and to assess their ability to treat wastewater and produce biomass that can be used for animal feed. The freshwater microalga, *Scenedesmus* sp. DDVG I was selected as a potential strain for biomass production. The freshwater cyanobacterium, *Limnothhrix* sp. DDVG II was used as an auto-flocculating strain. The Bioenergy Lab isolated both strains from a swampy region of the Indian Institute of Technology Guwahati (IITG), Indai. DDVG I and DDVG II microalgal isolates were molecularly characterized using 18S and 16S rRNA gene sequence analysis. The sequences were submitted to NCBI GenBank as MN630585 and MN630310, respectively. DDDVG I and DDVG II strains grew the fastest in a normal BG11 medium at pH 7 and 27 °C, with specific growth rates of 0.12±0.005 d^{-1} and 0.11±0.00 d^{-1}, respectively. Further supplementation of the medium with 1.05 g/L urea, 0.04 g/L K_2HPO_4, and 6 g/L glucose resulted in increased biomass and LY of up to 8.5 g/L & 39.5% for DDDVG I and 3.3 g/L & 19.9% for DDVG II, respectively.

Another method for increasing biomass recovery from culture broth is to use microalgae as the biofilm. The extracellular polymeric substance (EPS) is a critical intrinsic component for the growth of microalgae as a biofilm. In this study, three distinct extraction procedures were used to evaluate the generation of EPS from DDVGI and DDVG II. We observed negligible EPS yield in DDVG I over 24 days of cultivation. However, DDVG II produced significant EPS with a maximum output on the 12th day of culture. Furthermore, by exposing EPS to various substrata, the adhesive

properties of the material as well as the formation of microalgal biofilms were confirmed with maximum adhesion on rough polylactic acid (PLA) sheet.

Nitrogen shortage is the most prevalent technique for lipid accumulation; nonetheless, this strategy severely limits cell development. Some researchers demonstrated the enhancement of biomass and biomass and lipid production under the combined effects of low nitrogen (N) and high phosphorus (P). However, the selection of a balanced N:P ratio remains ambiguous among microalgal species and is subject to debate. We investigated the effect of N:P ratios ranging from 2:1 to 44.11:1 with supplementation of glucose in the BG 11 medium. The experiment was carried out by exposing DDVG I, to these diverse conditions in heterotrophic and mixotrophic modes. Under mixotrophic mode, the N:P of 100:50 or N-deficient P-over excessive (N_{def} P_{oexcs}) condition had the highest growth rate of 0.15 d^{-1} ± 0.01, with a maximum BP and LY of 41.1 0.5 mg/L.d and 39.1 1.2% dry cell weight (DCW), respectively. To improve the harvesting efficiency, we co-cultured DDVG I and DDVG II mixotrophically under different inoculum ratios in the N_{def} P_{oexcs} condition. The results showed that the 1:1 co-culture system achieved the highest biomass harvesting efficiency of 99.9± 0.5 %, with increased BP and LY up to 42.0 ± 0.9 mg/L.d and 40.2 ± 1.0 % DCW, respectively. The fatty acid methyl ester (FAME) compositions of co-culture 1:1 was also suitable for biodiesel production, with high levels of C18:2, C16:0, C18:1, and C18:0. The biodiesel derived from the co-culture 1:1 also met standard specifications for biodiesel production.

To test the feasibility of employing wastewater as a low-cost nutrient, we cultured DDVG I in primary municipal wastewater (PMWW) from Minneapolis, USA, in heterotrophic and mixotrophic modes. The experiment was expanded to a 3-L bubbling bioreactor. Over 10 days in the mixotrophic mode, DDVG I exhibited superior BP (0.069 g/L. d), LY (22.5%), and FAME content (22.04% in DCW). The biomass had a high essential amino acid content (159.8 mg/g DCW) and an EAAR of 0.45. The chemical oxygen demand (COD) and total nitrogen (TN) by *Scenedesmus* sp. were 75.6% and 99.8% respectively. Meanwhile, ammonia nitrogen (NH_3-N) and total phosphorus (TP) were removed at up to 100%.

Additionally, this study demonstated the growth of microalgae in low strength domestic wastewater (DWW). Urea was added to the DWW at two different levels to balance its nutritional content before being utilized to grow microalgae. The results showed that the optimal nutritional state (N_{250}/P_5) consisted of TN of 250 mg/L and TP of 5 mg/L. In this ideal medium, DDVG I increased COD, TN, and TP removal by up to 89.5%, 99.98%, and 99.1%, respectively. Further, co-cultivation of DDVG I and DDVG II in N_{250}/P_5 medium achieved 99.5% biomass harvesting efficiency with efficient wastewater treatment. Their corresponding biodiesel met the required standards as well. The analysis of the biomass's essential amino acid content and in vitro digestibility demonstrated its utility as a feed supplement. Overall, this study showed a future for a cleaner environment and greener energy production.

Abbreviations

ANOVA	Analysis of variance
AFM	Atomic force microscopy
APHA	American Public Health Association
ASTM	American standards for testing material
ATP	Adenosine triphosphate
BG-11	Blue-green medium
Blast	Basic local alignment search tool
BSA	Bovine serum albumin
C	Carbon
C/N/P	Carbon to nitrogen to phosphorus
$CaCl_2$	Calcium dichloride
CFPP	Cloud filter plugging point
$CHCl_3$	Chloroform
CN	Cetane number
CO_2	Carbon dioxide
COD	Chemical Oxygen Demand
CP	Cloud point
DCW	Dry cell weight
DMSO	Dimethyl sulfoxide
DU	Degree of unsaturation
DWW	Domestic wastewater
EAA	Essential amino acid
EAAR	Essential amino acid ratio
EDTA	Ethylene diamine tetraacetic acids
EDX	Electron dispersive x-ray spectroscopy
EPS	Extracellular polymeric substance
EU	European Union
FAME	Fatty acid methyl ester
FBS	Fetal bovine serum
FESEM	Field emission scanning electron microscope
FID	Flame ionization detector

FM	Filter membrane
FP	Flash point
FRP	Fiber-reinforced plastic
FTIR	Fourier transformation infrared spectroscopy
GC	Gas Chromatography
GHG's	Green House Gases
GS	Glass slide
H_2O	Water
H_2SO_4	Sulphuric Acid
HCL	Hydrochloric acid
HHV	High heating value
HPLC	High-Performance Liquid Chromatography
IV	Iodine value
IVD	Invitro digestibility
IVPD	Invitro protein digestibility
K_2HPO_4	dipotassium hydrogen phosphate
KBr	Potassium Bromide
KH_2PO_4	Potassium dihydrogen phosphate
KOH	Potassium Hydroxide
LCSF	Long-chain saturated factors
MEGA	Molecular Evolutionary Genetic Analysis
MeOH	Methanol
$MgCl_2$	Magnesium chloride
$MgSO_4.7H_20$	Magnesium sulphate heptahydrate
MTT	Thiazolyl blue tetrazolium bromide
N	Nitrogen
N/P	Nitrogen to Phosphorus
$Na_2B_4O_7$	Sodium tetraborate
Na_2CO_3	Di sodium carbonate
Na_2HPO_4	Di sodium hydrogen phosphate
NaN_3	Sodium azide
$NaNO_3$	Sodium nitrate

NaOH	Sodium hydroxide
Na_2SO_4	Sodium sulphate
NCBI	National Centre for Biotechnology Information
NCCS	National Centre for Cell Science
NH_3-N	Ammonia-nitrogen
NO_3-N	Nitrate nitrogen
OS	Oxidative stability
P	Phosphorus
PLA	Poly lactic acid sheet
PMWW	Primary municipal wastewater
PO_4-P	Phosphate phosphorous
PP	Pour point
PSII	Photosystem II
PUFA	Polyunsaturated fatty acid
rFRP	Rough fiber reinforced plastic
rGS	Rough glass slide
rPLA	Rough Polylactic acid sheet
RPMI	Roswell Park Memorial Institute Medium
rRNA	Ribosomal ribonucleic acids
SFA	Saturated fatty acid
SV	Saponification value
TAA	Total amino acid
TAG	Triacylglycerol
TN	Total nitrogen
TP	Total phosphorus
UTEX	University of Texas
UV	Ultraviolet
η	Viscosity
ρ_i	Density

Symbols and units

° C	Degree centigrade
%	Percent
µg/mL	Micro gram per milliliter
µmol/m^2. s	Photon
d^{-1}	Per day
g/L	Gram per liter
g/m^2. d	Milli gram per meter square per day
h	Hour
kWh/m^3	Kilowatt hour per cubic meter
L	Liter
mg	Milli gram
mg/g DCW	Milli gram per gram of dry cell weight
mg/L	Milli gram per liter
mg/L. d	Milli gram per liter per day
mg/mL	Milli gram per milli liter
min	Minute
MJ/Kg	Milli joule per kilo gram
mJ/m^2	Milli joule per meter square
mm	Milli meter
mM	Milli molar
mm^2/s	Milli meter square per second
N	Normality
nm	Nanometer

List of Tables

List of Figures

CHAPTER 1

Introduction and Literature Review

Background

Current status

Objectives

Thesis Organisation

This work has been published as Nongmaithem Debeni Devi, Angana Chaudhuri, Vaibhav V. Goud (2022). Algae biofilm as a renewable resource for production of biofuel and value-added products: A review. Sustainable Energy Technologies and Assessments, 53, 102749. https://doi.org/10.1016/j.seta.2022.102749.

Introduction and Literature Reviews

This chapter includes the current energy scenario, microalgae as a potential feedstock for biofuel production. The rationale for pursuing the current study has been described, and background information on the key challenge of energy security and the country's current energy situation has been developed. Besides, a thorough analysis of the literature has been discussed.

1.1. Introduction

A rise in global population and the growth of industrialization led to excessive use of non-renewable energy mainly petroleum, coal, and natural gas. According to Energy Information Administration (EIA) outlook 2021, global energy consumption will rise from 2020 to 2045, by 50% (Figure 1.1). At this rate of consumption, the fossil fuel reserve will run out in the next 45 years (EIA, 2021). The price hike in oil in the last decades due to finite fossil fuel reserves and increase energy demand become a baleful threat to economic development. According to the Petroleum Planning & Analysis Cell (PPAC), India is the world's third-largest oil consumer, spent $62.2 billion importing 196.5 million tonnes of crude oil in 2020–21, and by the end of the fiscal year in 2021–22, it is expected to have spent $110–115 billion on imports (Chaturvedi et al., 2022). Therefore, to strengthen the economy, the government planned to produce renewable energy and reduce energy imports by 50% by 2030 (Charles Rajesh Kumar and Majid, 2020). Besides, the extensive use of fossil fuels increases the emission of Greenhouse gases (GHGs) like CO_2 and methane. By 2050, CO_2 emissions are projected to have risen by 51 % from 2005 levels (Zhang et al., 2021). This poses a serious threat to global warming, the environment as well as human life. Therefore, it is high time to find an alternative way of sustainable and renewable resources.

Nowadays, several forms of renewable energy are emerging. Biofuel is attracting the greatest attention and is anticipated to play a vital part in the future global energy infrastructure. The term "biofuel" refers to any solid, liquid, or gaseous fuel that is primarily derived from biomass. Biodiesel has emerged as the most significant biofuel as a substitute for petroleum diesel. Biodiesel is a mono-alkyl ester produced by the interaction of fatty acids with alcohol. It offers comparable energy efficiency and

enormous potential for use in compression-ignition engines (Knothe, 2005). Based on the source of biomass and production technologies, biodiesel is classified into first-generation (edible oil crop) and second-generation biofuels (lignocellulose biomass) as presented in Figure 1.2 (Brennan and Owende, 2010a). However, both generations with certain limitations like food security issues, air pollution, requirements for modifications in the existing engine, etc. Recently, third-generation biodiesel has been produced from microalgae biomass. They offer significant advantages that potentially outweigh the downsides of first-generation and second-generation biodiesel. Moreover, the microalgae-based biodiesel has the compatibility with the existing engine with neutral gas emission characteristics (Subhadra, 2010). Thus, microalgae-based biodiesel will play a pivotal role in the future global energy infrastructure.

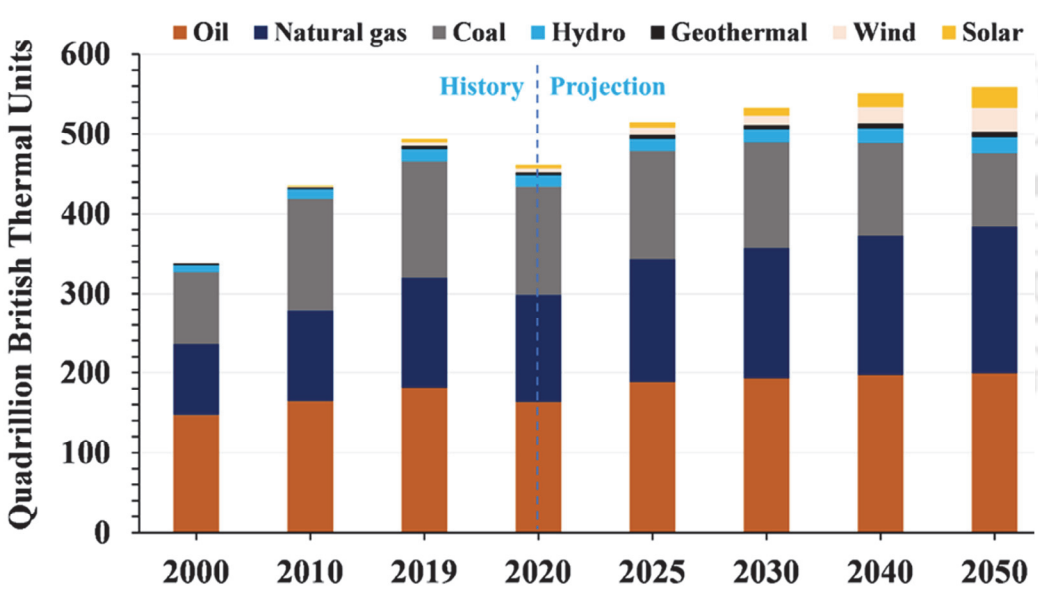

Figure 1.1: Global energy consumption and its projection, 2000-2050 (EIA, 2021).

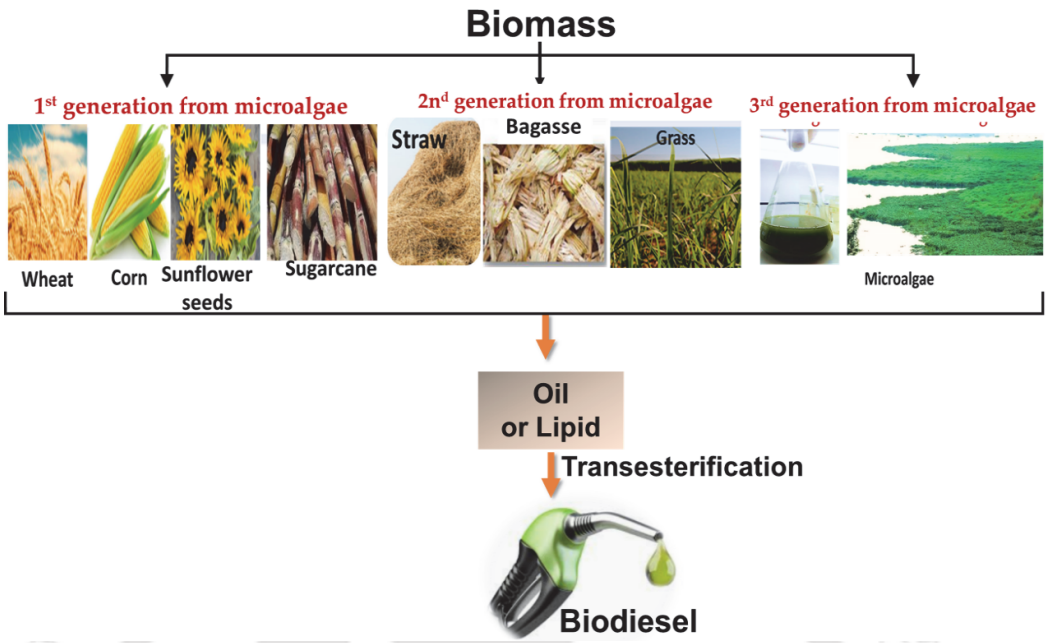

Figure 1.2: Various types of biomasses for the production of biodiesel.

Microalgae are a group of photosynthetic organisms that can transform light energy into chemical energy, especially in the form of biomolecules like carbohydrates, proteins, and lipids. The higher photosynthetic efficiency and high lipid yield of microalga has made the mini 'cell factories' of microalgae into a 'superior biomass' (Chisti, 2008). According to Table 1.1, microalgae may generate 15–300 times more oil than conventional crops per unit of land area. Microalgae have a short harvesting cycle (~1-10 days depending on the process), the capability of capturing greater light, and conversion efficiencies. They can be cultivated even in wastewater, marine water, or on marginal or non-arable land. Moreover, they have the potential to mitigate atmospheric carbon dioxide (at least 1.83 kg of CO_2 is being sequestered for the growth of 1 kg of algal biomass). Biodiesel generated from microalgae stands out as notable alternative energy due to its renewability, intrinsic lubricity, biodegradability, reduction in noxious gas emissions, safer handling, and compatibility with existing engines (Knothe, 2005). All these characteristics grab attention to expand the commercial cultivation of microalga (Brennan and Owende, 2010a).

Table 1.1: List of potential feedstocks for lipid production (Mata et al., 2010).

Feedstock source	Lipid yield (%)	Gallons of oil per acre per year
Coconut (*Cocos nucifera*)	35.3	276
Oil Palm (*Elaeis guineensi*)	35.3	610
Jatropha (*Jatropha curcas*)	28	194
Sunflower (*Helianthus annuus*)	47.3	98
Castor bean (*Ricinus communis*)	48	145
Rubber Seed (Hevea brasiliensis)	24-46	26
Rapeseed (*Brassica napus*)	30	122
Microalgae	25-75	6275-14,635

The utilization of microalgae as a potential natural resource is in the exploratory stage. Out of 200,000-800,000 microalgae species that exist on this planet, only 35,000 are identified for their high biomass productivity, lipid content, and ability to synthesize value-added products (Chisti, 2007). Therefore, bioprospecting is vital to explore prospective microalgae strains with superior growth and superior harvesting characteristics, high adaptability, bioremediation, and extra metabolite synthesis. Nowadays, the economic viability of microalgae is presented through a biorefinery strategy by producing biodiesel along with a variety of by-products. However, the absence of modern growing techniques and cost-economic constraints continue to impede the commercialization of microalgae biomass. Consequently, more extensive research employing a variety of cutting-edge approaches is required for the cultivation and process optimization of microalgae. Additionally, the commercial feasibility of microalgae biomass will benefit from the integration of the microalgae biodiesel system with wastewater treatment and co-product synthesis. This provides the framework for a comprehensive state-of-the-art analysis of the literature.

1.2. Literature

1.2.1 Biodiesel as renewable energy

An alternative fuel that is comparable to "conventional petroleum" diesel is biodiesel. Biodiesel is a liquid fuel made from biomass lipids or oils with similar combustion characteristics to petroleum-based diesel fuel. Biodiesel is biodegradable and so less dangerous to the environment. It has no sulphur. Its refineries are simpler and more environmentally friendly (Demirbas, 2009). In many circumstances, biodiesel is suitable for catalytic converters. Biodiesel includes more octane and lubricity-scoring chemicals than petroleum-based diesel fuel. Biodiesel can increase engine efficacy and are often long-lasting. The American Society for Testing and Materials (ASTM) standard D6751 and European Union (EU) 14214 are used to assess the commercial fuel quality of biodiesel. The guidelines require that biodiesel be completely reacted, with no remnants of glycerine, catalyst, or alcohol. It also guarantees that it is devoid of free fatty acids (FFA) and has a low sulphur level. Biodiesel can be used either alone or in combination with petroleum diesel. The most prevalent biodiesel blend is B20, which is a 1:4 ratio of biodiesel and petroleum diesel (Borugadda and Goud, 2012).

In comparison, biodiesel is more expensive than petroleum diesel fuel. The local temperature, geographic location, local soil environment, and agricultural culture of each nation all affect the availability of feedstock for generating bio-diesel. Consequently, it is crucial to identify the natural sources of cheap feedstock (Srivastava et al., 2018).

1.2.2 Microalgae as potential biomass

Microalgae biomass is one of the feedstocks that is gaining popularity for the production of biodiesel. This biomass is superior to other oil-rich feedstocks owing to the following reasons: (a). they have high oil content as shown in Table 1.1 (2-75 %) (b) ability to sequester atmospheric CO_2 through photosynthesis (20-60 times more efficiently than the terrestrial crops) (Xu et al., 2019) (c) fast growth rate and short life cycle (d) ability to grow in wastewater and marine water (Kothari et al., 2012; Wang et al., 2010) (e) can grow in non-arable land and no land competition with the edible crops

(Chisti, 2007; Ozkan et al., 2012; Sajjadi et al., 2018; Uduman et al., 2010), and (f) microalgal based biofuels are cleaner, non-hazardous and environmental sustainability. Moreover, the biomass of microalgae contains carbohydrates, proteins, vitamins, pigments, etc. that can be utilized for the production of food supplements, nutraceuticals, pharmaceuticals, cosmetics, etc. (Chen et al., 2016).

North East India houses a diverse range of microalgae, making it a hub for the study of microalgae-based biofuels. Several genome research and RNA sequencing investigations are now looking into the variety of microalgae. For instance, Talukdar et al., (2013) identified a novel strain *Botryococcus braunii* from the North East region of India which showed high lipid content of 57.14 %. They observed that the biomass had a high hydrocarbon content of 52.6%, suggesting its potential for biofuel generation.

Difusa et al., (2015) also reported a novel strain, *Chloromonas* sp. ADIITEC-III from North East India has a total lipid content of 36.5 ± 0.75. They reported that the lipid content ramped up to 37.35 ± 0.32 % when cultivated in BG 11 medium supplemented with urea as a nitrogen source.

Desmodesmus GS12 *and Chlorella sorokiniana* CG12, other novel strains from this region were reported by Srivastava et al., (2017). Their finding showed that when these two strains were cultivated in a salt stress environment with $CaCl_2$ as a source, their lipid content increased to 44.9 % and 40.02 % respectively. In addition, they observed high oleic acid content ranging from 53.46-64.18 %, demonstrating their potential as biomass for biodiesel production.

Monoraphidium sp. KMC4 was isolated from a local sewage treatment plant in North East India by Mishra and Mohanty (2019). The strains showed high biomass growth (1.47 ± 0.08 g/ L) and lipid content of 436.01 ± 0.06 mg/ L when cultivated in unsterilized domestic wastewater. They further reported that the saturated fatty acid content of the biomass was 55.32 % of the total FAME, which indicated its viability for biodiesel production.

Nevertheless, microalgae have the potential to become a substantial driver in the development of a bio-based economy, large-scale applications of microalgae

biotechnology are hampered by the current energy-intensive or non-eco-friendly chemical harvest technology. Along with the high nutrient and water requirements, the success of the large-scale open ponds for algae production is challenged by the invasion of local biota. Due to the small cell size of algae with specific gravities being very similar to that of culture medium, negative surface charges on the algae that result in dispersed stable algal suspensions, and the necessity of large volumes of water for cultivation results in low biomass to liquid ratio, which increases the downstream processing cost to about 30–40 % of the total costs of production (Cheng et al., 2013). Conventional algae harvest technology is generally based on centrifugation, filtration, flocculation, and flotation or a combination of these methods. It is evident from Table 1.2 that commonly used harvesting techniques such as chemical, flocculation, and centrifugation are intensive energy (0.015-7.6 kWh/m^3) and high cost (Uduman et al., 2010). To overcome this issue, recent studies have developed advanced cultivation of microalgae which is also known as the "biofilm system"(Gross et al., 2013a; Ozkan et al., 2012).

1.2.3 Microalgal biofilm cultivation

In natural ecosystems, most microbes exist as part of a complex, dynamically changing, microbial consortia, and the metabolic interactions between microbial species could be for various reasons including, the exchange of molecules, which may benefit one or both species. Biofilm is the assemblage of microbial communities that are embedded either on supporting materials or grow as a periphytic form on the aquatic surface (Flemming et al., 2007; Xiao and Zheng, 2016). The mechanism of biofilm formation is a complex process that varies from species to species. It is believed that extracellular polymeric substances (EPS) are the intrinsic factor for the assemblage of the microbial communities (Flemming et al., 2007). The EPS is self-secreting adhesive biomolecules that are released by certain microorganisms. A previous study has reported that the primary component of EPS is heteropolysaccharides, which contain a variety of monomer units (such as glucose, galactose, mannose, arabinose, and xylose) (Devi et al., 2021). It has also confirmed the presence of non-sugar components such as inorganic carbon, uronic acid, humic acid, nucleic acid, proteins, phospholipids, etc. Kawaguchi and Decho, (2000) showed that the presence of such biochemical contents

determines the hydrophobic and hydrophilic of the EPS. These characteristics are connected to the adhesion of microalgal cells onto the substrata, thus promoting early colonization (Domozych et al., 2005; Flemming et al., 2007). According to Domozych et al., (2005), the presence of different heteropolysaccharides in EPS creates a bridge that anchors the link between the cells to cell and cell to substrata. The existence of many elements such as carbon (C), oxygen (O), and a variety of minerals, including magnesium (Mg), sodium (Na), chloride (Cl), calcium (Ca), sulphur (S), etc., are also confirmed in EPS (Chen et al., 2021; Devi et al., 2021; Kawaguchi and Decho, 2000). These elemental compositions have a binding affinity for other mineral ions present in the culture medium, such as phosphate (PO_4^{3-}) and ammonia (NH_3^-), and they produce mineral salts by electrostatic, complex-ligand interaction, or ion exchange (Zhao et al., 2022). Thus, the EPS matrix could harbor mineral ions and provide nutrients to the developing cells (Xiao and Zheng, 2016). Previous research has shown that the quantity of EPS has a significant impact on how well cells adhere to one another through it. In turn, the production of EPS is affected by the stage of the microalgal life cycle, the availability of nutrients, and the stress environment (Devi et al., 2021; Rossi and De Philippis, 2015; Tong and Derek, 2021). According to several studies, the highest biofilm thickness and EPS production happened during the late logarithmic stage or early stationary stage of the culture life cycle. Cells from the biofilm were shown to separate and slough off after the late stationary phase (Boelee et al., 2014a).

Many reports are suggesting the benefits of microbial biofilm in a synthetic ecosystem for a variety of applications; specifically, to perform functions requiring multiple steps, including bio-remediation (Wijeyekoon et al., 2004). Recently, microalgae-based biofilms have been cultivated in two different systems: attached cultivation systems and co-cultivation systems (Zhao et al., 2022). The mechanisms for biofilm development are discussed in the forthcoming sections.

Table 1.2: Comparison of commonly used harvesting techniques for suspended microalgae (Uduman et al., 2010).

Technique	Advantages	Disadvantages
Centrifugation	• High biomass recovery (>90 %) • Quick separation • No chemical requirement • Feasible for all types of microalgae	• Requirement of expensive equipment • Energy-intensive (1.43 kWh/m^3) • Risk of cell disruption due to shear and gravitational force • Difficult for large culture volume
Filtration	• High cell recovery efficiency (20–87 %) • Inexpensive • No chemical requirement • Availability of wide varieties of filter designs with different pore sizes (ranging from 0.02 to10 µm)	• Slow process • Requirement of pressure and energy (0.77-1.22 kWh/m^3) • Filter membrane clogging
Floatation	• Rapid process with high cell recovery efficiency (83.4 %) • Suitable for small scale • Low-cost equipment	• High energy requirement (0.015-7.6 kWh/m^3 • Requirement of flocculants
Flocculation	• Fast process • High biomass recovery efficiency (50–90 %)	• Energy-intensive (0.15 kWh/m^3) • Requirement of flocculants • Sensitive to charge density, pH, and ionic strength of the flocculants
Electrophoresis	• High cell recovery efficiency (>98 %) • Cost-effective • No chemicals required • Recyclable process	• Requirement of energy (0.8-1.5 kWh/m^3) • High-density current cause the change in cell composition

1.2.3.1 Attached cultivation system

In attached cultivation, microalgae are grown on any supporting materials/ or substrata. Some studies reported the development of attached cultivation systems by using

polylactic acid (PLA), polyurethane (PU) foam, filter membrane (FM), cotton duct (CD), sheet, pine sawdust, muslin cloth, filter paper, cardboard, cotton duct, polyurethane foam, etc. (Boelee et al., 2014a; Finlay et al., 2002; Gayen et al., 2019; Genin et al., 2014; Ista et al., 2004; Ozkan and Berberoglu, 2013) (Table 1.3). There are two different designs of the attached photobioreactor systems: fixed systems and fluidized systems (Rosli et al., 2020). In a fixed system, the substrata are configured in different orientations such as rotating (including disk, flat panel, and rope), vertical (such as column, tubular, submerged flat panel, and permeated flat panel) and horizontal (like flat panel and tubular). While the fluidized bed is designed as a mobilized radial, immobilized packed bed, and immobilized flat-panel membrane systems (Wang et al., 2018).

The mechanism for the interaction between microalgae cells and substrata is driven by the adhesive force, while the cohesive force causes the interaction between cells. (Shen et al., 2014b). The schematic diagram in Figure 1.3 illustrated the different stages of attached biofilm formation on substrata. The planktonic microalgal cells are first moved onto the substratum through hydrodynamic or gravitational force, subsequently, the actual cells-substratum interaction (attachment of cells) begins (Bartley et al., 2014). This attachment is reversible where the microalgal cells can easily be removed from this interaction because of the turbulence in the media. For this attachment of the cells, the EPS secretion and physico-chemical characteristics of the substratum (such as surface hydrophobicity, surface charge, and surface texture) are taken into consideration (Sekar et al., 2004).

Some studies suggested that substrata having greater roughness facilitate the initial colonization of cells onto the surface. For example, Danaee et al., (2021) found that the formation of grooves on rough surfaces enhanced cell attachment by 22 % when compared to the smooth surface. Likewise, a gas-permeable membrane photobioreactor coupled with a rough surface (GMPBR-RS) showed an improvement in cell accumulation by 28.27% as compared to the normal surface (Guo et al., 2019). According to Zhang et al., (2020), the aerial biomass accumulation rose from 6.89 to 23.92 g/·m^2.·d as surface roughness increased from 13.03 to 45.15 m, respectively. The reason for effective cell recovery on the rough surface could be due to the presence of

crevices and cracks on rough substrata or material. Those uneven features offer a bigger surface area for cell adhesion, resulting in greater biomass accumulation (Zhang et al., 2020). Additionally, the cracks on rough surfaces tend to increase the fluid velocity of nearby areas by creating a hydrodynamic environment including low flow velocity areas to retain colloids (Zhang et al., 2020).

Surface hydrophobicity is another crucial parameter promoting cell adherence to the substrata. This mechanism can be explained via contact angle measurement, and surface wettability (Zhang et al., 2018). Ozkan and Berberoglu, (2013) reported that hydrophobic microalgae, *Botryococcus* showed higher attachment on hydrophobic substrata like plastic showed greater cell attachment than hydrophilic substrata such as metals or glass. Similarly, Finlay et al., (2002) observed a better attachment of *Amphora* cells on a hydrophobic surface. The reason behind this can be explained by the water exclusion theory, that is hydrophobic surfaces propel the water and thus provide the sites for cell adhesion. Conversely, Finlay et al., (2002) noticed a higher attachment of *Enteromorpha* cells on hydrophilic than hydrophobic substrata. Likewise, Genin et al., (2014) reported the effective growth of algal biofilm on hydrophilic substrata such as hydrophilic filter membranes such as cellulose nitrate (CN), cellulose acetate (CA), nylon (JN 6), and polyethersulfone (PES). However, some studies found no correlation between surface hydrophobicity and cell adhesion (Irving and Allen, 2011). This ambiguity led to further investigation of the biofilm formation mechanism through the thermodynamic model. The thermodynamic model implies that the favorability of interaction between microalgal cells and substratum is governed by the adhesion free energy (ΔD_{adh}) (Cheah and Chan, 2021). The higher cell attachment on the substratum is stable when $\Delta D_{adh} < 0$. As presented in Table 1.4, substrata like Polypropylene (ΔG_{adh}=-53 mJ/m^2) (Hadjiev et al., 2007), Nylon 6,/6 (ΔG_{adh}= -50 mJ/m^2) (Cui and Yuan, 2013) and polycarbonate (ΔG_{adh}= -53) (Hadjiev et al., 2007) showed high negative ΔD_{adh} resulting greater affinity for cell adhesion.

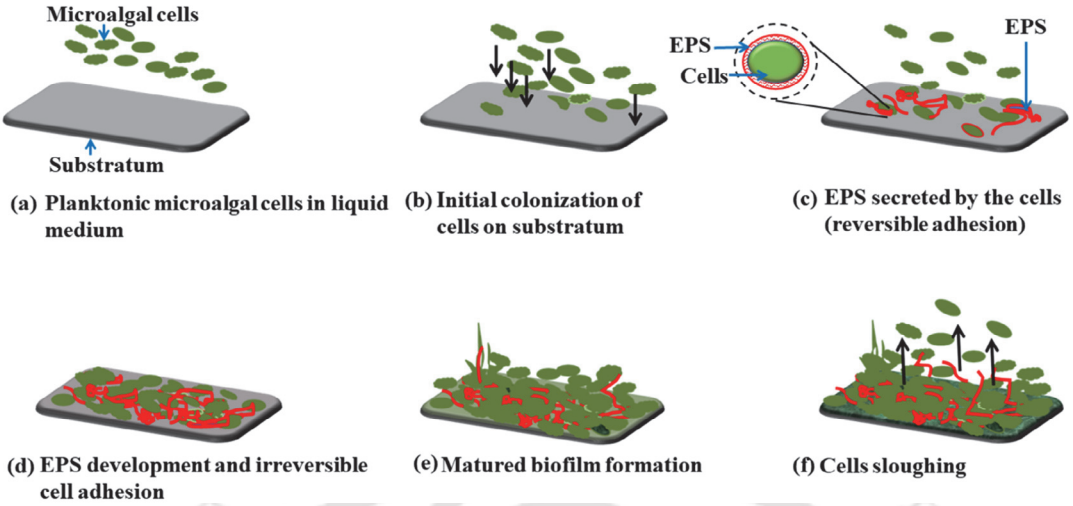

Figure 1.3: Schematic diagrams illustrating the developmental stages of microalgae biofilm on substrata via EPS.

1.2.3.2. Co-cultivation system

Co-cultivation is another type of biofilm cultivation to overcome the harvesting issue. In this system, the planktonic microalgal cells aggregate into biofilm or sessile cells through symbiotic association with other auto-flocculating microbes (Alam et al., 2016). The co-cultivation system has been extensively employed for in situ harvestings as well as enhanced biomass production of microalgae. Some of the common symbiotic associations such as algae-algae, algae-bacteria, and algae-fungi strategies have been explained in the following sections. Results in Table 1.5 summarise different types of co-cultivation system and their productivities.

Table 1.3: Comparison of different types of attached cultivation systems in different culture media. The notation "-" represents the data that is not presented in the sources.

Sl. No.	Species	Substratum	Type of Bioreactor	Culture medium	BP (g/ m^2. d)	LY/ FAME (%)	LP/ FP (g/ m^2. d)	References
1	*Chlorella vulgaris*	Stainless steel, polypropylene, acrylic, polycarbonate sheet	Fluidized Bed	Modified Bold 3N medium (MB3N)	5.3–12.2	-	-	(Roostaei et al., 2018)
2	*Scenedesmus* sp. DDVG I	Polylactic acid sheet	Vertical plate	BG 11 medium	31.6 ± 1.20	-	-	(Devi et al., 2021)
3	Mixed cultures (including *Diatoma, Pediastrum,* and *Chlorella*)	Cotton cord	Rotating	Tertiary municipal wastewater	20–31	-	2.2–2.5 (FP)	(Christenson and Sims, 2012)

4	*Scenedesmus obliquus*	Flat plate parallel horizontal photobioreactor	Synthetic medium with mineral nutrients of the CHU-10 diatom medium	2.1	0.18 (LP)	(Schnurr et al., 2013)
5	*N. palea* (CPCC 160)	Flat plate parallel horizontal photobioreactor	Synthetic medium with mineral nutrients of the CHU-10 diatom medium	2.8	-	0.45 (LP) (Schnurr et al., 2013)

(continued)

Note: BP-Biomass productivity; LY: lipid yield, LP: lipid productivity, FAME: fatty acid methyl ester; FP: FAME productivity

Table 1.4: The adhesion free energy, ΔG_{adh} (mJ/m^2) of different substrata for cell attachment.

Substratum	**ΔG_{adh} (mJ/ m^2)**	**Reference**
Polycarbonate	-48	(Hadjiev et al., 2007)
Polypropylene	-53	(Hadjiev et al., 2007)
Nylon 6/6	-50	(Cui and Yuan, 2013)
Teflon	-42	(Cui and Yuan, 2013)
Polysulfone	-36	(Schakenraad et al., 1988)
Polyethylenvinylacetate	-37	(Hadjiev et al., 2007)
Polyethylene	-43	(Hadjiev et al., 2007)

Bioflocculation through algae-algae interaction

Certain microalgal strains have the potential of either auto-flocculation or growing as biofilm mats. *Botryococcus braunii*, *Scenedesmus obliquus*, *Tribonema* sp. (Cheng et al., 2020a), *Scenedesmus abundans* (Mahesh et al., 2019), *Ankistrodesmus* sp. (Lananan et al., 2016), *Chlorella vulgaris* (Alam et al., 2014), etc. have been reported as auto-flocculating species. The co-cultivation of auto-flocculating species with the non-flocculating microalgae can provoke cell aggregation, resulting in higher cell recovery. For instance, auto-flocculating *Chlorella vulgaris* JSC-7 could enhance the sedimentation and flocculation of freely suspended *Chlorella vulgaris* CNW-11 (Alam et al., 2014). Tejido-Nuñez et al., (2020) investigated the co-cultivation of *Chlorella vulgaris* and *Tetradesmus obliquus* SAG 276 in an inoculum ratio of 1:1 in a thin layer photobioreactor. The study demonstrated higher biomass productivity (13.3 g/m^2. d) than the monoculture conditions. Likewise, co-cultivation of *Chlorella* sp. HS-2 and *Ettlia* sp. YC001 in an inoculation ratio of 1:08 could increase biomass productivity (0.74 ± 0.06 g/L. d) significantly ($p<0.05$) (Rashid et al., 2019). Salim et al., (2011) also observed an increased harvesting efficiency of non-flocculated algae such as *Neochloris oleoabundans* and *Chlorella vulgaris* via auto-flocculated algae such as *Scenedesmus obliquus* and *Ankistrodesmus falcatus.* Tiron et al., (2017) co-cultivated filamentous microalga, *Phormidium* sp. with *Chlorella* sp., resulting in higher harvesting efficiency (99 %). Several studies suggested that flocculation occurs due to patching and clumping up the cells together (Guo et al., 2013; Mahesh et al., 2019).

The EPS secreted by the flocculating microalgal species underlie the mechanism to aggregate the cells together (Guo et al., 2013; Taylor et al., 2012). Nevertheless, excessive EPS production may hinder mass transfer and block nutrient uptake to the cultures (Ishika et al., 2017). Hence, the selection of the potential microalgal strains to undergo co-culture should be taken carefully.

Bioflocculation through algae bacterial interaction

Microalgae-bacterial consortia are ubiquitous in the natural ecosystem. Considering this natural phenomenon, several researchers grew interested in adopting this strategy in bioremediation (Khoo et al., 2021). As reported by Croft et al., (2005), the possibility for the existence of a microalgae-bacterial consortium is because bacteria act as the exogenic source providing the growth promoter factors such as thiamine (vitamin B1), biotin (vitamin B7), cobalamin (vitamin B12) to microalgae. Moreover, indole-3-acetic acid produced by bacteria could promote the microalgae-bacteria interaction and enhance the overall lipid productivity (De-Bashan et al., 2008). Hence, several researchers have extended the microalgae-bacteria consortium in the aspect of biomass and lipid enhancement (Hu et al., 2020; Leong et al., 2020; Ruiz-Ruiz et al., 2020). This strategy could also facilitate the flocculation of microalgal partners through bacteria, improving the harvesting efficiency of the biomass. For instance, the co-culture of *Paenibacillus* sp. and *Chlorella vulgaris* could enhance the harvesting efficiency by 83 % (Oh et al., 2001). Co-culture of *Paenibacillus polymyxa* and *Scenedesmus* sp. resulted in high harvesting efficiency (95%) (Kim et al., 2011). In another study, *Solibacilus silvestris* was co-cultivated with *Nannochloropsis oceanica*, achieving more than 90% cell recovery and reducing the harvesting cost (Wan et al., 2013). Co-cultivation of aerobic activated sludge bacterium from municipal wastewater with microalgae including *Chlorella* sp., *Pediastrum* sp., *Phormidium* sp., and *Scenedesmus* sp. could result in consortium formation, resulting in more than 98 % harvesting efficiency (Van Den Hende et al., 2011). Efficient harvesting of *Pleurochrysis carterae* was attained by mixed bacterial cultures including *Pseudomonas stutzeri* and *Bacillus cereus* (Branyikova et al., 2018). Jiang et al., (2021) reported a mixed culture of bacterium *Citrobacter freundii* (No. W4) and fungi *Mucor circinelloides* could effectively harvest *Chlorella pyrenoidosa*, with a harvesting efficiency of 97.45%.

According to Wang et al., (2012), there are two possible mechanisms responsible for the aggregation of algae-bacteria. They are (1) bio flocculants released by the bacteria, and (2) direct interaction through flagella or proteins presents on the bacterial cell wall. The bio flocculants released by bacteria consist of EPS, polysaccharides, proteins, etc. These components impart different functional groups which were confirmed by Comte et al., (2006) via Fourier-transform infrared spectroscopy (FTIR) The presence of different functional groups could help in bridging and aggregating microalgae-bacteria cells (Kawaguchi and Decho, 2000). Cellulose derived from the bacterium *Gluconacetobacter xylinus* was effective for in situ harvesting of nearly 92 % *Chlorella vulgaris* and 90 % *Scenedesmus obliquus* and *Chlamydomonas reinhardtii* (Chen et al., 2018). In addition, algae-bacteria association could be facilitated by the nutrient-exchange process. Bacteria present in the symbiotic system utilize the oxygen released by the photosynthetic process of algae. In turn, the algae partner consumes the carbon dioxide (CO_2) liberated by bacteria resulting in a symbiotic association (Saravanan et al., 2021). Such a type of consortium has been explored mainly for wastewater treatment (Gross et al., 2015).

Bioflocculation through algae-fungal interaction

Co-culture of algae and fungi has been reported to enhance flocculation or pelletization. Some researchers found that filamentous fungi specifically *Rhizopus oryzae*, *Penicillium expansum*, *Mucor circenelloids* are useful to pelletize the microalgal cells (Rajendran and Hu, 2016). Xie et al., (2013) reported the use of *Cunninghamella echinulate* to harvest *Chlorella vulgaris*, resulting in 99 % cell recovery. Another study showed that a consortium of *Aspergillus oryzae* and *Chlorella vulgaris* increased cell pelletization by 93% (Zhou et al., 2013). Rajendran and Hu, (2016) developed a mycoalgae system using *Chlorella pyrenoidosa* cells with *Aspergillus fumigatus*, resulting in 99 % cell pelletization. Likewise, *Aspergillus* sp. could flocculate 92 % *Chlorella* MJ 11/11 (Lal et al., 2021). Pei et al., (2021) also found the effective harvesting of *Scenedesmus* sp. through *Aspergillus niger*, with 99.4 % harvesting efficiency. The co-cultivation of *Spirulina platensis* and *Aspergillus niger* was investigated and found to give nearly 100% biomass sedimentation within 2 h (Nazari et al., 2021). According to Zhu et al., (2013), the co-existence of the algae-fungi consortium is possible due to the synergistic metabolism developed between algae and

fungi. Fungi generally released extracellular enzymes thereby converting organic matters into soluble nutrients and CO_2 which can be easily assimilated by microalgae. While the oxygen released by the algae supports the respiration of fungi. Other factors for the pelletization of cells could be fungal hyphae. Chu et al., (2021) reported that fungal hyphae generally possess a positive charge that tends negatively charged microalgal cells accomplishing cell aggregation. Moreover, the release of polysaccharides or EPS from the mycelium provides the sites for better attachment of microalgal cells resulting in pelletization. Hence, the co-culture of robust fungal strains with microalgae can overcome harvesting issues and services for efficient biomass production.

1.2.4. General factors affecting the growth and lipid production of microalgae

1.2.4.1 Carbon

Carbon is the most critical factor for the growth of microalgae. In general, diversified carbon sources i.e., either inorganic (CO_2, bicarbonates, etc.) or organic (methanol, acetate, glucose, and so on) carbon are used for microalgal cultivations. Depending on the source of carbon, the cultivation can be classified into three major types: phototrophic, heterotrophic, and mixotrophic mode. Each type of cultivation is discussed in the forthcoming sections.

Phototrophic cultivation

Under phototrophic cultivation, the microalgal cells harvest light energy and assimilate inorganic carbon sources (CO_2 or bicarbonates) to form chemical energy through photosynthesis (Brennan and Owende, 2010). As illustrated in Table 1.6 Under phototrophic cultivation, there is a large variation in lipid content, biomass, and lipid productivity of different marine and freshwater microalgae species. The lipid content and biomass productivity can reach up to 0.02-15.79 g/ L. d and 8.1-63 % respectively, showing significant differences between the various microalgal species (Abd El Baky et al., 2012; Illman et al., 2000; Rodolfi et al., 2009). In some literature, lipid productivity is about 69.2 mg/L. d by *Scenedesmus obliquus* under phototrophic cultivation using 2.2 % CO_2 (Abd El Baky et al., 2012). The major advantage of using phototrophic cultivation is the consumption of CO_2 coming from flue gas of power plants and industrial activities. In a literature survey, (De Morais and Costa, 2007)

reported the raceway pond cultivation of *Spirulina* through fixation of CO_2 that is emitted in the combustion of coal in a thermo-electric power plant (UTPM, Brazil). The utilization of CO_2 as a substrate reduces carbon footprint when the gained microalgae biomass can be utilized to produce biofuels or other value-added products (Yen et al., 2015). Thus, phototrophic cultivation is considered to be ideal and reasonable from the perspective of economic feasibility for scaling up in the outdoor open or raceway ponds (Mata et al., 2010).

Heterotrophic cultivation

Heterotrophic is the type of cultivation in which the microalgae species can directly use organic carbon (such as glucose, acetate, glycerol, fructose, and maltose) in the presence or absence of a light supply (Han et al., 2012). The photosynthetic products such as simple organic sugar (glucose or sucrose) are converted into polysaccharide starch in plants. Starch is then hydrolyzed and used for cellular metabolic activities in the absence of light. This phenomenon is known as dark respiration and it becomes a major source of energy for the maintenance metabolism of photosynthetic organisms in the absence of light (Hu et al., 2018). The heterotrophic type of cultivation could avoid the problem associated with the light limitation that hinders high cell density in large-scale photobioreactors during phototrophic cultivation (Berberoglu et al., 2007). In this way, the lipid content and productivity reported in literature could reach up to 50.3–57.8 % and 1209.6–3701.1 mg/ L. d respectively by *Chlorella protothecoides*. using 15-60 g/ L glucose (Xiong et al., 2008). In recent years, there has been a tremendous focus on finding cheaper organic carbon sources as well as an integrated waste treatment. As illustrated in Table 1.6, *Chlorella sorokiniana* could effectively utilize aquaculture wastewater under heterotrophic conditions, resulting in high biomass (0.353 g/ L. d) and lipid (138.17 mg/ L. d) productivities and a significant removal of phosphate (PO_4^{-3}; 100 %), ammonium (NH_4^+; 98.21 %), and nitrate (NO_3^-; 75.76 %) (Guldhe et al., 2017). Biodiesel-derived crude glycerol is another excellent carbon source that *Chlorella protothecoides* and *Schizochytrium limacinum* can utilize to produce significant amounts of total lipid and docosahexaenoic acid (DHA, C22:6 *n*−3) under heterotrophic cultivation (Chen and Walker, 2011; Chi et al., 2007).

Table 1.5: Comparison of different types of co-cultivation systems in different culture media. The notation "-" represents the data that is not presented in the sources.

Sl. No.	**Species**	**Culture ratio**	**Culture medium**	**Harvesting efficiency (%)**	**Biomass Concentration (BC)/ Biomass productivity (BP)**	**Lipid Yield (%)**	**Lipid productivity (LP)/ Fatty Acid productivity (FAP)**	**References**
1	*Tribonema* sp. and *Chlorella zofingiensis*	1:1	Swine wastewater diluted with fishery wastewater	88.6	1.95 g/ L (BC)	44.12	-	(Cheng et al., 2020a)
2	*Ettlia* sp. and *Chlorella* sp. HS-2	1:0.8	BG 11 medium	99	3.23 ± 0.04 g/ L (BC) 0.74 ± 0.06 g/ L/ d (BP)	33	180.8 ± 15 mg/ g (FA)	(Rashid et al., 2019)

3	Mixed cultures (including *Chlorella* sp., *Acutodesmus* sp., *Scenedesmus* sp., *Flavobacterium* sp. *Leptolyngbya* sp. *Rhodobacter* sp., *Pseudomonas* stutzeri)	-	Municipal wastewater	99	117.1 ± 2.7 g/ L/ d (BP)	-	17.2 ± 0.2 g/ L/ d (LP)	(Cho et al., 2017)
4	*Chlorella vulgaris* UTEX 259 and C. *echinulata* (Strain ID: NRRL 3655)	1:1	Tris Acetate Phosphate buffer	100	-	-	-	(Xie et al., 2013)
5	*Chlorella* sp. MJ 11/11 and *Aspergillus* sp.	1:3	Tris Acetate Phosphate buffer	> 92	2.37 ± 0.12 g/ L (BC)	14	-	(Lal et al., 2021)
6	*Scenedesmus* sp. Z-4 and *Aspergillus niger* X-5	-	BG 11	99.4	2 g/ L (BC)	-	-	(Pei et al., 2021)

(continued)

Mixotrophic cultivation

Microalgae that are cultivated in a mixotrophic mode find both the advantages of phototrophic and heterotrophic conditions. Under this condition, microalgae undergo photosynthesis by assimilating organic carbon and CO_2 as a carbon substrate. The main advantage of this condition is that during microalgal respiration, CO_2 is released and then the cells recaptured and recycled CO_2 during the phototrophic mode (Devi et al., 2021). As indicated in Table 1.6, *Chlorella vulgaris* 31 shows higher lipid productivity of 0.226, 0.195, and 0.170 g/L. d by utilizing glucose, maltose, and sodium acetate respectively by altering the culture conditions from heterotrophic to mixotrophic (Kong et al., 2020). Like in heterotrophic conditions, the high biomass productivity of 3.88 g/ L. d and DHA productivity of 0.52 g/ L. d could be achieved by *Schizochytrium limacinum* SR21 (ATCC MYA-1381) under mixotrophic conditions using biodiesel derived crude glycerol (Lung et al., 2016).

1.2.4.2 Nutrient supply

Lipid productivity is influenced by both lipid content and biomass production by the algae. and hence, it is particularly important to be taken into account in large-scale microalgal lipid production (Rodolfi et al., 2009). Suitable media formulation or composition of nutrients at various concentrations is a crucial factor to increase the lipid production performance of microalgae species (Mandalam and Palsson, 1998). Under nutrient stress conditions, a general trend toward the accumulation of higher neutral lipids (predominantly triacylglycerols (TAG) or carbohydrates has been observed in several microalgal species (Sharma et al., 2012). A study on the lipid content of *Chlorella vulgaris* could be considerably increased by 40% in a low nitrogen-containing medium. Hu et al., (2006) conducted a study on the nitrogen stress response, indicating that 10%–20% higher lipid content could be achieved by microalgae, cyanobacteria, and diatoms than under normal conditions. It has been suggested that when microalgae are cultivated under nitrogen stress conditions, the proteins in microalgae will be disintegrated and converted to energy-rich products, such as lipids as a long-term storage mechanism (Hu et al., 2006; Siaut et al., 2011). Besides, phosphorus limitation could significantly increase the fatty acid and lipid composition of *Monodus subterraneus, Chaetoceros* sp*., Isochrysis galbana,* and *Pavlova lutheri,*

but decrease lipid content in *Nannochloris atomus* and *Tetraselmis* sp. (Khozin-Goldberg and Cohen, 2006; Reitan et al., 1994). The proportion of phospholipids *Monodus subterraneus* decreased from 8.3% to 1.4% of total lipids, while the TAG content increased from 6.5% up to 39.3% of total lipid under phosphorus limitation (Khozin-Goldberg and Cohen, 2006). In literature reported by Feng et al., (2012) suggested that nitrogen deficiency condition is the best and most effective strategy to enhance TAG production, indicating the highest lipid productivity (87.1 mg/L· d) by *Chlorella zofingiensis* under nitrogen starvation than that of phosphorus. In recent years, wastewaters, particularly municipal and agricultural wastewaters, are becoming a potential source of nitrogen and phosphorus (Chiu et al., 2015; Guldhe et al., 2017). In a literature survey, Chiu et al., (2015) reported the feasibility of growing different microalgae species (*Chlorella* sp., *Chlorella vulgaris, Chlorella zofingiensis, etc.*) using various types of wastewaters, containing ammonium (5-900 mg/ L), total phosphorus (3-500 mg/ L) and total nitrogen (30-900 g/ L) concentrations (Alkayal et al., 2010). Takagi et al., (2006) reported a higher intracellular lipid content (70%) and TAG (70%) in *Dunaliella* cells. In some studies, various sodium salts have been used to induce lipid accumulation and 20 g/ L NaCl was found to increase the lipid productivity of 67.08 mg/ L. d and better biodiesel quality in *Desmodesmus abundans* (Xia et al., 2014). Pancha et al., (2015b) reported 24.77% of lipid (containing 74.87% neutral lipid) along with higher biomass in *Scenedesmus* sp. under two-stage cultivation of salinity stress with 400 mM NaCl for 3 days. *Chlorella vulgaris* has also been grown in 5 L fermenter by applying the salinity stress strategies, resulting in lipid yield of 3.81 g/L at 180 h, which was 30.1% higher than the control condition (Duan, 2012). Salinity stress is also suggested as another approach to lipid overproduction as being feasible (Srivastava et al., 2017).

1.2.4.3 Cultivation of microalgae by using wastewater

Nowadays, there have been uses for a variety of low strength (domestic and municipal wastewaters) and high strength (carpet mill effluent, centrate wastewater, tannery effluent, animal effluent, such as cattle farm, poultry, piggery, diary, anaerobic digestate,) wastewaters (Christenson and Sims, 2011; Johnson and Wen, 2010; Luo et al., 2014; Pandey et al., 2016; Tsavatopoulou et al., 2019; L. Wang et al., 2021; Wang

et al., 2010, Yadav et al., 2021). However, the concentrations of nutrients in the wastewater especially tertiary wastewater are inadequate to support the growth of microalgae. While, the high strength nutrient such as anaerobic digestates, piggery wastewaters were reported to have relatively low C/N and N/P ratios that could not meet the optimal stoichiometric ratios. In addition, based on the Redfield theory, the molar stoichiometric C/N/P ratio for optimal microalgae growth should be 106:16:1 (Geider and La Roche, 2002). Hence, to achieve the desired N/ P and maximum biomass, the high strength wastewaters were diluted using low strength wastewater and were adjusted to the optimal ratio (Jain et al., 2022). Some studies reported the adjudgment of nutrient concentrations of wastewater by adding sodium nitrate ($NaNO_3$), industrial-grade urea, phosphorus, different wastewater, or anaerobic digestate (Boelee et al., 2014b; Cho et al., 2011; Christenson and Sims, 2011; Maurya et al., 2022; Mishra and Mohanty, 2019).

It is believed that biofilm growth follows a certain trend and responds differently to uptake nutrients when compared to suspension cultures (Kesaano and Sims, 2014; Shen et al., 2014a). During the initial biofilm growth or cell colonization stage, the nutrient uptake was comparatively low due to fewer microalgal cells. As growth increased, the rate of nutrient removal accelerated and then gradually decreased in the final stage (Boelee et al., 2014b). Fierro et al., (2008) reported 70 % nitrate removal and 94 % phosphate removal by the chitosan immobilized *Scenedesmus* sp. within 12 h of incubation. However, the same biomass grown in suspension cultures removed only 20% nitrate and 30% phosphate within 36 h of incubation. Some researchers reported that nutrient starvation does not stimulate neutral lipid accumulation in biofilm growth, unlike the suspended cells that accumulate lipid in nutrient starvation conditions (Ji et al., 2011). According to Schnurr et al., (2013), *Nitzschia palea* and *Scenedesmus obliquus*, grown in a biofilm system could not accumulate significant neutral lipid compared to the suspended culture. Likewise, Kesaano et al., (2015) observed that nutrient starvation was ineffective for accumulating neutral lipid in the rotating algal biofilm. This reason could be stemmed from how well the cells in the biofilm were deprived of nutrients. The researchers who reported the lower lipid content of biofilm, investigated the biofilm growing in a thicker layer (up to 1 mm) using non-sterilized wastewater for a longer period. This provoked the growth of bacterial cells and the

production of bacterial EPS over time (Bernstein et al., 2014). The EPS in the biofilm developed as a matured matrix and stored the nutrient, allowing continuous mass transfer of nutrients across the biofilm. This phenomenon facilitated the nutrients for the growth and development of microalgal cells during prolonged growth (Decho, 2000). Ultimately, the cells could obtain adequate nutrients continuously via ion exchange resin mechanisms even during a stress situation (Bernstein et al., 2014; Schnurr and Allen, 2015). This confirmed that the cells were not completely starved. Conversely, Shen et al., (2015) observed the enhanced lipid production by algal biofilm under the famine condition. The studies showing the enhanced biomass and lipid production during the famine condition grew the biofilm relatively thinner and for a shorter period of incubation. Those studies utilized sterilized wastewater or synthetic medium, inhibiting bacterial growth. During this short period of cultivation, the EPS concentration in the biofilm was less, preventing the well-developed EPS matrices. Hence, proper distribution of nutrients throughout the cells could not be achieved thereby leading to effective nutrient deprivation (Cheng et al., 2013; Shen et al., 2015). In addition, the study of effective nutrient deprivation could be accomplished if the biofilm was grown in a porous and rigid membrane. Such type of cultivation caused significant transportation of nutrients out of the biofilm through the substratum as well as from the waterside thus resulting in nutrient starvation (Liu et al., 2013).

1.2.4.4 pH

pH is another main factor influencing the rate of absorption of inorganic carbon in the culture medium. In general, pH 7-9 is considered to be an optimal condition for microalgal growth because most of the algae have neutral or slightly alkaline cytosolic pH containing pH-sensitive enzymes. Thus, the extreme pH undesirably affects the growth and CO_2 fixation by disrupting cellular processes (Kumar et al., 2011). Liu et al., (2007) reported that the normal range of pH (pH 7.5–8.5) was favorable for the growth of *Chattonella marina,* while a significant decrease in microalgal growth was observed when pH was increased beyond 9.0. However, in some studies, *Spirulina* sp. could thrive efficiently at a pH greater than 10 and thus minimizing the chances of contamination when cultivation was done in the raceway pond system (Kumar et al., 2011). Similarly, Belkin and Boussiba, (1991) found that *Spirulina platensis* exhibited

optimal growth at pH 9.0–10.0. This indicates that the suitable pH range for the growth of microalgae and cyanobacteria is greatly species-dependent.

1.2.4.5 Temperature

Temperature is another element for growing algae as it strongly influences nutrient solubility, nutrient uptake, protein structure, and algal growth rates. Change in temperature affects the lipid accumulation in microalgal cells by diverting the biosynthetic metabolism to lipid synthesis (Zhang et al., 2019). At high temperatures, essential cellular enzymes and proteins get denatured causing causes an inhibitory effect on the physiology of the growing cells (Wei et al., 2014). Hence, to maintain the growth of microalgae at optimal temperature, a controlled environment is required in the cultivation system. While, for large-scale microalgae cultivation in an outdoor system, the temperature change is dependent on photo duration and seasonal change. Several studies have been reported on the growth and lipid content of different microalgae due to varying temperatures. *Monoraphidium* sp. achieved its maximum biomass concentration (650 mg/ L) and lipid productivity (29.2 mg/L. d) at 30 °C (Wu et al., 2013). For the highest biomass growth of *Chlorella minutissima*, 25 °C was found to be the optimal temperature (Cao et al., 2014). Another study reported the increased cultivation temperature increased monosaturated fatty acids (MUFAs) and saturated fatty acids (FAs) while the neutral lipid and polyunsaturated FAs decreased (Wei et al., 2014) With increased temperature, the cetane number of fatty acid methyl esters (FAME) increased from 52.3 to 60.3 and 45.3 to 47.6 in *Nannochloropsis oculata* and *Tetraselmis subcordiformis* respectively (Wei et al., 2014). Thus, optimizing culture temperatures is vital for improving microalgal biodiesel production on a large scale. from temperature fluctuation (Kesaano and Sims, 2014; Mantzorou and Ververidis, 2019; Ozkan et al., 2012). Moreover, the cultivation of biofilm at high temperatures is critical due to the loss of water during evaporation. Ozkan et al., (2012) reported the water loss (~1.09 L/m^2. d) due to evaporation from the horizontal flat plate biofilm photobioreactor. Similarly, Posadas et al., (2013) reported that seasonal increase in the temperature led to evaporation of water from the culture medium at the rate of 3 to 4.7 ± 0.8 L/m^2. d in algae-bacterial biofilm photobioreactor. Considering this, a pilot-scale attached cultivation system should be developed and designed with a properly controlled system to prevent water loss and requirements.

Table 1.6: Biomass, lipid productivity and lipid content of different microalgae species under different mode of cultivations.

Microalgae species	**Mode of cultivation**	**Carbon source**	**Biomass productivity (g/ L. d)**	**Lipid %**	**Lipid productivity (mg/ L/ d)**	**References**
Chlorella vulgaris	Phototrophic	1 g/ L $NaHCO_3$	0.99	-	-	(Mokashi et al., 2016)
Scenedesmus sp. CCNM 1077	Phototrophic	0.6 g/ L $NaHCO_3$	-	34.44	-	(Pancha et al., 2015a)
Chlorella sp. HS2	Phototrophic	0.5 g/ L $NaHCO_3$ & 1 % CO_2	0.53	-	-	(Nayak et al., 2018)
Chlorella minutissima MCC27	Heterotrophic	Crude glycerol	0.446	34.36	165.15	(Katiyar et al., 2017)
Chlorella protothecoides	Heterotrophic	15-60 g/ L glucose	2.2–7.4	50.3–57.8	1209.6–3701.1	(Xiong et al., 2008)
Chlorella protothecoides UTEX 256	Heterotrophic	Biodiesel derived crude glycerol	5.5	-	2900	(Chen and Walker, 2011)
Chlorella sorokiniana	Heterotrophic	Aquaculture wastewater	0.353	31.9	138.17	(Guldhe et al., 2017)
Chlorella vulgaris FACHB 31	Heterotrophic	18 g/ L glucose	2.77	30.1	-	(Han et al., 2012)
Chlorella vulgaris #259	Heterotrophic	Glucose & acetate	0.08–0.15	23.0–36.0	27.0–35.0	(Liang et al., 2009)
Chlorella vulgaris 31	Heterotrophic	2 & 10 g/L glucose	0.159	-	0.19	(Kong et al., 2020)

Chlorella vulgaris 31	Mixotrophic	2 & 10 g/ L glucose	0.196	-	0.226	(Kong et al., 2020)
Chlorella vulgaris #259	Mixotrophic	Glucose & glycerol	0.09–0.25	21.0–34.0	22.0–54.0	(Liang et al., 2009)
Nannochloropsis sp.	Mixotrophic	2 g/ L glucose	0.587	25.3	148.3	(Cheirsilp and Torpee, 2012)
Schizochytrium limacinum SR21 (ATCC MYA-1381)	Mixotrophic	Biodiesel derived crude glycerol	3.88	-	-	(Ethier et al., 2011)

(continued)

1.2.4.6 Light

Photosynthesis and cell photo-acclimatization are both light-driven processes. Hence, types of light sources are a major constraint for the growth of microalgae. The response of photosynthetic cells to light intensity, absorption spectra, and photoperiod may vary for different microalgal species. The light energy spectrum, ranging from 400-700 nm wavelength is considered the actual photon range desirable for the photosynthesis of microalgae and cyanobacteria (Berberoglu et al., 2007). The light intensity required for growing microalgae in phototrophic mode is divided into several light phases: limitation phase, saturation phase, and inhibition phase (Ogbonna and Tanaka, 2000). The light saturation phase varying from 50-200 μmol/m^2 s is the maximum light intensity that can be accommodated with the photosynthetic cells of different microalgae (Goldman, 1979). Liu et al., (2012) investigated the effects of light intensity, ranging from 50-400 μmol/m^2 s on growth of *Scenedesmus* sp. The highest biomass yield (3.88 g/ L), lipid content (41.1 %), and neutral lipid content (32.9 %) were achieved at 400 μmol/m^2 s. In PBR, the high cell concentration can experience photoinhibition due to the self-shading effect between individual cells, causing a productivity decrease. Evenly distribution of light saturation phase over the whole microalgal cultivation can induce maximum biomass productivity. To circumvent the effect of light inhibition or photo shading in the high cell density, the light path should be reduced to get the optimum light intensity (Goldman, 1979).

1.3. Knowledge Gap

Microalgae show numerous applications in biofuel production as well as several by-products. It has the advantages of fast growth, high oil content, the ability to grow in a wide range of stress environments, and grow in varieties of wastewater. Nevertheless, the commercial cultivation of microalgae is still a challenge. The main obstacle to the economic viability of the microalga biomass can be overcome by strategic planning. The main knowledge gap in the commercialization of microalgal biomass is as follows:

1. Limited research on appropriately balanced nitrogen: phosphorus ratio in the culture medium for enhancement growth.
2. Cost-intensive harvesting and dewatering issue.

3. Limited research on microalga-cyanobacteria consortium for amalgamation of efficient harvest and biomass production
4. The coupling of co-product synthesis along with biodiesel is a prerequisite to making sustainable microalgal biomass.

1.4. Objectives

Based on the review of works of literature and research gaps, the following major objectives have been formulated for the present project study. Hence, this Ph.D. thesis with the title 'STUDY OF ALGAL BIOFILM GROWTH TO ENHANCE BIOMASS AND LIPID PRODUCTION', aims to achieve the following major objectives

1. Molecular identification; selection of initial pH and temperature; optimization of ideal nutrient source for highest growth and lipid yield enhancement.
2. Characterization of biofilm/ mat via extraction of EPS and attached cultivation on different substrata
3. Co-cultivation of microalgae and cyanobacteria in a balanced ratio of nitrogen and phosphorus in a synthetic medium for enhancement of efficient harvesting, biomass productivity, and lipid content
4. Study of microalgae cultivation in municipal wastewater as a source of low-cost nutrient medium
5. Co-cultivation of microalga and cyanobacterium in domestic wastewater optimizing N/P ratio towards the production of biodiesel and protein-rich biomass for its feasibility as animal feed.

1.5. Organization of the Thesis

The doctoral thesis is organized into seven chapters as follows:

Chapter 1: This chapter includes the current energy scenario, microalgae as a potential feedstock for biofuel production. The rationale for pursuing the current study has been described, and background information on the key challenge of energy security and the country's current energy situation has been developed. Besides, a thorough analysis of the literature has been discussed. This chapter provides comprehensive knowledge to design this Ph.D. research.

Chapter 2: In this chapter, a complete list of materials and procedures was used throughout this thesis research. This chapter also explains the detailed experimental design, and methodology used to process optimization of the cultivation of microalgae for enhanced oil content. The study's approach is exclusively based on a review of the literature. Standardization, process optimization, statistical analysis, and confirmatory analysis were carried out based on experimental needs.

Chapter 3: This chapter dealt with molecular identifications of microalga and cyanobacterium which were already isolated by our Bioenergy group, from the waterlogged area of the Indian Institute of Technology Guwahati, Assam. A preliminary examination was discussed to study the growth profile of the strains under various physical parameters (temperature, and pH). The study also encompasses further optimization of the chemical parameter (different sources of nitrogen, phosphorus, and glucose concentration) for enhanced lipid production. Further addition of different glucose concentrations on lipid accumulation and FAMEs composition in microalgae are also presented in this chapter

Chapter 4: This chapter dealt with the evaluation of intrinsic factors produced by microalga and cyanobacterium which are responsible for biofilm formation. The study includes an estimation of EPS production during various stages of microalgal growth and its characterization. This chapter also includes physio-chemical characterization of various substrata, and the synergistic interaction between the physio-chemical properties of substrata and EPS on efficient microalgal biomass accumulation.

Chapter 5: From the previous chapter, it was found that optimization of cultivation conditions (i.e., physicochemical parameters) could augment the lipid in microalga but the increase was not substantial. In this chapter, attempts are made to investigate the effect of varying nitrogen to phosphorus molar ratios on enhanced lipid accumulation in microalgae. This chapter also includes a selection of optimal microalga/cyanobacterium inoculum ratios to improve flocculation and efficient biomass harvesting. The interactive impact of the microalgal cultivation condition on fatty acid profiles and biodiesel properties is also presented.

Chapter 6: This chapter illustrates the utilization of municipal wastewater for microalgal cultivation, selection of culture conditions for simultaneous efficient growth, lipid production, and waste remediation. The study includes further scaling up the cultivation of bioreactors, and assessment of fatty acid profiles and biodiesel properties.

Chapter 7: This chapter discusses the issue of inadequate nitrogen to phosphorus proportion in wastewater for use as a microalgal culture medium. The study includes optimization of the chemical and physical parameters (N/P ratio, heterotrophic and mixotrophic mode) for an increase in lipid production. This chapter also encompasses the co-cultivation of microalga and cyanobacterium to improve harvesting efficiency, and lipid accumulation. In addition, the chapter intends to assess microalgal-based biodiesel properties, *in vitro* digestion of whole biomass, and its cytotoxicity to establish a sustainable solution for cleaner energy by animal feed production.

Chapter 8: In this chapter, the overall conclusions and scope for future work are summarized.

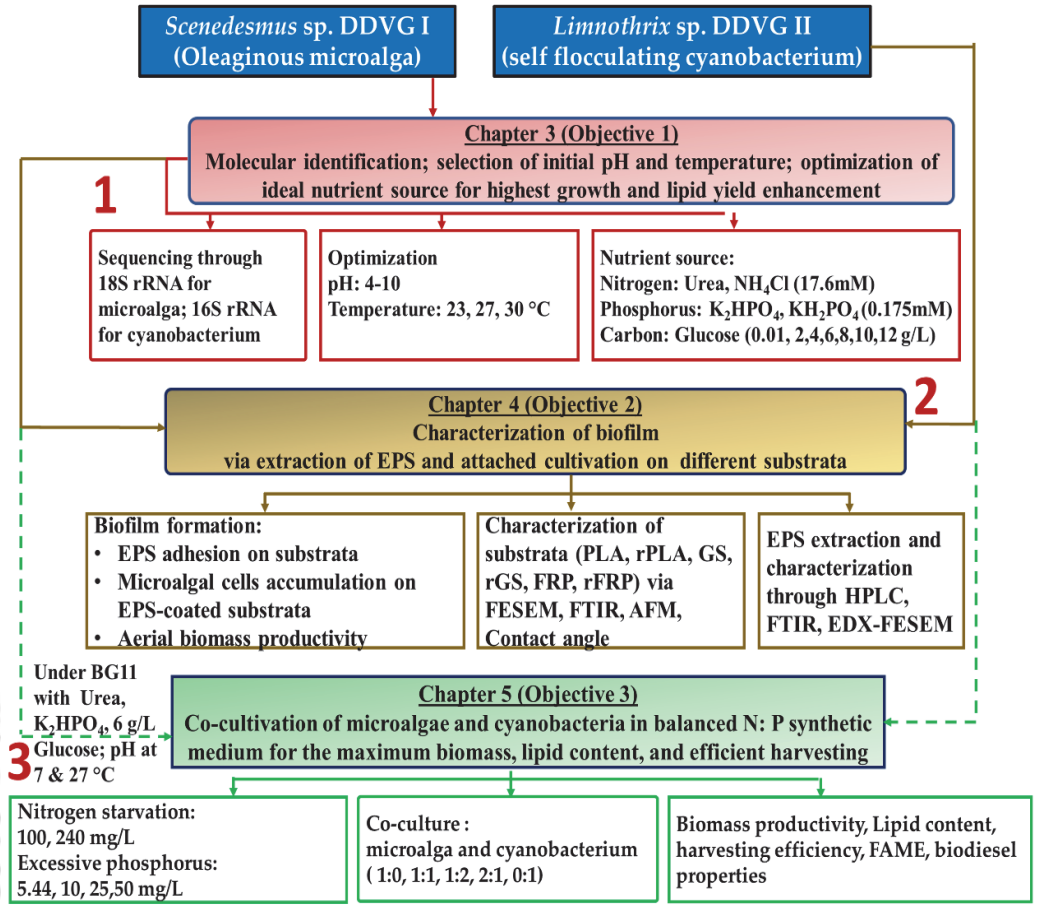

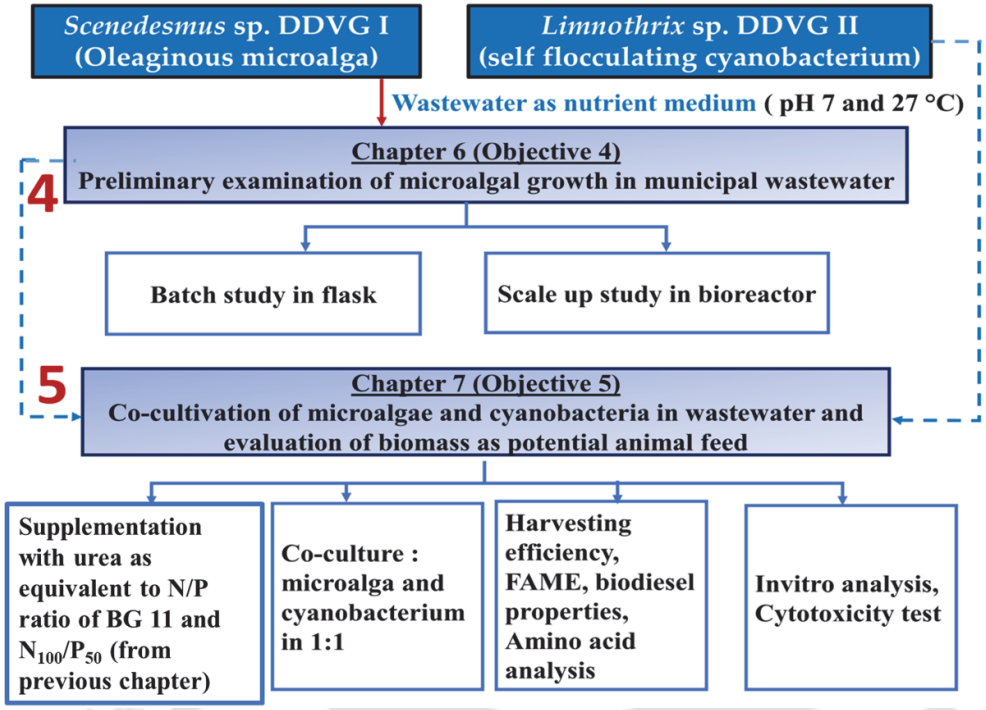

Figure 1.4: Flow chart of PhD thesis work.

CHAPTER 2

Materials and Methods

Materials

Methods

Procedures

CHAPTER 2

Materials and Methods

This chapter deals with a complete list of materials and procedures used throughout this thesis research. This chapter also explains the detailed experimental design, and methodology used to process optimization of the cultivation of microalgae for enhanced oil content. The study's approach is exclusively based on a review of the literature. Standardization, process optimization, statistical analysis, and confirmatory analysis were carried out based on experimental needs.

2.1 Materials

2.1.1 Chemicals

The chemicals employed for the present study were procured from M/s Merck India Pvt. Ltd. and M/s Himedia. Water quality analysis Kit for ammonia, total phosphate, total nitrate, and chemical oxygen demand (COD) were procured from M/s Hach (USA) and M/s Palintest Ltd. (United Kingdom). The cell line BHK-21 was procured from the National Centre for Cell Science (NCCS) (Pune, India).

2.1.2 Substratum

The four different substrata were employed in this study. The substrata were glass slide (GS), polylactic acid (PLA) sheet, millipore filter membrane (FM), and fiber-reinforced plastic (FRP). The substrata were modified with sandpaper Grit-100 to represent rough surfaces, i.e., rough glass slide (rGS), rough polylactic acid (rPLA) sheet, rough filter membrane (rFM), and rough fiber-reinforced plastic (rFRP). The dimension of the substrata was length × breadth = 7 × 2 cm. All the substrata were procured from a local market, Amingaon, Assam except PLA, it was a gift from the CoE-SusPol, IIT Guwahati.

2.1.3 Media composition

The blue-green medium–11 (BG-11), as proposed by the University of Texas (UTEX), was chosen as a growth medium for microalgae. The medium components include all the macro and micronutrients which are responsible for the growth of both the microalgae. The composition of the medium is summarised in Table 2.1 as follows:

2.1.4 Source of wastewater

Wastewater was used as a low-cost nutrient supply for the cultivation of microalgae. The waste materials such as Primary Municipal wastewater (PMWW) and Domestic wastewater (DWW) were used for media formulations. The PMWW was collected from a local Wastewater Treatment Plant in Saint Paul, Minnesota, USA. The DWW was located in a local Sewage Treatment Plant at the Indian Institute of Technology Guwahati (IITG), Assam. Large solid particles that were present in the wastewater were eliminated using sedimentation and filtration with Whatman filter paper (grade 42). The filtered wastewater was collected in a sterilized container and put under UV irradiation for about 45 min for disinfection.

2.1.5 Inoculum preparation

The freshwater microalgae DDVG I and cyanobacteria DDVG II were previously isolated by our Bioenergy laboratory, from the local waterlogged area of the IITG (26° 11′ N, 91° 41′ E). Selection of the microalgae strain was based on its fast growth rate, high biomass and oil production (Difusa et al., 2015; Tsavatopoulou et al., 2019). Furthermore, we opted the cyanobacterium, DDVG II because of its filamentous morphology and secretion of extracellular polymeric substances (EPS), which contribute to cell aggregation or auto-flocculation and facilitate the harvesting process (Gaignard et al., 2019). The individual cultures were maintained using a 100 mL normal BG11 medium in a 250 mL Erlenmeyer flask. The inoculum was kept at 25 °C in an orbital shaker with 150 rpm under the white fluorescent light of 4000 lux with a photoperiod of 12 h:12h light: dark condition. After attaining the exponential growth phase i.e., after 10 days, the inoculum was used for the experiment.

2.1.6. Growth conditions

The growth of microalga was performed in a 500 mL Erlenmeyer flask with 250 mL of culture medium and an initial inoculum optical density at 680 nm ($OD_{680\ nm}$) of ~0.4 (0.45 g/L). All flasks were incubated inside an orbital shaker at 150 rpm with a photoperiod of 12 h:12 h light: dark conditions and a light intensity of 6000 lux. Similar lighting conditions were provided for the mixotrophic regime. However, flasks were covered with aluminium foil during heterotrophic regimes to keep out light. All the

experiments were performed in triplicates. The microalgae growth conditions that did not adhere to the same parameters were specified when necessary.

2.2 Optimization of culture conditions

To ensure optimal growth and lipid content of the chosen microalgae, a multi-step culture approach was created. Each step was tailored to the selected microalgae strains and used a growth medium supplemented with different nutrient sources, different levels of N/P initial culture pH, temperature, and organic extracts (PMWW and DWW). To investigate the potential for auto-flocculation of the selected strains, an approach for EPS production followed by attached cultivation on different substrata was designed. For the enhancement of easy harvesting and recovery of biomass, a co-cultivation step was developed. According to the culture growth and performance, the cultivation period for each step varied from 10-20 days. The evaluation of microalgal biomass as animal feed was also performed through *in vitro* digestibility assay and cytotoxicity test via 3-(4,5-dimethylthiazol-2-yl)-2,5-diphenyltetrazolium bromide (MTT) assay. The biomass was harvested at the end of the culture period for each step. The best culture conditions were chosen based on the maximal growth and lipid output from the dried biomass. The following multi-step cultivation strategies were carried out in order.

2.2.1 Screening of initial pH and temperature

Scenedesmus sp. DDVG I and *Limnothrix* sp. DDVG II were grown at various temperatures of 23°C, 27°C, and 30°C. For each temperature setting, several batches of the experiments were done at pH levels ranging from 4 to 10. The initial pH value of all the conditions was adjusted by using 0.1N HCl or 0.1N NaOH solution. The culture was grown for 16 days. The cultivation condition with the highest growth was further chosen for the optimization of nutritional sources.

2.2.2. Effect of different nutritional sources

One variable at a time was altered in each of these investigations. The BG11 medium served as the baseline medium with the addition of 0.034 g/L of glucose which was also equivalent to 0.19 mM of Na_2CO_3 in the normal BG 11 medium. For the nitrogen source, we chose 1.05 g/L of urea and 0.94 g/L of NH_4Cl, which were equivalent to

17.6 mM of $NaNO_3$ in normal BG11 medium. For phosphorus supply, besides 0.04 g/L of K_2HPO_4 (which was equivalent to 0.23 mM) in BG 11, we also chose an equimolar concentration of 0.031 g/L of KH_2PO_4. Prior to glucose addition, all the media were autoclaved at 121 °C for 30 mins. Subsequently, concentrated glucose solution was added into the medium after sterilization using a sterile 0.22 μm filter. Table 2.2 summarises the concentrations and sources of carbon, nitrogen, and phosphorus in normal BG 11 medium and the experimental condition. The composition of micronutrients in the normal BG 11 medium was presented in Table A1 in Appendix. The pH of all the media was adjusted according to the optimized condition and was used for the cultivation of *Scenedesmus* and *Limnothrix* sp. To investigate the impact of glucose concentration variation on the lipid content of *Scenedesmus* sp. and *Limnothrix* sp., glucose was varied from 0.034, 2, 4, 6, 8, to 12 g/L. After 16 days grown, the biomasses were harvested through centrifugation and were used for the analysis of lipid content, and fatty acid profile.

Table 2.1: Composition of normal BG-11 medium for microalgae cultivation.

Macro-nutrients	**BG-11 Stock (g/500 mL)**	**Working volume (mL/L)**	**Final concentration (mg/L)**	**Final Molar Concentration (mM)**
$NaNO_3$	7.5	10	1500	17.6
$MgSO_4.7H_2O$	3.75	10	75	0.3
K_2HPO_4	2	10	40	0.23
$CaCl_2.2H_2O$	1.80	10	36	0.24
Citric Acid	0.30	10	6	0.031
Ferric Ammonium Citrate	0.3	10	6	0.021
Na_2EDTA	0.05	10	1	0.0027
Na_2CO_3	1	10	20	0.19
Micro-nutrients				
$ZnSO_4$	0.22	1 mL		See Table A1 in Appendix
$MnCl_2.4H_2O$	1.81			
$CuSO_4.5H_2O$	0.08			
$Co(NO_3)_2.6H_2O$	0.05			
H_3BO_3	2.86			

Table 2.2: Source of carbon, nitrogen, phosphorus and their concentration employed in the experimental condition for the study of the nutrient optimization. The concentrations were taken with respect to the equimolar concentrations of the normal BG 11 medium.

Nutrient	Source of Nutrient	Concentrations (g/L)
Nitrogen	Urea/ NH_4Cl	1.05 (~17.6 mM)
Phosphorus	K_2HPO_4/ KH_2PO_4	0.04 (0.23 mM)
Carbon	Glucose	0.034 (0.19 mM)

2.2.3 Evaluation of EPS production

The purpose of this step is to determine the production of EPS by *Scenedesmus* sp. and *Limnothrix* sp. in a typical habitat. To investigate this, *Scenedesmus* sp. and *Limnothrix* sp. were cultivated in normal BG 11 medium for 20 days. Meantime in a parallel batch of an experiment, the EPS produced periodically was evaluated for its adherence to various substrates (as mentioned in section 2.1.2). Briefly, a batch reactor was set up in jam bottles (total volume= 500 mL) with 300 mL of BG11 medium in different batches. The substrata were immersed vertically inside the jam bottles by an initial inoculation of *Limnothrix* sp. culture. Those substrata coated with EPS were removed from the jam bottles periodically after 4 days. Subsequently, the substrata coated with EPS-4, EPS-8, EPS-12, EPS-16, and EPS-20 were transferred into other jam bottles by an initial inoculation of *Scenedesmus* sp. culture. The systems were operated for at least 20 days and harvested after reached a steady state. *Scenedesmus* sp. biofilm was harvested from the substrata through scrapping. The overall experimentation is also illustrated in the schematic diagram (Figure 2.1).

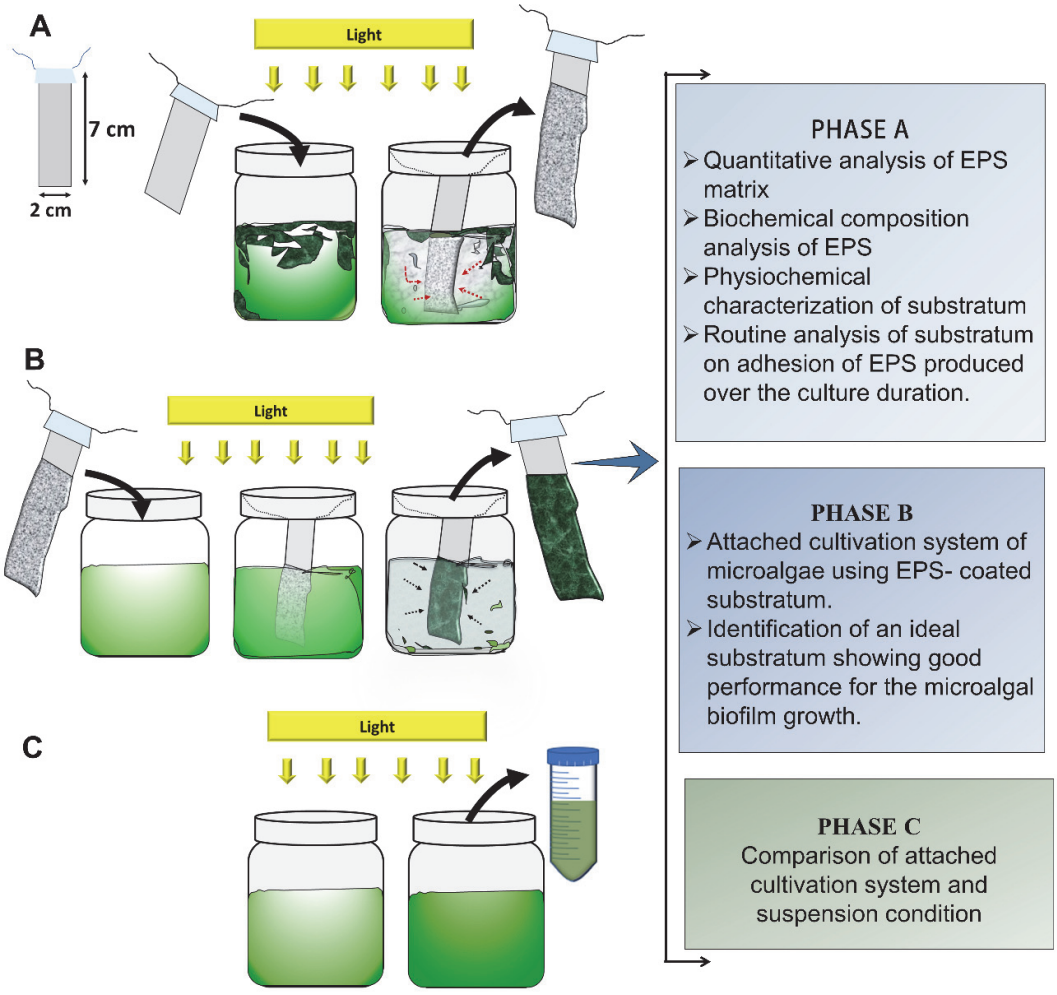

Figure 2.1: Schematic diagram of experimentation conducted under three phases using 500 mL jam bottles at 4000 lux light intensity with 300 mL BG 11. (a) Substratum (length × breadth = 7 × 2 cm) is immersed vertically inside the jam bottle with initial inoculation of *Limnothrix* sp. DDVG II (red dashed arrows represents adhesion of EPS from *Limnothrix* cells on the substratum. (b) EPS-coated substratum is used for the attached cultivation of microalgae, *Scenedesmus* sp. DDVG I (black dashed arrow represents an accumulation of cells as biofilm). (c) Microalgae cultivation in suspension condition.

2.2.4 Medium supplemented with appropriate N/P concentrations

In this study, BG 11 with the addition of 6000 mg/L of glucose was used as basal medium, but N and P supply were modified. Using the basal medium, five types of media were designed by substituting $NaNO_3$ by urea at various concentration with combination of different phosphorus level. The selections of glucose and urea for the present study were based on the preliminary examination (section 2.2.2). The initial concentrations of N and P for each modified medium were denoted with different designations (to be used elsewhere in the thesis) and the corresponding N:P values were compared with the BG11 medium, control (Table 2.3). The BG11 consisted of 240 mg/L of N-$NaNO_3$ and 5.44 mg/L of P-K_2HPO_4. Here, we described the five urea-based medium as follows: sufficient N and sufficient P (N_s P_s) as 240 mg/L of N and 5.44 mg/L of P, deficient N and over excessive P (N_{def} P_{oexcs}) as 100 mg/L of N and 50 mg/L of P. The deficient N and excessive P (N_{def} P_{excs}) was described by 100 mg/L of N and 25 mg/L of P, deficient N and moderately excessive P (N_{def} P_{mexcs}) as 100 mg/L of N and 10 mg/L of P, and sufficient and moderately excessive P (N_s P_{mexcs}) as 240 mg/L of N and 10 mg/L of P. The initial pH of all the media was adjusted to 7±0.1 by using 0.1 N NaOH and 0.1N HCl and autoclaved at 121 °C for 20 min. But for the media containing glucose, autoclave was done before addition of glucose. After autoclaved, sterilized glucose with 0.2µm pore size syringe filter (Axiva Sichem Biotech, India) was added into the medium and then pH was adjusted to 7±0.1. Each culture condition was performed in a 500 mL Erlenmeyer flask with 250 mL of medium, and an inoculum $OD_{680\ nm}$ of 0.4 (10:100 v/v). The study was conducted in both heterotrophic and mixotrophic modes for sixteen days at 27 °C in an orbital shaker (150 rpm) under a light intensity of 6000 lux with 12h (dark): 12h (light). In heterotrophic conditions, the flasks were wrapped with aluminium foil to avoid light illumination. Samplings were done every second day to estimate growth profile, Chlorophyll-a (Chl-a) content. After 16 days of growth, the biomass was harvested through centrifugation at 10,000 rpm for 10 mins. Based on the superior biomass and lipid content, the optimal condition was subsequently utilized for co-cultivation experiment.

Table 2.3: Overview of nutrient concentrations of the media.

Nutrient concentrations	**N_{def} P_{oexcs}**	**N_{def} P_{excs}**	**N_{def} P_{mexcs}**	**N_s P_{mexcs}**	**N_s P_s**	**BG 11**
N-Urea (mg/L)	100	100	100	240	240	240 (N-NaNO3)
P-K_2HPO_4 (mg/L)	50	25	10	10	5.44	5.44 (P-K_2HPO_4)
N:P	2:1	4:1	10:1	24:1	44.1:1	44.11:1
Glucose (mg/L)	6000	6000	6000	6000	6000	20 mg/L Na_2CO_3

2.2.4.1 Co-cultivation

For co-cultivation, the inoculum was prepared by combining the individual cells of *Scenedesmus* sp. DDVG I (S). and *Limnothrix* sp. DDVG II (L) at different levels of 1:1, 1:2 and 2:1 v/v to obtain a total initial $O.D_{680\ nm}$ of 0.4. Their corresponding systems were denoted as co-culture 1:1, co-culture 1:2 and co-culture 2:1, (to be used elsewhere in the manuscript), respectively. Each inoculum (10:100 v/v) was cultivated in 250 mL of the medium using 500 mL Erlenmeyer flask. The study was conducted using the optimized culture medium and condition as mentioned in section 2.2 for 16 days. Light and temperatures were also kept similar with the section 2.2. The cultures were maintained at 50 rpm (to increase the time of contact between the cultures).

2.2.5. Primary municipal wastewater as a source of low-cost nutrient media

This process was thought to be an efficient screening step for choosing the microalgae strains and creating a low-cost nutrient media for bulk production. The PMWW was used for the cultivation of microalgae. *Scenedesmus* sp. DDVG I was cultivated in mixotrophic and heterotrophic modes for ten days using PMWW. The similar culture condition (as mentioned in section 2.2.4) was employed in this study. A batch of blank containing wastewater medium but without the microalgal culture was set up simultaneously to observe any other microbial growth besides microalgae. Routine analyses including growth study and Chl-a content were determined during the culturing to examine the favorable cultivation mode. At the end of the 10-day, the biomass was collected through vacuum filtration and dried. The optimal cultivation

regime was selected and scaled up for enhanced biomass accumulation and biochemical analysis.

2.2.5.1. Bioreactor study using PMWW

The optimized culture condition in section 2.2.5 was scaled-up to a 3 L bioreactor (BR) (Biostat A plus, Sartorius, USA), with a 2 L working volume as illustrated in Figure 2.2. The base plate of the reactor was connected with a sparger to provide bubble aeration. The aeration was achieved by compressed air from an air pump (Tetra Whisper AP 150, 2.5 W) through the sparger. The bubbling air-flow rate was controlled by a flow meter (Cole Parmer, USA) at the rate of 80 mL/min. The bioreactor was connected to a pH probe and a temperature probe for monitoring pH and temperature regularly. A sample collecting port was installed at the top of the reactor. At the end of the 10-day, the biomass was collected through vacuum filtration and dried. Dried biomass was later used for biochemical analysis.

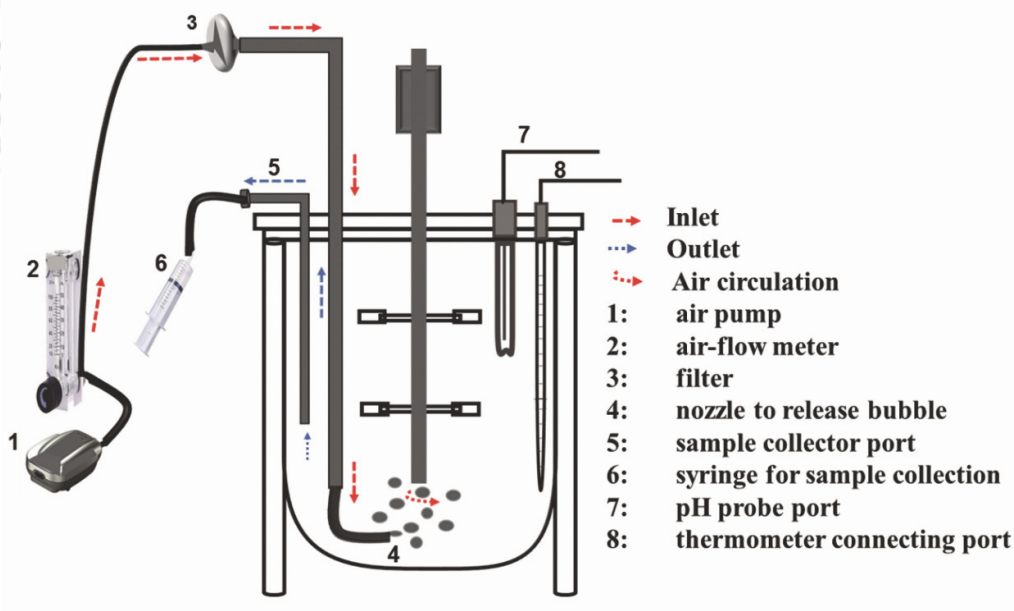

Figure 2.2: Configuration of 3 L bioreactor (BR) (Biostat A plus, Sartorius, USA) for mixotrophic cultivation of microalgae, *Scenedesmus* DDVG I in PMWW.

2.2.6 Nutritional balance of domestic wastewater for utilization in microalgae cultivation

Discharging domestic wastewater (DWW) containing organic contaminants and inorganic pollutants like phosphates and nitrates has the notable side effect of eutrophicating freshwater ecosystems (Azam et al., 2020). Thus, extra physical and chemical tertiary treatments are necessary before any freshwater disposal, but this process is often prohibitively expensive (Graham et al., 2014). One possible strategy for overcoming the high cost of microalgae farming is to use wastewater as a source of nutrients to obtain microalgae biomass as a by-product for biodiesel synthesis. Several research papers on the use of microalgae to treat various low- and high-strength wastewaters have been published (Geider and La Roche, 2002; Mishra and Mohanty, 2019; Mohan Singh et al., 2020; Ummalyma et al., 2022). However, one main difficulty with low-strength wastewater is the insufficient nitrogen (N) to phosphorus (P) ratio (N/P), thus limiting algae growth and poor bioremediation and biomass production. (Beuckels et al., 2015; Choi and Lee, 2015). Municipal wastewater has typically low N/P ratios of about 10 (Maurya et al., 2022) while wastewater from livestock farms, poultry, and toilet effluent shows high N/P ratios of ~ 40 (Kumar et al., 2010; Tuantet et al., 2014). To date, an optimized strategy for N/P balance of domestic wastewater for improved effluent quality and microalgae development has not been thoroughly documented.

Therefore, this study attempts to determine the optimal N/P condition of domestic wastewater to maximize the performance of total nutrient removal and biomass production of *Scenedesmus* sp. DDVG I. Subsequently, to establish an easy biomass harvesting approach, the study chose auto-flocculating *Limnothrix* sp. DDVG II and was co-cultivated with *Scenedesmus* sp. DDVG I in the optimal nutritional balance wastewater. Physicochemical characteristics of the domestic wastewater (DWW) are outlined in Table 2.4. The DWW was rich in COD (130. ± 8.5 mg/L), TN (3.99±1.9 mg/L), and TP (12.53±0.5). The two different levels of N/P conditions in DWW were set up at the ratios of 250:5 (denoted as DWW with N_{250}:P_5) and 100:50 (denoted as DWW with N_{100}:P_{50}). All the conditions were achieved by adding urea to the DWW effluent. These particular N/P levels were chosen based on the superior growth in the

preliminary study (see section 2.2.4). The pH of the media was adjusted to 7±0.1 by using 0.1 N NaOH or 0.1 N HCl. To disinfect the media, they were exposed to UV light for 45 min. The microalga growths in different wastewater media were compared with the normal BG 11 condition (control condition). Each wastewater media but no microalga culture (blank condition) was also incubated in parallel to explore any additional microbial growths. The effect of different N/P conditions on *Scenedesmus* sp. DDVG I growth was evaluated in both mixotrophic and heterotrophic regimes. Each culture condition was inoculated into a 500 mL flask with 250 mL of culture medium at an $OD_{680\ nm}$ of 0.4. The study was performed in a similar condition as mentioned in section 2.2.5. Samplings were done every second day to estimate growth profile, Chl-a content, and nutrient removal efficiency. The culture was harvested at the end of 12 days (when the biomass concentration reached the maximum level) through centrifugation at 10,000 rpm for 10 mins. Based on the superior growth, the optimal culture condition was subsequently employed for the co-cultivation experiment.

Table 2.4: Physicochemical characteristics of Domestic Wastewater (DWW) compared with the basal BG 11 media. All measurements were performed in triplicate, and results are expressed as mean value ± standard deviation (SD).

Parameter	**BG11 (control)**	**DWW**	**DWW with N_{100}:P_{50}**	**DWW with N_{250}:P_5**
COD mg/ L	450	130±2.5	192.7±1.9	1700±1.9
TN (mg/L)	250	3.99±1.9	25.06±1.9	576±1.9
TP (mg/L)	5.44	12.53±0.5	12.5±1.9	12.53±1.9
N/P	45.9:1	0.31:1	2:1	45.9:1
pH	7.0±0.01	7.0±0.01	7±0.01	7±0.01

2.2.6.1 Co-cultivation

The cyanobacterium strain, *Limnothrix* sp. DDVG II was employed as a flocculant /consortium partner to harvest the suspended *Scenedesmus* sp. DDVG I cell. To determine the growth of co-cultivation, the inoculum ratio of *Scenedesmus* sp. DDVG

I and *Limnothrix* sp. DDVG II inoculum was set as 1:1 v/v to get the total initial $O.D_{680\,nm}$ of 0.4. The inoculum was cultured in a 250 mL optimized medium (as optimized in section 2.2.6) using a 500 mL Erlenmeyer flask and a similar orbital shaker condition (as mentioned in section 2.2.4.1). The culture parameters (i.e., temperature and light intensity) were kept similar as mentioned in section 2.2.5. Samplings were done every second day to estimate growth profile, Chl-a content, and nutrient removal efficiency. All the experiments were carried out in triplicate for 12 days.

2.3 Analytical techniques

2.3.1 Phylogenetic analysis

To identify the microalga DDVG I and cyanobacterium strain, DDVG II, genomic DNA was extracted using the CTAB method prescribed by Mukherjee et al., (2016). Isolated DNA samples were stored at -20 °C. The partial 18S rRNA and 16S rRNA sequences of the microalga and cyanobacterium respectively were analyzed for classification. The universal oligos for amplification of the 18S rRNA include the forward oligo (NS 1 5′ GTAGTCATATGCTTGTCTC 3′) and the reverse oligo (NS 4 5′ CTTCCGTCAATTCCTTTAAG 3′). The universal oligos for amplification of the 16S rRNA include the forward oligo (CYA 106F 5’ CGGACGGGTGAGTAACGCGTGA 3’) and the reverse oligo (CYAN 1281R 5’ GCAATTACTAGCGATTCCTCC 3’) (Mukherjee et al., 2016). The PCR thermal program included an initial denaturing step for 5 min at 95 °C followed by 30 cycles of 30 s at 95 °C, 30 s at 61 °C, and 1 min at 72 °C, with a final extension step of 10 min at 72 °C. The PCR products were run on 0.8% agarose gel, and the amplicon was outsourced for sequencing to Eurofins Genomics Services, India. The obtained sequences of 18S and 16S rRNA were aligned through the Basic Local Alignment Search Tool (BLAST) in National Center for Biotechnology Information (NCBI) database for pairwise similarity. The multiple sequence alignment of both the species was generated through the program CLUSTAL W and MEGA 6 (Kumar et al., 2018; Larkin et al., 2007). The phylogenetic trees were built through Neighbor-Joining (NJ) trees (Saitou and Nei, 1987). All ambiguous positions were removed for each sequence pair (pairwise deletion option). Bootstrap analysis was done with 1000 re-samplings to determine the support for each clade.

2.3.2 Evaluation of microalgae growth

The growth profiles of the selected strains were monitored regularly over 10-24 days based on the culture condition. A specific volume of culture was withdrawn every second day and the OD of the sample was measured at 680 nm. The dry cell weight (DCW) was calculated using corresponding standard curves that were generated for each strain and growth medium ($R^2 > 0.99$).

While, the growth profile of microalgae cultivated in wastewater was measured in terms of the total solids (TS) and total volatile solids (TVS), which represent biomass concentration and were determined according to the standard methods (APHA, 1995). The biomass concentration for the growth profile of the microalgae was determined as the total biomass minus the biomass in wastewater that was not inoculated with algae (or blank condition).

Specific growth rate (μ, d^{-1}) was estimated according to the following equations (2.1) (Mishra and Mohanty, 2019).

$$\mu = \left[\ln(X_f) - \ln(X_i)\right] / \Delta t \quad (2.1)$$

where X_f and X_i were biomass concentrations at the period 'Δt' (d) during the exponential phase.

2.3.3 Total chlorophyll content

Chlorophyll-a (Chl-a) was determined according to the following method and equation (2.2) (Pruvost et al., 2011). Briefly, one mL of microalgal culture was centrifuged at 10,000 rpm for 10 min. The cell pellet was lysed with 1.5 mL of methanol by incubating in a water bath at 45 °C for 30 min. Then the sample was centrifuged at 10,000 rpm for 10 min, and the absorbances at 652 nm and 665 nm were measured using Hach DR 5000 Spectrophotometer:

$$Chl - a = 16.5169A_{665} - 8.0962A_{652} \quad (2.2)$$

2.3.4 Harvesting of cells from suspension and co-cultivation system

The suspended algal cells grown in the Erlenmeyer flasks were harvested through centrifugation at 10,000 rpm for 10 mins. While the suspended cells in the bioreactor were collected through vacuum filtration using Whatman filter paper (grade 4). For the

co-cultivation system, the agglomerated biomass was harvested via the sieving method using a muslin cloth (pore size: 0.7 mm) as illustrated in Figure 2.3. The harvested biomass was subjected to hot oven drying at 80 °C for 10 h to ensure complete drying. The dried biomass was stored at -20°C for further analysis. The biomass productivity was expressed as milligram per unit of volume divided by the duration of culture.

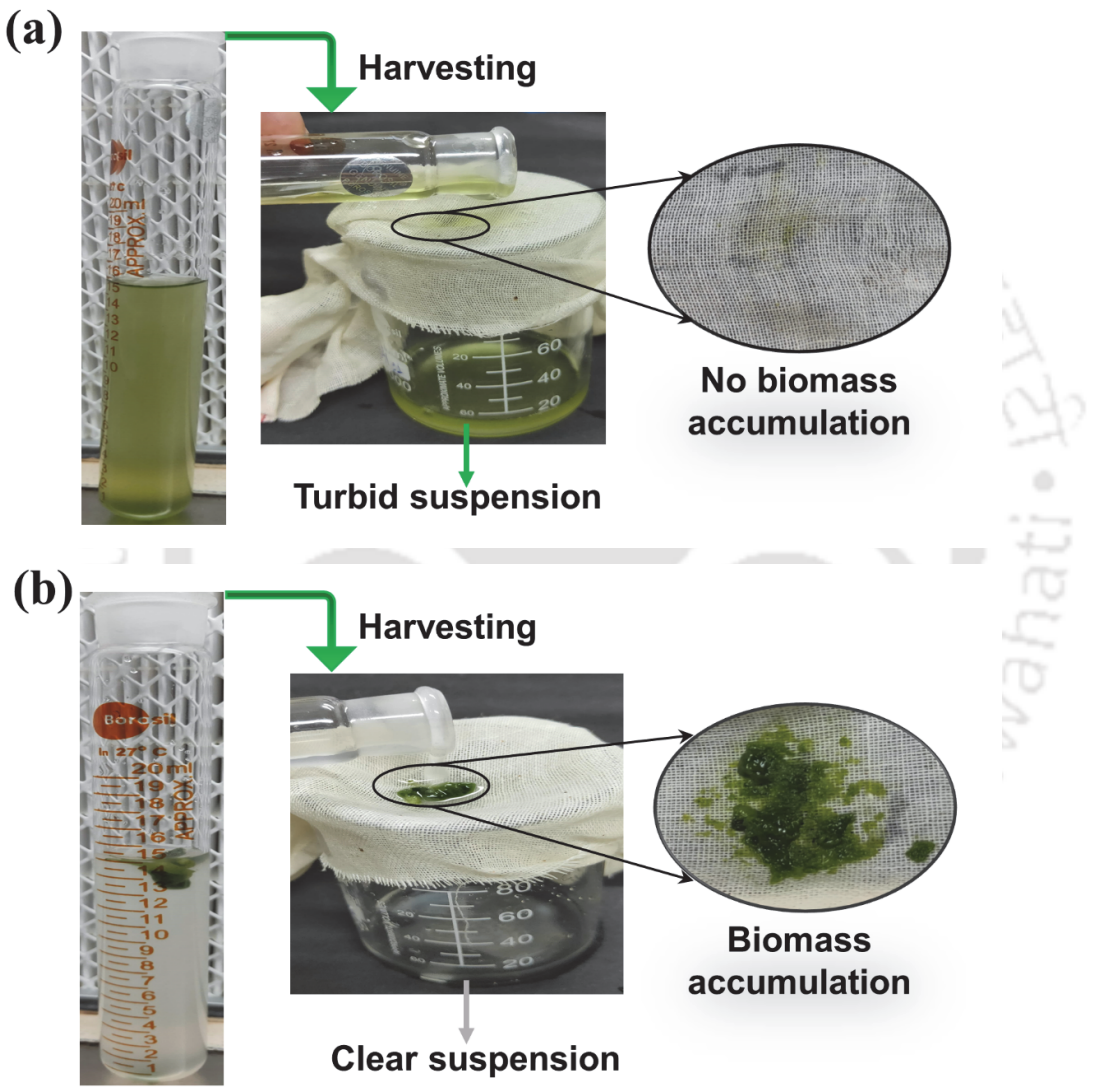

Figure 2.3: Comparison of biomass harvesting by using simple filtration with muslin cloths (pore size:0.7 mm). (a) *Scenedesmus* sp. DDVG I (b) co-culture of *Scenedesmus* sp. DDVG I and *Limnothrix* sp. DDVG II at a 1:1 ratio v/v.

2.3.5 Biomass harvesting efficiency

The flocculation efficiency of the co-culture system was compared with that of individual strains by using equation (2.3) (Leong et al., 2021).

$$Harvesting\ efficiency\ (\%) = \left(OD_{680}t_i - OD_{680}t_f\right) \times 100/OD_{680}t_i \quad (2.3)$$

where $OD_{680}\ (t_i)$ and $OD_{680}\ (t_f)$ denote the turbidity of broth taken on initial and final days.

2.3.6 Biochemical analysis of algal biomass

2.3.6.1 Nile red assay of co-cultures

The confocal laser scanning microscopy was done to examine the presence of lipid droplets in *Scenedesmus* sp., *Limnothrix* sp., and co-culture through the Nile Red staining as described by Ren et al., (2013). Briefly, the cell pellets were collected by centrifugation from 5 mL of culture and then re-suspended in 5 mL of 25 % DMSO. The pellets were then mixed with 3 µL of Nile Red stock solution (0.15 mg/mL of Nile Red dissolved in acetone) and further incubated at 50 °C with shaking at 150 rpm for 5 min. The Nile Red stained pellets were viewed under Zeiss LSM 880 microscope. The fluorescence of the stained lipid droplets (excitation at 543 nm, emission at 555–650 nm) and autofluorescence of the chlorophyll (excitation at 405 nm, emission >650 nm) were detected.

2.3.6.2 Lipid estimation

The lipid content in the microalga and cyanobacterium biomasses was estimated by Bligh and Dyer method (1959). Briefly, a known amount of finely ground biomass was soaked in the solvent mixture of $CHCl_3$: MeOH (2:1 v/v). After 16 h of incubation, distilled water (dH_2O) was added to the sample to achieve the final solvent mixture of $CHCl_3$: MeOH: dH_2O (2:1:1 v/v). The sample was vortexed for 1 min and subsequently centrifuged at 6000 rpm for 10 min. A biphasic layer with cell debris in the upper layer and a bottom organic ($CHCl_3$) layer with lipid were obtained. The bottom layer ($CHCl_3$) containing lipid components was collected and washed with 0.9 % NaCl two to three times to remove cell residues. Subsequently, the sample was transferred into pre-weighed vail (W_i). The vials were kept in a water bath at 60 °C to evaporate the solvent.

Then, the lipid extract was dried in a desiccator using anhydrous Na_2SO_4. After dryness, the vial was weighed again (W_f). The lipid content of the sample was determined by subtracting the W_i from W_2. The lipid content was estimated gravimetrically and the percentage of lipid content was determined by using the following equation (2.4).

$$Lipid\ content\ (\%\ of\ dried\ biomass) = \frac{Lipid\ weight}{Dried\ biomass} \times 100 \quad (2.4)$$

2.3.6.3 Transesterification of fatty acid

The extracted lipid was transesterified to obtain fatty acid methyl ester (FAME) with the following method (Morrison and Smith, 1964). Briefly, 14–16 mg of extracted lipid was mixed with a 1 mL solution of BF_3–methanol (10% v/v, Sigma Aldrich). The sample was incubated at 90 °C for 30 min in a water bath. After incubation, FAME was extracted by adding 2 mL of hexane and 2 mL of water, the upper phase was recovered and the esters were evaporated to dryness under a nitrogen stream. Finally, hexane (chromatography grade) was added to obtain a final volume of 1 mL.

2.3.6.4 Gas Chromatography with Flame Ionization Detection. (GC-FID)

The FAME compositions were analyzed by the GC-FID (PerkinElmer Clarus 590). The GC-FID was equipped with a BPX-70 column (film thickness 0.25µm, and 50 m × 0.22 mm i.d.) and hydrogen was used as the carrier gas at a flow rate of 2 mL/min on split mode. The initial column temperature was set as 100 °C for zero min and gradually increased to 240 °C at a 3 °C/min rate of 10 min. The injector and FID temperatures were set at 250 °C. The FAME compositions of microalgal lipid were compared with the FAME standard (Supelco 37 component FAME mix) and literature reports.

2.3.6.5 Assessment of biodiesel properties

The biodiesel quality can be calculated from the parameters of the biodiesel with empirical equations (2.5) to (2.17) (Bagul et al., 2017; Sergeeva et al., 2017). All the parameters were calculated based on the composition and content of individual fatty acids in the biomass of the microalgae.

The degree of unsaturation (DU) was calculated with the following equation (2.5):

$$DU = \sum_{i=0}^{n} MUFA_i + \sum_{i=0}^{n} PUFA_i \quad (2.5)$$

where $MUFA_i$ and $PUFA_i$ are contents of the individual monounsaturated fatty acid and polyunsaturated in the sum of total fatty acids, respectively.

The saponification value (SV, mg KOH/ g oil) was calculated by using the following equation (2.6):

$$\text{SV} = \sum_{i=0}^{n} (560\, w_i)/M_i \quad (2.6)$$

where, w_i is the content of the individual fatty acid in the sum of total fatty acids, and M_i is the molecular weight of the fatty acid (or its methyl ester).

The iodine value (IV, g I_2/ 100 g) was calculated with the equation (2.7):

$$IV = \sum_{i=0}^{n} (254\, N\, w_i)/M_i \quad (2.7)$$

where N is the number of double bonds in the fatty acid molecule.

The cetane number (CN) was estimated with the equation [2.8]:

$$CN = \sum_{i=0}^{n} w_i\, \phi_i \quad (2.8)$$

where ϕ_i is the cetane number of the individual FAME which can be calculated with the following formula:

$$\phi_i = -7.8 + 0.302\, M_i - 20\, N$$

The long-chain saturated factors (LCSF) can be determined with the formula (2.9)

$$LCSF = 0.1\, w_{C16:0} + 0.5\, w_{C18:0} + 1\, w_{C20:0} \quad (2.9)$$

where, $w_{C16:0}$, $w_{C18:0}$ and $w_{C20:0}$ is the weight content of C16:0, C18:0 and C20:0, respectively.

The cold flow plugging properties (CFPP, °C) was calculated with the following equation (2.10):

$$CFPP = 3.1417\, LCSF - 16.477 \quad (2.10)$$

The cloud point (CP, °C) was determined with the following formula (11):

$$CP = 0.526\, w_{C16:0} - 4.99 \quad (2.11)$$

The pour point (PP, °C) was calculated with the formula (12):

$$PP = 0.571\, w_{C16:0} - 12.24 \quad (2.12)$$

The oxidative stability (OS, h) was determined with the following equation (2.13):

$$OS = 117.9295/[w_{C18:2} + w_{C18:3} + 2.5905] \quad (2.13)$$

where, $w_{C18:2}$ and $w_{C18:3}$ is the weight content of C18:2 and C18:3, respectively.

The higher heating value (HHV, MJ/kg) was calculated with the equation (2.14):

$$HHV = \sum_{i=0}^{n} w_i\, \delta_i \quad (2.14)$$

where δ_i is the higher heat value of the individual FAME obtained from the formula, $\delta_i = 46.19 - 1794/M_i - 0.21\, N$

The flash point (FP, °C) was calculated with the formula (2.15):

$$FP = 23.36\, \sum_{i=0}^{n} w_i C_i + 4.854 \sum_{i=0}^{n} w_i N_i \quad (2.15)$$

where C_i is the number of carbons of the individual FAME.

The density (ρ_i, g/cm^3) was calculated with the formula (16):

$$\rho_i = \sum_{i=0}^{n} w_i\, \rho_i \quad (2.16)$$

where $\rho_i = 0.8463 + 4.9/M_i + 0.0118\, N$

Kinematic viscosity (η, mm^2/s) was calculated with the following equation (2.17):

$$\eta = \exp(\sum_{i=0}^{n} w_i\, \ln(\eta_i)) \quad (2.17)$$

where $\ln(\eta_i) = -12.503 + 2.496\, \ln(M_i) - 0.178\, N$

2.3.6.6 High Performance Liquid Chromatography-Diod Array Detection (HPLC-DAD) for amino acids profile

The amino acid content of the biomass was determined based on the following protocol (Barnharst et al., 2021). Fifty mg of each dried and ground sample was hydrolyzed with 1.0 mL of 6.0 M HCl in a 2 mL sealed centrifuge tube at 110 °C for 24 h. Each tube was purged with pure nitrogen before hydrolysis to avoid the oxidation of certain amino acids (cysteine and methionine). The derivatization of amino acids in each sample and standards were done by 9-fluorenyl-methyl chloroformate (FMOC) and ortho-phthalaldehyde (OPA) with the autosampler (G1329A, Agilent Technologies) before injection (Sun et al., 2021). Further, the amino acids were quantified using HPLC-DAD (1200 Infinity Series, Agilent Technologies) equipped with a C18 column (4.6 × 250 mm, 3.5 µm) (Agilent Technologies). For detection, two mobile phases were used, A: 10 mM Na_2HPO_4, 10 mM $Na_2B_4O_7$, 5 mM NaN_3 with pH 8.2, and B (by volume): acetonitrile, methanol, ultra-pure water in the ratio of 4.5: 4.5: 1. The flow rate was 1.5 mL/min. The injection volume of the sample was 40 µL and the amino acids in each sample were separated within a 40 min retention time at a column temperature of 40 °C. The essential amino acid ratio (EAAR) of the sample was calculated with the following formula (2.18) (Oser, 1951). Based on the EAAR, the protein quality was evaluated.

$$EAAR = \frac{EAA}{TAA} \quad (2.18)$$

where *EAA* is the essential amino acids and *TAA* is the total amino acids.

2.3.7 EPS extraction

Since there is no particular standard protocol for EPS extraction, EPS yield could not have relied on a single extraction method. Hence, two chemical methods i.e., Methods A and B were adopted according to conditions referred by Kawaguchi and Decho, (2000) and Klock et al., (2007) with slight modifications. Method C was also carried out as a control. The production of EPS was analyzed periodically every after 4 days for 20 days of the culture growth. Here, the types of EPS produced were named according to days of culture. For instance, EPSs produced on days 4, 8, 12, 16, and 20 were represented as EPS-4, EPS-8, EPS-12, EPS-16, and EPS-20, respectively. The

EPS extraction procedures are summarized in Figure 2.4 Briefly, the cell suspension was treated with different reagents: (Method A) 0.05-mM EDTA for 30 min at 40 °C, (Method B) 4-mM EDTA with 10% NaCl for 15 min at 40 °C. In Method C (control condition), the cell suspension was treated only with distilled water for 20 min at 50 °C. In the separation step, the EPS was separated by ultracentrifugation at 4 °C at different speeds: (Method A) 12,000 rpm for 15 min and followed by precipitation with ice-cold ethanol, (Method B) 10,000 rpm for 20 min and followed by precipitation with ice-cold ethanol, (Method C) 10,000 rpm for 20 min. Furthermore, the extracted EPS was purified using a dialysis membrane (Sigma-Aldrich, USA). Finally, the EPS was lyophilized and stored at -20 °C for further characterization. The quantification of EPS was measured by subtracting weight of the empty vial and final weight of the vial with EPS divided by unit of the volume. The yield was expressed as milli gram per unit of volume. The EPS with the highest concentration was further qualitatively analyzed for biochemical compositions.

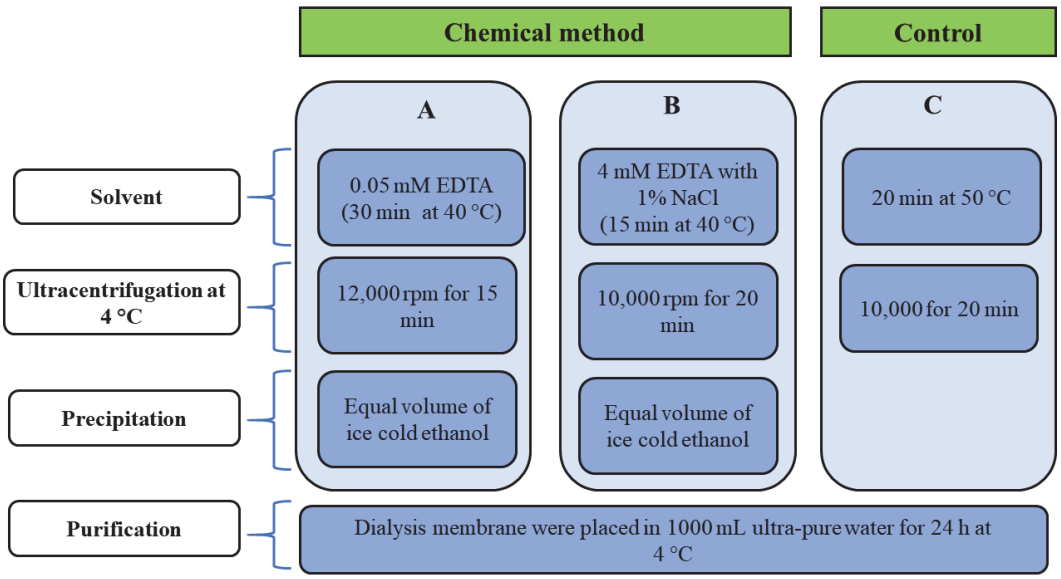

Figure 2.4: Procedures for the extraction of EPS. Chemical methods are represented as Method A and Method B while the control as Method C.

2.3.8 Evaluation of EPS productivity from the substrata

The EPS scraped from the substrata were transferred to a preweighed vial (*Wi*)and freeze-dried. The vial containing the freeze-dried EPS was reweighted (W_f). The difference between the W_f and W_i was recorded as EPS yield. The EPS productivity was calculated as EPS yield per unit of surface divided by culture duration which was presented in equation (2.19). The yield was expressed as milligram per unit of surface area by day.

$$EPS\ productivity\ (mg/m^2.d) = \frac{(W_f - W_i)}{(A_s \times d)} \quad (2.19)$$

where A_S represents the surface area of the substrata and d represents the days of the culture duration.

2.3.9 Microalgae cell harvest from the substrata

The total biofilm grown over the EPS-coated substrata was scraped off and put into a pre-weighed vial (X_i). The vial was freeze-dried and weighed (X_f). The difference in X_f and X_i represented the total biomass of the biofilm. The aerial biomass productivity of microalgal cells on the substrata was estimated by subtracting the EPS yield from the total biomass of the biofilm per surface area divided by culture age which is represented in the following equation (2.20).

$$Aerial\ biomass\ productivity\ of\ microalgae = \frac{X_f - X_i}{A_s \times d} \quad (2.20)$$

2.3.9.1 Adhesion capacity of microalgae cells on substrata

The percentage adhesion capacity is the amount of microalgal cells attached to the substrata over the total algae biomass produced in suspension which is demonstrated in Equation (2.21) (Rajendran and Hu, 2016).

$$Adhesion\ capacity\ (\%) = \left(\frac{B_b}{B_s}\right) \times 100 \quad (2.21)$$

where B_b is the microalgal biomass accumulated as a biofilm on substratum and B_s is the total biomass produced in the suspension culture condition.

2.3.10 Characterization of the chemical composition of EPS

The freeze-dried EPSs were subjected to quantitative analysis of protein, polysaccharides, and elemental composition. The following procedures have been incorporated to analyze both the quantitative and qualitative characteristics of EPS.

2.3.10.1 Total protein content

Total protein content was determined using a modified version of Lowry's technique (Lowry et al., 2000). In this method, the amino acids tyrosine and tryptophan present in the protein reduces the phosphomolybdic-phosphotungstic component of the folin-ciocalteau reagent resulting blue color.

The test sample was weighed and resuspended in SDS buffer (1%). The cell suspension was kept at -80 °C for 20 mins, thawed, and sonicated at 30 amplitudes in 10-second bursts with 25 second resting period for a total period of 30 minutes. The sample was centrifuged at 12000 rpm for 15 mins. From the supernatant 0.2 and 0.5 mL of the samples were taken for total protein estimation. The optical density of the colored solution produced during the reaction was measured at 750 nm. Bovine Serum Albumin (BSA-fraction V) was used as the standard to create a calibration curve with increments of 0, 2, 5, 10, 20, and 40 µg. The calibration curve was used to determine the protein content, which was then converted to mg of protein per gram of the sample by applying the following equation. The following equation was used to determine the percentage (%) value from the result (2.22):

$$Total\ protein\ content\ (\%) = \frac{CVD}{w} \times 100 \qquad (2.22)$$

where C is the concentration of protein obtained from the standard curve, V represents the volume of the buffer used, D is the dilution factor and w is the amount of the sample.

2.3.10.2 Sugar Analysis

The carbohydrate content was determined by following the phenol-sulphuric acid method (Dubois et al., 1956). In this method, the 2.5 N HCl was used to hydrolyze carbohydrates into simple sugars. Carbohydrates are dehydrated by reaction with strong sulfuric acid to yield furfural derivatives in this process. The interaction of furfural derivatives with phenol produces a yellow-orange color.

The test sample was weighed and resuspended in 2.5 N HCl. The sample was hydrolyzed at 100 °C for 3 h. The sample was cooled down to room temperature and neutralized with anhydrous calcium carbonate until the effervescence ceases. The solution volume was made up to 100 mL with distilled water and centrifuged at 6000 rpm for 10 min. The supernatant was collected and an aliquot of 0.2 mL was used for analysis. Before analysis, the volume was made up to 1 mL with distilled water. To this mixture 1 mL of phenol solution (5%) and 5 mL of H_2SO_4 (96%) were added and shaken well. The mixture sample was placed in a water bath (30 °C) for 20 min. After the heat treatment mixture was rapidly cooled to 4ºC. The optical density of the resultant dark green colored solution was measured at 490 nm. A calibration curve was prepared using glucose as standard at the concentration of 0.2 mg to 1 mg. The quantity of polysaccharides (sugar) present in the sample was calculated from the calibration curve using equation (2.23). The percentage (%) value was calculated from the final result as represented below.

$$Polysaccharides\ content(\%) = \frac{Carbohydrates\ yield\ from\ the\ standard\ curve}{Volume\ of\ test\ sample} \times 100 \quad (2.23)$$

2.3.10.3 HPLC for analysis of sugar

The monosaccharide composition of the EPS was further analyzed according to the method by Comte et al., (2006). Briefly, the lyophilized EPS was methanolized in 0.4-mL 2-M HCl in methanol (14 h at 85 °C). It was subsequently hydrolyzed with 2-M trifluoroacetic acid (TFA) in a sealed glass test tube (1 h at 121 °C). Before analysis, the sample was filtered through a 0.22-µm Nylon syringe filter (Axiva, India). The monosaccharide compositions of the hydrolysate were determined by HPLC (Perkin Elmer, Series 200, USA) equipped with an RI detector using a carbohydrate analysis column (Agilent Hi-Plex series, USA) and eluted with the solvent system 0.008-N H_2SO_4 at a flow rate of 0.5 mL/min.

2.3.10.4 Field emission scanning electron microscopy with energy-dispersive X-ray spectroscopy (FESEM-EDX):

The morphology of EPS was observed at a magnification of 10Kx, and the elemental composition was investigated by using a Zeiss Sigma 300 microscope (Germany) with a voltage accelerated from 1 to 20 kV.

2.3.10.5 Fourier transform infrared (FTIR)

The lyophilized EPS was ground to a powder using a mortar-pestle to identify its functional groups. One milligram of EPS powder was mixed with 180 mg of KBr and compacted to form a pellet. The transmission spectra from 4000 to 500 cm^{-1} were acquired using an FTIR spectrometer (Shimadzu IRAffinity-1, Japan). Powdered EPS samples were analyzed directly on marked glass slides through a 100× water immersion objective with an exposure time of 100 s.

2.3.11 Physiochemical characterization of substratum

Substrata that were mentioned in section 2.1.2 were evaluated for their physiochemical properties via the following methods.

2.3.11.1 Contact Angle measurement

Substrata were screened for their hydrophobicity through contact angle measurements. It was performed using Drop Shape Analyzer (KRUSS DSA25, Germany). The probe liquids used were Milli-Q water (as a polar solvent) and diiodomethane (non-polar solvent).

2.3.11.2 Atomic Force Microscopy (AFM)

The texture and topography of the surfaces were investigated by atomic force microscope (Agilent 5500 series, Model: Cypher, Oxford) on a quartz substrate in acoustic mode (non-contact) using a silicon cantilever with a force constant of 33 N/m and a resonance frequency of 304 kHz. The roughness of the substrata was analyzed by using WSxM 5.0 Develop software.

2.3.11.3 Confocal laser scanning microscopy (CLSM)

Confocal laser scanning microscopy (CLSM) was used to analyze the pattern of *Scenedesmus* cells developed within the EPS matrix. Images at discrete focal planes (z-stack) were taken using the microscope (JSM-7610F Jeol, USA). Chlorophyll within the cells was excited using an argon laser with a wavelength of 488 nm and emitted fluorescence was observed using a 505-nm long-pass filter and a 20 Kx magnification objective lens.

2.3.12 In vitro digestibility of biomass

A sequential in vitro enzymatic hydrolysis using pepsin (Pepsin 1:1,000, 1000 pepsin units per mg solids, Himedia) and pancreatin (P0636, TCI) was performed to determine the in vitro digestibility of microalgal biomass. The assay simulated the gastric and small intestine digestion of the monogastric animal and was performed as described by Sun et al. (2021).

2.3.12.1 Estimation of biomass digestibility

The following equation (2.24) was used to calculate the percentage *in vitro* dry matter digestibility (IVD in %). The IVD was calculated as the difference between the initial biomass and the undigested biomass divided by the initial biomass and multiplied by 100 as mentioned in equation (2.24) (Sun et al., 2021).

$$IVD\ (\%) = \frac{(X_i - X_r)}{X_i} \times 100 \quad (2.24)$$

where X_i represents the initial weight of the whole biomass while X_r represents the weight of residual biomass which remains undigested.

2.3.12.2 Estimation of protein digestibility of whole biomass

The protein content was determined through the Lowry method (2000). The *in vitro* protein digestibility of the biomass (IPVD %) was estimated by using equation (2.25) (Subhash et al., 2020).

$$IVPD = \frac{(P_i - P_r)}{P_i} \times 100 \quad (2.25)$$

where P_i represents the initial protein content of the biomass while P_r represents the residual protein content present in the undigested biomass.

2.3.13 Procedures for cytotoxicity test

To evaluate the cytotoxicity test, the cell extraction was performed according to the modified method of Niccolai et al., (2017). The dried cells were subjected to MilliQ water to achieve a concentration of 100 g/L (w/v). The cell suspension was sonicated at 30 amplitudes in 15 s bursts with a 40 s resting period for a total period of 30 min. Then, the sonicated sample was centrifuged at 12000 RCF for 30 min at 4 °C. After

centrifuge, the supernatant was filtered using a 0.40 µM filter to completely remove extra cell debris and the suspension was lyophilized. Subsequently, the lyophilized extract was resuspended in 500 µL of MilliQ water as a stock concentration at 200 mg/mL. Finally, using the MTT test, the cytotoxicity of various doses of extracts from *Scenedesmus* sp. DDVG I, *Limnothrix* sp. DDVG II, and co-culture (0–10 mg/mL) on BHK 21cells was assessed (Mosmann, 1983). To do this, the cells were cultured using Roswell Park Memorial Institute Medium (RPMI-1640) supplemented with 10% fetal bovine serum (FBS), and an antibiotic solution comprising 100 units/mL penicillin and 100 µg/mL streptomycin. Cultures were incubated at 37 °C in a humidified environment with 5% CO_2 and subcultured with a trypsin/EDTA solution. BHK 21 cells were seeded at a density of 5×10^4 cells per well per well in a 96-well cell culture plate with 200 L/well for cytotoxicity testing (Deniz et al., 2016). After 36 h, cells were treated 0, 0.001, 0.01, 0.1, 1 and 10 mg/mL of the extract, or Actinomycin D (500 nM) or DMSO (0.05%) in fresh treatment medium for 24 h. Actinomycin D-treated cells were considered a positive control to mark the cell cytotoxicity and cell death. The MTT was used to determine the viable cell percentage after incubation of cells with extracts for 24 h.

2.3.13.1 MTT assay

An MTT assay is a colorimetric assay to count living cells indirectly and is based on the activity of enzymes that reduce 3-(4,5-dimethylthiazol-2-yl)-2,5-diphenyltetrazolium bromide to a water-insoluble purple formazan product.
Briefly, Water insoluble formazan crystals were dissolved with 100 µL/well dimethyl sulfoxide (DMSO) and absorbance values were read with a spectrophotometer (Molecular Devices, UK) at 570 nm (with a reference filter, 690 nm). The percentage (%) viability values of cultures were calculated using the following equation (2.26) (Foo et al., 2019):

$$Cell\ viability\ (\%) = \frac{OD_{570-630}\ Treatment}{OD_{570-630}\ Control} \times 100 \qquad (2.26)$$

where OD_{570} and OD_{630} represent the optical density at 570 and 630 nm, respectively.

2.3.14 Nutrient removal efficiency

A definite volume of cultures was collected at regular intervals and subsequently centrifuged at 6000 rpm for 10 min. The supernatant was filtered through a 0.45 µm membrane and the filtrate was used for the determination of nutrients concentration. The concentration of glucose in the medium was determined through the phenol-sulphuric acid method (Dubois et al., 1956) by using D-glucose as the standard. Nitrogen, COD, TP, and TN were analyzed by using the Hach kits and the Palintest Kits. The nutrient removal efficiency was calculated with the following formula (2.27) where C_i and C_f are the initial and the final concentration of the nutrient.

$$Nutrient\ removal\ efficiency\ (\%) = \frac{(C_i - C_f)}{C_i} \times 100 \quad (2.27)$$

CHAPTER 3

Molecular identification; selection of initial pH and temperature; optimization of ideal nutrient source for highest growth and lipid yield enhancement.

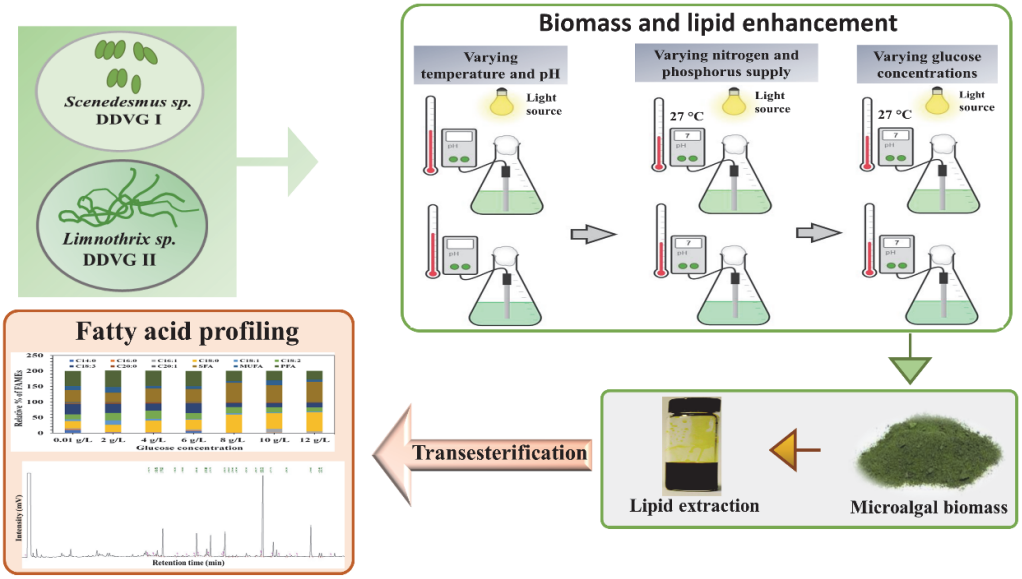

A part of this work has been published as Nongmaithem Debeni Devi, Chandan Mukherjee, Gaurav Bhatt, Lata Rangan, Vaibhav. V. Goud (2022). Co-cultivation of microalgae-cyanobacterium under various nitrogen and phosphorus regimes to concurrently improve biomass, lipid accumulation and easy harvesting. Biochemical Engineering Journal, 108706. https://doi.org/10.1016/j.bej.2022.108706

CHAPTER 3

Molecular identification; selection of initial pH and temperature; optimization of ideal nutrient source for highest growth and lipid yield enhancement.

This chapter covers microalgae identification, early growth studies, and lipid content estimation. The molecular identifications of microalga and cyanobacterium were outsourced at Eurofins Scientific India Pvt Ltd., Karnataka, India for 18S and 16S rRNA sequencing, respectively. Further, the microalgae were grown under various physicochemical conditions and optimization studies were performed for enhanced lipid accumulation.

3.1 Molecular characterization and phylogenetic placement

The novel microalga and cyanobacterium were originally isolated by our Bioenergy Group from the local waterlogged area of the IITG, Assam, India (26° 11′ N, 91° 41′ E). The partial 18S and 16S rRNA gene sequences of the microalga and cyanobacterium respectively were performed for sequence similarity. The partially sequenced data of 1024 nucleotides of DDVG I (accession no. MN630585) (https://www.ncbi.nlm.nih.gov/nuccore/MN630585.1/) and 1102 nucleotides of DDVG II (accession no. MN630310) (https://www.ncbi.nlm.nih.gov/nuccore/MN630310) were analyzed through BLAST in NCBI. According to the 18S rRNA-based NJ tree analysis (Figure 3.1a), the isolate DDVG I formed a distinct clade with different *Scenedesmus* species namely BCP-SNI 2, BCP-HAF2-VF10, FS with high bootstrap values. Likewise, from the 16S rRNA-based NJ tree analysis (Figure 3.1b), the isolate DDVG II formed a cluster with various *Limnothrix* species such as NGPC 10/37, LMECYA, 145, CHAB 751, etc. with high bootstrap values. The phylogenetic analyses of the isolates were found to have sequence similarities with the data obtained by the BLAST program and thus, the isolates were identified with high confidence values.

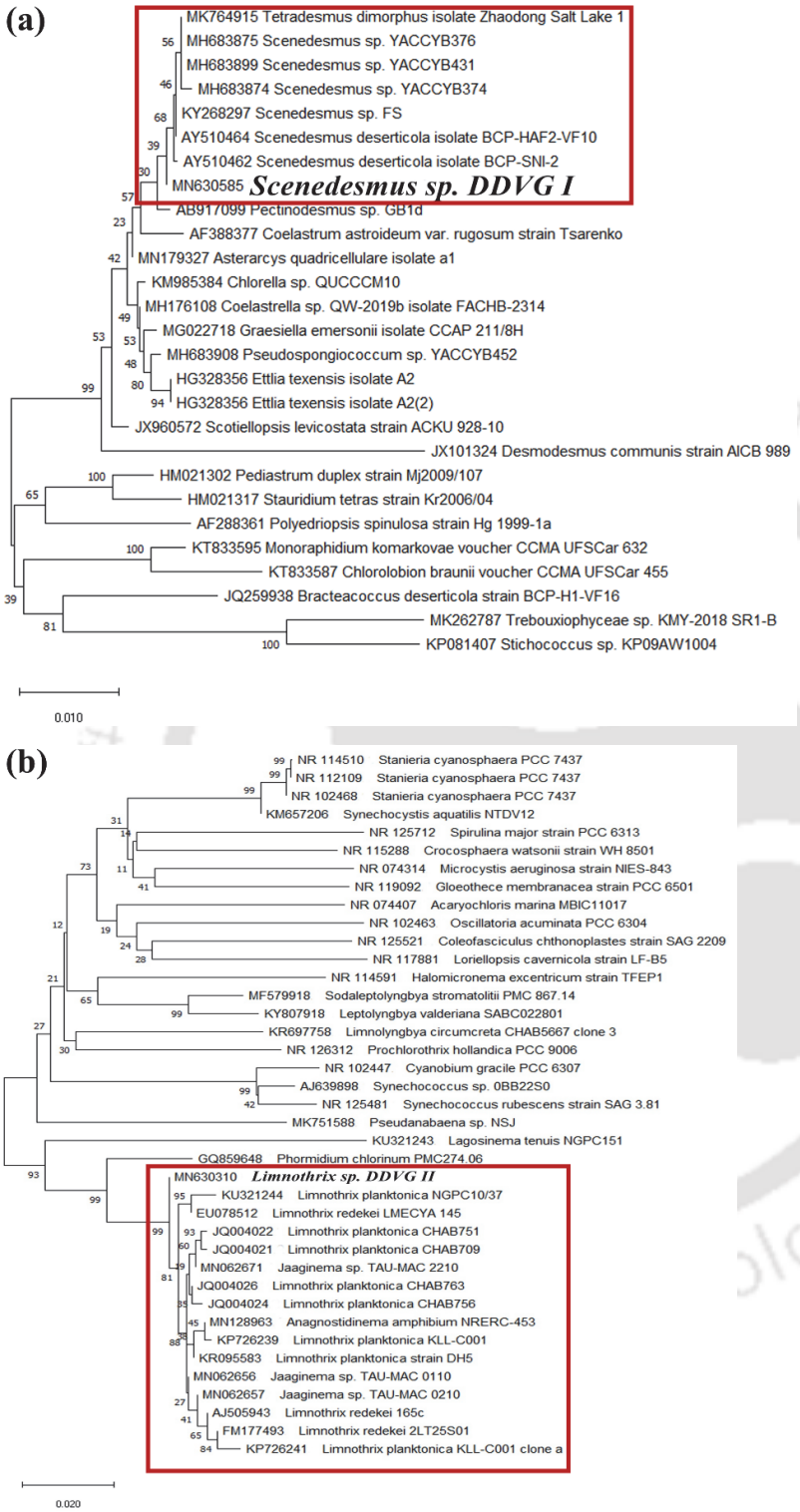

Figure 3.1: Phylogenetic tree of (a) microalga (DDVG I) and (b) cyanobacterium (DDVG II) constructed by using the Neighbor-Joining (NJ) method. The horizontal part of each segment represents the evolutionary distance among other corresponding strains.

3.2 Effect of initial pH and temperature

Results in Figure 3.2 showed that the growth behavior of both *Scenedesmus* sp. DDVG I and *Limnothrix* sp. DDVG II were significantly affected by varying pH and temperature. At a temperature of 23 °C, both the strains showed an irregular behavior of growth between pH 7 to pH 10, resulting in statistically insignificant trends (p=0.1). However, at a temperature of 27 °C and 30 °C, the cell biomasses increased steadily with increasing pH. Among all the tested pH values, the highest cell biomass for *Scenedesmus* sp. and *Limnothrix* sp. DDVG II were observed at pH 7 followed by pH 8. At a pH value of 7 and a temperature of 27 °C, the biomass concentrations of *Scenedesmus* sp. and *Limnothrix* sp. were 4.0 g/L and 1.8 g/L, respectively, with maximum specific growth rates of 0.12±0.005 d^{-1} and 0.11±0.000 d^{-1} (Table 3.1). The minimum biomass concentrations of *Scenedesmus* sp. and *Limnothrix* sp. at a pH value of 4 and a temperature of 23 °C were 1.19 g/L and 0.52 g/L, respectively, with the minimum specific growth rate of 0.05 d^{-1} after 16 days of the growth. These results indicated that an acidic pH medium and low-temperature conditions inhibit the growth of the cells. The reason may be that an acidic environment causes photosynthetic enzyme inhibition, which alters nutrient intake and hence inhibits algae growth (Loganathan et al., 2020). Similarly, Bartley et al., (2014) showed that *Nannochloropsis salina* could grow at a pH value ranging from 7-9, but optimally at a pH of 7.7. The reduction in cell growth in low or high temperatures may be caused by the cold/heat stress inducing the deactivation of enzymes and denaturation of proteins involved in photosynthesis, resulting in cell retardation (Bartley et al., 2014). Moreover, the cell growth, rate of various metabolic reactions, environmental temperature, and pH have a nonlinear relation. As temperature deviates, the balance of the rates of those reactions shifts, causing other enzyme-mediated reactions to become rate-limiting, which are then affected by enzymes with different pH optima due to different amino acid compositions in the active site, thus affecting the cell growth (Bartley et al., 2014).

Table 3.1: Effect of different pH and temperature on the specific growth of *Scenedesmus* sp. DDVG I, and *Limnothrix* sp. DDVG II.

Condition	**Specific growth rate, μ (d^{-1})**					
	***Scenedesmus* sp. DDVG I**			***Limnothrix* sp. DDVG II**		
	23 °C	**27 °C**	**30 °C**	**23 °C**	**27 °C**	**30 °C**
pH 4	0.05±0.004	0.072±0.008	0.06±0.001	0.05±0.000	0.08±0.001	0.06±0.002
pH 5	0.07±0.000	0.08±0.000	0.07±0.008	0.07±0.001	0.08±0.002	0.07±0.000
pH 6	0.08±0.005	0.09±0.005	0.08±0.005	0.08±0.003	0.09±0.001	0.08±0.001
pH 7	0.09±0.003	0.12±0.005	0.11±0.002	0.09±0.001	0.11±0.000	0.10±0.001
pH 8	0.09±0.000	0.1±0.008	0.1±0.000	0.09±0.001	0.1±0.001	0.095±0.000
pH 9	0.08±0.002	0.09±0.002	0.09±0.005	0.08±0.000	0.09±0.002	0.09±0.002
pH 10	0.07±0.01	0.08±0.005	0.08±0.000	0.07±0.002	0.09±0.001	0.08±0.002

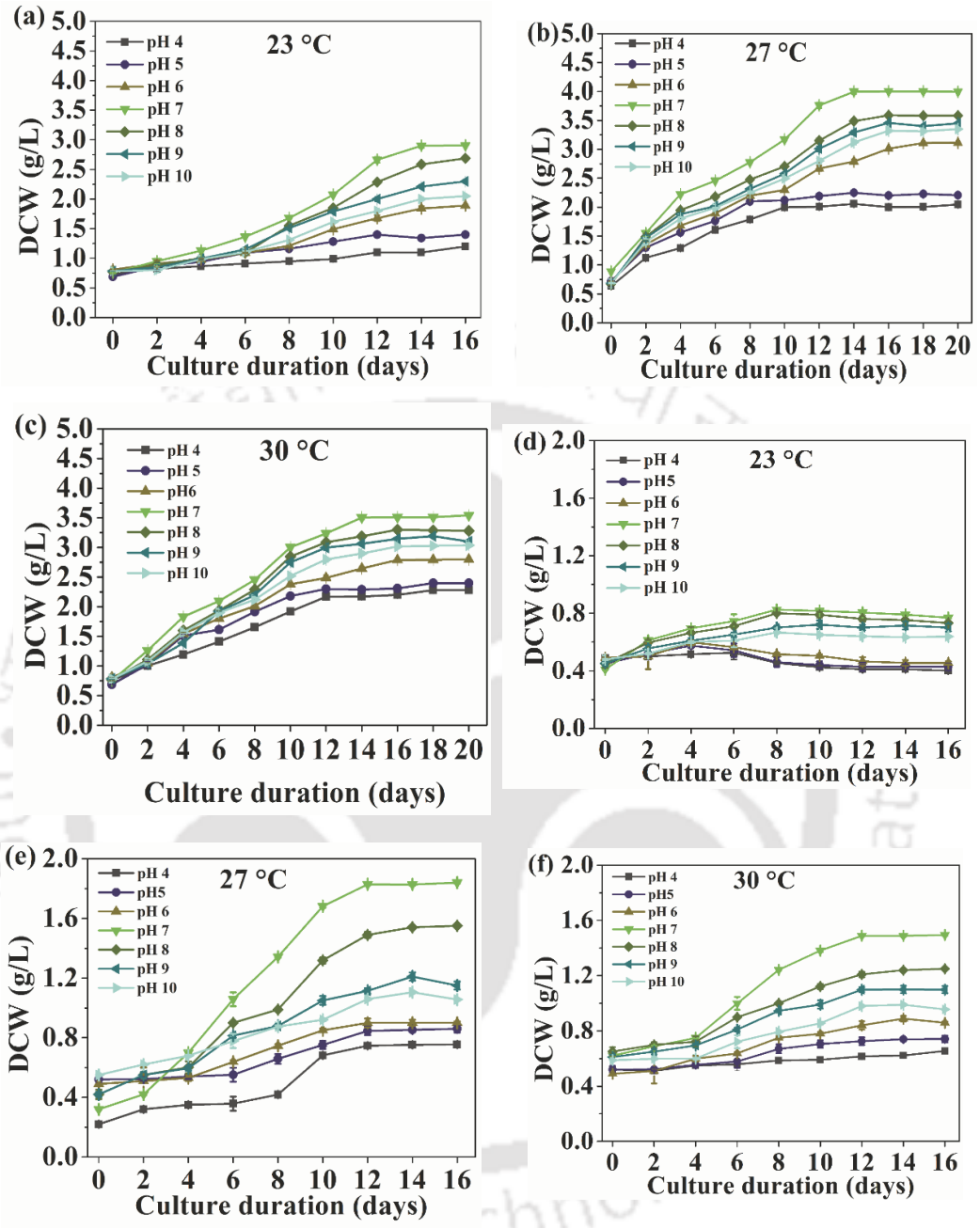

Figure 3.2: Effect of different pH and temperature on the growth: (a)-(c) *Scenedesmus* sp. DDVG I, and (d)-(f) *Limnothrix* sp. DDVG II.

The growth behavior of *Scenedesmus* sp. and *Limnothrix* sp. in different N and P supplies with the addition of glucose in the medium is presented in Figure 3.3a and Figure 3.3b, respectively. The experiment was conducted at the optimal pH value of 7 and temperature of 27 °C. The maximum biomass concentration of 4.5 g/L for

Scenedesmus sp. and 2.27 g/L for *Limnothrix* sp., were recorded with urea and K_2HPO_4 condition, followed by 4.1 g/L for *Scenedesmus* sp. and 1.9 g/L for *Limnothrix* sp. with urea & KH_2PO_4. However, the minimum biomass concentrations were recorded with NH_4Cl and KH_2PO_4 medium with the values of 0.86 g/L for *Scenedesmus* sp. and 0.67 g/L for *Limnothrix* sp. A similar study was reported by Podevin et al., (2015), stating that there was a pH drop from pH 7.5 to pH 3.7 in the culture medium containing NH_4Cl. The reason for the pH drops in NH_4Cl can be inferred from the following equations (3.1) and (3.2), which show the release of free NH_3 and H^+ (Sun and Fan, 2010). Moreover, low pH in NH_4Cl conditions inhibited growth (Dai et al., 2014). This reason could be correlated with our present study that free NH_3 directly might photodamage PSII of *Scenedesmus* sp. and *Limnothrix* sp. Moreover, as mentioned in section 3.2, low pH was unfavorable for the growth of *Scenedesmus* sp. and *Limnothrix* sp. conditions. Thus, the trend for favorable growth medium of *Scenedesmus* sp. and *Limnothrix* sp. in this study was glucose+ urea + K_2HPO_4 > glucose+ urea + KH_2PO_4 > BG11 > glucose+ NH_4Cl + K_2HPO_4 > glucose+ NH_4Cl + KH_2PO_4. Previous research on *Chlorococcum* sp. *Spirulina platensis*, and *Chlorella* sp. found similar findings, with the highest growth utilizing urea as a nitrogen source (Danesi et al., 2002; Fatini et al., 2021; Hsieh and Wu, 2009). Because each molecule of urea provides two nitrogen atoms to the cell, sodium nitrate ($NaNO_3$) and ammonium chloride (NH_4Cl) each deliver one nitrogen atom to the cell (Fatini et al., 2021).

$$NH_4Cl \leftrightarrow NH_4^+ + Cl^- \quad (3.1)$$

$$NH_4^+ \rightleftharpoons NH_3 + H^+ \rightarrow Organic - N + H^+ \quad (3.2)$$

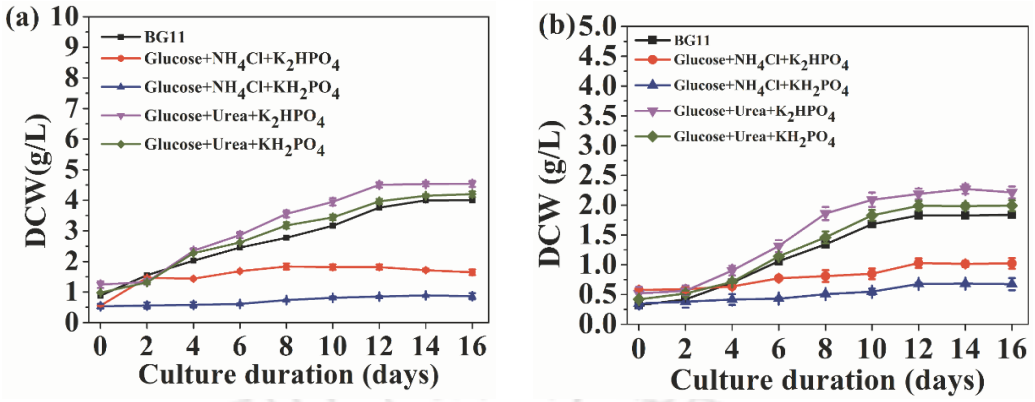

Figure 3.3: Growth behavior of (a) *Scenedesmus* sp. DDVG I and (b) *Limnothrix* sp. DDVG II with different nitrogen and phosphorus source under glucose supplementation.

Results in Figure 3.4a and Figure 3.4b showed the growth behavior and lipid content of *Scenedesmus* sp. and *Limnothrix* sp. when the glucose concentrations in the medium varied from 0.034 g/L to 12 g/L. It was observed that increase in glucose concentration from 0.034 g/L to 6 g/L ramped up the cell growth and lipid content from 3.31 g/L & 29.9 % to 8.5 g/L & 39.5 % in *Scenedesmus* sp. and 2.21 g/L &12.2 % to 3.3 g/L & 19.9 % in *Limnothrix* sp., respectively. However, further increases in glucose concentration up to 12 g/L showed an insignificant increase in cell growth and lipid content. This result was consistent with literature reports suggesting that 6 g/L of glucose was optimal for the growth of microalgae, but higher glucose concentration caused growth inhibition, attributed to substrate inhibition (Nouri et al., 2021). Some studies reported that glucose was the ideal carbon source for microalgal growth and lipid accumulation. Because, adding glucose to the culture medium activates the membrane-bound H^+- glucose symport system and promotes glucose uptake (Nouri et al., 2021). According to Patel et al., (2019), microalgae effectively utilize glucose through glycolysis, the pentose phosphate pathway, and produce acetyl-CoA from pyruvate, thus enhancing the lipid biosynthesis pathway. Additionally, during oxidative phosphorylation, the reducing equivalents ($FADH_2$ and NADPH) are created from glucose metabolism. As a result, all of the ATPs created are utilized to fuel cell growth and lipid synthesis (Nouri et al., 2021).

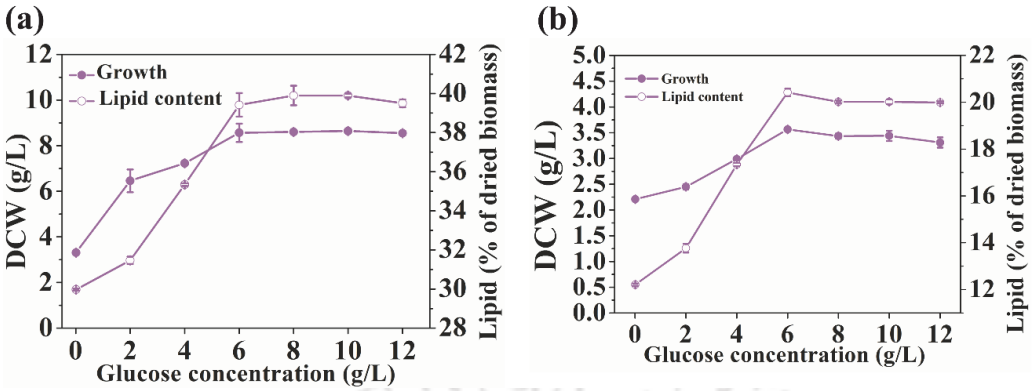

Figure 3.4: The biomass productivity and lipid content of (a) *Scenedesmus* sp. and (b) *Limnothrix* sp. were recorded after supplementation of varying glucose concentrations after 16 days of growth.

3.4 Fatty acid analysis

The viability of microalgae as a biofuel feedstock is determined by the amount of saturated and unsaturated fatty acids. Result in Figure 3.5a and Figure 3.5b illustrated the variation in FAMEs composition derived from *Scenedesmus* sp. and *Limnothrix* sp. respectively grown in different glucose concentration. In *Scenedesmus,* the fatty acids were predominant with C18:0 (22.8-57.79 %), C18:1 (1.9-14.6 %), C18:2 (13.3-23.7 %), and C18:3 (13.4-32.7 %). Moderate amount of C16:0 (0.3-3.1%), C16:1 (0.1-12.1%) and C14:0 (0.4-23.4 %) were also present in *Scenedesmus* sp. However, in *Limnothrix* sp., there was predominance of C18:0 (1.7-83 %), C18:1 (2.0-78%), C16:0 (1.7-59.3%), and C16:1 (0.2-52.95 %). Moderate amount of C18:2 (2.1-5.3 %) and C14:0 (0.4-23 %) were also present in *Limnothrix* sp. These results were consistent with the literature report showing that C14 to C18 were prevalent fatty acid components in the microalgal lipids (Devi et al., 2022; Mahesh et al., 2019). The presence of high amounts of C16:0 and C16:1 is indicated to be utilized for the production of biofuel and lubricating oils (Chiranjeevi and Mohan, 2016). Moreover, C18:0, C18:1, C18:2, and C18:3 determined the high quality of biodiesel for efficacy in engine combustion, lubrication, emulsification, and solubilization (Mahesh et al., 2019; Oliveira et al., 2020; Pandey et al., 2020). This study showed that *Scenedesmus* sp. DDVG I and *Limnothrix* sp. DDVG II could be an excellent candidate for biodiesel production.

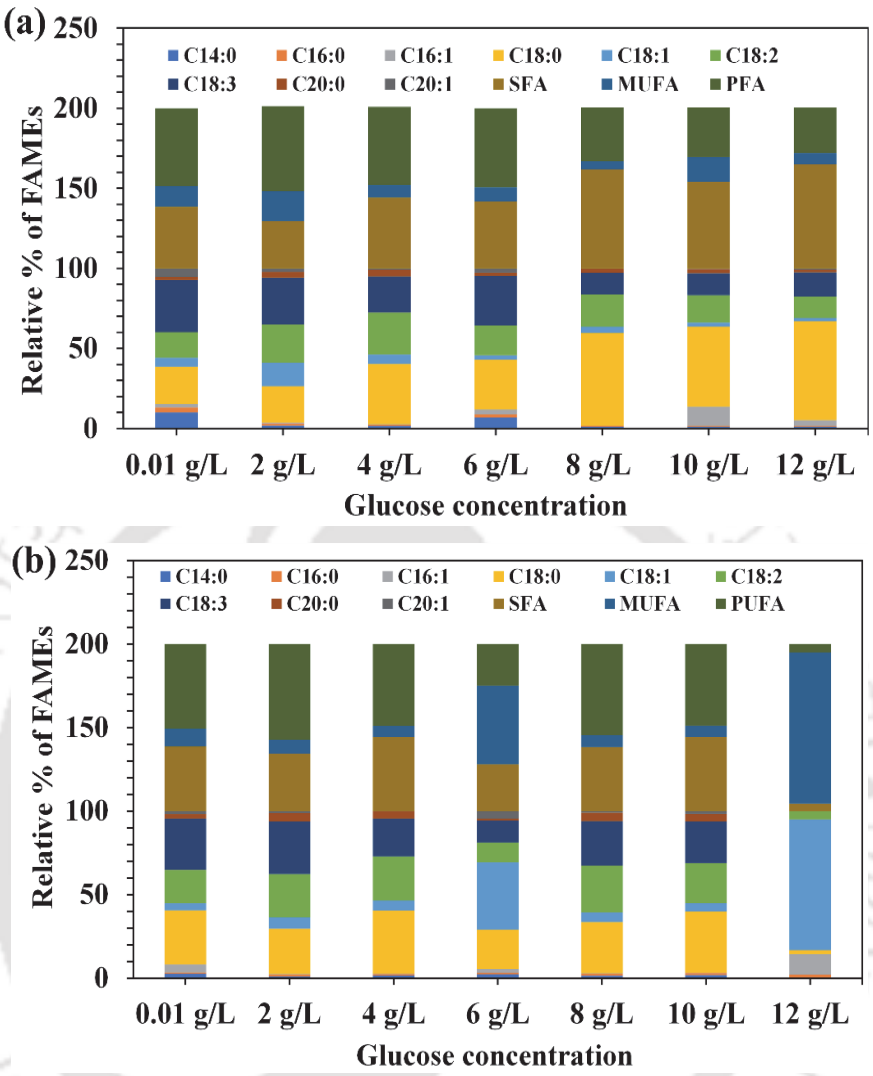

Figure 3.5: Variation in FAMEs composition of (a) *Scenedesmus* sp. and (b) *Limnothrix* sp. grown in glucose concentrations medium.

3.5 Conclusion

This chapter concludes that the freshwater microalga and cyanobacterium are DDVG I and DDVG II belong to the division *Scenedesmus* and *Limnothrix*. A growth study reveals that both the strains luxuriantly grew at a pH value of 7 in a normal BG11 medium with a specific growth rate of 0.12 d^{-1} and 0.09 d^{-1}, respectively at a temperature of 27 °C. The biomass concentration and lipid content reached up to 8.5 g/L & 39.5 % in *Scenedesmus* sp. and 3.3 g/L & 19.9 % in *Limnothrix* sp., respectively

when grown in urea, K_2HPO_4, and 6 g/L of glucose supplemented medium. The gas chromatography analysis revealed that their fatty acid profiles in *Scenedesmus* sp. and *Limnothrix* sp. were predominant in SFA and MUFA (60–90% in total FAME). This indicates that the biomasses showed their feasibility for biodiesel production.

CHAPTER 4

Characterization of biofilm/ mat via extraction of EPS and attached cultivation on different substrata

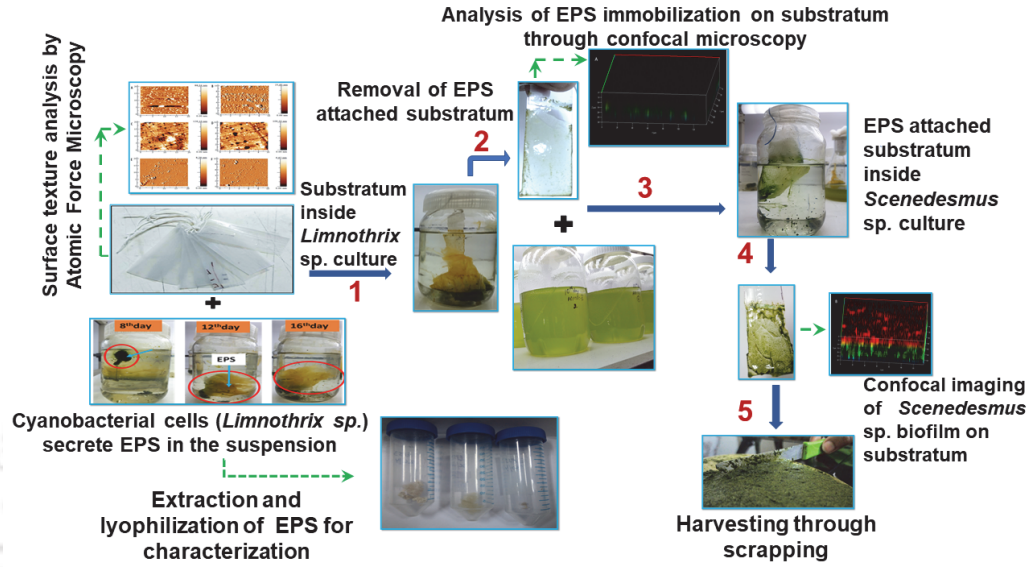

This work has been published as Nongmaithem Debeni Devi, Rahul Tiwari, Vaibhav. V. Goud, (2021). Cultivating Scenedesmus sp. on substrata coated with cyanobacterial-derived extracellular polymeric substances for enhanced biomass productivity: a novel harvesting approach. Biomass Conversion and Biorefinery, 1-13. https://doi.org/10.1007/s13399-021-01432-x.

CHAPTER 4

Characterization of biofilm/ mat via extraction of EPS and attached cultivation on different substrata

The attached cultivation system has emerged as a cost-effective approach for the cultivation of microalgae. However, few microalgae species are still restricted to grow as biofilm due to the lack of adhesive elements known as extracellular polymeric substances (EPS). The main objective of our study is to develop a novel attached cultivation strategy for EPS-lacking microalgae, Scenedesmus sp. DDVG I. We also aimed to identify cost-effective substratum showing good performance for biofilm growth. The approach was experimentally studied by conditioning a variety of substrata with EPS derived on varying days from cyanobacteria, Limnothrix sp. DDVG II. The EPS-coated substrata were used for the attached cultivation system of Scenedesmus sp. Additionally, we compared the biochemical properties of the EPS matrix derived on varying days using different extraction methods, their performance on adhesion strength, and microalgal growth. As a result, rough substrata were highly prone to the colonization of the EPS matrix than the normal one. The EPS derived from 12 days old Limnothrix sp. culture (EPS-12) showed the highest potential for adhesion strength. Rough substrata coated with EPS-12 showed the maximum growth of Scenedesmus sp. DDVG I as a biofilm. Among the rough substrata, rough polylactic acid (rPLA) sheet coated with EPS-12 was found to be the best substratum showing the highest adhesion capability of 94.60±4.2 % and the maximum aerial biomass productivity of 31.6±1.20 g/m^2. d. The results indicate that EPS-lacking Scenedesmus sp. can be cultured with the attached cultivation technique to improve its biomass productivity

4.1 Growth and EPS production

Result in Figure 4.1a shows the biomass growth curve of *Limnothrix* sp. DDVG II over a cultivation period of 24 days. *Limnothrix* sp. achieved its exponential state after day 4 where the biomass concentration increased from 0.32±0.037 g/ L to 0.69±0.05 g/ L. The maximum biomass concentration reached up to 1.82±0.06 g/ L in ten days. The culture did not show a further increase in biomass concentration after ten days which

marked the beginning of the stationary state. Meanwhile, the production of EPS and the yield were determined periodically using three different extraction methods. Results in Figure 4.1b showed that during the initial four days of *Limnothrix* sp. growth, EPS-4 concentration was very low with the yield of 1.5±0.05 mg/L (for Method A), 0.9±0.02 mg/L (Method B), and 0.72±0.00 mg/L (Method C). The EPS concentration was significantly increased ($p < 0.001$) over 12 days of growth where the culture, *Limnothrix* sp. reached an early stationary state. The yields of EPS-12 extracted using Method A, B, and C was 21.5±1.5 mg/ L, 21.0±1.1 mg/ L, and 18.1±1.0 mg/ L respectively. After day 12, there was an insignificant increase in EPS concentration. Moreno et al., (1998) demonstrated that *Anabaena* sp. could produce 17 mg/ L of EPS during the stationary phase. Likewise, Trabelsi et al., (2009) also reported that the maximum EPS yield (120 mg/ L) from *Arthrospira platensis* was obtained during the stationary phase. A study by De Philippis and Vincenzini, (1998) reported that cyanobacterial EPS are the specialized metabolites released by the organism when its growth is limited by different factors such as temperature, nitrogen concentration, or irradiance. Mainly during the late exponential or stationary phase, EPS provides a protective shield for the physiological adaptation to external changes (De Philippis and Vincenzini, 1998). On the other hand, when we quantitatively analyzed the EPS produced from *Scenedesmus* sp. DDVG I, the yield was almost negligible.

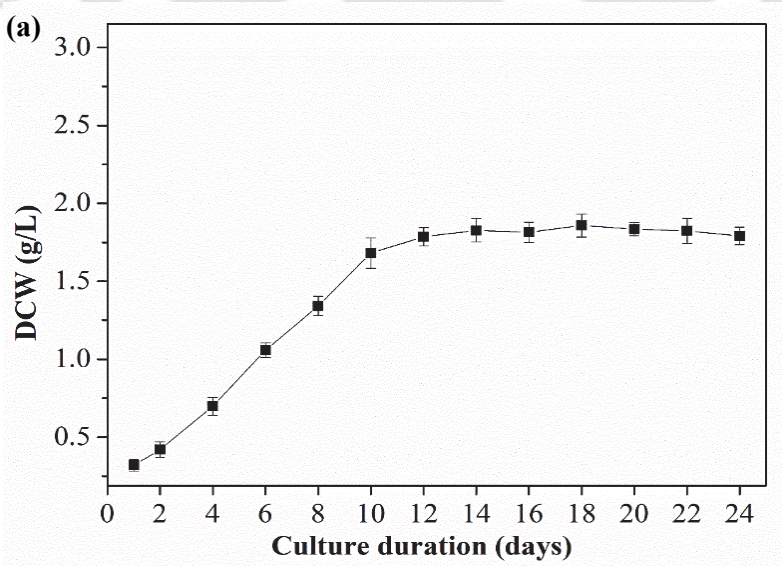

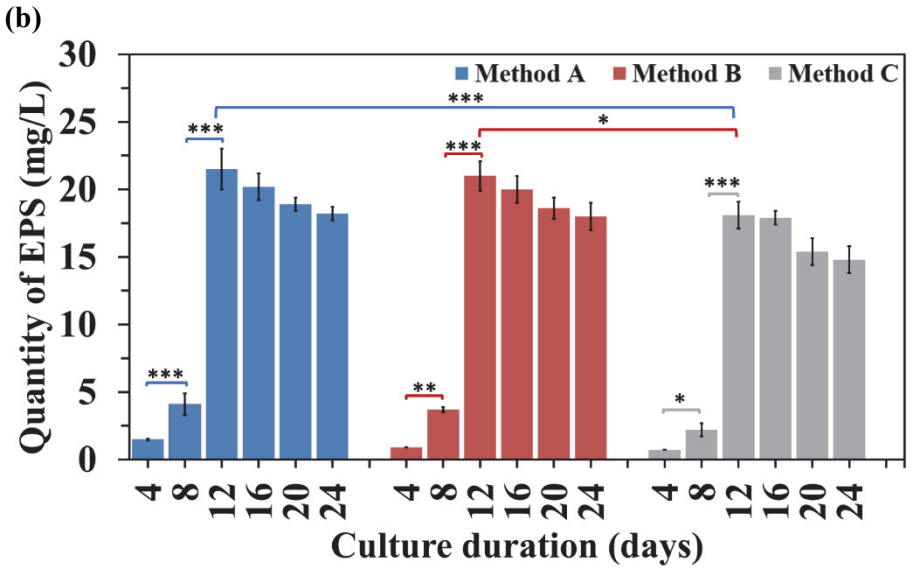

Figure 4.1: Biomass growth of (a) *Limnothrix* sp. DDVVG II (presented as mean ± standard deviation of triplicate experiments). (b) EPS yield (mg/ L) extracted during specific cultivation period of *Limnothrix* sp. DVVG II through the different extraction methods. Bars represent the average values over three replicates; error bars depict the standard error of the mean (n = 3). Data were analyzed by ANOVA and Tukey's HSD (***$p < 0.001$, **$p < 0.01$, *$p < 0.05$).

Overall, by comparing the EPS yield, we observed that the extraction methods, Method A and B were more efficient when compared with Method C (control condition). However, the yield obtained from Method A and B did not differ significantly from each other. The reason for higher extraction yield through chemical methods may be influenced by the use of chemical solvents. The metal ions such as NaCl and EDTA from the reagents, form strong interchain linkages and chelate divalent ions present within the EPS (Comte et al., 2006). They form EPS complexes that loosen EPS from cell surfaces and also reduce the strength of the EPS matrix (Liu and Fang, 2002). The motive for the addition of NaCl in Method B was that the sodium salts such as NaCl, NaOH, and CH_3COONa would increase the pH of the system. Hence, the dissociation of acidic groups in EPS would take place and cause repulsion between the negatively charged moieties. Thus, the solubility of EPS might increase in the solvent and facilitate the extraction process (Kawaguchi and Decho, 2000). Furthermore, ethanol precipitation and dialysis are common techniques for the isolation and purification of the EPS against the solvent (Underwood et al., 1995). The present study also showed

the effective isolation and purification of the polymeric fraction of EPS through ethanol precipitation in combination with dialysis.

4.2 Biochemical composition of EPS

According to Parikh and Madamwar, (2006), cyanobacterial EPS is mainly composed of heteropolysaccharides consisting of monomer units like neutral sugars (glucose, galactose, mannose, arabinose, and xylose) and at least one uronic acid. Likewise, results from Table 4.1 clearly showed the presence of polysaccharides (489.1–829.4 mg/ g) and proteins (17.45–29.36 mg/ g) abundantly in the purified EPS. While the monomer units of the polysaccharides were rich in neutral sugars specifically glucose (15.2–29.74 %), galactose (14.61–21.25 %), xylose (12.85–24.6 %), and uronic acid (0.6–2.5 %) (Table 4.1). The variations in the compositions of polysaccharides, uronic acids, and proteins in the EPS are due to the influence of centrifugation, incubation time, and the solvents (NaCl, EDTA, acetone, ethanol, etc.) (Klock et al., 2007). According to Higgins and Novak, (1997), varieties of protein moieties and hexose sugar present in the EPS matrix play a major role to signify the hydrophobic and hydrophilic behavior of EPS.

Table 4.1: Biochemical composition of EPS-12 extracted through three different methods.

Extraction method	**Dry weight of EPS (mg/ g)**		**Monosaccharide percentage of EPS (%)**			
	Proteins	Polysaccharides	Glucose	Galactose	Xylose	Glucuronic acid
Method A	29.36±1	829.43±15	29.74	21.25	24.6	2.5
Method B	27.43±1.5	779.67±10	28.89	20.5	23.74	1.8
Method C	17.45±1.1	489.10±12	15.2	14.61	12.85	0.6

4.2.1 FTIR spectroscopy

The FTIR spectra of EPS are shown in Figure 4.2 and band assignments corresponding to the IR spectra are represented per literature (Table A2 in Appendix) (Allen et al., 2004; Comte et al., 2006). The spectral band at 3750–3747 cm^{-1} attributed to the

vibrational stretching of OH- group of the polymeric compounds. The intense band at 3290–3288 cm^{-1} represents NH- stretching vibrations of amide and amine. The broad absorption peak at 2977–2950 cm^{-1} was assigned to asymmetrical stretching vibrations of C-H from an aliphatic CH_2 group, which reveals the presence of lipids and proteins. Peak intensity at 2877–2870 cm^{-1} attributed to the asymmetrical stretching of CH_3 from the lipids. The peak observed at 2380–2300 cm^{-1} could be due to the presence of -C=O- group and asymmetrical vibrational stretching of the C=N group. The asymmetrical absorption peak at 1760–1746 cm^{-1} represents the stretching vibration of C=O of esters. The intense broad peak at 1680–1670 cm^{-1} corresponds to the stretching vibration of the C-N and deformation vibration of N-H of the amide group. The peak at 1540–1523 cm^{-1} represents C-H bends and side-chain stretching of C-N of the amide group. The intense peak at 1377 cm^{-1} reveals the phosphorylated protein. The stretching of C-O-C and C-O at 1236 cm^{-1} corresponds to the presence of carbohydrates and the peak at 1125–1000 cm^{-1} confirms the presence of uronic acids (O-acetyl ester linkage bonds). Furthermore, several visible bands obtained at 1000–600 cm^{-1} correspond to the presence of phosphate and sulfur functional groups. Many studies documented that uronic acids and sulfated sugars in EPS have an affinity towards substratum and support in initial immobilization (Dubois et al., 1956). Domozych et al., (2005) reported the presence of xylose, fucose, and glucuronic acid after analyzing different functional groups in EPS of *Penium margaritaceum*. It was also confirmed that the presence of varieties of biochemical contents in EPS could aid in forming a cross-bridge between cells and the solid surface.

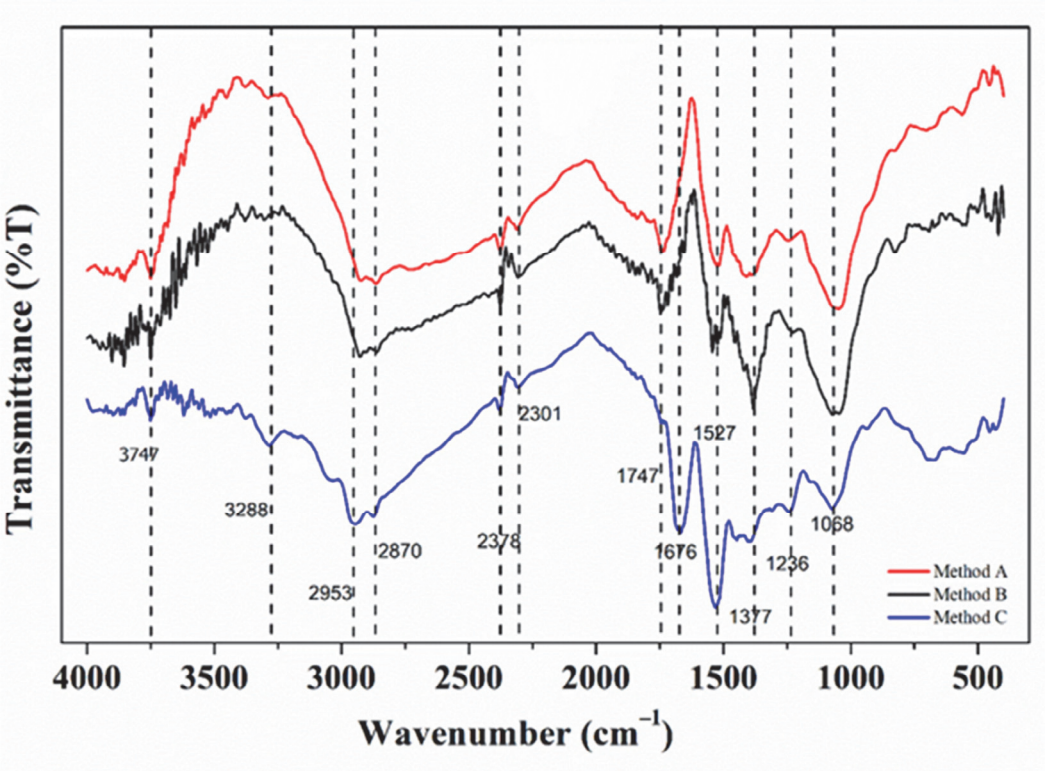

Figure 4.2: FTIR spectra of EPS extracted by Method A and Method B (chemical method) and Method C (control).

4.2.2 FESEM and EDX analysis

The morphology and the major elemental composition of EPS were analyzed through FESEM and EDX respectively. The EPS was observed as ribbon, cross-linking, and mesh-like structures because of the rich polysaccharides (Figure 4.3). The observed morphology of EPS was comparable to the typical structure of EPS obtained from cyanobacteria and bacteria (such as Gluconacetobacter xylinus) (Fang and Catchmark, 2014; Rossi and De Philippis, 2015). A high distribution of carbon (C) and oxygen (O) was detected in the EPS. A mixture of minerals such as calcium (Ca), phosphorus (P), sodium (Na), and sulfur (S) was detected in low quantities. Silicon (Si), magnesium (Mg), chloride (Cl), and other trace minerals namely sulfur (S) were also detected in the EPS (Table 4.2). According to Rossi and De Philippis, (2015), the distribution of cations such as Na and Ca in the EPS enhances its binding capacity with the negative charges of the sulfate groups. The advantage of having elements in EPS is that EPS

could provide a mini-environment by harboring these elements as mineral salt which is essential for the growth and development of microalgae (Rossi and De Philippis, 2015).

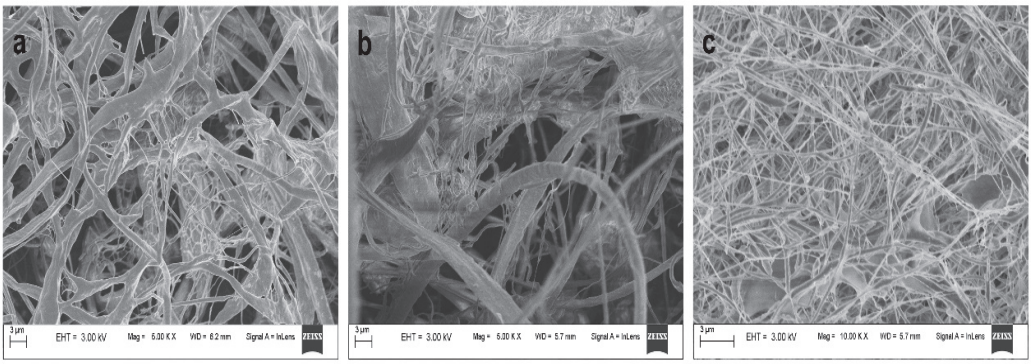

Figure 4.3: Morphology of EPS-12 extracted by (a) Methods A, (b) Method B, and (c) Method C and examined under FESEM at a magnification of 10 Kx.

Table 4.2: Major elemental composition of the extracted EPS obtained from EDX analysis.

Extraction methods	**Weight percentage (%)**						
	C	**O**	**N**	**F**	**S**	**Na**	**Ca**
Method A	65.6	32.3	0.3	0.1	0.4	0.1	1.2
Method B	64.6	27.2	6.1	0.1	0.4	0.2	0.8
Method C	64	27.1	4.8	1.1	0.3	0.3	1.4

4.3 Evaluation of the appropriate substratum

4.3.1 Surface hydrophobicity and texture

The physicochemical properties of the substrata including water and diiodomethane contact angle, the free surface energy of the substrata, and the textures are summarised in Table 4.3. The static water contact angle, θ of rPLA, PLA rGS, GS, FRP, and rFRP were measured as 53.0, 67.4, 20.7, 72, and 81.3 respectively, showing slightly hydrophilic, while, FM showed a higher θ of 122 being more hydrophobic (Arima and Iwata, 2007). Ji et al., (2014) observed that attachment of *Pseudochlorococcum* was stronger on the hydrophilic fiberglass than the hydrophobic surfaces. However, Sekar

et al., (2004) observed that hydrophobic surfaces favor higher attachment of bacterial EPS and microbial cells, which is mediated by the water exclusion mechanism. In this study, all the substrata were prone to the colonization of EPS, resulting in a significant accumulation of EPS ($p < 0.001$) (Figure 4.6). Further, the result in Table 4.3 shows the surface energy of the substrata to be in the range of 39.3–70.7 mJ/ m^2. (Gross et al., 2013) suggested that substrata like metals, plastics, and rubbers, having surface energy in the range of 20-60 mJ/ m^2 provide a site for adhesion of microalgae or cyanobacterial EPS.

Table 4.3: Physicochemical properties of the substrata.

Substratum	**Liquid contact angle (°)**		**Surface energy (mJ/ m^2)**	**Roughness (nm)**
	Water	**Diiodomethane**		
Polylactic acid (PLA)	67.4	44.8	39.3	79±21
Glass slide (GS)	32.6	47.4	65.9	7±3
Filter membrane (FM)	122	35.5	37.5	ND
Fibre-reinforced plastic (FRP)	72	45.8	43.5	50±14
Rough Polylactic acid (rPLA)	53.0	41.9	42.0	82±25
Rough Glass slide (rGS)	20.7	49.1	70.7	20±6
Rough Fibre-reinforced plastic (rFRP)	81.3	21.3	49.5	72±19

Note: ND denotes not determined. FM roughness could not be determined because of extreme roughness.

Results in Figure 4.4 demonstrates the formation of micropatterns over the substrata after modification with sandpaper grit-200 when compared to normal substrata. The surface of rPLA, PLA, and rFRP became more irregular and their roughness increased

to 82±25 nm, 79±21 nm, and 72±19 nm respectively. However, the roughness of FM was unable to be analyzed as the surface roughness was beyond the detection limit. According to Characklis et al., (1990) rough surfaces favor more attachment of EPS because of the increased convection associated with rough surfaces.

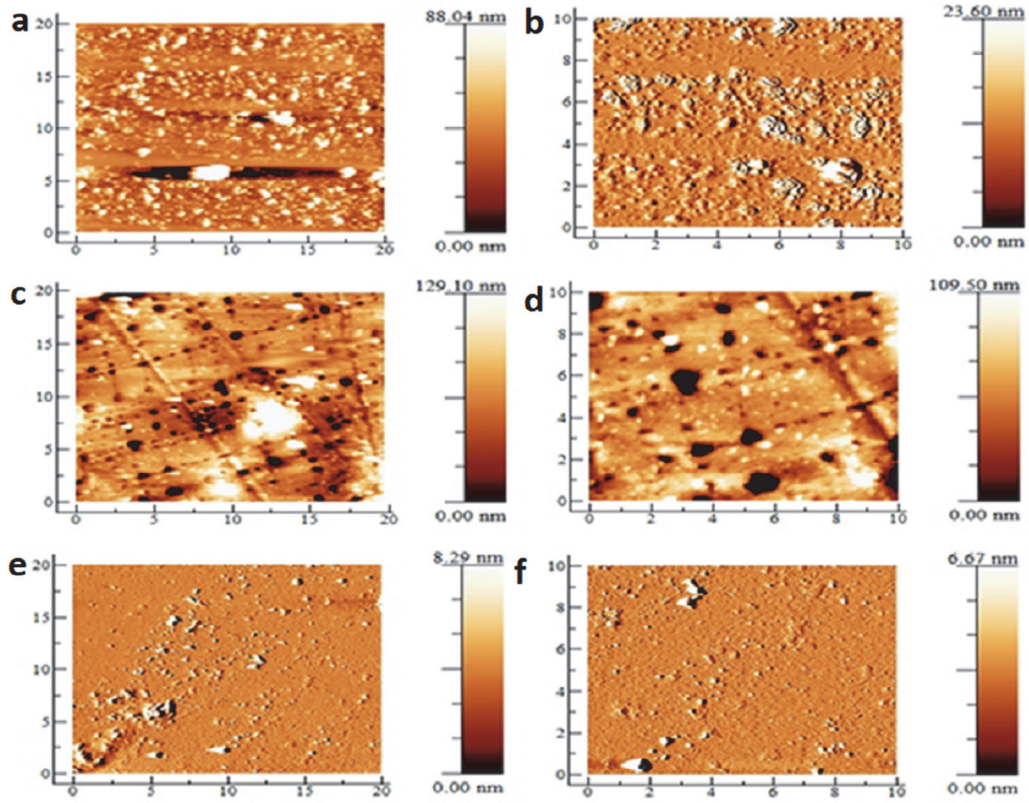

Figure 4.4: AFM analysis of (a) PLA, (b) rPLA, (c) FRP, (d) rFRP, (e) GS, and (f) rGS.

4.4 Effect of substrata on EPS adhesion

The substrata immobilized with EPS derived on different culture periods represented as EPS-4, EPS-8, EPS-12, EPS-16, and EPS-20. The EPS secreted during the initial four days i.e., EPS-4 of *Limnothrix* sp. growth poorly immobilized on the substrata that the aerial EPS yield was negligible. The substratum was covered with a thin film of EPS-12 significantly ($p < 0.001$) over the 12 days (as illustrated in Figure 4.5 and Figure 4.6). Among the substrata, the rough substrata showed higher adhesion for EPS-12 than the normal one. rPLA with EPS-12 showed the highest aerial EPS yield

(2.25±0.02 g/m^2. d) followed by rFRP (2.24±0.02 g/m^2. d), rGS (2.08±0.04 g/m^2. d) and FM (2.01±0.1 g/m$^{2.}$ d). Figure 4.5a also confirmed the proper immobilization of EPS-12 on the rPLA with a thickness of ~2 µm. However, all the substrata showed an insignificant increase ($p > 0.3$) in coverage of aerial yield of EPS-14, EPS- 16, and EPS-20 over twenty days of operation. Overall, the findings showed that rough substrata were ideal for adhesion (Figure 4.6). Gross et al., (2016) found a rough surface to be more suitable for biofilm formation than normal substrata. Characklis et al., (1990) found the increased biofilm formation on rough surfaces due to the increase in the surface area for the attachment. Moreover, we observed that EPS-12 produced during the early stationary phase of the culture showed good adhesion strength on substrata. We have discussed earlier in the previous section 4.2 about the correlation between the biochemical composition of EPS and its adhesion properties. Characklis et al., (1990) reported the deterioration in adhesion strength of EPS with an increase in culture age.

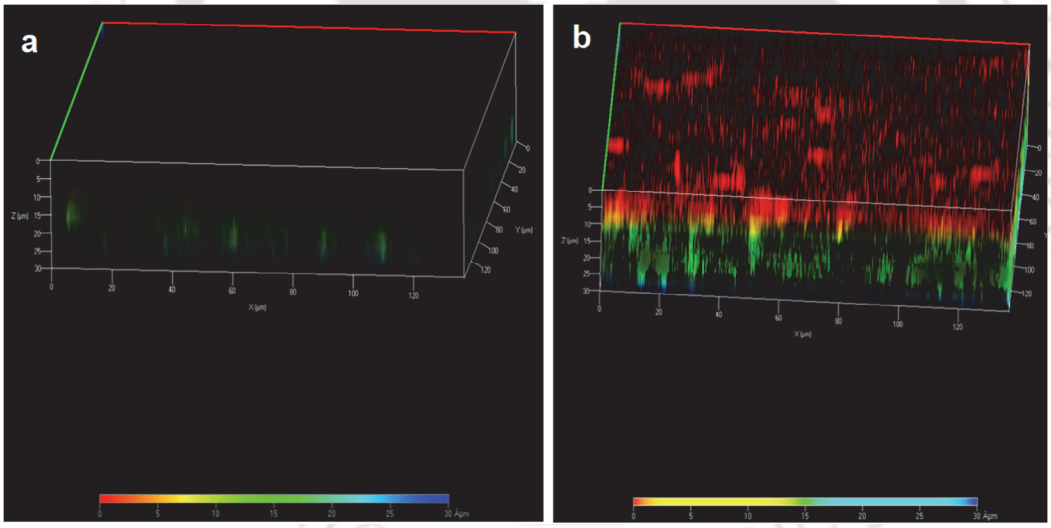

Figure 4.5: Confocal Z-stack images. (a) EPS colonization on rPLA with a thickness of ~2 µm. (b) Accumulation of *Scenedesmus* cells on rPLA with EPS-12. Red fluorescence is emitted from the chlorophyll content of algal biomass that is distributed over the rPLA with a thickness of ~10 µm (excitation and emission wavelength of 488 and 505 nm, respectively).

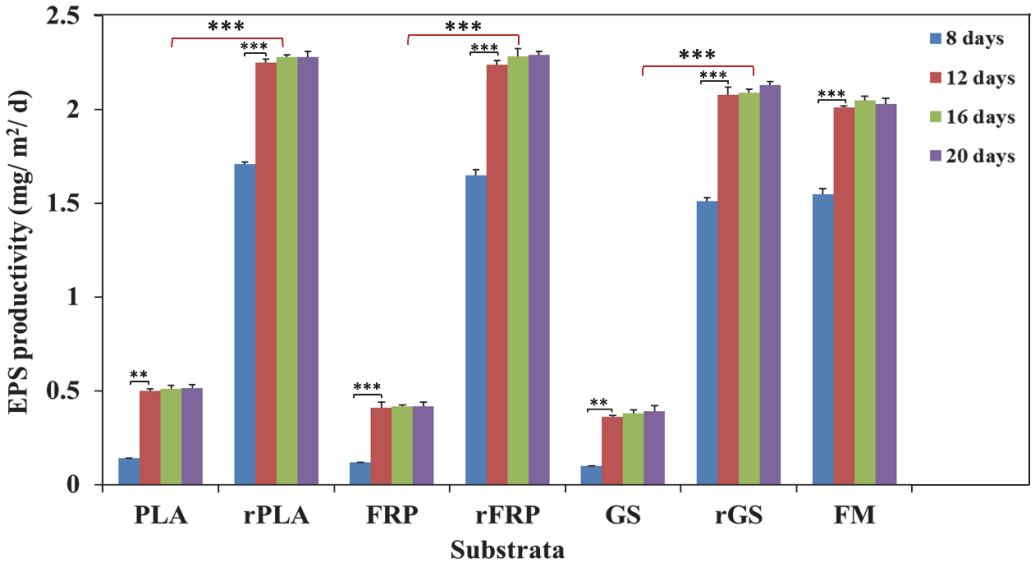

Figure 4.6: Aerial EPS productivity (mg/m^2. d) developed on different substrata due to adhesion of EPS produced from *Limnothrix* sp. over 20 days of the culture growth. Bars represent the average values over three replicates; error bars depict the standard error of the mean (n = 3). Data were analyzed by ANOVA and Tukey's HSD (***p < 0.001, **p < 0.01, *p < 0.05).

4.5 Microalgal accumulation on substrata

Results in Table 4.4 show that rough substrata coated with EPS-12 exhibit a high adhesion rate of *Scenedesmus* cells. The accumulation of *Scenedesmus* cells on different substrata is also illustrated in Figure A1in Appendix. Among the substrata, rPLA with EPS-12 showed the highest adhesion capacity (94.6±4.2 %) for microalgae accumulation with maximum biomass productivity of 31.6±1.2 g/m^2. d ($p< 0.001$). The pattern of biomass accumulated over rPLA coated with EPS-12 was observed through confocal microscopy. In Figure 4.5b, we observe red fluorescence with a thickness of ~10 µm developed over the substratum. The red fluorescence was emitted by the chlorophyll content of the microalgal biomass, which showed the proper accumulation of cells. EPS-12 coated rFRP, rGS and FM showed the adhesion capacity of 87.6±2.8 %, 79.28±2.8 %, 88.9±2.2 % respectively, and achieved algal biomass productivity of 30.9±1.20 g/m^2. d, 29.8±1.10 g/m^2. d and 27.6±0.90 g/m^2. d respectively. However, all the substrata without EPS showed a negligible amount of *Scenedesmus* sp. cell

accumulation. The adhesion capacity as well as the biomass productivity for the substrata without EPS were significantly very low ($p < 0.0001$). Even the aerial biomass productivity accumulated over rPLA with EPS-4 was higher (1.20±0.02 g/m^2. d) significantly ($p < 0.02$) when compared with aerial biomass productivity (0.90±0.00 g/m^2. d) over rPLA without EPS. (Table 4.4). This suggested that the presence of EPS as a film on substrata induced the microalgal attachment. It was also confirmed that *Scenedesmus* sp. DDVG I is a type of species that does not secrete its EPS but it somehow can grow on substrata with the aid of EPS derived from other sources. In suspension cultivation, *Scenedesmus* sp. cells did not show adhesion even on the jam bottles over 20 days of cultivation. The culture in the suspension medium took more than 36 h to settle down. Hence, the biomass was harvested through centrifugation, resulting in biomass productivity of 22±1.01 g/L. d. According to documented literature, the adhesion strength of EPS is not dependent on the quantity of EPS; rather, the age of EPS and its varieties of biochemical composition play a major role in the adhesion of EPS (Ohashi and Harada, 1996). In another study, Wagner et al., (2009) reported that with increasing EPS age, the chemical diversity of EPS changes tremendously. The mesh-like inter-crossed structure of EPS provides the sites for entrapment of microalgae cells, and thereby biomass accumulation occurs. In this study, 12 days old EPS showed the highest potential of microalgae adhesion. However, some studies reported that the EPS content does not influence adhesion (Flemming et al., 2007). There is no good reason to believe that adhesive properties and the attraction of microbial cells are related. These conflicting results may be explained by the complexity of EPS and its structure (Ahimou et al., 2007). Overall, rPLA would be ideal for attached cultivation and its performance is also compared with the documented literature reports in Table 4.5.

Table 4.4: Percentage adhesion capacity of *Scenedesmus* sp. DDVG I on different types of substrata which were attached with different duration of EPS and without EPS and its biomass productivity being scrapped off after 20 days.

Substratum	Nature of substratum	Percentage adhesion capacity (%)	Biomass productivity (g/m^2. d)
PLA	Without EPS	0.01±0.00	0.20±0.00
	EPS-4	0.09±0.00	0.13±0.00
	EPS-8	27.21±1.4	1.47±0.01
	EPS-12	63.5±1.70	18.5±0.02
	EPS-16	58.9±1.20	17.4±0.02
	EPS-20	41.5±1.40	16.7±0.08
rPLA	Without EPS	0.19±0.01	0.90±0.00
	EPS-4	9.40±0.09	1.20±0.02
	EPS-8	44.30±2.1	10.5±0.20
	EPS-12	94.60±4.2	31.6±1.20
	EPS-16	82.10±2.1	30.5±1.80
	EPS-20	55.4±3.20	29.9±0.90
FRP	Without EPS	0.06±0.00	0.15±0.00
	EPS-4	0.07±0.00	0.12±0.00
	EPS-8	26.4±1.10	1.04±0.00
	EPS-12	62.9±1.60	17.9±1.50
	EPS-16	55.1±1.40	16.5±1.10
	EPS-20	42.0±1.30	15.7±1.20
rFRP	Without EPS	0.17±0.00	0.70±0.01
	EPS-4	7.60±0.07	1.18±0.00
	EPS-8	43.8±2.30	9.90±0.02
	EPS-12	87.6±2.80	30.9±1.20
	EPS-16	82.5±2.50	29.1±1.10
	EPS-20	52.0±2.20	28.4±1.10

GS	Without EPS	0.05±0.00	0.10±0.00
	EPS-4	0.06±0.00	0.70±0.00
	EPS-8	26.1±1.70	0.90±0.00
	EPS-12	61.5±1.90	16.5±0.60
	EPS-16	56.1±1.60	15.2±0.60
	EPS-20	33.5±1.60	13.5±0.20
rGS	Without EPS	0.16±0.00	0.60±0.00
	EPS-4	6.8±0.070	0.05±0.00
	EPS-8	41.2±1.80	9.50±0.00
	EPS-12	79.0±2.80	29.8±1.10
	EPS-16	77.6±2.40	27.6±1.10
	EPS-20	48.5±1.90	25.8±1.30
FM	Without EPS	0.17±0.00	0.60±0.00
	EPS-4	7.75±0.09	0.90±0.00
	EPS-8	40.5±2.30	8.72±0.05
	EPS-12	88.9±2.20	27.6±0.90
	EPS-16	65.7±2.20	26.8±1.00
	EPS-20	33.2±1.80	26.2±1.20

(*continued)*

Table 4.5: Attached cultivation system of microalgae.

Microalgae species	**Types of substrata**	**Biomass productivity (g/m^2. d)**	**Reference**
Scenedesmus sp. DDVG I	Rough polylactic acid (PLA sheet) with EPS	31.6 ± 1.20	This study
Tribonema minus	Non-woven fabric	9.73 ± 2.19	(Roostaei et al., 2018)
Chlorella sp.	Polystyrene foam	25.65	(Zhang et al., 2020)
Algal-bacterial consortium	Cotton cord	20–31	(Tsavatopoulou et al., 2019)
Chlorococcum sp.	Glass fiber-reinforced plastic	4.26	(Kawaguchi and Decho, 2000)
Chlorella vulgaris UTEX #265	Cotton duct	7	(Allen et al., 2004)
Microalgae-bacteria consortium	Acrylic, cellulose acetate, glass, cellulose polycarbonate, polystyrene, and silicone rubber	1.10–2.08	(Yuan et al., 2019)

4.6 Conclusions

This chapter demonstrated the possibilities of growing non-adhesive microalga as a biofilm on substrata coated with EPS. The study reported an inclusive study for the extraction of EPS during different stages of cyanobacterial growth and the effect of the physicochemical properties on the initial colonization. Chemical extraction was found to be a good method for quantitative and qualitative analysis of EPS. Rough substrata showed to be effective for the adhesion of EPS. Among them, rPLA coated with EPS-12 showed the maximum algal accumulation of 31.6±1.2 g/m^2. d. For scaling up the system, we should need emphasis the total cost. The total capital cost for all the substrata in this study did not exceed $30. They are easily available in the local market. Moreover, the substrata can be either reused several times after scrapping off the biofilm. The results indicated that *Limnothrix* sp. would be a potential candidate to improve biomass harvesting of suspended *Scenedesmus* sp.

CHAPTER 5

Co-cultivation of microalgae and cyanobacteria in a balanced ratio of nitrogen and phosphorus in a synthetic medium for efficient harvesting, biomass productivity, and lipid content

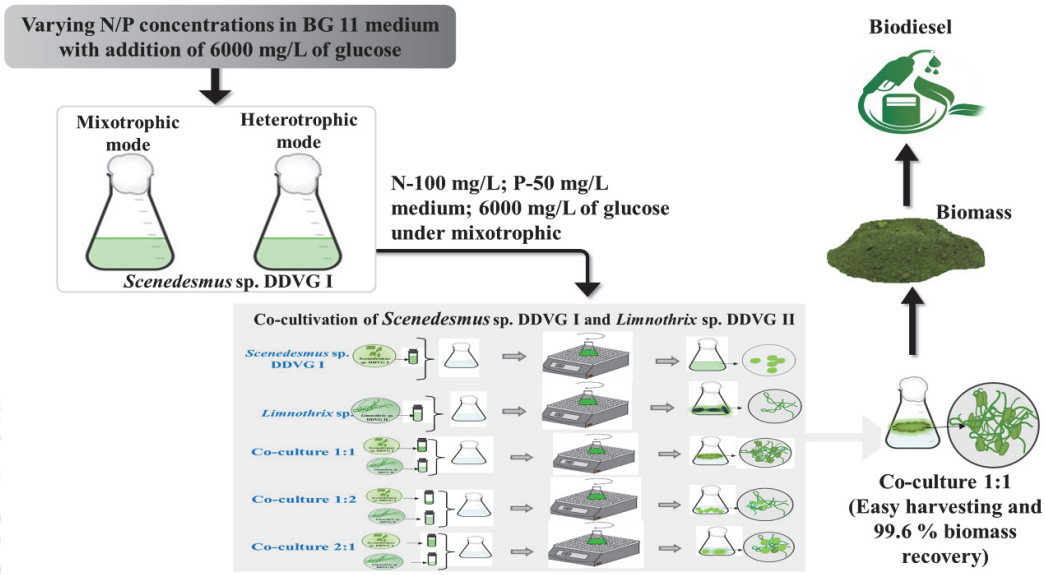

This work has been published as Nongmaithem Debeni Devi, Chandan Mukherjee, Gaurav Bhatt, Lata Rangan, Vaibhav. V. Goud (2022). Co-cultivation of microalgae-cyanobacterium under various nitrogen and phosphorus regimes to concurrently improve biomass, lipid accumulation and easy harvesting. Biochemical Engineering Journal, 108706. https://doi.org/10.1016/j.bej.2022.108706.

CHAPTER 5

Co-cultivation of microalgae and cyanobacteria in a balanced ratio of nitrogen and phosphorus in a synthetic medium for efficient harvesting, biomass productivity, and lipid content

Due to due to high-cost harvesting method, low biomass productivity (BP), and lipid yield (LY), commercialization of microalgae biomass is still impeded. Some researchers discovered that the combined effects of low nitrogen (N) and high phosphorus (P) resulted to an increase in biomass and lipid production. However, the choice of a balanced N:P ratio is still ambiguous between microalgal species and is up for debate. Here, we set various ranges of N:P ratios from 2:1 to 44.11:1 with the addition of glucose in the BG 11 medium to examine its influence on the growth of microalgae. The investigation was performed by subjecting a novel strain, Scenedesmus sp. DDVG I to these various mediums under heterotrophic and mixotrophic modes. The N:P of 100:50 or N-deficient P-over excessive (N_{def} P_{oexcs}) condition under mixotrophic mode had the highest growth rate of 0.15 d-1±0.01, with a maximum BP and LY of 41.1±0.5 mg/L. d and 39.1±1.1 % dry cell weight (DCW), respectively. Further, in attempting to facilitate the harvesting step, we co-cultured Scenedesmus sp. with Limnothrix sp. DDVG II mixotrophically under inoculum ratio of 1:1, 1:2, 2:1 in the N_{def} P_{oexcs} condition. The co-culture 1:1 system achieved the maximum biomass harvesting efficiency of 99.6±0.3 % with an increase in BP and LY up to 42.0±1.0 mg/L. d and 40.2±1.0 % DCW, respectively. The fatty acid methyl ester compositions of co-culture 1:1 was rich in C18:2 (36.05 %), C16:0 (32.25 %), C18:1 (16.86 %), and C18:0 (7.68 %). The biodiesel derived from the co-culture 1:1 also complied with standard specifications, making it appropriate for the production of biodiesel. The overall findings demonstrated a unique co-culture approach toward easy harvesting while concurrently maximizing biomass and lipid yield when grown in a balanced N:P ratio of 100:50. The techno-economic analysis of the system, biodiesel cost, and its implementation toward biorefinery approach can be envisaged in the future study.

5.1 Effect of N and P on biomass concentration, its productivity, and lipid content

To amalgamate biomass and lipid production, the concurrent effect of N and P with the addition of 6000 mg/L of glucose was studied in a single-step process. Urea and K_2HPO_4 were used as nitrogen and phosphorus supply. The growth behavior of *Scenedesmus* sp. DDVG I over 16 days of cultivation period under heterotrophic and mixotrophic modes is shown in Figure. 5.1 The growth of *Scenedesmus* sp. DDVG I was greatly influenced by different N and P regimes and cultivation modes. As evident from Figure 5.1a, the DCW of *Scenedesmus* sp. DDVG I was 1.15-fold higher in the N_s P_s condition under mixotrophic mode as compared to that of normal BG 11 medium. The increase in growth under mixotrophic glucose supplementation might be attributed to the production of reduced equivalents ($FADH_2$ and NADPH) during oxidative phosphorylation from glucose metabolism. Consequently, every ATP produced is used to drive cell growth and lipid synthesis (Gim et al., 2016). The favorable mixotrophic growth of *Scenedesmus* sp. DDVG I in the N_s P_s condition was correlated with the increase in Chl-a concentration which reached up to 4.40 ± 0.02 mg/L after 16 days of cultivation (Figure 5.1b). However, as shown in Figure 5.1c, *Scenedesmus* sp. DDVG I growth was almost linear under heterotrophic mode. The reduction in the cell growth in heterotrophic cells was consistent with the decrease in the Chl-a concentration due to the chlorosis condition (Figure 5.1d). Moreover, the corresponding biomass productivity and lipid content in the heterotrophic mode was reduced significantly to 22.1 ± 0.6 mg/L. d and 21.5 ± 0.7 % DCW, respectively. In a study by Li et al., (2020), the mixotrophic growth of *Asterarcys* sp. resulted in 18.5-fold higher biomass production when compared to heterotrophic growth. Similarly, Bhatnagar et al., (2011) reported that mixotrophic growth of *Scenedesmus bijuga*, *Chlorella minutissima,* and *Chlamydomonas globosa* produced 3–10 times more biomass than phototrophic growth conditions. The superior growth under the mixotrophic mode was mainly due to the capability to achieve substantial energy from both the light source and organic nutrients, resulting in enhanced cell growth (Sajjadi et al., 2018). However, microalgae species such as *T. obliquus* (Caprio et al., 2019), *Tetraselmis suecica* (Azma et al., 2011), *Acutodesmus obliquus* (Kim et al., 2016), *Haematococcus pluvialis* (Kang et al., 2006)

showed favorable growth in heterotrophic mode with simultaneous removal of nitrogen and phosphorus from the growth medium. Nevertheless, not all strains of microalgae can be sustained in total darkness (Tan et al., 2021). This experiment showed that *Scenedesmus* sp. DDVG I could adapt to an environment in which glucose is the source of organic carbon while being cultured in both light and dark conditions.

Results in Figure 5.1a and Figure 5.1b showed that the cell growth of *Scenedesmus* sp. in N_s P_{mexcs} was almost linear, achieving DCW of 2.95±0.01 g/ L and Chl-a concentration of 2.16±0.2 mg/L during 16 days of cultivation. However, in the N_{def} P_{mexcs} condition, the biomass production of *Scenedesmus* sp. reached up to 4.4±0.01 g/L. The maximum biomass production was recorded in the N_{def} P_{oexcs} condition with DCW of 10.25±0.14 g/L, followed by 5.84±0.17 g/L for N_{def} P_{excs}, and 4.77±0.15 g/L for N_{def} P_{mexcs}. The corresponding specific growth rates and biomass productivities were 0.15 d^{-1} & 41.1±0.5 mg/ L. d for N_{def} P_{oexcs}, 0.13 d^{-1} & 39.5±0.2 mg/L. d for N_{def} P_{excs} and 0.103 d^{-1} & 37±1.2 mg/L. d for N_{def} P_{mexcs} respectively (Table 5.1). These findings were similar to those by (Fu et al., 2017), who reported that *Chlorella regularis* showed higher biomass productivity of 0.72 g/L. d in limited N and excess P condition when compared to the biomass productivity of 0.48 g/L. d in limited N and adequate P condition. Their study also found the upregulation of certain genes such as CYP735A, BAS1, and ROT3 under nitrogen-deficient and abundant-phosphorus conditions. These genes encode enzymes such as zeatin and brassinosteroid that are involved in carbon and amino acid metabolism, carbon fixation, and hormone regulation, cell division during N and P stress conditions (Boelee et al., 2014b). Besides, microalgal cells also convert and store the excessive P as Poly-P inside the cells which serve as storage energy during the anabolism of DNA, RNA, and protein in stress conditions for cell growth (Harold, 1966).

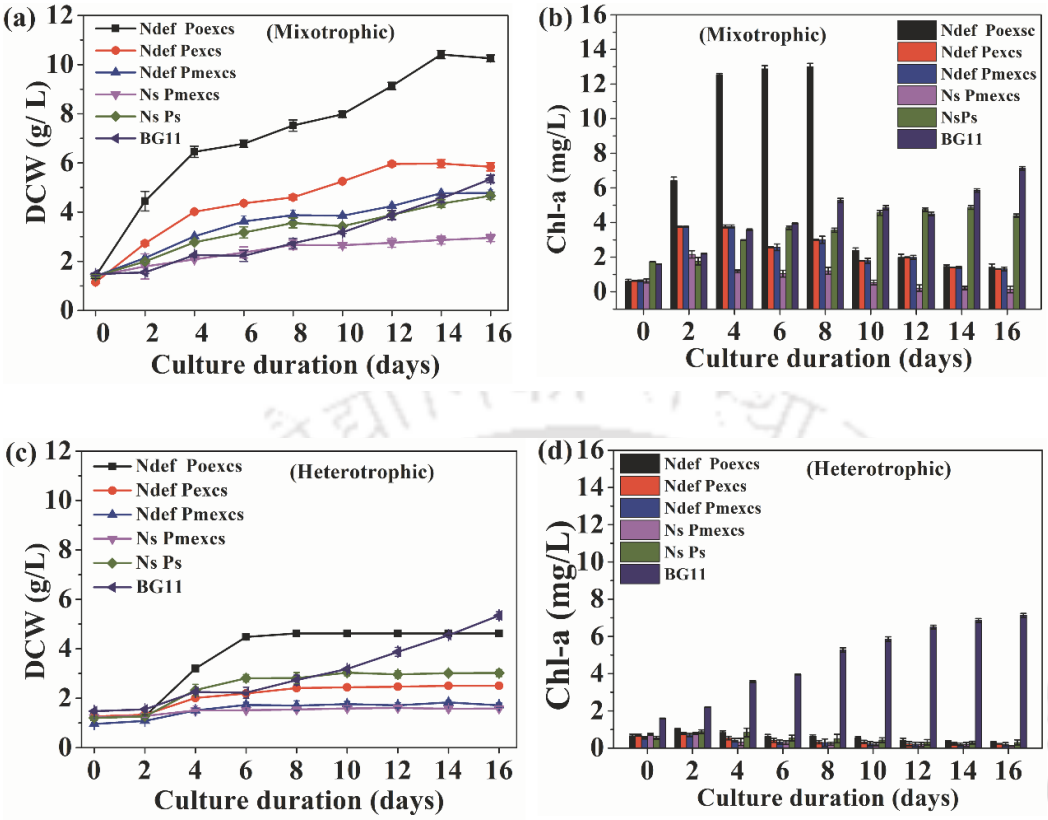

Figure 5.1: (a) Mixotrophic growth profiles, and (b) Chl-a concentration of *Scenedesmus* sp. DDVG I grown in different nitrogen and phosphorus concentration conditions over 16 days culture period. (c) Heterotrophic growth profiles, and (d) Chl-a concentration of *Scenedesmus* sp. DDVG I respectively in different nitrogen and phosphorus concentration conditions over 16 days culture period.

Results in Figure 5.1b showed that Chl-a concentration in all the N deficient conditions initially increased and decreased abruptly at the end of 16 days of cultivation. The Chl-a concentration in N_{def} P_{oexcs} was maximum on day 8 with the value of 12.9±0.2 mg/ L which decreased rapidly to 1.41±0.19 mg/ L on the 16th day. A similar trend was observed in N_{def} P_{excs} and N_{def} P_{mexcs} conditions, achieving Chl-a concentrations of 3.1±0.02 mg/ L and 3.0±0.2 mg/L during 8-day and declining abruptly to 1.31±0.01 and 1.30±0.01 mg/L respectively after day-16. This decrease in Chl-a revealed cell growth and photosynthetic activity under N-deficient conditions, indicating the utilization of chlorophyll as an intracellular nitrogen source (Pancha et al., 2014). A similar trend of a 2-fold increase in biomass concentration and reduction in chlorophyll

content by *Nannochloropsis gaditana* in N-deficiency condition was reported (Janssen et al., 2018). According to Pancha et al., (2014), deficiency of nutrients induces the breakdown and enables assimilation of the intracellular N-rich compounds including chlorophyll, protein, and DNA as an instant energy source for maintaining growth.

The maximum lipid content based on the dry weight of N_{def} P_{oexcs}, N_{def} P_{excs}, and N_{def} P_{mexcs} in mixotrophic culture conditions was 39.1±1.2 %, 38±1.5 %, 27.9, and 31.1±0.0 %, respectively. The lipid content in N_{def} P_{oexcs} was 1.6-fold higher than that of the normal BG11 condition (Table 5.1). Similarly, Fu et al., (2017) reported that the lipid content of *C. regularis* in N-deficient and P-supplementation conditions (50 mg/L of N and 45 mg/ L of P) was ~2-fold higher than that of N-sufficient and P-sufficient conditions (240 mg/ L of N and 5.5 mg/ L of P). It can be deduced that a balanced N/P regime can only stimulate the amalgamation of biomass productivity and lipid content. The study further suggested that the increase in lipid content during nitrogen stress and P supply could be possibly due to the following reasons: (i) N-deficiency upregulated the malic enzyme-producing NADPH, resulting in enhanced lipid production (Li et al., 2013); (ii) N-deficiency causes upregulation of glutamate dehydrogenase and enhances the tricarboxylic acid cycle, offering intermediates and energy for lipid biosynthesis; and (iii) excessive phosphorus assimilation downregulates ADP-glucose pyrophosphorylase activity of microalgae preventing starch synthesis, and stimulating intracellular carbon allocation towards the lipid biosynthesis pathway (Fu et al., 2017; Zhu et al., 2015).

Table 5.1: Mixotrophic and heterotrophic growth of *Scenedesmus* sp. DDVG I under different nitrogen and phosphorus conditions and their corresponding specific growth rate, biomass productivity, lipid content after 16 days of cultivation.

	Heterotrophic			**Mixotrophic**		
	Specific growth (d^{-1})	**Biomass productivity (mg/L. d)**	**Lipid (% DCW)**	**Specific growth (d^{-1})**	**Biomass productivity (mg/L. d)**	**Lipid (% DCW)**
BG11	-	-	-	0.08	29±1.1	25±1.8
N_{def} P_{oexcs}	0.082	22.1±0.6	21.5±1.0	0.15	41.1±0.51	39.1±1.2
N_{def} P_{excs}	0.042	21.1±0.1	16.23±0.2	0.13	39.5±1.1	38±1.5
N_{def} P_{mexcs}	0.036	17.8±0.0	14.5±0.1	0.103	39±1.2	31.1±0.0
N_s P_{mexcs}	0.015	11±0.1	8±0.5	0.069	26.1±0.5	24.4±0.5
N_s P_s	0.029	14.5±0.2	9.5±1.1	0.11	35.9±1.1	26.4±0.1

5.1.1 Co-cultivation of Scenedesmus sp. DDVG I and Limnothrix sp. DDVG II

The auto flocculating strain, *Limnothrix* sp. DDVG II was co-cultivated with *Scenedesmus* sp. DDVG I to facilitate the harvesting of biomass. The previous study reported that both the species were isolated from freshwater (Devi et al., 2021). Hence, it gave us a clue that they should be able to grow together since both originated from the same habitat, freshwater. Moreover, it was indispensable to identify under which inoculation ratio they offer strong symbiosis; the stronger the symbiosis greater would be the harvesting efficiency. The co-culture system was set up at different inoculation ratios of S: L as 1:1, 1:2, and 2:1. As evident from Figure 5.2a, *Limnothrix* sp. DDVG II could grow and thrive well in the N_{def} P_{oexcs} under the mixotrophic mode, achieving DCW of 4.18±0.11g/ L. Among the co-culture systems, co-culture 1:1 showed the highest DCW of 10.7±0.2 g/L which was higher than the biomass productions by the monocultures. The result in Figure 5.2b shows the presence of Chl-a in all the co-culture systems. Similar trends of increase in Chl-a content up to day 8 and subsequent reduction were observed during the growth of co-cultures. The maximum Chl-a content

was recorded in co-culture 1:1, followed by co-culture 1:2, co-culture 2:1 with the values of 13.57±0.5 mg/ L, 3.79±0.12 mg/ L, and 7.42±0.4 mg/ L respectively on day-8. However, their corresponding Chl-a contents were reduced to 1.5±0.1 mg/L, 0.85±0.0 mg/L, and 0.87±0.0 mg/L, respectively after 16 days. The reduction in Chl-a content attributes to photosynthetic activity under N-deficient conditions and being utilized as an intracellular nitrogen source (Pancha et al., 2014). Results in Table 5.2 showed that the biomass productivity of 42±0.9 mg/ L. d for the co-culture 1:1 was higher than biomass productivities of 41±1.0 mg/L. d for monoculture *Scenedesmus* sp. DDVG I and 28.4± 0.5 mg/L. d for *Limnothrix* sp. DDVG II. This study was in accordance with the findings from Gonçalves et al., (2016) who showed that the co-culture of microalgae and cyanobacteria (1:1 w/w inoculation ratio) achieved higher biomass productivity of 64 to 97 mg/L. d when compared to biomass productivity of 41 to 60 mg/L. d for the individual cultures. Additionally, co-culture 1:1 exhibited the highest lipid content (40.2±1.0 % of DCW) which was higher significantly than that of *Scenedesmus* sp. DDVG I (38.9±1.1 % of DCW), and *Limnothrix* sp. DDVG II (25.3±0.9 % of DCW). Some studies have proposed that the interactive effects of the symbiotic species and the competition on nutrient intake, nutrient starvation, are directly linked to the increase in lipid accumulation under co-culture conditions (Cheng et al., 2020b). Moreover, the intracellular lipid accumulations in the co-cultures 1:1 and the individual species were confirmed through the Nile red staining. According to Ren et al., (2013), the lipophilic Nile Red fluorescent dye selectively binds to triacylglycerol (TAG) and the lipids are reflected as red yellow fluorescence when visualized under the microscope. It is evident from Figure 5.3 that the golden yellow fluorescence indicated the high accumulation of neutral lipid in the co-culture cells. We also observed the emission of red colour from the cells due to the auto-florescence of the chlorophyll in microalgae. The advantage of the auto-florescence is that they give the reliability of the result, as Nile dye sometimes do not stain all microalgae successfully, even the technique is advanced (Ren et al., 2013).

As evident in Figure 5.2c and Table 5.2, the biomass harvesting efficiency was highest for co-culture 1:1, achieving 99.9 ± 0.5 %, followed by 79.1 ± 3.2 % for co-culture 1:2, 65.8 ± 3.1 % for individual *Limnothrix* sp. DDVG II, and 57.9 ± 2.1 % for co-culture 2:1. However, the biomass harvesting efficiency of *Scenedesmus* sp. DDVG I was as

low as 0.02 ± 0.0 %. The results signified that the co-culture 1:1 was an effective strategy for harvesting non-flocculating *Scenedesmus* sp. DDVG I. The reason for effective biomass recovery in co-culture could be attributed to the presence of *Limnothrix* sp. DDVG II. This strain is filamentous which forms a cross-link mat and entraps the minute Scenedesmus sp. cells. They also have gas vesicles which can enable them to buoyant on the water bodies as biofilm under nutrient starvation (Gkelis et al., 2005). Moreover, it was evident from the previous study that the sheath of the *Limnothrix* sp. DDVG II secretes EPS that helps to bind with the microalgal cells (Devi et al., 2021). reported that EPS played a major role in bio granulations of suspended *Ankistrodesmus falcatus* var. *acicularis*, resulting in efficient harvesting.

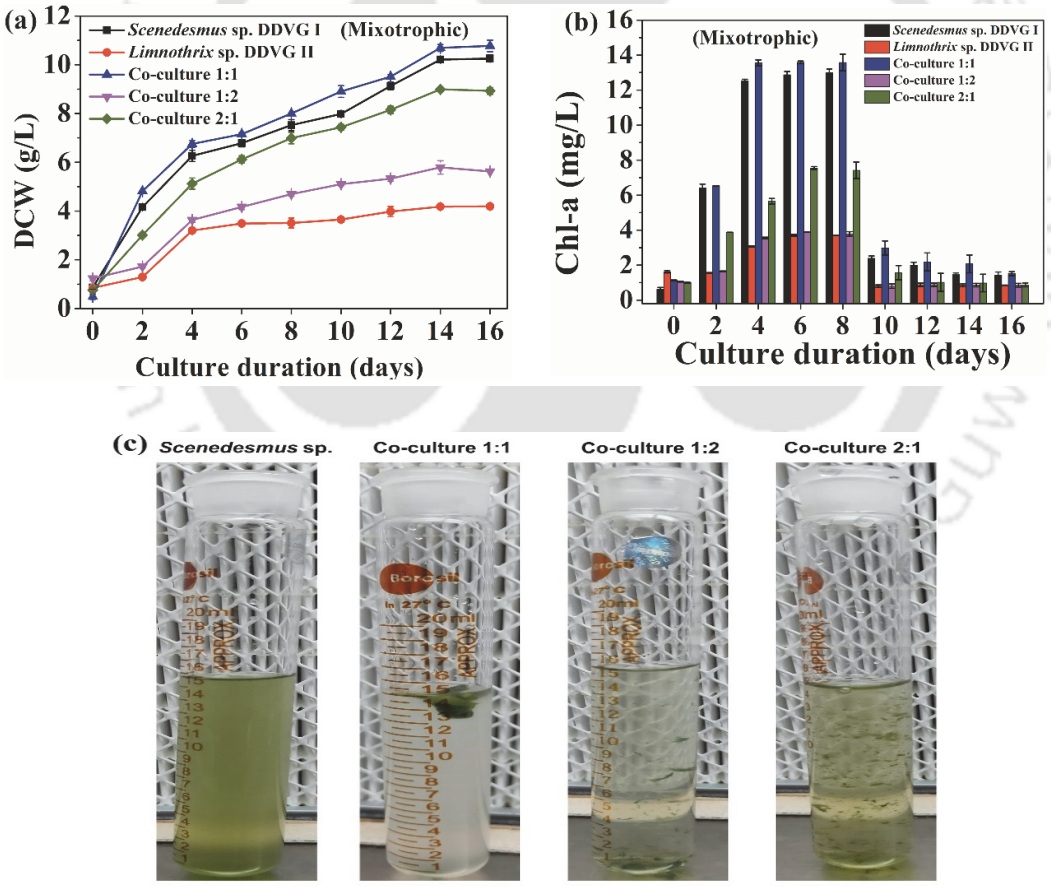

Figure 5.2: Mixotrophic growth profile (b) Chl-a concentration (c) Co-culture of *Scenedesmus* sp. DDVG I: *Limnothrix* sp. DDVG II at different inoculum ratios.

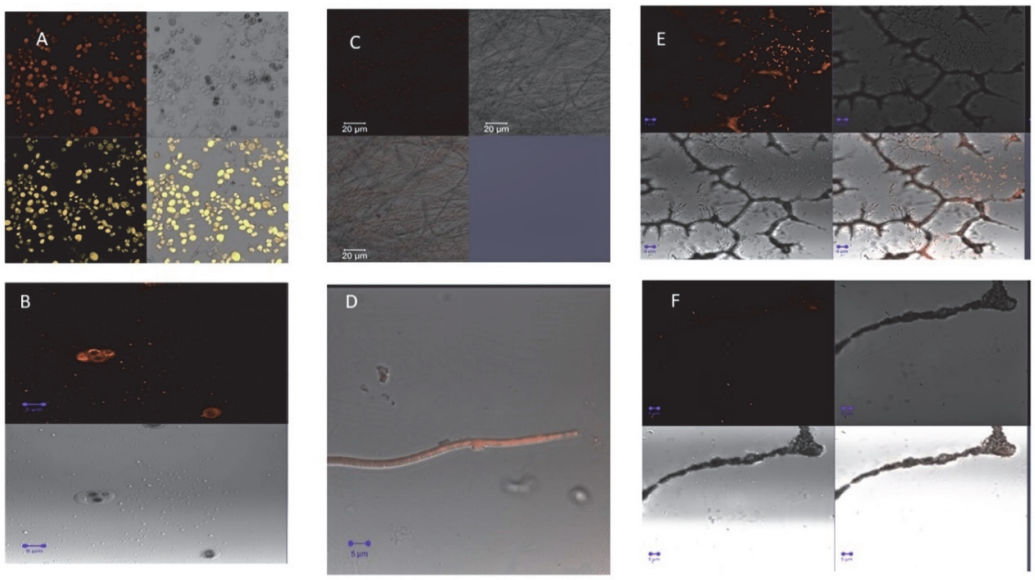

Figure 5.3: Confocal imaging of cells using Nile red reagent and chlorophyll as autofluorescence with excitation/ emission of 543nm/ 555-652 nm (Nile) and 405/650 nm (chlorophyll) respectively. (A) *Scenedesmus* cells under dark field, Nile autofluorescence and merge field observed under the magnification of 20 Kx (B) *Scenedesmus* sp. under the magnification of 60 Kx (oil immersion) (C) Filamentous structure of *Limnothrix* cells under dark field, Nile autofluorescence and merge field, observed under the magnification of 20 Kx (D) *Limnothrix* cells under the magnification of 60 Kx (oil immersion) (E) *Scenedesmus* cells attached on the filamentous structure of *Limnothrix* cells, under dark field, Nile autofluorescence and merge field, observed under the magnification of 20 Kx (F) *Scenedesmus* sp. and *Limnothrix* sp. cells under the magnification of 60 Kx (oil immersion).

Table 5.2: Comparative study of *Scenedesmus* sp. DDVG I, *Limnothrix* sp. DDVG II and *Scenedesmus* sp.: *Limnothrix* sp. (co-culture 1:1, co-culture 1:2, and co-culture 2:1) on biomass productivity (mg/L. d), and lipid content (%) cultivated in N_{def} P_{oexcs} medium after 16 days of mixotrophic cultivation.

Culture types	**Biomass productivity (mg/L. d)**	**Lipid content (% DCW)**	**Harvesting efficiency (%)**
Scenedesmus sp. DDVG I	41±1.0	38.9±1.1	0.02±0.0
Limnothrix sp. DDVG II	28.4±0.4	25.3±0.9	65.83±3.1
Co-culture (1:1)	42±0.9	40.2±1.0	99.9±0.5
Co-culture (1:2)	37±0.56	35.5±0.8	79.1±3.2
Co-culture (2:1)	39±1.5	36.2±0.8	57.9±2.1

5.2.2 Removal of glucose, urea-N, and PO_4^{3-}-P

The result in Figure 5.4 shows the assimilation of glucose, urea-N, and PO_4^{3-}-P by the different co-culture systems and the monocultures over 16 days of cultivation from N_{def} P_{oexcs} medium under mixotrophic mode. The glucose consumption rates were consistent with the cell growth behavior. The glucose in the medium was almost exhausted after 16 days of cultivation in a co-culture 1:1 system and pure *Scenedesmus* sp. As evident in Figure 5.4a, the glucose concentration in the co-culture 1:1 system and *Scenedesmus* sp. removed glucose up to 99.9±4.1 % and 99.97±1.1 % respectively. While the glucose removal efficiency for *Limnothrix* sp., co-culture 1:2 and 2:1 was 64±1.8, 78.9±1.8, and 92.6±1.5% respectively. The removal efficiencies of PO_4^3-P exhibited by co-culture 1:1 and pure *Scenedesmus* sp., from the medium were almost 100 % after 16 days of mixotrophic cultivation. However, removal efficiencies of PO_4^3-P by *Limnothrix* sp., co-culture 1:2, and co-culture 2:1 were 63±1.8 %, 68±1.5 %, and 92.1±1.3 % respectively (Figure 5.4b). The result in Figure 5.4c showed that the urea-N concentrations were almost assimilated (100 % removal efficiency) by co-culture 1:1 and pure *Scenedesmus* sp. respectively. However, the removal efficiencies of urea-N

by *Limnothrix* sp., co-culture 1:2, and 2:1 were 80.15±1.5, 88.77±1.8, and 97.9±1.3 % respectively from the medium (Figure 5.4c). These findings were in accordance with literature reports (Fu et al., 2017; Gonçalves et al., 2016; Rashid et al., 2019; Tsolcha et al., 2018b, 2018a, 2017). Generally, excess P was assimilated and converted into intracellular Poly-P inside microalgae, offering storage energy. The energy stored as Poly-P was related to the ATP supply. The stored Poly-P was released and utilized for biosynthesis during the nutrient deficiency (Jiménez et al., 2017).

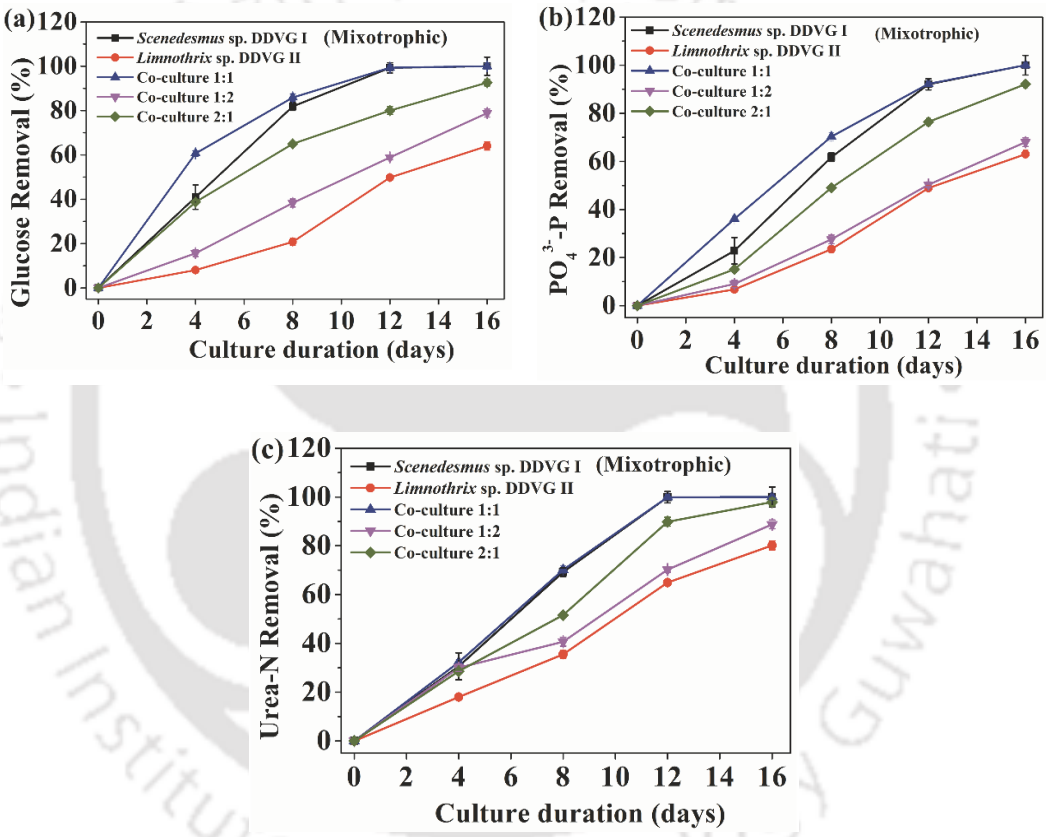

Figure 5.4: Removal efficiencies of (a) glucose, (b) PO_4^{3-}-P, and (c) Urea-N by different co-culture systems over 16 days mixotrophic cultivation in N_{def} P_{oexcs} condition.

5.3 FAME profile and assessment of biodiesel quality

The highest lipid content acquired by the co-culture 1:1 was further evaluated for the fatty acid profile. The FAME compositions of co-culture 1:1 was compared to those of monocultures which are summarized in Table 5.3. Most of the FAME produced in all

the conditions had a carbon chain ranging from C14 to C20. In co-culture 1:1, the FAME profile was predominant in C18:2 (36.05 %), followed by C16:0 (32.25 %), C18:1 (16.86 %), and C18:0 (7.68 %). The major FAME composition of monoculture *Scenedesmus* sp. were C18:2 (34.66 %), C16:0 (29.72 %), C18:1 (19.15) and C18:0 (8.30 %). While in *Limnothrix* sp., a high concentration of FAME was contributed from C18:1 (46.43 %), followed by C18:3 (25.98 %) and C16:0 (14.65 %).

Table 5.3: FAME profile of *Scenedesmus* sp. DDVG I, *Limnothrix* sp. DDVG II and *Scenedesmus* sp.: *Limnothrix* sp. (co-culture 1:1) cultivated in N_{def} P_{oexcs} medium after 16 days mixotrophic cultivation.

Fatty acid composition	***Scenedesmus* sp. DDVG I**	***Limnothrix* sp. DDVG II**	**Co-culture (1:1)**
C14:0 (myristic)	1.37	0.28	1.15
C16:0 (palmitic)	29.72	14.65	32.25
C16:1 (palmitoleic)	2.92	0.70	1.74
C18:0 (stearic)	8.30	1.38	7.68
C18:1 (oleic)	19.15	46.43	16.86
C18:2 (linoleic)	34.66	2.93	36.05
C18:3 (linolenic)	0.35	25.98	0.37
C20:0 (arachidic)	0.73	2.35	0.76
C20:1 (gadoleic)	0.58	5.02	0.65
C22:1 (erucic)	0.42	0.26	0.48
C24:1 (nervonic)	1.80	0.00	2.01
SFA	40.12	18.67	41.84
MUFA	24.88	52.42	21.74
PUFA	35.00	28.91	36.42
%FAME in total FAME	100	100	100

Additionally, using equations 2.5–2.17 (as mentioned in section 2.3.6.5), the properties of biodiesel derived from co-culture 1:1 and the monocultures were also evaluated based on the FAME profile. Results in Table 5.4 summarized the significant properties of biodiesel and the standard norms recommended by the European biodiesel system (EN) 14214 and American standard system (ASTM) D6751. The IV values of 81.80 g I2/ 100 g for *Scenedesmus* sp., 117.29 g I2/ 100 g for *Limnothrix* sp., and 81.41 g I_2/ 100 g for co-culture met the current standard limit of the IV (it should be < 120). This reflected the stability of biodiesel. In the present study, CN in all the cultures ranged from 48.6 to 56.02 which exceeded the minimum standard value of CN values of 47, and 51 according to the ASTM D6751, and European Standard EN 14214, respectively. This suggested the good ignition performance of the biodiesel. Cloud point (CP) determines the flow properties at low temperatures (Knothe et al., 2003). The CP of *Scenedesmus* sp. and co-culture 1:1 was 10.64 °C and 11.97 °C respectively, which fall well within standard limits (−3 to +12 °C). However, the CN (−2.71 °C) of *Limnothrix* sp. did not meet the standard limit. This reflected that biodiesel derived from *Scenedesmus* sp. and co-culture 1:1 would be more appropriate in a low-temperature climate. The FP determines the temperature at which the fuel must be heated and ignited. The FP in all cultures varied from 412.08° to 423.38°C which met the standard norm of the EU (> 120 °C), and ASTM (> 93 °C). According to the analysis, the HHV value of *Scenedesmus* sp. (39.75 MJ/ kg), *Limnothrix* sp. (39.78 MJ/kg), and co-culture 1:1 (39.75 MJ/kg) achieved the minimum standard limit (>35 MJ/ kg). This parameter allowed estimation of the energy potential and economic efficacy. The corresponding density (ranging from 0.87 to 0.88 g/cm^3) and viscosity (ranging from 4.2 to 4.33 mm^2/s) complied with the standard values (Table 5.4). Moreover, the OS signifies the storage capacity, fuel compatibility, and stability of biodiesel. The biodiesel of all the conditions in this experiment ranged between 3.02 and 3.74 h which met the minimum standard limit (>3 h).

Besides, it is worthwhile to mention that co-cultivation produced an elevated level of omega-6 fatty acids, which are highly beneficial to human health. It validates the feasibility of employing co-cultivation for biodiesel production as well as other value-added bio-products generation. Despite variation in the FAME profile among co-culture 1:1 and individual cultures, the co-cultivation strategy still holds a good

prospect for biodiesel production on a mass scale. This finding provides evidence that mixotrophic co-cultivation can be targeted to utilize microalgae for fuel purposes.

Moreover, this work provided a novel cultivation system to boost simultaneous biomass and lipid productivity. There was no sign of contamination or culture crash in our experiment. Several studies reported the successful implementation of a co-culture system in biodiesel production as well as value-added products toward biorefinery prospects (Debeni et al., 2022; Shahid et al., 2020; Wang et al., 2021). Likewise, in the present study, the effective performance of nutrient removal by this co-cultivation approach depicts the feasibility of using it in the biorefinery approach. Additionally, this system aims to demonstrate that algae-cyanobacterium consortium models are more sustainable and similar to natural ecosystems. Nevertheless, various factors such as procurement of inoculum in bulk, light input during continuous process, etc. may become major constraints while scaling up the system. Thus, future investigation should be planned to evaluate the economic viability of co-culture system using techno-economical and life cycle analysis studies.

Table 5.4: Properties of biodiesel derived from *Scenedesmus* sp. DDVG I, *Limnothrix* sp. DDVG II and *Scenedesmus* sp.: *Limnothrix* sp. (co-culture 1:1) cultivated in N_{def} P_{oexcs} medium after 16 days mixotrophic cultivation.

Properties	***Scenedesmus* sp. DDVG I**	***Limnothrix* sp. DDVG II**	**Co-culture (1:1)**	**EN 14214**	**ASTM D6751**
DU	94.88	110.24	94.57	NR	NR
SV (mg KOH/g oil)	194.65	191.15	194.69	NR	NR
IV (g I_2/ 100 g)	81.80	117.29	81.41	<120	NR
CN	55.94	48.6	56.02	>51	>47
LCSF	7.12	4.51	7.06	NR	NR
CFPP (°C)	5.90	-2.31	5.71	NR	NR
CP (°C)	10.64	2.71	11.97	NR	-3 to +12
PP (°C)	4.73	-3.88	6.81	NR	NR
OS (h)	3.14	3.74	3.02	NR	>3h
HHV (MJ/kg)	39.75	39.78	39.75	NR	>35
FP (°C)	412.14	423.38	412.08	>120	>93
ρ_i at 15 °C (g/cm^3)	0.87	0.88	0.87	0.86-0.90	0.82-0.90
η at 40 °C (mm^2/s)	4.33	4.2	4.33	3.5–5.0	1.9–6.0

NR: not reported

5.4. Conclusions

This study concluded that (i) deficient nitrogen and over excessive phosphorus (N_{def} P_{oexcs}) which included 100 mg/L of N and 50 mg/L of P enhanced the growth and lipid content of *Scenedesmus* sp. DDVG I; (ii) co-cultivation of *Scenedesmus* sp. DDVG I with *Limnothrix* sp. DDVG II in a 1:1 ratio demonstrated efficient biomass harvesting of 99.9 %; (iii) empirical analysis revealed that the FAME produced by co-culture 1:1 fulfilled standard specifications for biodiesel property. Studies on upgrading the quality of biodiesel by blending it with different oils or additives, cost analysis of the fuel are envisaged in the future.

CHAPTER 6

Study of microalgae cultivation in municipal wastewater as a source of low-cost nutrient medium

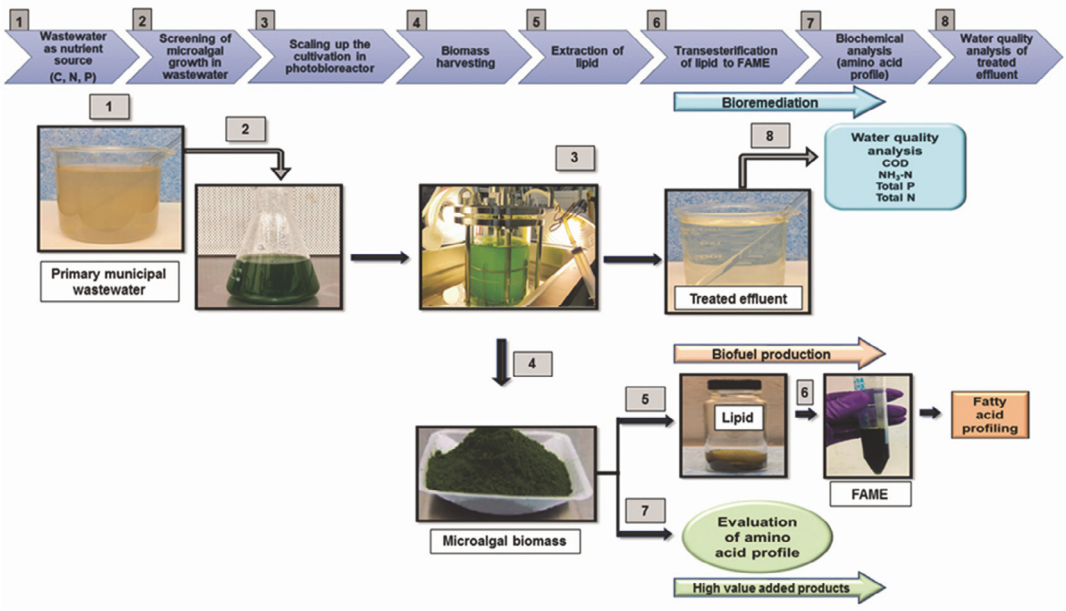

This work has been published as Nongmaithem Debeni Devi, Xiao Sun, Lingkan Ding, Vaibhav V. Goud Bo Hu, (2022). Mixotrophic growth regime of novel strain Scenedesmus sp. DDVG I in municipal wastewater for concomitant bioremediation and valorization of biomass. Journal of Cleaner Production. 365, 132834. https://doi.org/10.1016/j.jclepro.2022.132834.

CHAPTER 6

Study of microalgae cultivation in municipal wastewater as a source of low-cost nutrient medium

The availability of cost-effective nutrients for the commercial cultivation of microalgae is one of the major challenges. The present study investigated the feasibility of primary municipal wastewater (PMWW) collected from a local wastewater treatment plant in Minnesota, USA as an alternative to fresh-water microalgae growth media for high-value bioenergy feedstock production. The novel strain Scenedesmus sp. DDVG I was cultivated in the PMWW under heterotrophic and mixotrophic modes in 250 mL Erlenmeyer flasks. The optimized cultivation mode was further scaled up to the 3-L bubbled bioreactor. The study confirmed the wastewater as a potential growth medium while Scenedesmus sp. DDVG I showed superior biomass productivity (0.069 g/L. d), lipid yield (22.5 %), and fatty acid content (4.25 % in dry cell weight) over 10 days in the mixotrophic mode. The biomass also showed high essential amino acid content (159.8 mg/ g DCW). The corresponding values for bioremediation efficiencies of COD and TN by Scenedesmus sp. were 75.2% and 99.85% respectively. Meanwhile, ammonia nitrogen (NH_3-N) and TP were removed at up to 100% removal efficiencies. Analyses of fatty acid profile and different parameters that were required for biodiesel characterization revealed the high-quality nature of the Scenedesmus-derived oil. Overall, the study concluded effective bioremediation of municipal wastewater by Scenedesmus sp. DDVG I with the recovery of valuable resources from the biomass.

6.1. Wastewater characterization

The physicochemical parameters of PMWW and the average data of the measurement are summarized in Table 6.1. The PMWW has a pH of 7.0 ± 0.01 which is favorable for the cultivation of microalgae without any pH adjustments. The PMWW showed the presence of COD (484.8 ± 8.5 mg/L), NH_3–N (40.2 ± 1.1 mg/L), TN (44.9±1.9 mg/L), and TP (7.9±0.5). Wang et al., (2010) used the primary municipal wastewater collected from the Metropolitan WWTP for the growth of *Chlorella* sp. The study showed the presence of 40.65 ± 0.07 mg/L of TN and 5.66±0.08 mg/L of TP, which is comparable to the nutrient content of the wastewater used in this study.

Table 6.1: Physicochemical characteristics of the PMWW. All measurements were performed in triplicate, and the results are expressed as mean values ± standard deviations (SD).

Parameter	**PMWW**
TS (mg/L)	245 ± 3.7
TVSS (mg/ L)	23 ± 0.03
COD (mg/L)	484.8 ± 8.5
NH_3-N (mg/L)	40.2 ± 1.1
TN (mg/L)	44.9 ± 1.9
TP (mg/L)	7.9 ± 0.5
pH	7.0 ± 0.01

6.2. Mixotrophic and heterotrophic cultivation of *Scenedesmus* sp. DDVG I in batch culture with PMWW

The biomass concentrations and chlorophyll content attained at regular intervals under heterotrophic and mixotrophic modes are illustrated in Figure 6.1a and Figure 6.1b, respectively. In mixotrophic mode, the biomass concentration of *Scenedesmus sp.* DDVG I increased significantly (p=0.001) from 0.36 ± 0.00 g/L to 1.5 ± 0.04 g/L after 2 days of inoculation. After 8 days, *Scenedesmus* sp. attained its stationary phase with

a biomass concentration of 3.27 ± 0.12 g/L. At the end of the culture period (10-day), the biomass concentration achieved by *Scenedesmus* sp. DVVG I was 3.4 ± 0.13 g/L. The maximum biomass productivity and lipid content achieved by *Scenedesmus* sp. were 0.065 ± 0.01 g/L. d and 21.9 %, respectively (Table 6.2). During the mixotrophic mode, the growth of unwanted microbes (like bacteria or protozoa) in the blank condition was insignificant when examined under microscopy. The occurrence of higher Chl-a content in the mixotrophic cells further confirmed the photosynthetic activity of the microalgal cells. The Chl-a content increased from 0.62 ± 0.1 mg/L to 5.46 ± 0.7 mg/L significantly ($p < 0.001$) over two days. The highest Chl-a reached up to 10.2 ± 0.16 mg/L over the 10 days cultivation period.

In heterotrophic mode, *Scenedesmus* sp. persisted in the lag phase over 3 days. No particular exponential phase was observed over the 10 days culture duration. The maximum biomass concentration achieved by the *Scenedesmus* sp. was 0.71 ± 0.05 g/L after 4 days. Thereafter, the growth declined slowly up to day 10 of the study. The biomass productivity and lipid yield at the end of the culture period were 0.021 g/L. d and 8.7%, respectively. However, the blank condition in heterotrophic mode showed a minor population of bacterial growth. A similar observation was reported by Khan and Diba, 2016) stating that the heterotrophic mode favored the growth of microbes. They further stated that the heterotrophic mode provided a dark fermentation environment for bacteria thus inducing the growth. The Chl-a content in the heterotrophic mode decreased gradually from 0.44 ± 0.09 mg/L to 0.40 ± 0.09 mg/L during the first two days. The Chl-a further declined to the lowest concentration of 0.10 ± 0.04 mg/L over 10 days in heterotrophic cultivation. Furthermore, *Scenedesmus* sp. in mixotrophic mode showed a higher specific growth rate of 0.16 d^{-1} (p= 0.001) as compared to the specific growth rate (0.06 d^{-1}) of heterotrophic mode. This suggested that the heterotrophic mode of cultivation is less efficient for *Scenedesmus* sp. as compared to the mixotrophic. The result behind the slower activity of *Scenedesmus* sp. DDVG I in heterotrophic mode could be related to the non-biodegradability of organic matter for utilization by the lesser cell densities (Ruiz et al., 2014). Cid et al., (1992) reported that the uptake of organic nutrients by photosynthetic microalgae was greatly influenced by light. In a mixotrophic mode, catabolism of organic matter during photosynthesis coupled with aerobic respiration provides higher energy required for the greater cell

densities (Mitra et al., 2012). A similar study was reported by Daneshvar et al., (2019) that the mixotrophically grown *Tetraselmis suecica* showed higher biomass concentration (0.58 g/L) and chlorophyll content (11.70 mg/L) as compared to heterotrophic growth with dairy wastewater. Likewise, *Chlorella vulgaris* JSC-6 could achieve higher biomass growth (3.96 g/L) under mixotrophic mode as compared to the heterotrophic growth (2.35 g/L) with swine wastewater (Wang et al., 2015). They further reported that the presence of light is a limiting parameter supporting the higher availability of organic matter to microalgal growth in a mixotrophic mode. The present study clearly suggested that heterotrophic cultivation of *Scenedesmus* sp. in PMWW is less efficient, compared to the mixotrophic mode. Thus, the further scale-up study was focused only on the mixotrophic mode to evaluate enhanced productivity with an increase in culture volume.

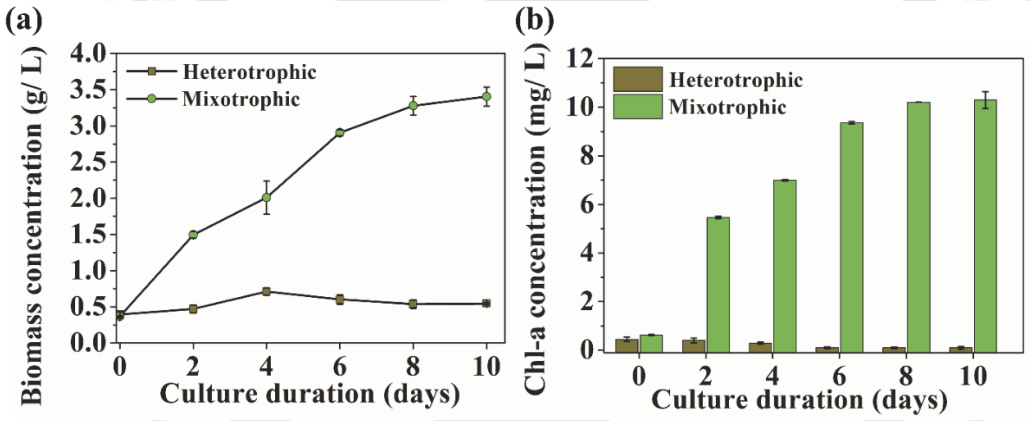

Figure 6.1: (a) Heterotrophic and mixotrophic growth curves of *Scenedesmus* sp. DDVG I in PMWW for 10 days cultivation period; (b) Chlorophyll-a content of *Scenedesmus* sp. DDVG I under heterotrophic and mixotrophic modes.

6.2.1 Nutrient removal by Scenedesmus sp. DDVG I cell from PMWW

The patterns of nutrient removal by S*cenedesmus* sp. from the culture medium (PMWW) in heterotrophic and mixotrophic mode over 10 days cultivation period are illustrated in Figure 6.2. As shown in Figure 6.2a, the concentration of COD decreased gradually in mixotrophic mode when compared to heterotrophic over 10 days of culture duration. In mixotrophic, the COD decreased from 484.8 ± 8.5 mg/L to 225 ± 5.5 mg/L when the cells were in the exponential phase (day 4) of the growth. The lowest residual

COD concentration in the culture medium after 10 days was 120 mg/L, achieving an overall COD removal efficiency of 75.2 ± 0.1%. In a study by Chaudhary et al., (2018), *Scenedesmus obliquus* ACHB 417 exhibited a COD removal efficiency of 75.9 % from municipal wastewater. Likewise, the higher concentration of COD (3429.33 mg/L) in the slaughterhouse wastewater was reduced to 855.6 mg/L by *Chlorella pyrenoidosa*, achieving a 75.4 % removal efficiency (Azam et al., 2020). These values were comparable with this present study. However, Wang et al., (2010) stated that the centrate sludge obtained after centrifugation of municipal wastewater generally had 20,180 mg/L of COD. The study further reported the effective reduction of COD to 6065 mg/L by *Chlorella* sp. with a 70 % removal efficiency which was relatively lower than the value of this present study.

Results in Figure 6.2b and Figure 6.2c indicated that the initial concentrations of NH_3-N (40.5 mg/L) and TN (44.9 mg/L) in the medium declined abruptly, resulting in 19.92 mg/L and 7.7 mg/L with removal efficiencies of 50.8 % and 82.8 ± 1.2 %, respectively after day 4, which corresponded to the exponential phase of *Scenedesmus* sp. DDVG I growth. At the end of the experiment (day 10), the lowest TN concentration remained in the culture medium was 0.05 mg/L, resulting in a nutrient removal efficiency of 99.8%. Meanwhile, the NH_3-N removal efficiency achieved by *Scenedesmus* sp. was 100 %. A study conducted by Daneshvar et al., (2019) reported that the removal efficiency of TN from dairy wastewater by *Scenedesmus quadricauda* was 87.6 %. Chaudhary et al., (2018) found out 91.5 % of NH_3-N removal by *Scenedesmus obliquus* ACHB 417 from municipal wastewater. Likewise, *Chlorella* sp. showed the highest removal of NH_3-N (91.3 %) from the centrate sludge (Wang et al., 2010). As shown in Figure 6.2d, the initial TP concentration (7.9 mg/L) in PMWW was reduced to 0.52 mg/L with a removal efficiency of 93.4 % after day 6. After day 10, the TP was removed efficiently by *Scenedesmus* sp., resulting in a 100 % removal efficiency. Daneshvar et al., (2019) reported that TP from the dairy wastewater was completely removed (100 % removal efficiency) by *Scenedesmus quadricauda*. Similarly, complete removal of TP (100 %) from dairy wastewater by *Acutodesmus dimorphus* was reported (Chokshi et al., 2016). Results in Figure 6.2 showed that in heterotrophic mode, the nutrient removal efficiency achieved by *Scenedesmus* sp. was relatively lower when compared to the mixotrophic condition. The COD removal efficiency was 46.9±1.1 % over 10

days of cultivation. While the removal of TN, NH_3-N, and TP over 10 days of cultivation were 89.9±1.1 %, 87.5 %, and 81.2±1.1 %, respectively. The high nutrient removal efficiency even after the lesser cell densities of *Scenedesmus* sp. might be contributed by the growth of other microbes in heterotrophic as mentioned in section 6.2. In such dark conditions, bacteria tend to assimilate nitrogen and phosphorus efficiently as instant energy is required for cell division and growth (Cid et al., 1992).

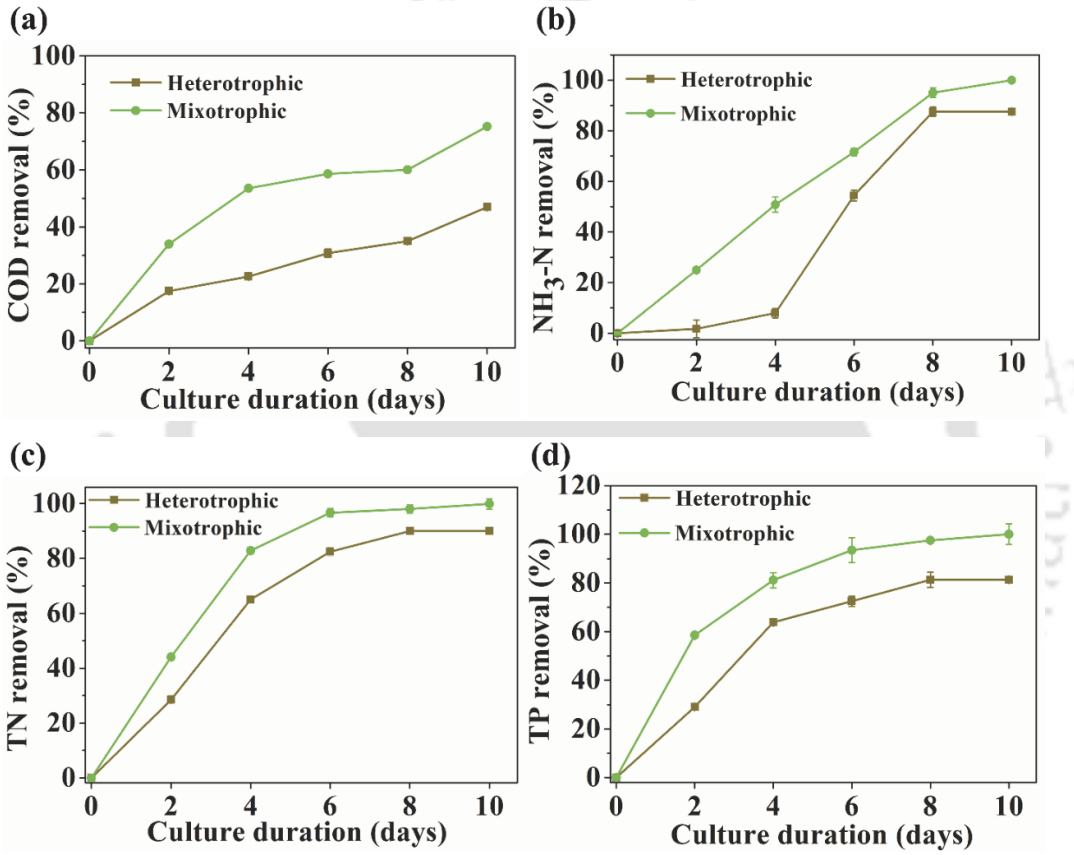

Figure 6.2: Nutrient removal efficiencies by *Scenedesmus* sp. during 10 days culture period in the PMWW. (a) COD removal; (b) NH_3–N removal efficiency; (c) TN removal efficiency; (d) TP removal efficiency.

6.3. Mixotrophic growth of *Scenedesmus* sp. DDVG I in 3 L bioreactor

The scale-up cultivation of *Scenedesmus* sp. DDVG I in mixotrophic mode using PMWW to a 3 L bioreactor (Figure 2.2) is illustrated in Figure A9 in Appendix. The growth in terms of biomass concentration over 10 days cultivation period is shown in

Figure 6.3a. The growth curve in the bioreactor study illustrated a similar trend to the mixotrophic growth curve of the flask. The initial biomass concentration (0.18 ± 0.04 g/L) increased significantly (p=0.001) up to 1.27 ± 0.13 g/L after day 2. After day 4 and day 8, the biomass concentration increased up to 2.12 ± 0.2 g/L and 3.21 ± 0.03 g/L, respectively. At the end of cultivation (day 10), the biomass concentration, biomass productivity, and lipid content were 3.39 ± 0.03 g/L, 0.069 ± 0.01 g/L. d, and 22.51%, respectively (Table 6.2). *Scenedesmus* sp. grown in a bioreactor exhibited a specific growth rate of 0.2 d^{-1}. During the growth, the Chl-a content increased from 0.56 ± 0.01 mg/L to 6.4 ± 0.6 mg/L over four days (Figure 6.3b). The highest Chl-a content (9.90 ± 0.06 mg/L) was achieved on day 10 of incubation. This revealed that *Scenedesmus* sp. DDVG I consumed organic matter in the PMWW efficiently in a mixotrophic mode. In agreement with this study, Engin et al., (2018) reported mixotrophic cultivation of *Micractinium sp. ME05* with vinasse in a 5-L bioreactor, achieving a higher biomass concentration of 1.95 ± 0.2 g/L of and 0.32 ± 0.2 mg/L. d of biomass productivity when compared to a 500 mL flask study. Similarly, mixotrophic growth of *Auxenochlorella protothecoides* UMN280 with concentrated municipal wastewater in a 25-L BIOCOIL reactor achieved high biomass concentration and biomass productivity of 1.30-1.78 g/L and 0.92 mg/L. d, respectively. Mitra et al., (2012) reported that mixotrophically grown *Chlorella vulgaris* in a 6L bioreactor could increase cell densities from 8.0 to 9.8 g/L and biomass productivities from 2.0 to 2.5 g/L. d by scaling up from 250 mL flask cultivation. The augmentation in the cell growth and biomass productivity with increased working volume signified a correlation between the working volume and biomass productivity. This might be due to more space for light exposure to microalgal cells and proper aeration in the bioreactor than in smaller flasks (Engin et al., 2018).

Table 6.2: Comparison of and mixotrophic and heterotrophic cultivation of *Scenedesmus* sp. DDVG I in PMWW in terms of lipid content, biomass productivity, and specific growth rate.

Growth condition	**Specific growth rate (μ, d^{-1})**	**Biomass productivity (g/L. d)**	**Lipid content (% DCW)**
Heterotrophic	0.06	0.021	8.7
Mixotrophic	0.16	0.065± 0.01	21.9
Mixotrophic in bioreactor	0.20	0.069 ± 0.01	22.51

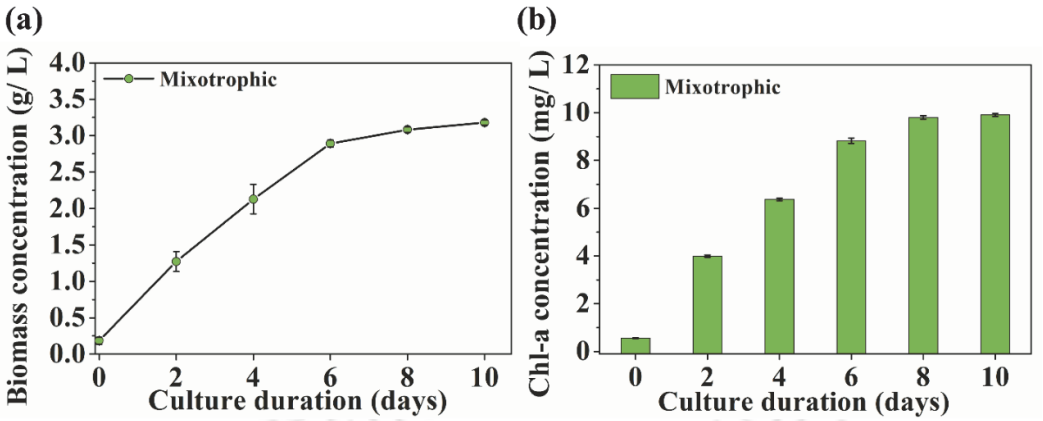

Figure 6.3: (a) Mixotrophic growth curve of *Scenedesmus* sp. DDVG I in the 3-L bioreactor for 10 days cultivation period, and (b) Chlorophyll-a content of *Scenedesmus* sp. DDVG I in the 3-L bioreactor.

6.3.1 Nutrient removal by Scenedesmus sp. DDVG I cell from the bioreactor

Scaling up of mixotrophic growth in a 3 L bioreactor showed the maximum removal efficiency of COD (75.6 ± 1.5 %), NH_3-N (100%), TN (99.8 %), and TP (100%) which were comparable with the literature report a shown in Table 6.3. But, the incomplete removal of COD might be due to the presence of intractable organic compounds in the wastewater, which cannot be easily degraded by microalgae. Nevertheless, the present study exhibited higher COD removal efficiency when compared to literature reports (Eladel et al., 2019; Leong et al., 2019). From all these analyses and results, we observed that when the cell densities increased, the extent of pollutants present in the culture medium gradually decreased which is represented in Figure A10 in Appendix. The nutrients were consumed by the microalgal cells, resulting in enhanced cell densities and the lowering of pollutants. Highly polluted municipal wastewater discharges are detrimental to the environment (Kothari et al., 2012; Wang et al., 2010). The mixotrophic cultivation of *Scenedesmus* sp. DDVG I could be an alternative method for the treatment of wastewater The mechanism of sequestering pollutants specifically N and P compounds in wastewater are performed by microalgae through assimilation. The general chemical equation for nitrogen assimilation is represented in Equation 6.1 (Su, 2021)

$$NO_3^- + 5e^- + 8H^+ + CO_2 \rightarrow (CH_2O) + NH_4^+ + 3H_2O \quad (6.1)$$

where NO_3^- is nitrate, e^- is an electron, H^+ is a hydrogen ion, CO_2 is carbon dioxide, (CH_2O) is a carbohydrate, and NH_4^+ is ammonium. The assimilation of P-compounds by microalgae can be represented as equation 6.2 (Dyhrman, 2016).

$$PO_4^{3-} + ADP + NADP^+ + H^+ + CO_2 + H_2O \rightarrow (CH_2O)_n + O_2 + P_i + ATP + NADPH \quad (6.2)$$

where PO_4^{3-} represents orthophosphate, *ADP* is adenosine diphosphate, $NADP^+$ is nicotinamide adenine dinucleotide phosphate, H^+ is a proton, CO_2 is carbon dioxide, H_2O is water, $(CH_2O)_n$ represents organic compounds such as sugars, *ATP* is adenosine triphosphate, *NADPH* is reduced nicotinamide adenine dinucleotide phosphate, O_2 is oxygen, and *Pi* is inorganic phosphate .

The overall equation shows that the microalgae assimilate N and P compounds and convert them into organic compounds such as sugars, while producing oxygen and ATP through photosynthesis. The organic compounds produced can be used for growth and other metabolic processes. The excess phosphorus can be stored as polyphosphate or other phosphorus-containing compounds within the microalgae cell (Su, 2021). Further studies are still required to improve the overall nutrient removal and biomass production. Some studies suggested that efficient removal of COD could be achieved via either introduction of cyanobacteria to the microalgal growth or a mixed microbial consortium (Tsolcha et al., 2021, 2018a, 2018b, 2017; Patrinou et al., 2020). Besides, an optimal N/P ratio in the medium would enhance the performance of bioremediation and microalgal growth (Choi and Lee, 2015). Hence, future research will focus on the microalgal-based consortium in balanced N/P medium to get efficient removal of the overall nutrient and enhanced biomass productivity.

6.4. Effect of mixotrophic cultivation on biochemical composition of *Scenedesmus* sp. DDVG I

6.4.1. Amino acid profile

The amino acid profile (in mg/g DCW) of whole dried algal cells obtained from *Scenedesmus* sp. DDVG I is summarized in Table 6.4. We observed that the biomass comprised nine EAA and eight NEAA. The EAAR value of the *Scenedesmus* sp. grown

in the PMWW was 0.45, which was slightly higher than the EAAR value (0.43–0.44) of soybean (Serretti et al., 1994). Miao et al., (2016) reported the EAAR value achieved by mixotrophically grown *Chlorella vulgaris* in domestic wastewater was 0.37. Furthermore, the EAA content (159.8 mg/g DCW) of this study was comparable to other reference proteins such as soybean (EAA content, ranging from 160 to 220.4 mg/g DCW) (Serretti et al., 1994), *Spirulina* (EAA content = 226.4 mg/g DCW) (Dewi et al., 2016), *Nannochloropsis granulate* (EAA content = 172.6 mg/g DCW) (Tibbetts et al., 2015), and *Scenedesmus acuminatus* (149.4 mg/g DCW of EAA) (Zhang et al., 2019). This indicated that PMWW could induce the accumulation of EAA in *Scenedesmus* sp. DDVG I, showing the feasibility for use in animal and aquaculture feed.

Despite its high nutritional values, precautions should be taken before the establishment and commercialization of microalga as feed supplements. Some algal species could accumulate heavy metals at higher concentrations higher from the environment and produce biogenic toxins including purines that cause neurodegenerative disorders (Jin et al., 2006; Lum et al., 2013). Some studies reported that the sequestration of toxic pollutants within the microalgae involves various complex mechanisms such as biosorption, bioaccumulation, detoxification, compartmentalization, efflux-transport (Chugh et al., 2022). These mechanisms are companied by phyto-chelators (like organic acids, peptides, enzymes, thiol containing molecules) that detoxify the pollutants into non-toxic organic compound. Thus, microalgae sequester pollutants into valuable biomass. This suggested that microalgae bioremediation is an eco-friendly system (Nur & Buma, 2019). Nevertheless, risk assessment is an important measure that needs to be addressed for production of microalgae as a viable and safe feed supplement. Therefore, future research is still required to understand the toxicological property of *Scenedesmus* sp. DDVG I for consuming as feed supplements.

Table 6.3: Comparison of biomass concentration and nutrient removal efficiency by *Scenedesmus* sp. DDVG I under 3L mixotrophic growth in primary municipal wastewater with previously reported bioremediation studies.

Species	Wastewater	Cultivation period (days)	Biomass content (g/ L)	Nutrient content in untreated wastewater (mg/ L)	Nutrient content in treated wastewater (mg/ L)	Nutrient removal efficiency (%)	Reference
Scenedesmus sp. DDVG I	Municipal wastewater	10	3.4	COD (484.8 ± 8.5) NH_3-N (40.2 ± 1.1) TN (44.9 ± 1.9) TP (7.9 ± 0.5)	COD (118.0 ± 1.5) NH_3-N (ND) TN (0.052) TP (NR)	COD (75.6 ± 1.1) NH_3 (100) TN (99.8) TP (100)	**This study**
Scenedesmus sp. LX1	Municipal wastewater	15	0.11	TN (15.5) TP (0.5)	TN (0.24) TP (0.01)	TN (98.45) TP (98)	(Xin et al., 2010)
Chlorella sp.	Centrate from sludge centrifuge	9	1.5	COD (20180) NH_3-N (1434.3)	COD (6054) NH_3-N (124.7)	COD (70) NH_3 (91.3)	(Wang et al., 2010)
Scenedesmus obliquus ACHB 417	Municipal Wastewater	10	0.8	COD (293 ± 3.3) NH_3-N (43.67 ± 0.72) PO_4^{3-} (18.53 ± 0.05)	COD (70.5) NH_3-N (3.7) PO_4^{3-} (1.6)	COD (75.9) NH_3 (91.5) PO_4^{3-} (91.3)	(Chaudhary et al., 2018)
Scenedesmus obliquus	Municipal wastewater	7	0.31	TN (8.7±0.5) TP (1.71±0.3)	TN (ND) TP (ND)	TN (100) TP (100)	(Ji et al., 2013)
Parachlorella kessleri sp.	Municipal wastewater	12	1.01 ± 0.01	NH_3-N (100) TN (130) PO_4^{3-} (65)	NH_3-N (ND) TN (2.6) PO_4^{3-}(0.65)	NH_3-N (100) TN (98) PO_4^{3-}(99)	(Aketo et al., 2020)
Chlorella vulgaris	Municipal wastewater	14	1.0 ± 0.03	COD (160-200)	COD (64-80)	COD (55.5-64.45)	(Leong et al., 2019)

				NH_3-N (43-46)	NH_3-N (ND)	NH_3-N (100)	
Chlorella sorokiniana	Municipal wastewater	10	0.07	COD (44) NH_3-N (0.5) TP (1.9)	COD (16.9) NH3-N (0.12) TP (0.32)	COD (61.5) NH3-N (76) TP (83.16)	(Eladel et al., 2019)
Scenedesmus quadricauda	Dairy wastewater	12	0.47	TN (85.99) PO_4^{3-} (8.7)	TN (10.66) PO_4^{3-} (0.87)	TN (87.6) PO_4^{3-} (90.0)	(Daneshvar et al., 2019)
Chlorella pyrenoidosa	Livestock slaughterhouse wastewater	15	0.4	COD (3429.33) BOD (1798.33) NO_3-N (331.66) PO_4-$^{3-}$ (34.13)	COD (855.6) BOD (547.6) NO_3-N (48.0) PO_4-$^{3-}$ (4.4)	COD (75.05) BOD (69.5) NO_3-N (85.5) PO_4-$^{3-}$ (87.1)	(Azam et al., 2020)

(continued)

ND, not detected

Table 6.4: Amino acid (mg/g DCW) composition of whole biomass produced from *Scenedesmus* sp. DDVG I grew in the 3-L bioreactor under a mixotrophic condition.

Amino acids	***Scenedesmus* sp. DDVG 1** [a]	***Scenedesmus acuminatus*** [b]	***Nannochloropsis granulate*** [c]	***Spirulina*** [d]	***Chlorella vulgaris*** [e]	**Soybean** [f]
Non-essential amino acid (NEAA)						
Alanine	34.6 ± 0.0	23.31	23.0	45.9	11.2 ± 0.1	19.1-24.4
Aspartic acid	28.2 ± 0.1	25.58	35.5	59.9	13.7 ± 0.3	50.8-67.4
Cystine	2.9 ± 0.0	2.85	2.7	5.9	2.4 ± 0.2	5.3-6.5
Glutamic acid	39.7 ± 0.0	43.76	40.4	91.3	15.7 ± 0.5	75.4-102.5
Glycine	23.2 ± 0.0	14.8	18.3	31.3	8.6 ± 0.1	18-23.4
Hydroxyproline	34.8 ± 0.3	12.74	0.3	NR	0.7 ± 0.0	NR
Serine	17.3 ± 0.0	11.27	14.8	27.6	7.5 ± 0.1	22.7-29.4
Tyrosine	11.7 ± 0.1	9.31	14.1	25	6.4 ± 0.2	15.5-19.5
Essential amino acid (EAA)						
Arginine	21.3 ± 0.0	38.74	25.4	43.1	9.8 ± 0.1	29.3-44.4
Histidine	6.7 ± 0.0	9.01	7.5	10	3.1 ± 0.2	12.3-16.4
Isoleucine	14.3 ± 0.0	11.08	17.4	35	6.5 ± 0.0	12.3-15.4
Leucine	33.7 ± 0.0	24.96	32.4	53.8	13.4 ± 0.1	28.9-37.6
Lysine	19.1 ± 0.0	15.88	24.1	4.8	9.2 ± 0.3	24.2-37.6
Methionine	6.3 ± 0.0	4.71	8.7	11.7	3.5 ± 0.1	5.0-6.2
Phenylalanine	20.2 ± 0.0	16.21	19.1	NR	8.2 ± 0.1	19.8-25.2
Threonine	18.9 ± 0.1	14.02	16.5	28.6	6.4 ± 0.2	15.5-21.2
Valine	19.3 ± 0.09	14.78	21.5	39.4	9 ± 0.0	12.7-16.4
Total EAA	159.8	149.4	172.6	226.4	69.1	160-220.4
Total EAAR	0.45	0.50	0.53	0.44	0.51	0.43-0.44

(continued)

**NR:* not reported;* [a] present study; [b] (Zhang et al., 2019); [c](Tibbetts et al., 2015); [d](Dewi et al., 2016); [e](Tibbetts et al., 2015); [f](Serretti et al., 1994)

6.5 Fatty acid profile, and biodiesel assessment

The fatty acid profile (together with C14–C24 content) of *Scenedesmus* sp. DDVG I obtained over the 10 days of cultivation is presented in Table 6.5. The FAME were consisting of saturated fatty acid (SFA), unsaturated fatty acid (MUFA), and polyunsaturated fatty acid (PUFA). The total FAME content of the mixotrophically grown *Scenedesmus* sp. DDVG I in wastewater was 22.04% in DCW. The MUFA content (65.8%) in total FAME was predominant, followed by PUFA (19.1%), and SFA (15.1%). A higher concentration of MUFA in the FAME indicated a better quality of the biodiesel, owing to the oxidative stability and low-temperature fluidity (Cao et al., 2014). Furthermore, *Scenedesmus* sp. DDVG I was rich in C18:2 (linoleic acid) or also known as omega 6 fatty acid (18.9%). This FA is generally deficient in the human diet and animal feed (Mitra et al., 2012; Sinclair, 1990). The remarkable content of C18:2 in the present study showed a promising solution for a dietary source of human, aquaculture, and animal feed**.**

Table 6.5: FAME compositions of *Scenedesmus* sp. DDVG I in mixotrophic growth using 3-L bioreactor in the PMWW for a culture duration of 10 days.

FAME	%FAME in DCW	% FAME in total FAME
C14:0 (myristic)	0.53	2.4
C16:0 (palmitic)	0.37	1.7
C16:1 (palmitoleic)	5.89	26.7
C18:0 (stearic)	2.07	9.4
C18:1 (oleic)	8.38	38.0
C18:2 (linoleic)	4.17	18.9
C18:3 (linolenic)	0.02	0.2
C20:0 (arachidic)	0.35	1.6
C20:1 (gadoleic)	0.09	0.4
C22:1 (erucic)	0.07	0.3
C24:1 (nervonic)	0.10	0.4
SFA	3.32	15.1
MUFA	14.53	65.8
PUFA	4.19	19.1
Total FAME	22.04	100

(continued)

Based on the FAME profile, biodiesel parameters (including, DU, SV, IV, CN, LCSF, CFPP, CP, PP, OSI, HHV, FP, ρi, and η) were determined and summarized in Table 6.6. The results were represented with correspondence to the characteristics of the biodiesel standards EN 14214 (Europe) and ASTM D6751 (United States). We observed that all the tested parameters were comparable to the corresponding standard values. The IV (89.3 g I_2/100 g) of *Scenedesmus* sp. meets the current standard limit of the IV (it should be < 120). Thus, the biodiesel found from the lipid of this strain showed high oxidative stability. As shown in Table 6, the CN value (54.8) exceeded the minimum standard value of CN (it should exceed >51) which suggested that the combustibility of the fuel obtained from this biomass might be appropriate.

According to the analysis, the HHV value of *Scenedesmus* sp. (39.9 MJ/kg) attained the minimum standard value (>35 MJ/kg). This parameter allowed estimation of the energy potential and economic efficacy. Furthermore, density (0.87 g/cm^3) and viscosity (4.4 mm^2/s) met their corresponding standard values (Table 6.6). This demonstrated superior biodiesel, allowing transfer of a small mass of fuel to the engine, effective atomization, energy efficiency, as well as less deposition of fuel in the engine. Thus, *Scenedesmus* sp. DDVG I-derived biodiesel showed the viability of use in automobiles.

Table 6.6: Properties of *Scenedesmus* sp. DDVG I-derived biodiesel grown mixotrophically in the primary municipal wastewater (PMWW).

Properties	*Scenedesmus* sp. DDVG I	EN 14214	ASTM D6751
DU	103.6	NR	NR
SV (mg KOH/g oil)	191.1	NR	NR
IV (g I_2/ 100 g)	89.3	<120	NR
CN	54.8	>51	>47
LCSF	8.4	NR	NR
CFPP (°C)	9.9	NR	NR
CP (°C)	-3.0	NR	NR
PP (°C)	-10.2	NR	NR
OSI	4.4	NR	>3h
HHV (MJ/kg)	39.9	NR	>35
FP (°C)	421.1	>120	>93
ρ_i at 15 °C (g/cm^3)	0.87	0.86-0.90	0.82-0.90
η at 40 °C (mm^2/s)	4.4	3.5–5.0	1.9–6.0

NR: not reported

6.6 Conclusions

The novel strain *Scenedesmus* sp. DDVG I isolated from a fresh water-logged area was proven to be a robust candidate for wastewater bioremediation. Depending on the high growth rate and biomass yield, municipal wastewater can be an alternative low-cost medium for mixotrophic cultivation of *Scenedesmus* sp. The operation of a 3-L bubble photobioreactor for 10 days provided net biomass productivity of 0.069 g/ L. d of dried algae, a lipid yield of 22.5% DCW, and a FAME content of 22.04% in DCW. This study identified that *Scenedesmus* sp. DDVG I had valuable fatty acids and amino acid profile (EAA of 159.8 mg/g DCW) that can be converted to biodiesel as well as animal feed, respectively.

CHAPTER 7

Co-cultivation of microalgae and cyanobacterium in domestic wastewater by optimizing N/P ratio towards the production of biodiesel and protein-rich biomass for its feasibility as animal feed.

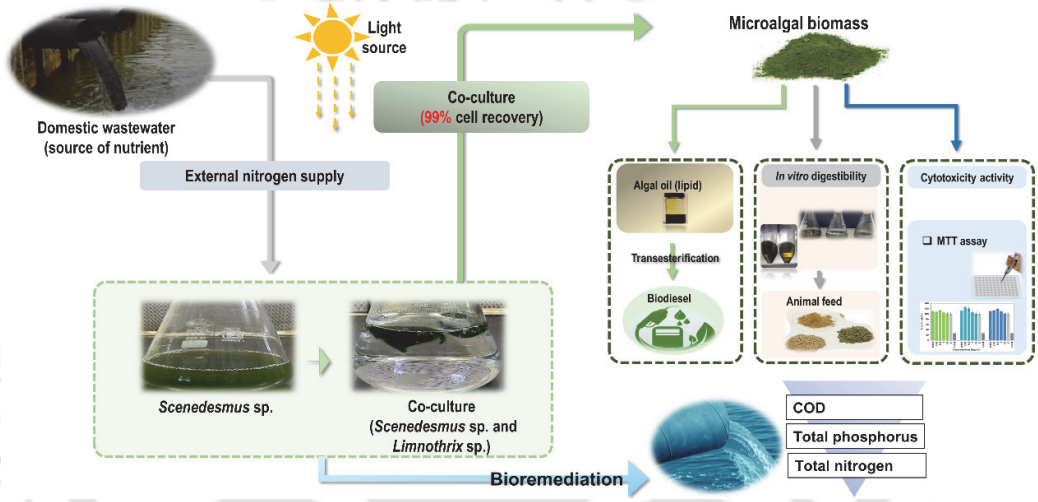

This work has been published as Nongmaithem Debeni Devi, Xiao Sun, Bo Hu, Vaibhav V. Goud, (2022). Bioremediation of domestic wastewater with microalgae-cyanobacteria co-culture by nutritional balance approach and its feasibility for biodiesel and animal feed production. Chemical Engineering Journal, 140197. https://doi.org/10.1016/j.cej.2022.140197.

CHAPTER 7

Co-cultivation of microalgae and cyanobacterium in domestic wastewater by optimizing N/P ratio towards the production of biodiesel and protein-rich biomass for its feasibility as animal feed.

Microalgae have been identified as a promising option for concomitant bioremediation of wastewaters and biodiesel generation. However, the nutritional composition of wastewater differs between locations, and some wastewater contains low nitrogen levels that inhibit microalgae growth, resulting in poor total nutrient removal and biomass output. Furthermore, the high cost of harvesting microalgae biomass is a barrier to commercial microalgae farming. This study aims to employ a novel microalga, Scenedesmus sp. DDVG I for bioremediation of low-nitrogen domestic wastewater. The nutritional balance of the wastewater was achieved with the addition of urea at two different levels and then was used for the cultivation of microalgae. The results showed that the optimized nutritional condition included total nitrogen (TN) of 250 mg/L and total phosphorus (TP) of 5 mg/L (N_{250}/P_5). The culture cultivated in this optimal medium improved chemical oxygen demand (COD), TN, and TP removal by as much as 89.5 %, 99.98 %, and 99.1 %, respectively. Scenedesmus sp. DDVG I growth was likewise at its peak, with a value of 5.1 g/L, but with a low harvesting efficiency (0.02 %). Subsequently, Scenedesmus sp. DDVG I was co-cultured with a novel cyanobacterium, Limnothrix sp. DDVG II under the optimal nutritional condition. The results revealed a 99.5 % increase in harvesting efficiency with effective wastewater treatment. The co-culture-derived biodiesel also complied with the standard specifications. Further, analysis of the essential amino acid content and in vitro digestibility of the biomass proved its usefulness as a feed supplement. Overall, this study demonstrated a promising future for a cleaner environment and sustainable bio-economy of microalgae.

7.1 Effect of varying N/P of wastewater in the heterotrophic and mixotrophic growth of *Scenedesmus* sp. DDVG I

Scenedesmus sp. DDVG I growth in mixotrophic and heterotrophic regimes was examined in DWW with varied N/P levels for 12 days. Results in Figure 7.1 showed that an increase in the N/P ratio in wastewater from 3.99/12.53 in DWW to 576/12.53 in the DWW with N_{250}/P_5 condition resulted in increased biomass production. The highest biomass concentration, 5.1 g/L, was recorded in the DWW with N_{250}/P_5 condition, followed by 4.5 g/L in the DWW with N_{100}/P_{50} condition after. Both of these values were significantly higher ($p=0.001$) than the biomass concentration of 3.1 g/L in the DWW condition over 12 days of cultivation in the mixotrophic mode (Figure 7.1c). Under a microscope observation, the mixotrophic regime showed negligible proliferation of unwanted microbes in the blank condition. The increase in Chl-a content in varying N/P conditions was also correlated with the increase in biomass in the mixotrophic regime. High Chl-a concentration in the mixotrophic cells further supported the ability of microalgae cells to photosynthesize and sustain in wastewater. Over 12 days, the Chl-a content of 8.0±0.05 mg/L was maximum in the DWW with N_{250}/P_5 condition, followed by 5.9±0.1 mg/L in DWW with N_{100}/P_{50} condition and 3.2±0.01 mg/L in DWW condition respectively (Figure 1d). In a study by Huo et al., (2020), the optimal N/P for the growth of *Tribonema* sp. was 30:1, producing maximum biomass of 2.04 g/L after 14 days cultivation. These values were significantly lowered than our present study (4.5 g/L). While *C. sorokiniana* showed a final average biomass concentration of 12 g/L with N:P ratios ranging between 15 and 26 (Fernandes et al., 2017). This clearly demonstrated that the ideal N/P condition in wastewater had a substantial impact on the growth and output of microalgae since they would assimilate nitrogen and phosphorus in a certain stoichiometric proportion (Beuckels et al., 2015; Choi and Lee, 2015).

The growth of *Scenedesmus* sp. DDVG I in the heterotrophic environment was, however, noticeably slower than in the mixotrophic regime. The maximal biomass content in the DWW with N_{250}/P_5 in heterotrophic mode was 0.7 g/L, which was even substantially lower ($p=0.001$) than 3.8 g/L in normal BG 11 (control condition) (Figure 7.1a). Contrary to the mixotrophic regime, a small population of bacterial growth was

evident in the heterotrophic blank condition. According to a similar finding by (Khan and Diba, (2016) and Devi et al., (2022), the heterotrophic mode encouraged microbial growth. They claimed that the heterotrophic mode provided bacteria with a dark fermentation environment and caused bacterial growth. The decrease in microalgal cell growth in heterotrophic was also correlated with the decrease in Chl-a content over 12 days of cultivation (Figure 7.1b). The Chl-a content in DWW with N_{250}/P_5, DWW with N_{100}/P_{50}, and DWW was as low as 0.4, 0.39 and 0.32 mg/L, respectively. This indicated that the photosynthetic pigment like Chlorophyll degrades in absence of light, resulting in an overall reduction of photosynthetic efficiency and thus inhibiting cell growth (Li et al., 2020). This signified that the heterotrophic mode of cultivation is unsuitable for *Scenedesmus* sp. DDVG I Similarly, our previous study reported that *Scenedesmus* sp. DDVG I was unable to grow in municipal wastewater under heterotrophic mode (Devi et al., 2022). According to similar findings by Roostaei et al., (2018), Patel et al., (2019), and Sajadian et al., (2018), mixotrophic culture yielded more microalgae biomass than heterotrophic growing modes. A mixotrophic mode produces the higher energy needed for higher cell densities through the catabolism of organic matter during photosynthesis in conjunction with aerobic respiration. They also stated that the presence of light is a limiting factor that promotes the higher availability of organic matter for mixotrophic microalgal growth. However, in heterotrophic mode, the non-biodegradability of organic resources for use by the lower cell caused lesser cell densities of microalgae (Patel et al., 2019).

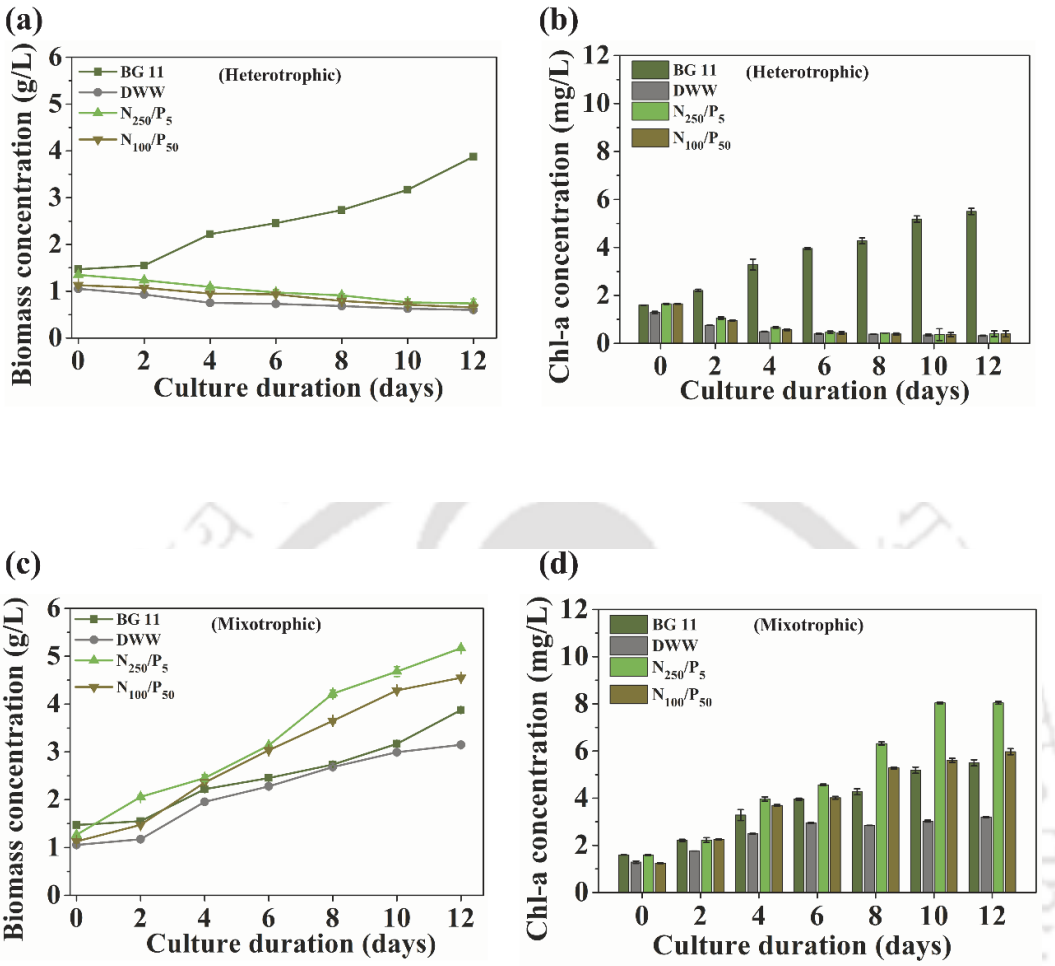

Figure 7.1: (a) Growth profile & (b) Chl-a content in heterotrophic mode (c) growth profile & (d) Chl-a content of *Scenedesmus* sp. DDVG I when grown in varying N/P concentrations of wastewater under heterotrophic and mixotrophic mode over 12 days.

7.2.1 Nutrient removal by Scenedesmus sp. DDVG I

Results in Figure 7.2 showed that the removal efficiencies of COD, TN, and TP by *Scenedesmus* sp. DDVG I in heterotrophic and mixotrophic mode. The content of COD in the wastewater varied with different N/P conditions. The maximum removal of COD (89.5±1.2 %) was achieved in DWW with N_{250}/P_5, followed by 75.2±0.89 % of N_{100}/P_{50} over 12 days of cultivation in mixotrophic mode. However, the COD removal (25±1.5 %) in DWW was significantly lower than 47.2±1.2 % in normal BG 11 conditions after 12 days of cultivation. The TP removal from DWW with N_{250}/P_5 and N_{100}/P_{50} were 99.1±1.2 % and 97.7±1.25 %, respectively. Their corresponding TN removal was as

high as 99 %. However, the TN and TP removal in DWW were 96.3±0.9 %, and 70.12±1.2 % respectively. The change in nutrient removal rate was consistent with the growth of *Scenedesmus* sp. DDVG I cell. Most importantly, Beuckels et al., (2015) reported that microalgae maintain the structural components by accomplishing the Redfield Ratio with N:P molar ratios ranging between 8:1 and 45:1. Apparently, the biomass achieved the desired N and P concentration in their biomass in relation to the surrounding N/P in the medium.

Under heterotrophic mode, the COD removal from DWW with N_{250}/P_5, DWW with N_{100}/P_{50}, and DWW were 46.9±1.1, 40.9±1.1, and 18.0±1.1 %, respectively (Figure 7.2a). The corresponding TN and TP removal from the three media were 82.6±1.1 and 76.1±1.1 %, 75.2±1.5 and 70.1±1.1 %, and 86.7±1.02 and 57.9±1.0 %, respectively (Figure 7.2d-f). The effective removal of nutrients even after less cell growth could be contributed by the growth of bacteria favoring a dark fermentation environment (Khan and Diba, 2016). In this study, we could confirm that the ideal N/P ratio for enhanced growth for *Scenedesmus* sp. DDVG I was 576/12.53 (DWW with N_{250}/P_5, see Table 2.4). Therefore, this ideal condition was further employed to evaluate the co-cultivation experiment.

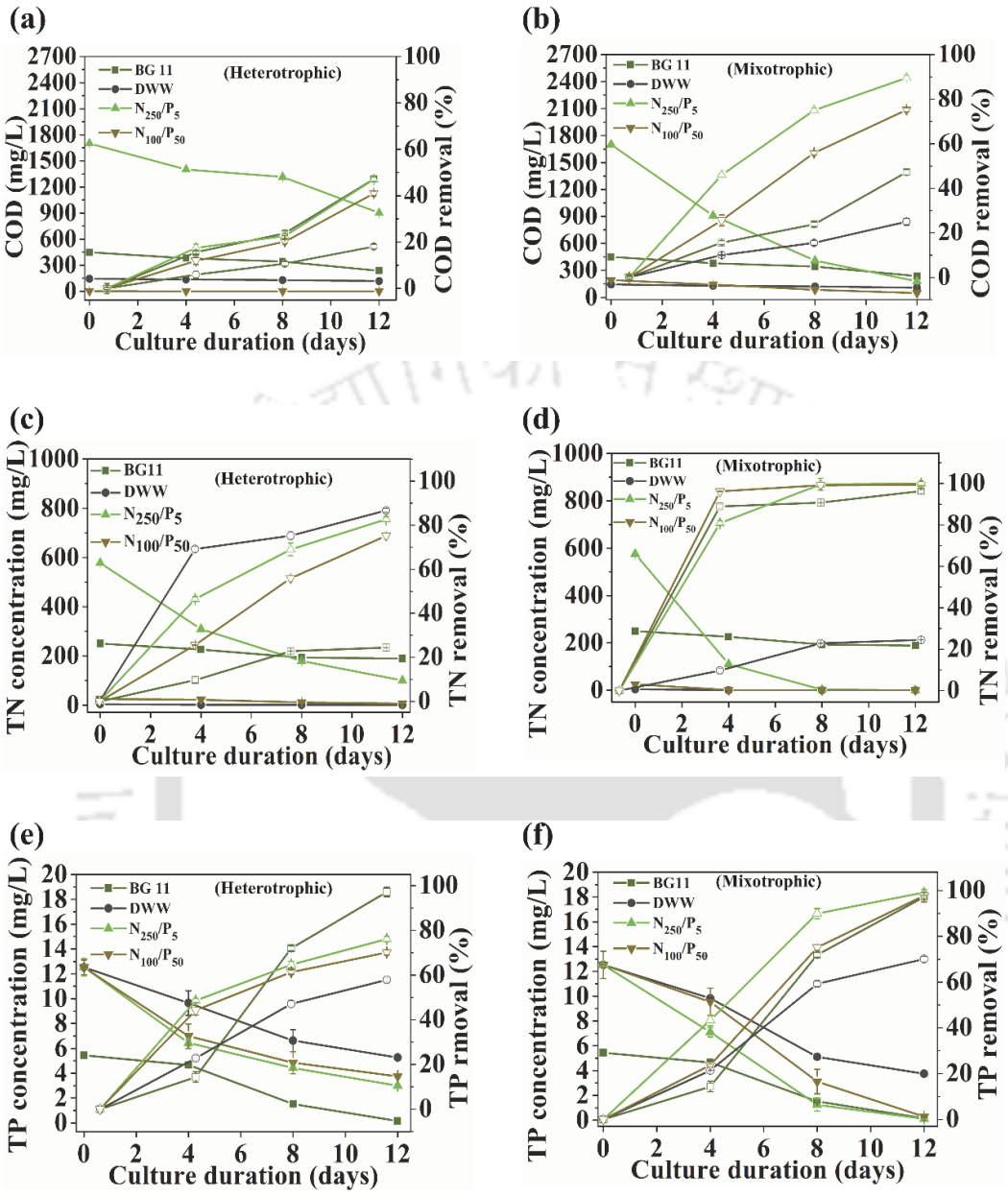

Figure 7.2: Nutrient removal efficiencies by *Scenedesmus* sp. from varying N/P concentrations of wastewater (a) COD removal under mixotrophic mode; (b) COD removal under heterotrophic mode; (c) TN removal under mixotrophic mode; (d) TN removal under heterotrophic mode; (e) TP removal under mixotrophic mode; (f) TP removal under heterotrophic mode.

7.3 Co-cultivation of *Scenedesmus* sp. DDVG I and *Limnothrix* sp. DDVG II in DWW with N_{250}/P_5 under mixotrophic mode

Scenedesmus sp. DDVG I and *Limnothrix* sp. DDVG II was co-cultivated in the ratio of 1:1 by volume. The cultivation was performed mixotrophically in DWW with N_{250}/P_5 and the characteristics of the growth were presented in Figure 7.3. It was evident from Figure 7.3a that the maximum biomass concentration of 5.5±0.03 g/L was produced by the co-culture system as compared to 5.1 g/L for *Scenedesmus* DDVG I and 4.5±0.01 g/L of *Limnothrix* sp. DDVG II. The results in Figure 7.3b showed the increase in Chl-a content in the co-culture system over 12 days of cultivation. The higher Chl-a content of 9.3±0.12 mg/L was recorded in the co-culture system when compared to 8.04±0.05 mg/L in *Scenedesmus* sp. DDVG I and 7.5±0.1 mg/L in *Limnothrix* sp. DDVG II. The highest cell harvesting efficiency of 99.5 % (see Table 7.1) was achieved by the co-culture system, resulting in biomass productivity of 70.8±1.1 mg/L. d. *Scenedesmus* sp. DDVG I and *Limnothrix* sp. DDVG II showed lower harvesting efficiency of 0.02 % and 65.9 %, resulting in biomass productivities of 52.5±1 mg/L. d and 26.5 mg/L. d, respectively. In astudy by Cheng et al., (2020a), the authors found that co-cultivation of *Tribonema* sp. and *Chlorella zofingiensis* in swine wastewater resulted in maximal biomass production of 1.95 g/L and cell recovery efficiency of 88.6 %, which were lower than in the current study. Harvesting of microalgal biomass is one of the major challenges in microalgal cultivation (Molina Grima et al., 2003). The present study represented an easy and high cell recovery performance through co-cultivation of *Scenedesmus* sp. DDVG I and *Limnothrix* sp. DDVG II. It was clearly evident from Figure 7.3c that filamentous *Limnothrix* sp. DDVG II established a criss-cross mat and entangled the minute *Scenedesmus* sp. DDVG I cell. Our previous study reported that filamentous *Limnothrix* sp. DDVG II secrets EPS favoring the formation of biofilm. In addition, *Limnothrix* sp. DDVG II possesses gas vesicles that support the floatation of the cells on the water bodies and thus enhance easy cell recovery (Devi et al., 2021).

Results in Table 7.1 showed that the lipid content of individual *Scenedesmus* sp. DDVG I, and *Limnothrix* sp. DDVG II in terms of dried biomass was 34% and 11.14 %, respectively. However, the lipid content in dried biomass of the co-culture system ramped up to 46.2 %. These results were comparable with the findings of (Cheng et al.,

2020b). In their study, the co-culture of *Tribonema* sp. and *C. zofingiensis* had higher lipid content of 44.12 % dried biomass when compared to the lipid content of 42.78% and 18.82 % in monoculture in *Tribonema* sp. and *C. zofingiensis*, respectively. The increased lipid content in co-culture might be correlated with the dense population of the cells. However, the actual mechanism behind the increase in lipid production by co-culture is still not understood. Some researchers suggested that the growth of bacteria within the microalgae consortium might trigger a stressful environment on microalgae and thus stimulate lipid biosynthesis (Cheng et al., 2020b). However, the hypothesis may not be applicable for enhanced lipid production in the current study because the bacterial growth was insignificant as mentioned in section 6.2. Some researchers also suggested that the synergistic effects between the symbiotic species and the competition on nutrient uptake (nutrient starvation) are directly associated with the augmentation in lipid yield under co-culture conditions (Magdouli et al., 2016). The significant lipids derived from *Scenedesmus* sp. DDVG I and the co-culture system were further analyzed for their feasibility for biodiesel production.

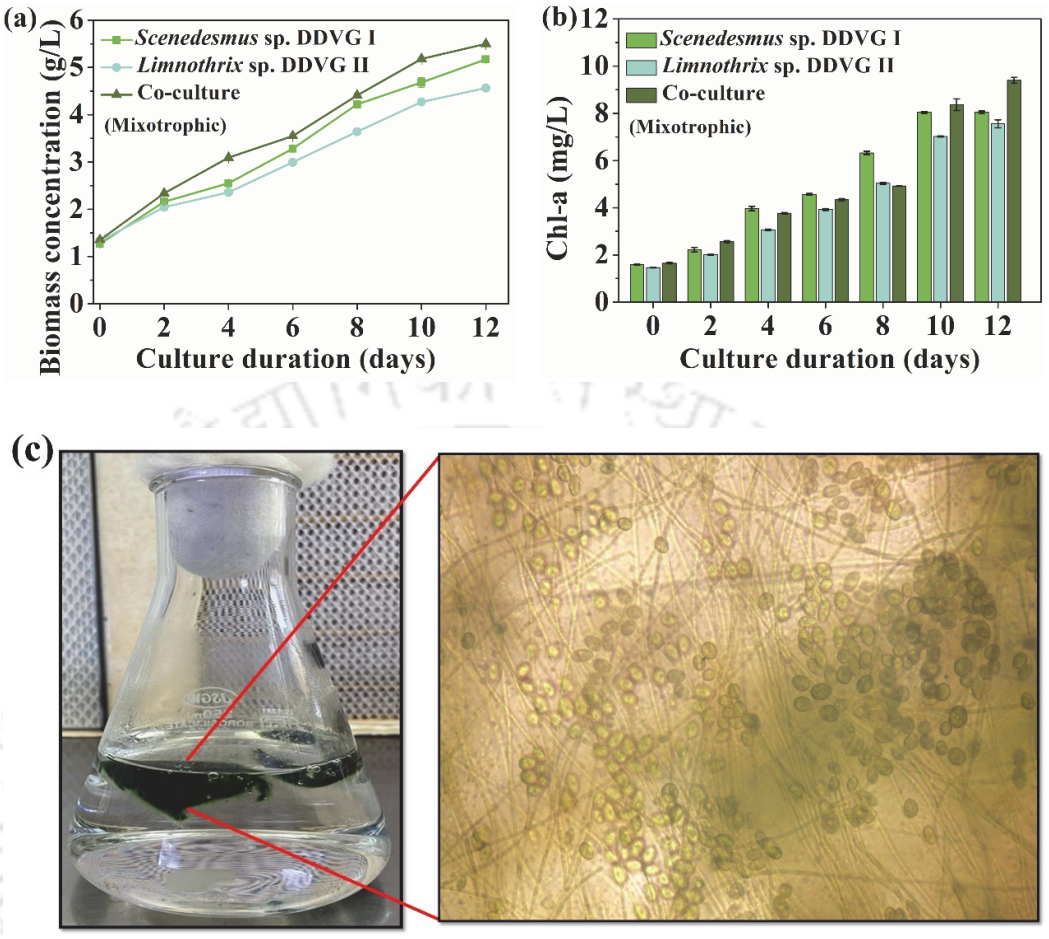

Figure 7.3: (a) Growth profile (b) Chl-a content and (b) co-culture of *Scenedesmus* sp. DDVG I and *Limnothrix* sp. DDVG II [inset: observation of symbiotic association of *Scenedesmus* sp. DDVG I and *Limnothrix* under 40X using light microscopy] grown in DDWW with N_{250}/P_5 in mixotrophic condition for 12 days.

7.3.1 Nutrient removal

The performance of nutrient removal (COD, TN, TP) by the co-culture system from the DWW with N_{250}/P_5 was evaluated periodically for 12 days. The values were compared with the performance of individual *Scenedesmus* sp. DDVG I, *Limnothrix* sp. DDVG II and literature reports as presented in Table7.1. The removal efficiency of COD by the co-culture system, *Scenedesmus* sp. DDVG I, and *Limnothrix* sp. DDVG II over 12 days were 90.2, 89.9 and 66.8 % respectively. The high removal of COD by the co-culture reflected the increased biomass production. This could be due to the domestic

wastewater containing high organic matter, that was assimilated by the culture and supported the growth. The existence of recalcitrant organic molecules in the wastewater, however, was difficult for microalgae to decompose. This might cause incomplete remediation of COD (Xia and Murphy, 2016). However, the present values were comparatively higher than the findings of literature reports (Cheng et al., 2020b; Devi et al., 2022; Tsolcha et al., 2018b) as shown in Table 7.1. The removal of TN and TP by *Scenedesmus* sp., DDVG I, *Limnothrix* sp. DDVG II and co-culture over 12 days were 99.9 & 99.1 %, 98.4 & 82.7 %, and 99.9 & 99.2 %, respectively. The reason for the effective removal of nitrogen and phosphorus from the wastewater by co-culture indicated that the N/P ratio in DWW with N_{250}/P_5 achieved the specific stoichiometric proportion. This ratio promoted the growth of the co-culture resulting in an increase in cell density and enhanced nutrient uptake from the wastewater (Choi and Lee, 2015; Zhang et al., 2020). Thus, the study demonstrated an effective bioremediation system and overall biomass productivity through co-cultivation.

7.4 Fatty acid profile, and biodiesel assessment

The fatty acid profile consisting of C14 to C24 for *Scenedesmus* sp. DDVG I and co-culture condition is outlined in Table 7.2. FAME is made up of saturated fatty acids (SFA), unsaturated fatty acids (MUFA), and polyunsaturated fatty acids (PUFA). FAME is made up of saturated fatty acids (SFA), unsaturated fatty acids (MUFA), and polyunsaturated fatty acids (PUFA). The following FAME profile was found in the total FAME content of the mixotrophically produced *Scenedesmus* sp. DDVG I in DWW with N_{250}/P_5: 15.1 % of SFA, 65.8 % of MUFA, and 19.1 % of PUFA. The FAME composition of the co-culture also had a high concentration of 47.5 % of SFA, 36.3 % of MUFA, and 16.02 % of PUFA. A higher MUFA concentration in the FAME suggested improved biodiesel quality due to oxidative stability and low-temperature fluidity (Cao et al., 2014). Furthermore, *Scenedesmus* sp. DDVG I was rich in C18:2 (linoleic acid) or also known as omega 6 fatty acid (18.9%). This FA is generally deficient in the human diet and animal feed (Mitra et al., 2012). The remarkable content of C18:2 in the present study showed a promising solution for a dietary source of human, aquaculture, and animal feed.

The properties of biodiesel derived from *Scenedesmus* sp. DDVG I and co-culture were determined using the FAME profile and reported in Table 7.3. The results were represented with respect to the characteristics of the biodiesel standards EN 14214 (Europe) and ASTM D6751 (United States). We observed that all the tested parameters were comparable to the corresponding standard values. The HHV value of *Scenedesmus* sp. DDVG I (39.9 MJ/kg) and co-culture (39.87 MJ/kg) met the minimal standard value (>35 MJ/kg), according to the analysis. This metric allows for the evaluation of energy potential as well as economic efficacy. Furthermore, the density (0.87 g/cm^3) and viscosity (4.8 and 4.6 mm^2/s) met the standards (Table 7.3). This appears to be excellent biodiesel, enabling a small mass of fuel to be transferred to the engine, effective atomization, energy efficiency, and reduced fuel deposition in the engine.

The IVs of *Scenedesmus* sp. DDVG I (67.96 g I_2/ 100 g) and co-culture (71.47 g I_2/ 100g) meet the current standard limit of the IV (it should be < 120). Thus, the biodiesel found from the lipid of this strain showed high oxidative stability. As shown in Table 7.3, the CN value of both the cultures exceeded the minimum standard value of CN (it should exceed >51). This suggested that the combustibility of the fuel obtained from this biomass might be appropriate. Thus, *Scenedesmus* sp. DDVG I and co-culture generated biodiesel show promise for their use in vehicles.

7.5 Evaluation of amino acid content

Results in Table 7.4 provides a summary of the amino acid profile of the completely dried algal cells produced from the co-culture system and individual cultures. We found that there were eight NEAA and nine EAA in the biomass. *Scenedesmus* sp. DDVG I and co-culture system cultivated in DWW with N_{250}/P_5 had an EAAR value of 0.46, whereas *Limnothrix* sp. DDVG II had an EAAR value of 0.44, which was marginally higher than the EAAR of soybean (0.43-0.44) (Serretti et al., 1994). Likewise, an earlier study revealed that *Scenedesmus* sp. DDVG I cultivated in the sewage treatment plant had an EAAR value of 0.45. According to Miao et al., (2016), mixotrophically grown *Chlorella vulgaris* in domestic wastewater produced an EAAR value of 0.37. Their value was comparatively lower when compared to the current study. Additionally, the EAA contents of these studies (159.8 mg/g DCW and 42.99 mg/g DCW) were

comparable to those of other reference proteins like soybean (EAA content, ranging from 160 to 220.4 mg/g DCW) (Serretti et al., 1994), *Spirulina* (EAA content = 226.4 mg/g DCW) (Dewi et al., 2016), *Nannochloropsis* granulate (EAA content = 172.6 (Zhang and Li, 2019)). This indicated that the nutrient balancing of DWW might cause EAA accumulation in *Scenedesmus* sp. DDVG I, *Limnothrix* sp. DDVG II and co-culture system. This shows the viability of using these organisms as animal and aquaculture feed.

Table 7.1: The biomass productivity, lipid content, cell harvesting and nutrient removal efficiency of *Scenedesmus* sp. DDVG I and co-culture cultivated mixotrophically in domestic wastewater treated with urea were compared to earlier investigations.

Species	**Culture medium**	**Initial concentration (mg/L)**			**Cell harvesting efficiency (%)**	**BC (g/L)**	**BP (mg/L.d)**	**Lipid (%)**	**Removal efficiency (%)**			**Ref.**
		COD	**TN**	**TP**					**COD**	**TN**	**TP**	
Scenedesmus sp. DDVG I	Domestic wastewater supplemented with urea	1700± 1.9	576± 1.9	12.5±1.9	0.02	5.17	52.5±1.1	34	89.5	99.9	99.1	**This study**
Limnothrix sp. DDVG II	Domestic wastewater supplemented with urea	1700± 1.9	576± 1.9	12.5±1.9	65.8 ±1.1	4.5±0.13	26.5	11.14	66.8	98.4	82.7	**This study**
Mixed culture (*Scenedesmus sp.* DDVG I and *Limnothrix* sp. DDVG II)	Domestic wastewater supplemented with urea	1700± 1.9	576± 1.9	12.5±1.9	99.5	5.4±0.09	70.8±1.1	46.2	89.9	99.9	99.2	**This study**

Tribonema sp. and *Chlorella zofingiensis*	Swine wastewater diluted with fishery wastewater	6280	965	96	88.6	1.95	-	44.12	89.1	80.5	84.7	(Cheng et al., 2020b)
Chlorella sp. MJ 11/11 and *Aspergillus* sp.	Tris Acetate Phosphate buffer	-	-	-	> 92	2.37 ± 0.12	-	14	-	-	-	(Lal et al., 2021)
S. obliquus and C. vulgaris	Urban wastewater sample	-	-	-	-	0.9 g/L.d	-	-	-	98	100	(Cuellar-Bermudez et al., 2017)
Chlorella vulgaris, Botrycoccus terribilis	Municipal wastewater	-	-	-	-	0.28 g/L.d	-	-	>70	-	-	(Cabanelas et al., 2013)

(continued)

Table 7.2: FAME compositions of *Scenedesmus* sp. DDVG I, and co-culture grown in DWW with N_{250}:P_5 medium under mixotrophic condition.

FAME	**% FAME in total FAME**	
	***Scenedesmus* sp. DDVG I**	**Co-culture (*Scenedesmus* sp. DDVG I and *Limnothrix* sp. DDVG II)**
C14:0 (myristic)	2.4	11.2
C16:0 (palmitic)	1.7	1.8
C16:1 (palmitoleic)	26.7	6.6
C18:0 (stearic)	9.4	15.8
C18:1 (oleic)	38.0	27.2
C18:2 (linoleic)	18.9	2.19
C18:3 (linolenic)	0.2	13.8
C20:0 (arachidic)	1.6	18.5
C20:1 (gadoleic)	0.4	2.06
C22:1 (erucic)	0.3	0.30
C24:1 (nervonic)	0.4	0.07
SFA	15.1	47.5
MUFA	65.8	36.3
PUFA	19.1	16.02
Total FAME	100	100

Table 7.3: Biodiesel characteristic of *Scenedesmus* sp. DDVG I and co-culture when cultured in DWW with N_{250}:P_5 medium under mixotrophic mode.

Properties	***Scenedesmus* sp. DDVG I**	**Co-culture (*Scenedesmus* sp. DDVG I and *Limnothrix* sp. DDVG II)**	**ASTM D6751**	**EN 14214**
HHV (MJ/kg)	39.9	39.87	>35	NR
FP (°C)	426.4	420.1	>93	>120
ρ_i at 15 °C (g/cm^3)	0.87	0.87	0.82-0.90	0.86-0.90
η at 40 °C (mm^2/s)	4.8	4.6	1.9–6.0	3.5–5.0
DU	66.74	68.51	NR	NR
SV (mg KOH/g oil)	188.06	191.71	NR	NR
IV (g I_2/ 100 g)	67.96	71.47	NR	<120
CN	60.02	58.6	>47	>51
LCSF	24.06	26.7	NR	NR
CFPP (°C)	59.1	67.45	NR	NR
CP (°C)	-3.7	-4.0	NR	NR
PP (°C)	-10	-11	NR	NR
OSI	6.6	6.31	>3h	NR

NR: not reported

Table 7.4: Amino acid content (mg/g DCW) of entire biomass generated by *Scenedesmus* sp. DDVG I, *Limnothrix* sp. DDVG II, and the co-culture system in the DWW with N_{250}:P_5 medium mixotrophically.

Amino acids	*Scenedesmus* sp. DDVG I	*Limnothrix* sp. DDVG II	Co-culture (*Scenedesmus* sp. DDVG I and *Limnothrix* sp. DDVG II)	*Spirulina* [a]	Soybean[b]
Non-essential amino acid (NEAA)					
Alanine	42.49 ± 0.0	17.69	34.78	45.9	19.1-24.4
Aspartic acid	28.07 ± 0.1	15.32	27.1	59.9	50.8-67.4
Cystine	0.72 ± 0.0	0.52	1.06	5.9	5.3-6.5
Glutamic acid	41.11 ± 0.0	17.50	33.05	91.3	75.4-102.5
Glycine	25.92 ± 0.0	11.96	24.84	31.3	18-23.4
Hydroxyproline	24.16 ± 0.3	16.59	19.82	-	-
Serine	17.42 ± 0.0	20.88	17.94	27.6	22.7-29.4
Tyrosine	10.4 ± 0.1	5.17	10.06	25	15.5-19.5
Essential amino acid (EAA)					
Arginine	17.52 ± 0.0	10.79	14.54	43.1	29.3-44.4
Histidine	5.34 ± 0.0	7.05	4.61	10	12.3-16.4
Isoleucine	15.76 ± 0.0	7.32	14.49	35	12.3-15.4
Leucine	34.88 ± 0.0	16.19	32.04	53.8	28.9-37.6
Lysine	18.40 ± 0.0	8.25	15.16	4.8	24.2-37.6
Methionine	7.7 ± 0.0	1.63	5.08	11.7	5.0-6.2
Phenylalanine	21.09 ± 0.0	9.82	19.53	NR	19.8-25.2
Threonine	19.88 ± 0.1	10.76	19.64	28.6	15.5-21.2
Valine	22.3 ± 0.09	10.34	20.53	39.4	12.7-16.4
Total EAA	162.87	82.14	145.62	226.4	160-220.4
Total EAAR	0.46	0.44	0.46	0.44	0.43-0.44

(continued) [a] (Tibbetts et al., 2015); [b] (Serretti et al., 1994)

7.6 Evaluation of IVD and cytotoxicity of microalgae

The utilization of *Scenedesmus* sp., DDVG I, *Limnothrix* sp. DDVG II, and co-culture as a feed supplement are indicated by the IVD of algal biomass. According to Table 7.5, the maximum IVD of biomass was achieved by *Scenedesmus* sp. DDVG I with 62±1.1 % of dried biomass, followed by co-culture and *Limnothrix* sp. DDVG II with values of 58±1 and 43±1.2 % dried biomass respectively. The corresponding *in vitro* digestibility of protein (IVPD) based on dried biomass was 89±0.9, 85.5±1.1, and 65±1.5 %, respectively. The IVPD is reflected in the availability of amino acids that can be easily utilized within the body. Kose et al., (2017) reported that almost 70% of *C. vulgaris* biomass and 97% of *S. platensis* were digestible. Their study stated that the incomplete digestibility of the biomass could be affected by the variations in compositions and structures in the cell wall (Kose et al., 2017). The cell wall of cyanobacteria is mainly made up of peptidoglycan resembling Gram-negative bacteria cell wall with a thickness of 40–60 nm while the microalgal cell wall is composed of thick cellulose. Thus, the presence of this highly rigid cell wall obstructs the organism from achieving the complete digestibility of the whole biomass (Monks et al., 2013).

Table 7.5: Evaluation of in vitro digestibility of *Scenedesmus* sp. DDVG I, *Limnothrix* sp. DDVG II and co-culture obtained from DWW with N_{250}/P_5.

Culture	**IVD (% dried biomass)**	**IVPD (% dried biomass)**
Scenedesmus sp. DDVG I	62±1.1	89±0.9
Limnothrix sp. DDVG II	43±1.2	65±1.5
Co-culture (*Scenedesmus* sp. DDVG I and *Limnothrix* sp. DDVG II)	58±1	85.5±1.1

The cytotoxic effect of different extracts from *Scenedesmus* sp. DDVG I, *Limnothrix* sp. DDVG II, and co-culture were tested against BHK 21 cells using MTT colorimetric assay. The viability of the cell lines was measured after 24 h exposure to the different concentrations (0.001, 0.01, 0.1, 1.0, and 10 mg/mL) of the extracts. Results in Figure 7.4 clearly demonstrated that treated concentrations of the microalgal extracts

stimulated the growth of the cells instead of causing inhibition, thus indicating there was no evidence for cytotoxicity. Similarly, Gürlek et al., (2020) reported that exposure to different microalgal extracts against the HepG2 cell line promoted cell growth. The reason for the enhancement of growth might be due to the presence of antioxidant metabolites and phenolic compounds in the microalgal extracts that prevent the cell lines from oxidative stress and even enhance their viability (Mukherjee et al., 2022). This suggested that the microalgal extracts are safe to use as feed supplements. Furthermore, this is the first study to describe the viability of *Scenedesmus* sp. DDVG I and *Limnothrix* sp. DDVG II for feed supplementation. Hence, more research including an *in vivo* study using a fish model is envisaged for safe consumption before establishing these strains as feed.

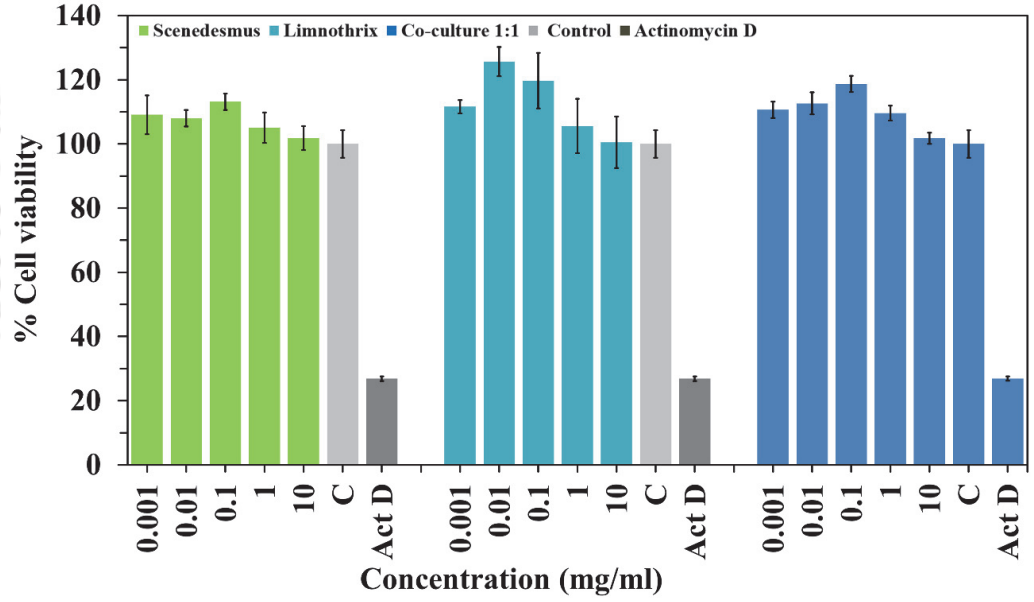

Figure 7.4: Effect of different concentrations of *Scenedesmus* sp. DDVG I, *Limnothrix* sp. DDVG II and co-culture extracts on BHK 21 cell viability at 24th h. C represents the control containing only DMSO but without microalgal extracts, Act D denotes Actinomycin d-treated cells as a positive control to mark the cell cytotoxicity and cell death.

7.7 Conclusion

We discovered a promising co-cultivation strategy of novel strains *Scenedesmus* sp. DDVG I and *Limnothrix* sp., DDVG II that not only thrived in DWW but also had a high performance for the treatment of the wastewater. The nutritional balancing at an N/P ratio of 576/12.53 might be the optimal method to obtain the highest removal rate of COD, TN, and TP toward DWW bioremediation. Moreover, the co-cultivation approach exhibited an efficient cell harvesting of 99.5 %. The biomass derived from this approach showed potential for the production of biodiesel as well as animal feed. Thus, it can be concluded that this unique co-cultivation strategy concomitantly facilitates easy harvest, generates valuable bioresources and provides a biorefinery prospect.

Chapter 8

Overall conclusion and future scope

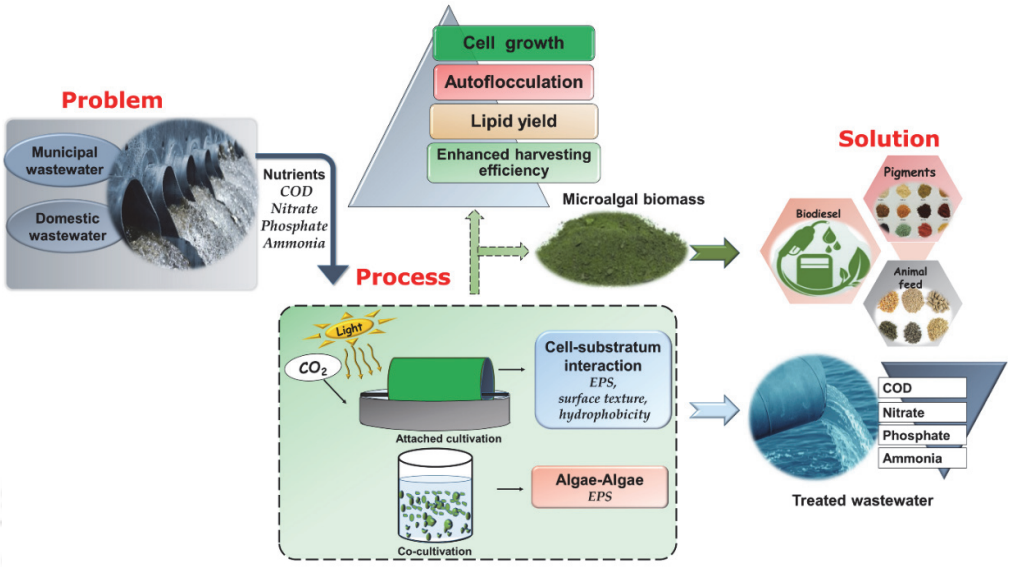

Chapter 8

Overall Conclusions and Future Scope

In this work, local freshwater microalgae species were isolated from relatively untapped microalgae resources in North East India, appropriate oleaginous microalgae species were identified and characterized, and several physicochemical parameters for biodiesel synthesis were tested. The key conclusions of the entire thesis are therefore presented below based on the investigation that was conducted:

8.1 Conclusions

- 18S rRNA and 16 S rRNA confirmed that microalga DDVG I and cyanobacterium DDVG II belonged to *Scenedesmus* sp. with accession no. MN630585 and *Limnothrix* sp. with accession no. MN630310 respectively. This genus has been extensively studied and documented for its remarkable characteristics such as rapid growth, as well as high biomass and oil yield, which makes it an ideal candidate for our research. The cyanobacterium is characterized by its filamentous morphology. At pH 7 and 27 °C, both the strains achieve optimal growth in BG 11 medium. The medium containing urea, K_2HPO_4 with glucose addition medium showed the ideal substrate resulting in increased biomass output of 4.1 g/L for *Scenedesmus* sp. DDVG I and 2.4 g/L for *Limnothrix* sp. DDVG II respectively. Under varied glucose concentrations, 6 g/L of glucose resulted in the maximum biomass growth and lipid content of 8 g/L & 40 % for *Scenedesmus* sp. DDVG I and 3.4 g/L & 18 % for *Limnothrix* sp. DDVG II, respectively. The lipid generated by both the strains included about 60–90 % of SFA and MUFA fatty acids. These observations provided insights into the characteristics and growth conditions of two strains of microalgae and cyanobacteria and their lipid production potential, which might have applications in biofuels and bioremediation.
- The genus *Limnothrix* is well known for its filamentous morphology and secretion of extracellular polymeric substances (EPS), which contribute to cell aggregation or auto-flocculation and facilitate the harvesting process. In this study, different extraction methods were employed to confirm the production of EPS by the novel *Limnothrix* sp. DDVG II. As expected, DDVG I produced significant EPS on 12 days or during the early stationary phase of the growth phase. However, DDVG II produced negligible amount of EPS over 12 days of culture period. By exposing EPS to various substrata, its adhesive quality was confirmed with maximum

adhesion on rough polylactic acid (PLA) sheet. The characterization of EPS revealed the mesh-like structure, presence of various polysaccharides, protein moieties, different cations in EPS that would support cell-cell interaction, and adhesion on substrata. The adhesion of EPS was maximum on rPLA over 12 days. The rPLA coated with EPS-12 showed the maximum biofilm formation of *Scenedesmus* sp. DDVG I cell, resulting in biomass accumulation of 31.6 ± 1.2 g/m^2. d. This work suggested the feasibility of co-cultivation of non-flocculting *Scenedesmus* sp. DDVG I and *Limnothrix* sp. DDVG II for form biofilm.

- Selection of balanced nitrogen (N): phosphorus (P) ratio in nutritional source is critical to achieve simultaneous enhancement of biomass and lipid production in microalgae. In this study, *Scenedesmus* sp. DDVG I was cultivated under various regimes of N:P ratio containing BG 11 with the supplementation of 6 g/L of glucose. The combined effect of N-limitation and over excessive P (N_{def} P_{oexcs}) (100 mg/L of N and 50 mg/L of P condition) showed an effective condition to enhance the growth and lipid content by *Scenedesmus* sp. DDVG I in mixotrophic mode. Further, in attempting to facilitate the harvesting step, we co-cultured *Scenedesmus* sp. with *Limnothrix* sp. DDVG II mixotrophically under inoculum ratio of 1:1, 1:2, 2:1 in the N_{def} P_{oexcs} condition. The co-culture 1:1 system achieved the maximum biomass harvesting efficiency of 99.9± 0.5 % with an increase in BP and LY up to 42.0 ± 0.9 mg/L. d and 40.2 ± 1.0 % DCW, respectively. The fatty acid methyl ester compositions of co-culture 1:1 was rich in C18:2 (36.05 %), C16:0 (32.25 %), C18:1 (16.86 %), and C18:0 (7.68 %). The biodiesel derived from the co-culture 1:1 also complied with standard specifications, making it appropriate for the production of biodiesel. The overall findings demonstrated a unique co-culture approach toward easy harvesting while concurrently maximizing biomass and lipid yield when grown in a balanced N:P ratio of 100:50. The techno-economic analysis of the system, biodiesel cost, and its implementation toward biorefinery approach can be envisaged in the future study.
- The study investigated the feasibility of primary municipal wastewater (PMWW) collected from a local wastewater treatment plant in Minnesota, USA as an alternative to growth media for novel strain, *Scenedesmus* sp. DDVG I cultivation.

The study confirmed the wastewater as a potential growth medium while *Scenedesmus* sp. DDVG I showed superior biomass productivity (0.069 g/L d), lipid yield (22.5%), and FAME content (22.04 % in dry cell weight) over 10 days in the mixotrophic mode. The biomass also showed high essential amino acid content (159.8 mg/g DCW). The corresponding values for bioremediation efficiencies COD and TN were 75.6% and 99.8% respectively. Meanwhile, NH_3–N and TP were removed at up to 100%. Analyses of fatty acid profile and different parameters that were required for biodiesel characterization revealed the high-quality nature of the *Scenedesmus*-derived biodiesel. This study identified that *Scenedesmus* sp. DDVG I had valuable amino acid profile (EAA of 159.8 mg/g DCW) that can be used as animal feed, respectively. Overall, the study concluded effective bioremediation of municipal wastewater by *Scenedesmus* sp. DDVG I with the recovery of valuable resources from the biomass.

- There is a variety of low strength (domestic and municipal wastewaters) and the nutritional compositions vary between locations. For example, DWW from IITG had lo nitrogen level that inhibit microalgae growth. In this study, the nutritional balance of the DWW was achieved with the addition of urea at two different levels and then was used for the cultivation of *Scenedesmus* sp.. *Scenedesmus* sp. showed maximum growth (5.1 g/L) in the modified DWW condition consisting of 250 mg/L of TN and 5 mg/Lof TP (N_{250}/P_5). The culture cultivated in this optimal medium improved COD, TN, and TP removal by as much as 89.5 %, 99.98 %, and 99.1 %, respectively. Subsequently, *Scenedesmus* sp. DDVG I was co-cultured with *Limnothrix* sp. DDVG II in DWW with N_{250}/P_5 mixotrophically. The results revealed a 99.5 % increase in harvesting efficiency with effective wastewater treatment. The co-culture-derived biodiesel also complied with the standard specifications. Analysis of the essential amino acid content and in vitro digestibility of the biomass proved its usefulness as a feed supplement. Using the MTT test, the evidence of no cytotoxicity of various doses of biomass extracts on BHK 21cells were confirmed. This suggested that the microalgal extracts are safe to use as feed supplements. Furthermore, this is the first study to describe the viability of *Scenedesmus* sp. DDVG I and *Limnothrix* sp. DDVG II for feed supplementation.

Hence, more research including an in vivo study using a fish model is envisaged for safe consumption before establishing these strains as feed.

8.2 Future scope

The findings of this work provided insights into molecular identification, selection of growth conditions, evaluation of EPS production for biofilm formation, optimization of physicochemical parameters for enhanced growth, and co-cultivation strategy for enhanced recovery of biomass and lipid accumulation studies by using synthetic and wastewater as a source of nutrients. The following studies which are listed below are envisaged in the future for the enrichment of the algal process, improvement of biodiesel quality, the economic viability of microalgal biomass, etc.

- Cultivation in semi-continuous system to understand the performance of the microalgae under more realistic and dynamic conditions.
- Real field implementation of the microalgal cultivation by co-utilization of different types of wastewaters to meet the required nutrients can be explored.
- Studies on the use of different materials such as meat and bone meals to improve the performance of flocculation are highly recommended.
- *In vivo* digestibility assay (such as the Fish model study) is highly recommended to ensure the utilization of microalgae as a feed supplement.
- Techno-economic analysis of the overall cultivation system is required

References

References

Abd El Baky, H.H., El-Baroty, G.S., Bouaid, A., Martinez, M., Aracil, J., 2012. Enhancement of lipid accumulation in Scenedesmus obliquus by Optimizing CO2 and Fe3+ levels for biodiesel production. Bioresour Technol 119, 429–432. https://doi.org/10.1016/j.biortech.2012.05.104

Ahimou, F., Semmens, M.J., Haugstad, G., Novak, P.J., 2007. Effect of protein, polysaccharide, and oxygen concentration profiles on biofilm cohesiveness. Appl Environ Microbiol 73, 2905–2910. https://doi.org/10.1128/AEM.02420-06

Aketo, T., Hoshikawa, Y., Nojima, D., Yabu, Y., Maeda, Y., Yoshino, T., Takano, H., Tanaka, T., 2020. Selection and characterization of microalgae with potential for nutrient removal from municipal wastewater and simultaneous lipid production. J Biosci Bioeng 129, 565–572. https://doi.org/10.1016/j.jbiosc.2019.12.004

Alam, A., Vandamme, D., Chun, W., Zhao, X., Foubert, I., Wang, Z., Muylaert, K., Yuan, Z., 2016. Bioflocculation as an innovative harvesting strategy for microalgae. Rev Environ Sci Biotechnol. https://doi.org/10.1007/s11157-016-9408-8

Alam, M.A., Wan, C., Guo, S.L., Zhao, X.Q., Huang, Z.Y., Yang, Y.L., Chang, J.S., Bai, F.W., 2014. Characterization of the flocculating agent from the spontaneously flocculating microalga Chlorella vulgaris JSC-7. J Biosci Bioeng 118, 29–33. https://doi.org/10.1016/j.jbiosc.2013.12.021

Alkayal, F., Albion, R.L., Tillett, R.L., Hathwaik, L.T., Lemos, M.S., Cushman, J.C., 2010. Expressed sequence tag (EST) profiling in hyper saline shocked Dunaliella salina reveals high expression of protein synthetic apparatus components. Plant Science 179, 437–449. https://doi.org/10.1016/j.plantsci.2010.07.001

Allen, M.S., Welch, K.T., Prebyl, B.S., Baker, D.C., Meyers, A.J., Sayler, G.S., 2004. Analysis and glycosyl composition of the exopolysaccharide isolated from the floc-forming wastewater bacterium Thauera sp. MZ1T. Environ Microbiol 6, 780–790. https://doi.org/10.1111/j.1462-2920.2004.00615.x

APHA, 1995. Standard Methods for the Examination of Water and Wastewater (19th edition American Public Health Association, Washington, D.C, USA. (accessed September 8, 2022).

Arima, Y., Iwata, H., 2007. Effect of wettability and surface functional groups on protein adsorption and cell adhesion using well-defined mixed self-assembled monolayers. Biomaterials 28, 3074–3082. https://doi.org/10.1016/j.biomaterials.2007.03.013

Azam, R., Kothari, R., Singh, H.M., Ahmad, S., Ashokkumar, V., Tyagi, V. V., 2020. Production of algal biomass for its biochemical profile using slaughterhouse wastewater for treatment under axenic conditions. Bioresour Technol 306, 123116. https://doi.org/10.1016/j.biortech.2020.123116

Azma, M., Mohamed, M.S., Mohamad, R., Rahim, R.A., Ariff, A.B., 2011. Improvement of medium composition for heterotrophic cultivation of green microalgae, Tetraselmis suecica, using response surface methodology. Biochem Eng J 53, 187–195. https://doi.org/10.1016/J.BEJ.2010.10.010

Bagul, S.Y., Bharti, R.K., Dhar, D.W., 2017. Assessing biodiesel quality parameters for wastewater grown Chlorella sp. Water Science and Technology 76, 719–727. https://doi.org/10.2166/wst.2017.223

Barnharst, T., Sun, X., Rajendran, A., Urriola, P., Shurson, G., Hu, B., 2021. Enhanced protein and amino acids of corn–ethanol co-product by Mucor indicus and Rhizopus oryzae. Bioprocess Biosyst Eng 44, 1989–2000. https://doi.org/10.1007/s00449-021-02580-0

Bartley, M.L., Boeing, W.J., Dungan, B.N., Holguin, F.O., Schaub, T., 2014. pH effects on growth and lipid accumulation of the biofuel microalgae Nannochloropsis salina and invading organisms. J Appl Phycol 26, 1431–1437. https://doi.org/10.1007/s10811-013-0177-2

Belkin, S., Boussiba, S., 1991. Resistance of spirulina platensis to ammonia at high pH values. Plant Cell Physiol 32, 953–958. https://doi.org/10.1093/oxfordjournals.pcp.a078182

Berberoglu, H., Yin, J., Pilon, L., 2007. Light transfer in bubble sparged photobioreactors for H2 production and CO2 mitigation. Int J Hydrogen Energy 32, 2273–2285. https://doi.org/10.1016/j.ijhydene.2007.02.018

Bernstein, H.C., Kesaano, M., Moll, K., Smith, T., Gerlach, R., Carlson, R.P., Miller, C.D., Peyton, B.M., Cooksey, K.E., Gardner, R.D., Sims, R.C., 2014. Direct measurement and characterization of active photosynthesis zones inside wastewater remediating and biofuel producing microalgal biofilms. Bioresour Technol 156, 206–215. https://doi.org/10.1016/j.biortech.2014.01.001

Beuckels, A., Smolders, E., Muylaert, K., 2015. Nitrogen availability influences phosphorus removal in microalgae-based wastewater treatment. Water Res 77, 98–106. https://doi.org/10.1016/j.watres.2015.03.018

Bhatnagar, A., Chinnasamy, S., Singh, M., Das, K.C., 2011. Renewable biomass production by mixotrophic algae in the presence of various carbon sources and wastewaters. Appl Energy 88, 3425–3431. https://doi.org/10.1016/j.apenergy.2010.12.064

Bligh, E.G. and Dyer W.J., 1959. A rapid method of total lipid extraction and purification. Can. J. Biochem. Physiol. 37, 911–917. https://doi.org/dx.doi.org/10,1139/cjm2014-0700

Boelee, N.C., Janssen, M., Temmink, H., Taparavičiute, L., Khiewwijit, R., Jánoska, Á., Buisman, C.J.N., Wijffels, R.H., 2014a. The effect of harvesting on biomass production and nutrient removal in phototrophic biofilm reactors for effluent polishing. J Appl Phycol 26, 1439–1452. https://doi.org/10.1007/s10811-013-0178-1

Boelee, N.C., Temmink, H., Janssen, M., Buisman, C.J.N., Wijffels, R.H., 2014b. Balancing the organic load and light supply in symbiotic microalgal-bacterial biofilm reactors treating synthetic municipal wastewater. Ecol Eng 64, 213–221. https://doi.org/10.1016/j.ecoleng.2013.12.035

Borugadda, V.B., Goud, V. V., 2012. Biodiesel production from renewable feedstocks: Status and opportunities. Renewable and Sustainable Energy Reviews 16, 4763–4784. https://doi.org/10.1016/j.rser.2012.04.010

Branyikova, I., Prochazkova, G., Potocar, T., Jezkova, Z., Branyik, T., 2018. Harvesting of microalgae by flocculation. Fermentation. 4, 93. https://doi.org/10.3390/fermentation4040093

Brennan, L., Owende, P., 2010. Biofuels from microalgae-A review of technologies for production, processing, and extractions of biofuels and co-products. Renewable and Sustainable Energy Reviews 14, 557–577. https://doi.org/10.1016/j.rser.2009.10.009

Cabanelas, I.T.D., Arbib, Z., Chinalia, F.A., Souza, C.O., Perales, J.A., Almeida, P.F., Druzian, J.I., Nascimento, I.A., 2013. From waste to energy: Microalgae production in wastewater and glycerol. Appl Energy 109, 283–290. https://doi.org/10.1016/J.APENERGY.2013.04.023

Cao, J., Yuan, H.L., Li, B.Z., Yang, J.S., 2014. Significance evaluation of the effects of environmental factors on the lipid accumulation of Chlorella minutissima UTEX 2341 under low-nutrition heterotrophic condition. Bioresour Technol 152, 177–184. https://doi.org/10.1016/j.biortech.2013.10.084

Cao, Y., Liu, W., Xu, X., Zhang, H., Wang, J., Xian, M., 2014. Production of free monounsaturated fatty acids by metabolically engineered Escherichia coli. Biotechnol Biofuels 7, 59. https://doi.org/10.1186/1754-6834-7-59

Caprio, F.D, Altimari, P., Iaquaniello, G., Toro, L., Pagnanelli, F., 2019. Heterotrophic cultivation of T. obliquus under non-axenic conditions by uncoupled supply of nitrogen and glucose. Biochem. Eng. J., 145, 127-136. https://doi.org/10.1016/j.bej.2019.02.020.

Characklis WG, McFeters GA, Marshall KC., 1990. Physiological ecology in biofilm systems. In: Characklis WG, Marshall KC, editors. Biofilms. New York: John Wiley & Sons. p. 341–94.

Chaturvedi, B.K., Nautiyal, A., Kandpal, T.C., Yaqoot, M., 2022. Projected transition to electric vehicles in India and its impact on stakeholders. Energy for Sustainable Development 66, 189–200. https://doi.org/10.1016/j.esd.2021.12.006

Chaudhary, R., Dikshit, A.K., Tong, Y.W., 2018. Carbon-dioxide biofixation and phycoremediation of municipal wastewater using Chlorella vulgaris and Scenedesmus obliquus. Environmental Science and Pollution Research 25, 20399–20406. https://doi.org/10.1007/s11356-017-9575-3

Cheah, Y.T., Chan, D.J.C., 2021. Physiology of microalgal biofilm: a review on prediction of adhesion on substrates. Bioengineered 12, 7577–7599. https://doi.org/10.1080/21655979.2021.1980671

Cheirsilp, B., Torpee, S., 2012. Enhanced growth and lipid production of microalgae under mixotrophic culture condition: Effect of light intensity, glucose concentration and fed-batch cultivation. Bioresour Technol 110, 510–516. https://doi.org/10.1016/j.biortech.2012.01.125

Chen, J., Wang, Y., Benemann, J.R., Zhang, X., Hu, H., Qin, S., 2016. Microalgal industry in China: challenges and prospects. J Appl Phycol 28, 715–725. https://doi.org/10.1007/s10811-015-0720-4

Chen, Q., Fan, Q., Zhang, Z., Mei, Y., Wang, H., 2018. Effective in situ harvest of microalgae with bacterial cellulose produced by Gluconacetobacter xylinus. Algal Res 35, 349–354. https://doi.org/10.1016/j.algal.2018.09.002

Chen, Y., Wang, M., Zhou, X., Fu, H., Qu, X., Zhu, D., 2021. Sorption fractionation of bacterial extracellular polymeric substances (EPS) on mineral surfaces and associated effects on phenanthrene sorption to EPS-mineral complexes. Chemosphere 263, 128264. https://doi.org/10.1016/j.chemosphere.2020.128264

Chen, Y.H., Walker, T.H., 2011. Biomass and lipid production of heterotrophic microalgae Chlorella protothecoides by using biodiesel-derived crude glycerol. Biotechnol Lett 33, 1973–1983. https://doi.org/10.1007/s10529-011-0672-y

Cheng, P., Chen, D., Liu, W., Cobb, K., Zhou, N., Liu, Y., Liu, H., Wang, Q., Chen, P., Zhou, C., Ruan, R., 2020a. Auto-flocculation microalgae species Tribonema sp. and Synechocystis sp. with T-IPL pretreatment to improve swine wastewater nutrient removal. Science of the Total Environment 725, 138263. https://doi.org/10.1016/j.scitotenv.2020.138263

Cheng, P., Cheng, J.J., Cobb, K., Zhou, C., Zhou, N., Addy, M., Chen, P., Yan, X., Ruan, R., 2020b. Tribonema sp. and Chlorella zofingiensis co-culture to treat swine wastewater diluted with fishery wastewater to facilitate harvest. Bioresour Technol 297, 122516. https://doi.org/10.1016/j.biortech.2019.122516

Cheng, P., Ji, B., Gao, L., Zhang, W., Wang, J., Liu, T., 2013. The growth, lipid and hydrocarbon production of Botryococcus braunii with attached cultivation. Bioresour Technol 138, 95–100. https://doi.org/10.1016/j.biortech.2013.03.150

Chi, Z., Pyle, D., Wen, Z., Frear, C., Chen, S., 2007. A laboratory study of producing docosahexaenoic acid from biodiesel-waste glycerol by microalgal fermentation. Process Biochemistry 42, 1537–1545. https://doi.org/10.1016/j.procbio.2007.08.008

Chiranjeevi, P., Mohan, S.V., 2016. Critical parametric influence on microalgae cultivation towards maximizing biomass growth with simultaneous lipid productivity. Renew Energy 98, 64–71. https://doi.org/10.1016/j.renene.2016.03.063

Chisti, Y., 2008. Biodiesel from microalgae beats bioethanol. Trends Biotechnol 26, 126–131. https://doi.org/10.1016/j.tibtech.2007.12.002

Chisti, Y., 2007. Biodiesel from microalgae. Biotechnol Adv. 25, 294-306. https://doi.org/10.1016/j.biotechadv.2007.02.001

Chiu, S.Y., Kao, C.Y., Chen, T.Y., Chang, Y. Bin, Kuo, C.M., Lin, C.S., 2015. Cultivation of microalgal Chlorella for biomass and lipid production using wastewater as nutrient resource. Bioresour Technol 184, 179–189. https://doi.org/10.1016/j.biortech.2014.11.080

Cho, H.U., Cho, H.U., Park, J.M., Park, J.M., Kim, Y.M., 2017. Enhanced microalgal biomass and lipid production from a consortium of indigenous microalgae and bacteria present in municipal wastewater under gradually mixotrophic culture conditions. Bioresour Technol 228, 290–297. https://doi.org/10.1016/j.biortech.2016.12.094

Cho, S., Luong, T.T., Lee, D., Oh, Y.K., Lee, T., 2011. Reuse of effluent water from a municipal wastewater treatment plant in microalgae cultivation for biofuel

production. Bioresour Technol 102, 8639–8645. https://doi.org/10.1016/j.biortech.2011.03.037

Choi, H.J., Lee, S.M., 2015. Effect of the N/P ratio on biomass productivity and nutrient removal from municipal wastewater. Bioprocess Biosyst Eng 38, 761–766. https://doi.org/10.1007/s00449-014-1317-z

Chokshi, K., Pancha, I., Ghosh, A., Mishra, S., 2016. Microalgal biomass generation by phycoremediation of dairy industry wastewater: An integrated approach towards sustainable biofuel production. Bioresour Technol 221, 455–460. https://doi.org/10.1016/j.biortech.2016.09.070

Christenson, L., Sims, R., 2011. Production and harvesting of microalgae for wastewater treatment, biofuels, and bioproducts. Biotechnol Adv. 29, 686-702. https://doi.org/10.1016/j.biotechadv.2011.05.015

Christenson, L.B., Sims, R.C., 2012. Rotating algal biofilm reactor and spool harvester for wastewater treatment with biofuels by-products. Biotechnol Bioeng 109, 1674–1684. https://doi.org/10.1002/bit.24451

Chu, R., Li, S., Zhu, L., Yin, Z., Hu, D., Liu, C., Mo, F., 2021. A review on co-cultivation of microalgae with filamentous fungi: Efficient harvesting, wastewater treatment and biofuel production. Renew. Sustain. Energy Rev. 139, 110689. https://doi.org/10.1016/j.rser.2020.110689

Chugh, M., Kumar, L., Shah, M.P., Bharadvaja, N., 2022. Algal Bioremediation of heavy metals: An insight into removal mechanisms, recovery of by-products, challenges, and future opportunities. Energy Nexus 7, 100129. https://doi.org/10.1016/J.NEXUS.2022.100129

Cid, A., Abalde, J., Herrero, C., 1992. High yield mixotrophic cultures of the marine microalga Tetraselmis suecica (Kylin) Butcher (Prasinophyceae), Journal of Applied Phycology. Kluwer Academic Publishers. 4, 31-37. https://doi.org/10.1007/BF00003958

Comte, S., Guibaud, G., Baudu, M., 2006. Relations between extraction protocols for activated sludge extracellular polymeric substances (EPS) and EPS complexation properties: Part I. Comparison of the efficiency of eight EPS extraction methods. Enzyme Microb Technol 38, 237–245. https://doi.org/10.1016/j.enzmictec.2005.06.016

Croft, M.T., Lawrence, A.D., Raux-Deery, E., Warren, M.J., Smith, A.G., 2005. Algae acquire vitamin B12 through a symbiotic relationship with bacteria. Nature 438, 90–93. https://doi.org/10.1038/nature04056

Cuellar-Bermudez, S. P., Aleman-Nava, G. S., Chandra, R., Garcia-Perez, J. S., Contreras-Angulo, J. R., Markou, G., Muylaert, K., Rittmann, B. E., & Parra-Saldivar, R., 2017. Nutrients utilization and contaminants removal. A review of two approaches of algae and cyanobacteria in wastewater. Algal Research, 24, 438–449. https://doi.org/10.1016/J.ALGAL.2016.08.018

Cui, Y., Yuan, W., 2013. Thermodynamic modeling of algal cell-solid substrate interactions. Appl Energy 112, 485–492. https://doi.org/10.1016/j.apenergy.2013.03.036

Dai, G.Z., Qiu, B.S., Forchhammer, K., 2014. Ammonium tolerance in the cyanobacterium Synechocystis sp. strain PCC 6803 and the role of the psbA

multigene family. Plant Cell Environ 37, 840–851. https://doi.org/10.1111/pce.12202

Danaee, S., Ofoghi, H., Heydarian, S.M., 2021. Acceleration of microalgal biofilm formation on PET by surface engineering. Korean Journal of Chemical Engineering 38, 1–12. https://doi.org/10.1007/s11814-021-0873-6

Daneshvar, E., Zarrinmehr, M.J., Koutra, E., Kornaros, M., Farhadian, O., Bhatnagar, A., 2019. Sequential cultivation of microalgae in raw and recycled dairy wastewater: Microalgal growth, wastewater treatment and biochemical composition. Bioresour Technol 273, 556–564. https://doi.org/10.1016/j.biortech.2018.11.059

Danesi, E.D.G., Rangel-Yagui, C.D.O., De Carvalho, J.C.M., Sato, S., 2002. An investigation of effect of replacing nitrate by urea in the growth and production of chlorophyll by Spirulina platensis. Biomass Bioenergy 23, 261–269. https://doi.org/10.1016/S0961-9534(02)00054-5

De Morais, M.G., Costa, J.A.V., 2007. Carbon dioxide fixation by Chlorella kessleri, C. vulgaris, Scenedesmus obliquus and Spirulina sp. cultivated in flasks and vertical tubular photobioreactors. Biotechnol Lett 29, 1349–1352. https://doi.org/10.1007/s10529-007-9394-6

De Philippis, R., Vincenzini, M., 1998. Exocellular polysaccharides from cyanobacteria and their possible applications. FEMS Microbiol Rev 22, 151–175. https://doi.org/10.1016/S0168-6445(98)00012-6

De-Bashan, L.E., Antoun, H., Bashan, Y., 2008. Involvement of indole-3-acetic acid produced by the growth-promoting bacterium Azospirillum spp. in promoting growth of Chlorella vulgaris. J Phycol 44, 938–947. https://doi.org/10.1111/j.1529-8817.2008.00533.x

Devi, N.D., Chaudhuri, A., Goud, V.V., 2022. Algae biofilm as a renewable resource for production of biofuel and value-added products: A review. Sustainable Energy Technologies and Assessments 53, 102749. https://doi.org/10.1016/J.SETA.2022.102749

Decho, A.W., 2000. Microbial biofilms in intertidal systems: An overview. Cont Shelf Res 20, 1257–1273. https://doi.org/10.1016/S0278-4343(00)00022-4

Demirbas, A., 2009. Progress and recent trends in biodiesel fuels. Energy Convers Manag 50, 14–34. https://doi.org/10.1016/j.enconman.2008.09.001

Deniz, I., Ozen, M.O., Yesil-Celiktas, O., 2016. Supercritical fluid extraction of phycocyanin and investigation of cytotoxicity on human lung cancer cells. Journal of Supercritical Fluids 108, 13–18. https://doi.org/10.1016/j.supflu.2015.10.015

Devi, N.D, Goud, V.V, Hu, B., 2021. 2 Algal cultivation systems and photobioreactor designs, in: Dalai, A.K., Goud, V.V., Nanda, S., Borugadda, V.B. (Eds.), Algal Biorefinery: Developments, Challenges and Opportunities, Taylor & Francis, United Kingdom (2021), p. 24.

Devi, N.D., Sun, X., Ding, L., Goud, V.V., Hu, B., 2022. Mixotrophic growth regime of novel strain Scenedesmus sp. DDVG I in municipal wastewater for concomitant bioremediation and valorization of biomass. J Clean Prod 365, 132834. https://doi.org/10.1016/j.jclepro.2022.132834

Devi, N.D., Tiwari, R., Goud, V.V., 2021. Cultivating Scenedesmus sp. on substrata coated with cyanobacterial-derived extracellular polymeric substances for enhanced biomass productivity: a novel harvesting approach. Biomass Convers Biorefin, 1-13. https://doi.org/10.1007/s13399-021-01432-x

Dewi, E.N., Amalia, U., Mel, M., 2016. The Effect of Different Treatments to the Amino Acid Contents of Micro Algae Spirulina sp. Aquat Procedia 7, 59–65. https://doi.org/10.1016/j.aqpro.2016.07.008

Difusa, A., Talukdar, J., Kalita, M.C., Mohanty, K., Goud, V. V., 2015. Effect of light intensity and pH condition on the growth, biomass and lipid content of microalgae Scenedesmus species. Biofuels 6, 37–44. https://doi.org/10.1080/17597269.2015.1045274

Domozych, D.S., Kort, S., Benton, S., Yu, T., 2005. The extracellular polymeric substance of the green alga Penium margaritaceum and its role in biofilm formation. Biofilms 2, 129–144. https://doi.org/10.1017/S147905050500181X

Duan, X., Ren, G. Y., Liu, L. L., & Zhu, W. X. (2012). Salt-induced osmotic stress for lipid overproduction in batch culture of Chlorella vulgaris. African J. Biotechnol. 11, 7072-7078. https://doi.org/10.5897/ajb11.3670

Dubois, M., Gilles, K.A., Hamilton, J.K., Rebers, P.A., Smith, F., 1956. Colorimetric Method for Determination of Sugars and Related Substances. Anal Chem 28, 350–356. https://doi.org/10.1021/ac60111a017

Dyhrman, S.T., 2016. Nutrients and Their Acquisition: Phosphorus Physiology in Microalgae. The Physiology of Microalgae 155–183. https://doi.org/10.1007/978-3-319-24945-2_8

EIA, 2021. Annual Energy Outlook 2021 (AEO2021), 2021, 33. 〈 https://www.eia.gov/outlooks/aeo/pdf/AEO_Narrative_2021.pdf〉 (accessed October 26, 2021).

Eladel, H., Abomohra, A.E.F., Battah, M., Mohmmed, S., Radwan, A., Abdelrahim, H., 2019. Evaluation of Chlorella sorokiniana isolated from local municipal wastewater for dual application in nutrient removal and biodiesel production. Bioprocess Biosyst Eng 42, 425–433. https://doi.org/10.1007/s00449-018-2046-5

Engin, I.K., Cekmecelioglu, D., Yücel, A.M., Oktem, H.A., 2018. Evaluation of heterotrophic and mixotrophic cultivation of novel Micractinium sp. ME05 on vinasse and its scale up for biodiesel production. Bioresour Technol 251, 128–134. https://doi.org/10.1016/j.biortech.2017.12.023

Ethier, S., Woisard, K., Vaughan, D., Wen, Z., 2011. Continuous culture of the microalgae Schizochytrium limacinum on biodiesel-derived crude glycerol for producing docosahexaenoic acid. Bioresour Technol 102, 88–93. https://doi.org/10.1016/j.biortech.2010.05.021

Fang, L., Catchmark, J.M., 2014. Characterization of water-soluble exopolysaccharides from Gluconacetobacter xylinus and their impacts on bacterial cellulose crystallization and ribbon assembly. Cellulose 21, 3965–3978. https://doi.org/10.1007/s10570-014-0443-8

Fatini, M.A., Basri, E.M., Wan Maznah, W.O., 2021. Effect of different nitrogen sources on cell growth and biochemical compositions of Chlorococcum sp. cultivated under laboratory conditions. IOP Conf Ser Earth Environ Sci 711, 012010. https://doi.org/10.1088/1755-1315/711/1/012010

Feng, P., Deng, Z., Fan, L., Hu, Z., 2012. Lipid accumulation and growth characteristics of Chlorella zofingiensis under different nitrate and phosphate concentrations. J Biosci Bioeng 114, 405–410. https://doi.org/10.1016/j.jbiosc.2012.05.007

Fernandes, T. V., Suárez-Muñoz, M., Trebuch, L.M., Verbraak, P.J., Van de Waal, D.B., 2017. Toward an ecologically optimized N:P Recovery from wastewater by microalgae. Front Microbiol 8. https://doi.org/10.3389/fmicb.2017.01742

Fierro, S., del Pilar Sánchez-Saavedra, M., Copalcúa, C., 2008. Nitrate and phosphate removal by chitosan immobilized Scenedesmus. Bioresour Technol 99, 1274–1279. https://doi.org/10.1016/j.biortech.2007.02.043

Finlay, J.A., Callow, M.E., Ista, L.K., Lopez, G.P., Callow, J.A., 2002. The influence of surface wettability on the adhesion strength of settled spores of the green alga Enteromorpha and the diatom Amphora. Integr Comp Biol 42, 1116–1122. https://doi.org/10.1093/icb/42.6.1116

Flemming, H.C., Neu, T.R., Wozniak, D.J., 2007. The EPS matrix: The "House of Biofilm Cells." J Bacteriol 189, 7945–7947. https://doi.org/10.1128/JB.00858-07

Foo, J.B., Ng, L.S., Lim, J.H., Tan, P.X., Lor, Y.Z., Loo, J.S.E., Low, M.L., Chan, L.C., Beh, C.Y., Leong, S.W., Saiful Yazan, L., Tor, Y.S., How, C.W., 2019. Induction of cell cycle arrest and apoptosis by copper complex Cu(SBCM)2 towards oestrogen-receptor positive MCF-7 breast cancer cells. RSC Adv 9, 18359–18370. https://doi.org/10.1039/c9ra03130h

Fu, L., Cui, X., Li, Y., Xu, L., Zhang, C., Xiong, R., Zhou, D., Crittenden, J.C., 2017. Excessive phosphorus enhances Chlorella regularis lipid production under nitrogen starvation stress during glucose heterotrophic cultivation. Chemical Engineering Journal 330, 566–572. https://doi.org/10.1016/j.cej.2017.07.182

Gayen, K., Bhowmick, T., Maity, S., 2019. Sustainable Downstream Processing of Microalgae for Industrial Application, Sustainable Downstream Processing of Microalgae for Industrial Application. https://doi.org/10.1201/9780429027970

Gaignard, C., Laroche, C., Pierre, G., Dubessay, P., Delattre, C., Gardarin, C., Gourvil, P., Probert, I., Dubuffet, A., Michaud, P., 2019. Screening of marine microalgae: Investigation of new exopolysaccharide producers. Algal Res 44. https://doi.org/10.1016/j.algal.2019.101711

Geider, R.J., La Roche, J., 2002. Redfield revisited: Variability of C:N:P in marine microalgae and its biochemical basis. Eur J Phycol. https://doi.org/10.1017/S0967026201003456

Genin, S.N., Stewart Aitchison, J., Grant Allen, D., 2014. Design of algal film photobioreactors: Material surface energy effects on algal film productivity, colonization and lipid content. Bioresour Technol 155, 136–143. https://doi.org/10.1016/j.biortech.2013.12.060

Gim, G.H., Ryu, J., Kim, M.J., Kim, P. Il, Kim, S.W., 2016. Effects of carbon source and light intensity on the growth and total lipid production of three microalgae under different culture conditions. J Ind Microbiol Biotechnol 43, 605–616. https://doi.org/10.1007/s10295-016-1741-y

Gkelis, S., Rajaniemi, P., Vardaka, E., Moustaka-Gouni, M., Lanaras, T., Sivonen, K., 2005. Limnothrix redekei (Van Goor) Meffert (Cyanobacteria) strains from Lake Kastoria, Greece form a separate phylogenetic group. Microb Ecol 49, 176–182. https://doi.org/10.1007/s00248-003-2030-7

Goldman, J.C., 1979. Outdoor algal mass cultures-II. Photosynthetic yield limitations. Water Res 13, 119–136. https://doi.org/10.1016/0043-1354(79)90083-6

Gonçalves, A.L., Pires, J.C.M., Simões, M., 2016. Biotechnological potential of Synechocystis salina co-cultures with selected microalgae and cyanobacteria: Nutrients removal, biomass and lipid production. Bioresour Technol 200, 279–286. https://doi.org/10.1016/j.biortech.2015.10.023

Graham, J.L., Stone, M.L., Rasmussen, T.J., Foster, G.M., Poulton, B.C., Paxson, C.R., Harris, T.D., 2014. Effects of Wastewater Effluent Discharge and Treatment Facility Upgrades on Environmental and Biological Conditions of Indian Creek , Johnson County , Kansas , June 2004 through June 2013 78.

Gross, M., Henry, W., Michael, C., Wen, Z., 2013. Development of a rotating algal biofilm growth system for attached microalgae growth with in situ biomass harvest. Bioresour Technol 150, 195–201. https://doi.org/10.1016/j.biortech.2013.10.016

Gross, M., Jarboe, D., Wen, Z., 2015. Biofilm-based algal cultivation systems. Appl Microbiol Biotechnol 99, 5781–5789. https://doi.org/10.1007/s00253-015-6736-5

Gross, M., Zhao, X., Mascarenhas, V., Wen, Z., 2016. Effects of the surface physico-chemical properties and the surface textures on the initial colonization and the attached growth in algal biofilm. Biotechnol Biofuels 9, 38. https://doi.org/10.1186/s13068-016-0451-z

Guldhe, A., Ansari, F.A., Singh, P., Bux, F., 2017. Heterotrophic cultivation of microalgae using aquaculture wastewater: A biorefinery concept for biomass production and nutrient remediation. Ecol Eng 99, 47–53. https://doi.org/10.1016/j.ecoleng.2016.11.013

Guo, C., Duan, D., Sun, Y., Han, Y., Zhao, S., 2019. Enhancing Scenedesmus obliquus biofilm growth and CO2 fixation in a gas-permeable membrane photobioreactor integrated with additional rough surface. Algal Res 43, 101620. https://doi.org/10.1016/j.algal.2019.101620

Guo, S.L., Zhao, X.Q., Wan, C., Huang, Z.Y., Yang, Y.L., Asraful Alam, M., Ho, S.H., Bai, F.W., Chang, J.S., 2013. Characterization of flocculating agent from the self-flocculating microalga Scenedesmus obliquus AS-6-1 for efficient biomass harvest. Bioresour Technol 145, 285–289. https://doi.org/10.1016/j.biortech.2013.01.120

Gürlek, C., Yarkent, Ç., Köse, A., Tuğcu, B., Gebeloğlu, I.K., Öncel, S., Elibol, M., 2020. Screening of antioxidant and cytotoxic activities of several microalgal

extracts with pharmaceutical potential. Health Technol (Berl) 10, 111–117. https://doi.org/10.1007/s12553-019-00388-3

Hadjiev, D., Dimitrov, D., Martinov, M., Sire, O., 2007. Enhancement of the biofilm formation on polymeric supports by surface conditioning. Enzyme Microb Technol 40, 840–848. https://doi.org/10.1016/j.enzmictec.2006.06.022

Han, F., Huang, J., Li, Y., Wang, W., Wang, J., Fan, J., Shen, G., 2012. Enhancement of microalgal biomass and lipid productivities by a model of photoautotrophic culture with heterotrophic cells as seed. Bioresour Technol 118, 431–437. https://doi.org/10.1016/j.biortech.2012.05.066

Harold, F.M., 1966. Inorganic polyphosphates in biology: structure, metabolism, and function. Bacteriol Rev 30, 772–794. https://doi.org/10.1128/br.30.4.772-794.1966

Higgins, M.J., Novak, J.T., 1997. Characterization of exocellular protein and its role in bioflocculation. Journal of Environmental Engineering 123, 479–485. https://doi.org/10.1061/(ASCE)0733-9372(1997)123:5(479)

Hsieh, C.H., Wu, W.T., 2009. Cultivation of microalgae for oil production with a cultivation strategy of urea limitation. Bioresour Technol 100, 3921–3926. https://doi.org/10.1016/j.biortech.2009.03.019

Hu, J., Nagarajan, D., Zhang, Q., Chang, J.S., Lee, D.J., 2018. Heterotrophic cultivation of microalgae for pigment production: A review. Biotechnol Adv 36, 54–67. https://doi.org/10.1016/j.biotechadv.2017.09.009

Hu, Q., Zhang, C., Sommerfeld, M., 2006. Biodiesel from algae: lessons learned over the past 60 years and future perspectives. J Phycol 42, 12.

Hu, X., Meneses, Y.E., Aly Hassan, A., 2020. Integration of sodium hypochlorite pretreatment with co-immobilized microalgae/bacteria treatment of meat processing wastewater. Bioresour Technol 304. https://doi.org/10.1016/j.biortech.2020.122953

Huo, S., Liu, J., Zhu, F., Basheer, S., Necas, D., Zhang, R., Li, K., Chen, D., Cheng, P., Cobb, K., Chen, P., Brandel, B., Ruan, R., 2020. Post treatment of swine anaerobic effluent by weak electric field following intermittent vacuum assisted adjustment of N:P ratio for oil-rich filamentous microalgae production. Bioresour Technol 314, 123718. https://doi.org/10.1016/j.biortech.2020.123718

Illman, A.M., Scragg, A.H., Shales, S.W., 2000. Increase in Chlorella strains calorific values when grown in low nitrogen medium. Enzyme Microb Technol 27, 631–635. https://doi.org/10.1016/S0141-0229(00)00266-0

Irving, T.E., Allen, D.G., 2011. Species and material considerations in the formation and development of microalgal biofilms. Appl Microbiol Biotechnol 92, 283–294. https://doi.org/10.1007/s00253-011-3341-0

Ishika, T., Moheimani, N.R., Bahri, P.A., 2017. Sustainable saline microalgae co-cultivation for biofuel production: A critical review. Renewable and Sustainable Energy Reviews 78, 356–368. https://doi.org/10.1016/j.rser.2017.04.110

Ista, L.K., Callow, M.E.; Finlay, J.A., Coleman, S.E., Nolasco, A.C., Simons, R.H., Callorw, J.A., Lopez, G.P., 2004. Effect of Substratum Surface Chemistry and Surface Energy on Attachment of Marine Bacteria and Algal Spores. Appl Environ Microbiol 70, 4151–4157. https://doi.org/10.1128/AEM.70.7.4151

Jain, R., Mishra, S., & Mohanty, K., 2022. Cattle wastewater as a low-cost supplement augmenting microalgal biomass under batch and fed-batch conditions. Journal of Environmental Management, 304. https://doi.org/10.1016/j.jenvman.2021.114213

Janssen, J.H., Kastenhofer, J., de Hoop, J.A., Lamers, P.P., Wijffels, R.H., Barbosa, M.J., 2018. Effect of nitrogen addition on lipid productivity of nitrogen starved Nannochloropsis gaditana. Algal Res 33, 125–132. https://doi.org/10.1016/j.algal.2018.05.009

Ji, B., Zhang, W., Zhang, N., Wang, J., Lutzu, G.A., Liu, T., 2014. Biofilm cultivation of the oleaginous microalgae Pseudochlorococcum sp. Bioprocess Biosyst Eng 37, 1369–1375. https://doi.org/10.1007/s00449-013-1109-x

Ji, C.F., Yu, X.J., Chen, Z.A., Xue, S., Legrand, J., Zhang, W., 2011. Effects of nutrient deprivation on biochemical compositions and photo-hydrogen production of Tetraselmis subcordiformis. Int J Hydrogen Energy 36, 5817–5821. https://doi.org/10.1016/j.ijhydene.2010.12.138

Ji, M.-K., Abou-Shanab, R.A.I., Hwang, J.-H., Timmes, T.C., Kim, H.-C., Oh, Y.-K., Jeon, B.-H., 2013. Removal of Nitrogen and Phosphorus from Piggery Wastewater Effluent Using the Green Microalga Scenedesmus obliquus. Journal of Environmental Engineering 139, 1198–1205. https://doi.org/10.1061/(asce)ee.1943-7870.0000726

Jiang, J., Jin, W., Tu, R., Han, S., Ji, Y., Zhou, X., 2021. Harvesting of Microalgae Chlorella pyrenoidosa by Bio-flocculation with Bacteria and Filamentous Fungi. Waste Biomass Valorization 12, 145–154. https://doi.org/10.1007/s12649-020-00979-6

Jiménez, J., Bru, S., Ribeiro, M.P.C., Clotet, J., 2017. Polyphosphate: popping up from oblivion. Curr Genet 63, 15-18. https://doi.org/10.1007/s00294-016-0611-5

Jin, D.Q., Lim, C.S., Sung, J.Y., Choi, H.G., Ha, I., Han, J.S., 2006. Ulva conglobata, a marine algae, has neuroprotective and anti-inflammatory effects in murine hippocampal and microglial cells. Neurosci Lett 402, 154–158. https://doi.org/10.1016/j.neulet.2006.03.068

Johnson, M.B., Wen, Z., 2010. Development of an attached microalgal growth system for biofuel production. Appl Microbiol Biotechnol 85, 525–534. https://doi.org/10.1007/s00253-009-2133-2

Kang, C.D., An, J.Y., Park, T.H., Sim, S.J., 2006. Astaxanthin biosynthesis from simultaneous N and P uptake by the green alga Haematococcus pluvialis in primary-treated wastewater. Biochem Eng J 31, 234–238. https://doi.org/10.1016/J.BEJ.2006.08.002

Katiyar, R., Gurjar, B.R., Bharti, R.K., Kumar, A., Biswas, S., Pruthi, V., 2017. Heterotrophic cultivation of microalgae in photobioreactor using low cost crude glycerol for enhanced biodiesel production. Renew Energy 113, 1359–1365. https://doi.org/10.1016/j.renene.2017.06.100

Kawaguchi, T., Decho, A.W., 2000. Biochemical characterization of cyanobacterial Extracellular Polymers (EPS) from modern marine stromatolites (Bahamas). Prep Biochem Biotechnol 30, 321–330. https://doi.org/10.1080/10826060008544971

Kesaano, M., Gardner, R.D., Moll, K., Lauchnor, E., Gerlach, R., Peyton, B.M., Sims, R.C., 2015. Dissolved inorganic carbon enhanced growth, nutrient uptake, and lipid accumulation in wastewater grown microalgal biofilms. Bioresour Technol 180, 7–15. https://doi.org/10.1016/j.biortech.2014.12.082

Kesaano, M., Sims, R.C., 2014. Algal biofilm based technology for wastewater treatment. Algal Res 5, 231–240. https://doi.org/10.1016/j.algal.2014.02.003

Khan, M., Diba, F., 2016. Heterotrophic Growth of Micro Algae Plasma Treatment View project Design, fabrication and development of coagulation/ flocculation simulator (Jar Tester) View project. www.esciencecentral.org/ebooks (accessed May 15, 2022)

Khoo, K.S., Chia, W.Y., Chew, K.W., Show, P.L., 2021. Microalgal-Bacterial Consortia as Future Prospect in Wastewater Bioremediation, Environmental Management and Bioenergy Production. Indian J Microbiol 61, 262-269. https://doi.org/10.1007/s12088-021-00924-8

Khozin-Goldberg, I., Cohen, Z., 2006. The effect of phosphate starvation on the lipid and fatty acid composition of the fresh water eustigmatophyte Monodus subterraneus. Phytochemistry 67, 696–701. https://doi.org/10.1016/j.phytochem.2006.01.010

Kim, D.G., La, H.J., Ahn, C.Y., Park, Y.H., Oh, H.M., 2011. Harvest of Scenedesmus sp. with bioflocculant and reuse of culture medium for subsequent high-density cultures. Bioresour Technol 102, 3163–3168. https://doi.org/10.1016/j.biortech.2010.10.108

Kim, H. C., Choi, W. J., Chae, A. N., Park, J., Kim, H. J., & Song, K. G., 2016. Treating high-strength saline piggery wastewater using the heterotrophic cultivation of Acutodesmus obliquus. Biochemical Engineering Journal, 110, 51-58. https://doi.org/10.1016/j.bej.2016.02.011

Klock, J.H., Wieland, A., Seifert, R., Michaelis, W., 2007. Extracellular polymeric substances (EPS) from cyanobacterial mats: Characterisation and isolation method optimisation. Mar Biol 152, 1077–1085. https://doi.org/10.1007/s00227-007-0754-5

Knothe, G., 2005. Dependence of biodiesel fuel properties on the structure of fatty acid alkyl esters. Fuel Processing Technology 86, 1059–1070. https://doi.org/10.1016/j.fuproc.2004.11.002

Knothe, G., Matheaus, A.C., Ryan, T.W., 2003. Cetane numbers of branched and straight-chain fatty esters determined in an ignition quality tester. Fuel 82, 971–975. https://doi.org/10.1016/S0016-2361(02)00382-4

Kong, W., Yang, S., Wang, H., Huo, H., Guo, B., Liu, N., Zhang, A., Niu, S., 2020. Regulation of biomass, pigments, and lipid production by Chlorella vulgaris 31 through controlling trophic modes and carbon sources. J Appl Phycol 32, 1569-1579. https://doi.org/10.1007/s10811-020-02089-1

Kose, A., Ozen, M.O., Elibol, M., Oncel, S.S., 2017. Investigation of in vitro digestibility of dietary microalga Chlorella vulgaris and cyanobacterium Spirulina platensis as a nutritional supplement. 3 Biotech 7, 1–7. https://doi.org/10.1007/s13205-017-0832-4

Kothari, R., Pathak, V. V., Kumar, V., Singh, D.P., 2012. Experimental study for growth potential of unicellular alga Chlorella pyrenoidosa on dairy waste water: An integrated approach for treatment and biofuel production. Bioresour Technol 116, 466–470. https://doi.org/10.1016/j.biortech.2012.03.121

Kumar, K., Dasgupta, C.N., Nayak, B., Lindblad, P., Das, D., 2011. Development of suitable photobioreactors for CO2 sequestration addressing global warming using green algae and cyanobacteria. Bioresour Technol 102, 4945-4953. https://doi.org/10.1016/j.biortech.2011.01.054

Kumar, M.S., Miao, Z.H., Wyatt, S.K., 2010. Influence of nutrient loads, feeding frequency and inoculum source on growth of Chlorella vulgaris in digested piggery effluent culture medium. Bioresour Technol 101, 6012–6018. https://doi.org/10.1016/j.biortech.2010.02.080

Kumar, S., Stecher, G., Li, M., Knyaz, C., Tamura, K., 2018. MEGA X: Molecular evolutionary genetics analysis across computing platforms. Mol Biol Evol 35, 1547–1549. https://doi.org/10.1093/molbev/msy096

Lal, A., Banerjee, S., Das, D., 2021. Aspergillus sp. assisted bioflocculation of Chlorella MJ 11/11 for the production of biofuel from the algal-fungal co-pellet. Sep Purif Technol 118320. https://doi.org/10.1016/j.seppur.2021.118320

Lananan, F., Mohd Yunos, F.H., Mohd Nasir, N., Abu Bakar, N.S., Lam, S.S., Jusoh, A., 2016. Optimization of biomass harvesting of microalgae, Chlorella sp. utilizing auto-flocculating microalgae, Ankistrodesmus sp. as bio-flocculant. Int Biodeterior Biodegradation 113, 391–396. https://doi.org/10.1016/j.ibiod.2016.04.022

Larkin, M.A., Blackshields, G., Brown, N.P., Chenna, R., Mcgettigan, P.A., McWilliam, H., Valentin, F., Wallace, I.M., Wilm, A., Lopez, R., Thompson, J.D., Gibson, T.J., Higgins, D.G., 2007. Clustal W and Clustal X version 2.0. Bioinformatics 23, 2947–2948. https://doi.org/10.1093/bioinformatics/btm404

Leong, W.H., Azella Zaine, S.N., Ho, Y.C., Uemura, Y., Lam, M.K., Khoo, K.S., Kiatkittipong, W., Cheng, C.K., Show, P.L., Lim, J.W., 2019. Impact of various microalgal-bacterial populations on municipal wastewater bioremediation and its energy feasibility for lipid-based biofuel production. J Environ Manage 249, 109384. https://doi.org/10.1016/j.jenvman.2019.109384

Leong, W.H., Kiatkittipong, K., Kiatkittipong, W., Cheng, Y.W., Lam, M.K., Shamsuddin, R., Mohamad, M., Lim, J.W., 2020. Comparative performances of microalgal-bacterial co-cultivation to bioremediate synthetic and municipal wastewaters whilst producing biodiesel sustainably. Processes 8, 1–12. https://doi.org/10.3390/pr8111427

Leong, W.H., Lim, J.W., Lam, M.K., Lam, S.M., Sin, J.C., Samson, A., 2021. Novel sequential flow baffled microalgal-bacterial photobioreactor for enhancing nitrogen assimilation into microalgal biomass whilst bioremediating nutrient-rich wastewater simultaneously. J Hazard Mater 409, 124455. https://doi.org/10.1016/j.jhazmat.2020.124455

Li, T., Yang, F., Xu, J., Wu, H., Mo, J., Dai, L., Xiang, W., 2020. Evaluating differences in growth, photosynthetic efficiency, and transcriptome of Asterarcys sp. SCS-1881 under autotrophic, mixotrophic, and heterotrophic

culturing conditions. Algal Res 45, 101753. https://doi.org/10.1016/j.algal.2019.101753

Li, Y., Yuan, Z., Mu, J., Chen, D., Feng, B., 2013. Proteomic analysis of lipid accumulation in chlorella protothecoides cells by heterotrophic N deprivation coupling cultivation. Energy and Fuels 27, 4031–4040. https://doi.org/10.1021/ef4000177

Liang, Y., Sarkany, N., Cui, Y., 2009. Biomass and lipid productivities of Chlorella vulgaris under autotrophic, heterotrophic and mixotrophic growth conditions. Biotechnol Lett 31, 1043–1049. https://doi.org/10.1007/s10529-009-9975-7

Liu, H., Fang, H.H.P., 2002. Extraction of extracellular polymeric substances (EPS) of sludges. J Biotechnol 95, 249–256. https://doi.org/10.1016/S0168-1656(02)00025-1

Liu, J., Yuan, C., Hu, G., Li, F., 2012. Effects of light intensity on the growth and lipid accumulation of microalga Scenedesmus sp. 11-1 under nitrogen limitation. Appl Biochem Biotechnol 166, 2127–2137. https://doi.org/10.1007/s12010-012-9639-2

Liu, T., Wang, J., Hu, Q., Cheng, P., Ji, B., Liu, J., Chen, Y., Zhang, W., Chen, X., Chen, L., Gao, L., Ji, C., Wang, H., 2013. Attached cultivation technology of microalgae for efficient biomass feedstock production. Bioresour Technol 127, 216–222. https://doi.org/10.1016/j.biortech.2012.09.100

Liu, W., Au, D.W.T., Anderson, D.M., Lam, P.K.S., Wu, R.S.S., 2007. Effects of nutrients, salinity, pH and light:dark cycle on the production of reactive oxygen species in the alga Chattonella marina. J Exp Mar Biol Ecol 346, 76–86. https://doi.org/10.1016/j.jembe.2007.03.007

Loganathan, G.B., Orsat, V., Lefsrud, M., Wu, B. Sen, 20. Bioprocess Biosyst Eng 43, 1445–1455. https://doi.org/10.1007/s00449-020-02338-0

Lowry, O.H., Rosebrough, N.J., Farr, A.L., Randall, R.J., 2000. Total protein estimation by Lowry's method. Experiment BL 301 1–3.

Lum, K.K., Kim, J., Lei, X.G., 2013. Dual potential of microalgae as a sustainable biofuel feedstock and animal feed. J Anim Sci Biotechnol 4, 1-7. https://doi.org/10.1186/2049-1891-4-53

Lung, Y.T., Tan, C.H., Show, P.L., Ling, T.C., Lan, J.C.W., Lam, H.L., Chang, J.S., 2016. Docosahexaenoic acid production from crude glycerol by Schizochytrium limacinum SR21. Clean Technol Environ Policy 18, 2209–2216. https://doi.org/10.1007/S10098-016-1126-Y/TABLES/4

Luo, W., Yang, C., He, H., Zeng, G., Yan, S., Cheng, Y., 2014. Novel two-stage vertical flow biofilter system for efficient treatment of decentralized domestic wastewater. Ecol Eng 64, 415–423. https://doi.org/10.1016/j.ecoleng.2014.01.011

Magdouli, S., Brar, S.K., Blais, J.F., 2016. Co-culture for lipid production: Advances and challenges. Biomass Bioenergy 92, 20-30. https://doi.org/10.1016/j.biombioe.2016.06.003

Mahesh, R., Naira, V.R., Maiti, S.K., 2019. Concomitant production of fatty acid methyl ester (biodiesel) and exopolysaccharides using efficient harvesting technology in flat panel photobioreactor with special sparging system via

Scenedesmus abundans. Bioresour Technol 278, 231–241. https://doi.org/10.1016/j.biortech.2019.01.091

Majid, M. A. (2020). Renewable energy for sustainable development in India: current status, future prospects, challenges, employment, and investment opportunities. Energy, Sustainability and Society, 10(1), 1-36. https://doi.org/10.1186/s13705-019-0232-1

Mandalam, R.K., Palsson, B., 1998. Elemental balancing of biomass and medium composition enhances growth capacity in high-density Chlorella vulgaris cultures. Biotechnol Bioeng 59, 605–611. https://doi.org/10.1002/(SICI)1097-0290(19980905)59:5<605::AID-BIT11>3.0.CO;2-8

Mantzorou, A., Ververidis, F., 2019. Microalgal biofilms: A further step over current microalgal cultivation techniques. Science of the Total Environment, 651, 3187-3201. https://doi.org/10.1016/j.scitotenv.2018.09.355

Mata, T.M., Martins, A.A., Caetano, N.S., 2010. Microalgae for biodiesel production and other applications: A review. Renewable and Sustainable Energy Reviews 14, 217–232. https://doi.org/10.1016/j.rser.2009.07.020

Maurya, R., Zhu, X., Valverde-Pérez, B., Ravi Kiran, B., General, T., Sharma, S., Kumar Sharma, A., Thomsen, M., Venkata Mohan, S., Mohanty, K., Angelidaki, I., 2022. Advances in microalgal research for valorization of industrial wastewater. Bioresour Technol 343, 126128. https://doi.org/10.1016/J.BIORTECH.2021.126128

Miao, M. S., Yao, X. D., Shu, L., Yan, Y. J., Wang, Z., Li, N., ... & Kong, Q. (2016). Mixotrophic growth and biochemical analysis of Chlorella vulgaris cultivated with synthetic domestic wastewater. Int Biodeterior Biodegradation 113, 120–125. https://doi.org/10.1016/j.ibiod.2016.04.005

Mishra, S., Mohanty, K., 2019. Comprehensive characterization of microalgal isolates and lipid-extracted biomass as zero-waste bioenergy feedstock: An integrated bioremediation and biorefinery approach. Bioresour Technol 273, 177–184. https://doi.org/10.1016/J.BIORTECH.2018.11.012

Mitra, D., van Leeuwen, J. (Hans), Lamsal, B., 2012. Heterotrophic/mixotrophic cultivation of oleaginous Chlorella vulgaris on industrial co-products. Algal Res 1, 40–48. https://doi.org/10.1016/j.algal.2012.03.002

Mokashi, K., Shetty, V., George, S.A., Sibi, G., 2016. Sodium Bicarbonate as Inorganic Carbon Source for Higher Biomass and Lipid Production Integrated Carbon Capture in Chlorella vulgaris. Achievements in the Life Sciences 10, 111–117. https://doi.org/10.1016/j.als.2016.05.011

Molina Grima, E., Belarbi, E.H., Acién Fernández, F.G., Robles Medina, A., Chisti, Y., 2003. Recovery of microalgal biomass and metabolites: Process options and economics. Biotechnol Adv 20, 491–515. https://doi.org/10.1016/S0734-9750(02)00050-2

Monks, L.M., Rigo, A., Mazutti, M.A., Vladimir Oliveira, J., Valduga, E., 2013. Use of chemical, enzymatic and ultrasound-assisted methods for cell disruption to obtain carotenoids. Biocatal Agric Biotechnol 2, 165–169. https://doi.org/10.1016/j.bcab.2013.03.004

Moreno, J., Vargas, M.A., Olivares, H., Rivas, J., Guerrero, M.G., 1998. Exopolysaccharide production by the cyanobacterium Anabaena sp. ATCC 33047 in batch and continuous culture. J Biotechnol 60, 175–182. https://doi.org/10.1016/S0168-1656(98)00003-0

Morrison, W.R., Smith, L.M., 1964. Preparation of fatty acid methyl esters and dimethylacetals from lipids with boron fluoride–methanol. J Lipid Res 5, 600–608. https://doi.org/10.1016/s0022-2275(20)40190-7

Mosmann, T., 1983. Rapid colorimetric assay for cellular growth and survival: Application to proliferation and cytotoxicity assays, Journal of Immunological Methods 65, 55-63. https://doi.org/10.1016/0022-1759(83)90303-4

Mukherjee, C., Chowdhury, R., Sutradhar, T., Begam, M., Ghosh, S.M., Basak, S.K., Ray, K., 2016. Parboiled rice effluent: A wastewater niche for microalgae and cyanobacteria with growth coupled to comprehensive remediation and phosphorus biofertilization. Algal Res 19, 225–236. https://doi.org/10.1016/J.ALGAL.2016.09.009

Mukherjee, C., Suryawanshi, P.G., Kalita, M.C., Deka, D., Aranda, D.A.G., Goud, V. V., 2022. Polarity-wise successive solvent extraction of Scenedesmus obliquus biomass and characterization of the crude extracts for broad-spectrum antibacterial activity. Biomass Convers Biorefin, 1-17. https://doi.org/10.1007/s13399-022-02432-1

Nayak, M., Suh, W.I., Lee, B., Chang, Y.K., 2018. Enhanced carbon utilization efficiency and FAME production of Chlorella sp. HS2 through combined supplementation of bicarbonate and carbon dioxide. Energy Convers Manag 156, 45–52. https://doi.org/10.1016/j.enconman.2017.11.002

Nazari, M.T., Rigueto, C.V.T., Rempel, A., Colla, L.M., 2021. Harvesting of Spirulina platensis using an eco-friendly fungal bioflocculant produced from agro-industrial by-products. Bioresour Technol 322, 124525. https://doi.org/10.1016/j.biortech.2020.124525

Niccolai, A., Bigagli, E., Biondi, N., Rodolfi, L., Cinci, L., Luceri, C., Tredici, M.R., 2017. In vitro toxicity of microalgal and cyanobacterial strains of interest as food source. J Appl Phycol 29, 199–209. https://doi.org/10.1007/S10811-016-0924-2

Nouri, H., Roushandeh, J.M., Hallajisani, A., Golzary, A., Daliry, S., 2021. The effects of glucose, nitrate, and pH on cultivation of Chlorella sp. Microalgae. Global Journal of Environmental Science and Management 7, 103–116. https://doi.org/10.22034/gjesm.2021.01.08

Nur, M.M.A., Buma, A.G.J., 2019. Opportunities and Challenges of Microalgal Cultivation on Wastewater, with Special Focus on Palm Oil Mill Effluent and the Production of High Value Compounds. Waste Biomass Valorization 10, 2079–2097. https://doi.org/10.1007/S12649-018-0256-3

Ogbonna, J.C., Tanaka, H., 2000. Light requirement and photosynthetic cell cultivation - Development of processes for efficient light utilization in photobioreactors, in: Journal of Applied Phycology. Springer Netherlands, pp. 207–218. https://doi.org/10.1023/a:1008194627239

Oh, H.M., Lee, S.J., Park, M.H., Kim, H.S., Kim, H.C., Yoon, J.H., Kwon, G.S., Yoon, B.D., 2001. Harvesting of Chlorella vulgaris using a bioflocculant from Paenibacillus sp. AM49. Biotechnol Lett 23, 1229–1234. https://doi.org/10.1023/A:1010577319771

Ohashi, A., Harada, H., 1996. A novel concept for evaluation of biofilm adhesion strength by applying tensile force and shear force. Water Science and Technology 34, 201–211. https://doi.org/10.1016/0273-1223(96)00647-6

Oliveira, C.Y.B. de, Viegas, T.L., Lopes, R.G., Cella, H., Menezes, R.S., Soares, A.T., Antoniosi Filho, N.R., Derner, R.B., 2020. A comparison of harvesting and drying methodologies on fatty acids composition of the green microalga Scenedesmus obliquus. Biomass Bioenergy 132, 105437. https://doi.org/10.1016/J.BIOMBIOE.2019.105437

Oser, B.L., 1951. Method for integrating essential amino acid content in the nutritional evaluation of protein. J Am Diet Assoc 27, 396–402. https://doi.org/10.1016/s0002-8223(21)30758-1

Ozkan, A., Berberoglu, H., 2013. Physico-chemical surface properties of microalgae. Colloids Surf B Biointerfaces 112, 287–293. https://doi.org/10.1016/j.colsurfb.2013.08.001

Ozkan, A., Kinney, K., Katz, L., Berberoglu, H., 2012. Reduction of water and energy requirement of algae cultivation using an algae biofilm photobioreactor. Bioresour Technol 114, 542–548. https://doi.org/10.1016/j.biortech.2012.03.055

Pancha, I., Chokshi, K., George, B., Ghosh, T., Paliwal, C., Maurya, R., Mishra, S., 2014. Nitrogen stress triggered biochemical and morphological changes in the microalgae Scenedesmus sp. CCNM 1077. Bioresour Technol 156, 146–154. https://doi.org/10.1016/j.biortech.2014.01.025

Pancha, I., Chokshi, K., Ghosh, T., Paliwal, C., Maurya, R., Mishra, S., 2015a. Bicarbonate supplementation enhanced biofuel production potential as well as nutritional stress mitigation in the microalgae Scenedesmus sp. CCNM 1077. Bioresour Technol 193, 315–323. https://doi.org/10.1016/j.biortech.2015.06.107

Pancha, I., Chokshi, K., Maurya, R., Trivedi, K., Patidar, S.K., Ghosh, A., Mishra, S., 2015b. Salinity induced oxidative stress enhanced biofuel production potential of microalgae Scenedesmus sp. CCNM 1077. Bioresour Technol 189, 341–348. https://doi.org/10.1016/j.biortech.2015.04.017

Pandey, A., Gupta, A., Sunny, A., Kumar, S., Srivastava, S., 2020. Multi-objective optimization of media components for improved algae biomass, fatty acid and starch biosynthesis from Scenedesmus sp. ASK22 using desirability function approach. Renew Energy 150, 476–486. https://doi.org/10.1016/J.RENENE.2019.12.095

Pandey, V.K., Anjum, N., Chandra, R., 2016. Algae as a biofuel: Renewable source for liquid fuel. Carbon - Science and Technology Applied Science Innovations Pvt. Ltd. India, pp 86–93.

Parikh, A., Madamwar, D., 2006. Partial characterization of extracellular polysaccharides from cyanobacteria. Bioresour Technol 97, 1822–1827. https://doi.org/10.1016/j.biortech.2005.09.008

Patel, A.K., Joun, J.M., Hong, M.E., Sim, S.J., 2019. Effect of light conditions on mixotrophic cultivation of green microalgae. Bioresour Technol 282, 245–253. https://doi.org/10.1016/j.biortech.2019.03.024

Patrinou, V., Tsolcha, O.N., Tatoulis, T.I., Stefanidou, N., Dourou, M., Moustaka-Gouni, M., Aggelis, G., Tekerlekopoulou, A.G., 2020. Biotreatment of poultry waste coupled with biodiesel production using suspended and attached growth microalgal-based systems. Sustainability (Switzerland) 12, 5024. https://doi.org/10.3390/su12125024

Pei, X.Y., Ren, H.Y., Liu, B.F., 2021. Flocculation performance and mechanism of fungal pellets on harvesting of microalgal biomass. Bioresour Technol 321, 124463. https://doi.org/10.1016/j.biortech.2020.124463

Podevin, M., De Francisci, D., Holdt, S.L., Angelidaki, I., 2015. Effect of nitrogen source and acclimatization on specific growth rates of microalgae determined by a high-throughput in vivo microplate autofluorescence method. J Appl Phycol 27, 1415–1423. https://doi.org/10.1007/s10811-014-0468-2

Posadas, E., García-Encina, P.A., Soltau, A., Domínguez, A., Díaz, I., Muñoz, R., 2013. Carbon and nutrient removal from centrates and domestic wastewater using algal-bacterial biofilm bioreactors. Bioresour Technol 139, 50–58. https://doi.org/10.1016/j.biortech.2013.04.008

Pruvost, J., van Vooren, G., le Gouic, B., Couzinet-Mossion, A., Legrand, J., 2011. Systematic investigation of biomass and lipid productivity by microalgae in photobioreactors for biodiesel application. Bioresour Technol 102, 150–158. https://doi.org/10.1016/j.biortech.2010.06.153

Rajendran, A., Hu, B., 2016. Mycoalgae biofilm: Development of a novel platform technology using algae and fungal cultures. Biotechnol Biofuels 9, 112. https://doi.org/10.1186/s13068-016-0533-y

Rashid, N., Ryu, A.J., Jeong, K.J., Lee, B., Chang, Y.K., 2019. Co-cultivation of two freshwater microalgae species to improve biomass productivity and biodiesel production. Energy Convers Manag 196, 640–648. https://doi.org/10.1016/j.enconman.2019.05.106

Reitan, K.I., Rainuzzo, J.R., Olsen, Y., 1994. Effect of Nutrient Limitation on Fatty Acid and Lipid Content of Marine Microalgae. J Phycol 30, 972–979. https://doi.org/10.1111/j.0022-3646.1994.00972.x

Ren, H.Y., Liu, B.F., Ma, C., Zhao, L., Ren, N.Q., 2013. A new lipid-rich microalga Scenedesmus sp. strain R-16 isolated using Nile red staining: Effects of carbon and nitrogen sources and initial pH on the biomass and lipid production. Biotechnol Biofuels 6, 1–10. https://doi.org/10.1186/1754-6834-6-143

Rodolfi, L., Zittelli, G.C., Bassi, N., Padovani, G., Biondi, N., Bonini, G., Tredici, M.R., 2009. Microalgae for oil: Strain selection, induction of lipid synthesis and outdoor mass cultivation in a low-cost photobioreactor. Biotechnol Bioeng 102, 100–112. https://doi.org/10.1002/bit.22033

Roostaei, J., Zhang, Y., Gopalakrishnan, K., Ochocki, A.J., 2018. Mixotrophic Microalgae Biofilm: A Novel Algae Cultivation Strategy for Improved Productivity and Cost-efficiency of Biofuel Feedstock Production. Sci Rep 8. https://doi.org/10.1038/s41598-018-31016-1

Rosli, S.S., Amalina Kadir, W.N., Wong, C.Y., Han, F.Y., Lim, J.W., Lam, M.K., Yusup, S., Kiatkittipong, W., Kiatkittipong, K., Usman, A., 2020. Insight review of attached microalgae growth focusing on support material packed in photobioreactor for sustainable biodiesel production and wastewater bioremediation. Renewable and Sustainable Energy Reviews 134. https://doi.org/10.1016/j.rser.2020.110306

Rossi, F., De Philippis, R., 2015. Role of cyanobacterial exopolysaccharides in phototrophic biofilms and in complex microbial mats. Life 5, 1218–1238. https://doi.org/10.3390/life5021218

Ruiz, J., Arbib, Z., Álvarez-Díaz, P.D., Garrido-Pérez, C., Barragán, J., Perales, J.A., 2014. Influence of light presence and biomass concentration on nutrient kinetic removal from urban wastewater by Scenedesmus obliquus. J Biotechnol 178, 32–37. https://doi.org/10.1016/j.jbiotec.2014.03.001

Ruiz-Ruiz, P., Gómez-Borraz, T.L., Revah, S., Morales, M., 2020. Methanotroph-microalgae co-culture for greenhouse gas mitigation: Effect of initial biomass ratio and methane concentration. Chemosphere 259. https://doi.org/10.1016/j.chemosphere.2020.127418

Saitou, N., Nei, M., 1987. The neighbor-joining method: a new method for reconstructing phylogenetic trees., Molecular biology and evolution 4, 406-425. https://doi.org/10.1093/oxfordjournals.molbev.a040454

Sajadian, S., Morowvat, M., Ghasemi, Y., 2018. Investigation of autotrophic, heterotrophic, and mixotrophic modes of cultivation on lipid and biomass production in Chlorella vulgaris. Natl J Physiol Pharm Pharmacol 8, 1. https://doi.org/10.5455/njppp.2018.8.0935625122017

Sajjadi, B., Chen, W.Y., Raman, A.A.A., Ibrahim, S., 2018. Microalgae lipid and biomass for biofuel production: A comprehensive review on lipid enhancement strategies and their effects on fatty acid composition. Renewable and Sustainable Energy Reviews 97, 200-232. https://doi.org/10.1016/j.rser.2018.07.050

Salim, S., Bosma, R., Vermuë, M.H., Wijffels, R.H., 2011. Harvesting of microalgae by bio-flocculation. J Appl Phycol 23, 849–855. https://doi.org/10.1007/s10811-010-9591-x

Saravanan, A., Kumar, P.S., Varjani, S., Jeevanantham, S., Yaashikaa, P.R., Thamarai, P., Abirami, B., George, C.S., 2021. A review on algal-bacterial symbiotic system for effective treatment of wastewater. Chemosphere 271. https://doi.org/10.1016/j.chemosphere.2021.129540

Schakenraad, J.M., Busscher, H.J., Wildevuur, C.R.H., Arends, J., 1988. Thermodynamic aspects of cell spreading on solid substrata. Cell Biophys 13, 75–91. https://doi.org/10.1007/BF02797367

Schnurr, P.J., Allen, D.G., 2015. Factors affecting algae biofilm growth and lipid production: A review. Renewable and Sustainable Energy Reviews 52, 418–429. https://doi.org/10.1016/j.rser.2015.07.090

Schnurr, P.J., Espie, G.S., Allen, D.G., 2013. Algae biofilm growth and the potential to stimulate lipid accumulation through nutrient starvation. Bioresour Technol 136, 337–344. https://doi.org/10.1016/j.biortech.2013.03.036

Sekar, R., Venugopalan, V.P., Satpathy, K.K., Nair, K.V.K., Rao, V.N.R., 2004. Laboratory studies on adhesion of microalgae to hard substrates, in: Hydrobiologia. Springer Netherlands, Dordrecht, pp. 109–116. https://doi.org/10.1023/B:HYDR.0000020315.40349.38

Sergeeva, Y.E., Mostova, E.B., Gorin, K. V., Komova, A. V., Konova, I.A., Pojidaev, V.M., Gotovtsev, P.M., Vasilov, R.G., Sineoky, S.P., 2017. Biodiesel fuel performance calculation on the basis of fatty acid composition of lipids of some biotechnologically important microorganisms. Biotekhnologiya 33, 53–61. https://doi.org/10.21519/0234-2758-2017-33-1-53-61

Serretti, C., Schapaugh Jnr, W.T., Leffel, R.C., 1994. Amino acid profile of high seed protein soybean. Crop Sci 34, 207–209. https://doi.org/10.2135/cropsci1994.0011183X003400010037x

Shahid, A., Malik, S., Zhu, H., Xu, J., Nawaz, M.Z., Nawaz, S., Asraful Alam, M., Mehmood, M.A., 2020. Cultivating microalgae in wastewater for biomass production, pollutant removal, and atmospheric carbon mitigation; a review. Science of the Total Environment 704. https://doi.org/10.1016/j.scitotenv.2019.135303

Sharma, K.K., Schuhmann, H., Schenk, P.M., 2012. High lipid induction in microalgae for biodiesel production. Energies (Basel) 5, 1532–1553. https://doi.org/10.3390/en5051532

Shen, Y., Chen, C., Chen, W., Xu, X., 2014a. Attached culture of Nannochloropsis oculata for lipid production. Bioprocess Biosyst Eng 37, 1743–1748. https://doi.org/10.1007/s00449-014-1147-z

Shen, Y., Xu, X., Zhao, Y., Lin, X., 2014b. Influence of algae species, substrata and culture conditions on attached microalgal culture. Bioprocess Biosyst Eng 37, 441–450. https://doi.org/10.1007/s00449-013-1011-6

Shen, Y., Zhang, H., Xu, X., Lin, X., 2015. Biofilm formation and lipid accumulation of attached culture of Botryococcus braunii. Bioprocess Biosyst Eng 38, 481–488. https://doi.org/10.1007/s00449-014-1287-1

Siaut, M., Cuiné, S., Cagnon, C., Fessler, B., Nguyen, M., Carrier, P., Beyly, A., Beisson, F., Triantaphylidès, C., Li-Beisson, Y., Peltier, G., 2011. Oil accumulation in the model green alga Chlamydomonas reinhardtii: Characterization, variability between common laboratory strains and relationship with starch reserves. BMC Biotechnol 11, 7. https://doi.org/10.1186/1472-6750-11-7

Sinclair, H.M., 1990. Essential fatty acids - An historical perspective. Biochem Soc Trans 18, 756–761. https://doi.org/10.1042/bst0180756

Singh, H. M., Tyagi, V. V., Kothari, R., Azam, R., Slathia, P. S., & Singh, B. (2020). Bioprocessing of cultivated Chlorella pyrenoidosa on poultry excreta leachate to enhance algal biomolecule profile for resource recovery. Bioresour Technol, 316, 123850. https://doi.org/10.1016/j.biortech.2020.123850

Srivastava, G., Nishchal, Goud, V. v., 2017. Salinity induced lipid production in microalgae and cluster analysis (ICCB 16-BR_047). Bioresour Technol 242, 244–252. https://doi.org/10.1016/j.biortech.2017.03.175

Srivastava, G., Paul, A.K., Goud, V. V., 2018. Optimization of non-catalytic transesterification of microalgae oil to biodiesel under supercritical methanol condition. Energy Convers Manag 156, 269–278. https://doi.org/10.1016/j.enconman.2017.10.093

Su, Y., 2021. Revisiting carbon, nitrogen, and phosphorus metabolisms in microalgae for wastewater treatment. Science of The Total Environment 762, 144590. https://doi.org/10.1016/J.SCITOTENV.2020.144590

Subhadra, B.G., 2010. Sustainability of algal biofuel production using integrated renewable energy park (IREP) and algal biorefinery approach. Energy Policy 38, 5892–5901. https://doi.org/10.1016/j.enpol.2010.05.043

Sun, A., Fan, D., 2010. Prediction, monitoring, and control of ammonium chloride corrosion in refining processes. NACE - International Corrosion Conference Series 10359.

Sun, X., Devi, N.D., Urriola, P.E., Tiffany, D.G., Jang, J.C., Shurson, G.G., Hu, B., 2021. Feeding value improvement of corn-ethanol co-product and soybean hull by fungal fermentation: Fiber degradation and digestibility improvement. Food and Bioproducts Processing 130, 143–153. https://doi.org/10.1016/j.fbp.2021.09.013

Takagi, M., Karseno, Yoshida, T., 2006. Effect of salt concentration on intracellular accumulation of lipids and triacylglyceride in marine microalgae Dunaliella cells. J Biosci Bioeng 101, 223–226. https://doi.org/10.1263/jbb.101.223

Talukdar, J., Kalita, M.C., Goswami, B.C., 2013. Characterization of the biofuel potential of a newly isolated strain of the microalga Botryococcus braunii Kützing from Assam, India. Bioresour Technol 149, 268–275. https://doi.org/10.1016/j.biortech.2013.09.057

Tan, H.L., Lam, M.K., Cheng, Y.W., Lim, J.W., Tan, I.S., Henry Foo, C.Y., Show, P.L., 2021. Heterotrophic and Mixotrophic Cultivation of Chlorella vulgaris using Chicken Waste Compost as Nutrients Source for Lipid Production, in: IOP Conference Series: Earth and Environmental Science. IOP Publishing Ltd. https://doi.org/10.1088/1755-1315/721/1/012011

Taylor, R.L., Rand, J.D., Caldwell, G.S., 2012. Treatment with Algae Extracts Promotes Flocculation, and Enhances Growth and Neutral Lipid Content in Nannochloropsis oculata-a Candidate for Biofuel Production. Marine Biotechnology 14, 774–781. https://doi.org/10.1007/s10126-012-9441-8

Tejido-Nuñez, Y., Aymerich, E., Sancho, L., Refardt, D., 2020. Co-cultivation of microalgae in aquaculture water: Interactions, growth and nutrient removal efficiency at laboratory- and pilot-scale. Algal Res 49. https://doi.org/10.1016/j.algal.2020.101940

Tibbetts, S.M., Bjornsson, W.J., McGinn, P.J., 2015. Biochemical composition and amino acid profiles of Nannochloropsis granulata algal biomass before and after supercritical fluid CO2 extraction at two processing temperatures. Anim Feed Sci Technol 204, 62–71. https://doi.org/10.1016/j.anifeedsci.2015.04.006

Tiron, O., Bumbac, C., Manea, E., Stefanescu, M., Lazar, M.N., 2017. Overcoming Microalgae Harvesting Barrier by Activated Algae Granules. Sci Rep 7, 1–11. https://doi.org/10.1038/s41598-017-05027-3

Tong, C.Y., Derek, C.J.C., 2021. The role of substrates towards marine diatom Cylindrotheca fusiformis adhesion and biofilm development. J Appl Phycol 33, 2845–2862. https://doi.org/10.1007/s10811-021-02504-1

Trabelsi, L., M'sakni, N.H., Ouada, H. Ben, Bacha, H., Roudesli, S., 2009. Partial characterization of extracellular polysaccharides produced by cyanobacterium Arthrospira platensis. Biotechnology and Bioprocess Engineering 14, 27–31. https://doi.org/10.1007/s12257-008-0102-8

Tsavatopoulou, V.D., Aravantinou, A.F., Manariotis, I.D., 2019. Biofuel conversion of Chlorococcum sp. and Scenedesmus sp. biomass by one- and two-step transesterification. Biomass Convers Biorefin 1–9. https://doi.org/10.1007/s13399-019-00541-y

Tsolcha, O.N., Patrinou, V., Economou, C.N., Dourou, M., Aggelis, G., Tekerlekopoulou, A.G., 2021. Utilization of biomass derived from cyanobacteria-based agro-industrial wastewater treatment and raisin residue extract for bioethanol production. Water (Switzerland) 13. https://doi.org/10.3390/w13040486

Tsolcha, O.N., Tekerlekopoulou, A.G., Akratos, C.S., Aggelis, G., Genitsaris, S., Moustaka-Gouni, M., Vayenas, D. V., 2018a. Agroindustrial wastewater treatment with simultaneous biodiesel production in attached growth systems using a mixed microbial culture. Water (Switzerland) 10, 1693. https://doi.org/10.3390/w10111693

Tsolcha, O.N., Tekerlekopoulou, A.G., Akratos, C.S., Aggelis, G., Genitsaris, S., Moustaka-Gouni, M., Vayenas, D.V., 2017. Biotreatment of raisin and winery wastewaters and simultaneous biodiesel production using a Leptolyngbya-based microbial consortium. J Clean Prod 148, 185–193. https://doi.org/10.1016/j.jclepro.2017.02.026

Tsolcha, O.N., Tekerlekopoulou, A.G., Akratos, C.S., Antonopoulou, G., Aggelis, G., Genitsaris, S., Moustaka-Gouni, M., Vayenas, D.V., 2018b. A Leptolyngbya-based microbial consortium for agro-industrial wastewaters treatment and biodiesel production. Environmental Science and Pollution Research 25, 17957–17966. https://doi.org/10.1007/s11356-018-1989-z

Tuantet, K., Janssen, M., Temmink, H., Zeeman, G., Wijffels, R.H., Buisman, C.J.N., 2014. Microalgae growth on concentrated human urine. J Appl Phycol 26, 287–297. https://doi.org/10.1007/s10811-013-0108-2

Uduman, N., Qi, Y., Danquah, M.K., Forde, G.M., Hoadley, A., 2010. Dewatering of microalgal cultures: A major bottleneck to algae-based fuels. Journal of Renewable and Sustainable Energy 2, 012701. https://doi.org/10.1063/1.3294480

Ummalyma, S. B., Sirohi, R., Udayan, A., Yadav, P., Raj, A., Sim, S. J., & Pandey, A. (2022). Sustainable microalgal biomass production in food industry wastewater for low-cost biorefinery products: a review. Phytochemistry Reviews, 1-23. https://doi.org/10.1007/s11101-022-09814-3

Underwood, G.J.C., Paterson, D.M., Parkes, R.J., 1995. The measurement of microbial carbohydrate exopolymers from intertidal sediments. Limnol Oceanogr 40, 1243–1253. https://doi.org/10.4319/lo.1995.40.7.1243

Van Den Hende, S., Vervaeren, H., Desmet, S., Boon, N., 2011. Bioflocculation of microalgae and bacteria combined with flue gas to improve sewage treatment. N Biotechnol 29, 23–31. https://doi.org/10.1016/j.nbt.2011.04.009

Venkata Subhash, G., Chugh, N., Iyer, S., Waghmare, A., Musale, A.S., Nandru, R., Dixit, R.B., Gaikwad, M.S., Menon, D., Thorat, R., Kumar, G.R.K., Nagle, V., Sagaram, U.S., Dasgupta, S., 2020. Application of in vitro protein solubility for selection of microalgae biomass as protein ingredient in animal and aquafeed. J Appl Phycol 32, 3955–3970. https://doi.org/10.1007/s10811-020-02235-9

Wagner, M., Ivleva, N.P., Haisch, C., Niessner, R., Horn, H., 2009. Combined use of confocal laser scanning microscopy (CLSM) and Raman microscopy (RM): Investigations on EPS – Matrix. Water Res 43, 63–76. https://doi.org/10.1016/j.watres.2008.10.034

Wan, C., Zhao, X.Q., Guo, S.L., Asraful Alam, M., Bai, F.W., 2013. Bioflocculant production from Solibacillus silvestris W01 and its application in cost-effective harvest of marine microalga Nannochloropsis oceanica by flocculation. Bioresour Technol 135, 207–212. https://doi.org/10.1016/j.biortech.2012.10.004

Wang, H., Laughinghouse, H.D., Anderson, M.A., Chen, F., Willliams, E., Place, A.R., Zmora, O., Zohar, Y., Zheng, T., Hill, R.T., 2012. Novel bacterial isolate from permian groundwater, capable of aggregating potential biofuel-producing microalga Nannochloropsis oceanica IMET1. Appl Environ Microbiol 78, 1445–1453. https://doi.org/10.1128/AEM.06474-11

Wang, J.H., Zhuang, L.L., Xu, X.Q., Deantes-Espinosa, V.M., Wang, X.X., Hu, H.Y., 2018. Microalgal attachment and attached systems for biomass production and wastewater treatment. Renewable and Sustainable Energy Reviews 92, 331–342. https://doi.org/10.1016/j.rser.2018.04.081

Wang, L., Addy, M., Cobb, K., Ma, H., Zhang, R., Chen, D., Chen, P., Wang, H., Liu, Y., Ruan, R., 2021. Interaction of Chlorella vulgaris and bacteria when co-cultivated in anaerobically digested swine manure. Bioresour Technol 320, 124250. https://doi.org/10.1016/j.biortech.2020.124250

Wang, L., Min, M., Li, Y., Chen, P., Chen, Y., Liu, Y., Wang, Y., Ruan, R., 2010. Cultivation of green algae Chlorella sp. in different wastewaters from municipal wastewater treatment plant. Appl Biochem Biotechnol 162, 1174–1186. https://doi.org/10.1007/s12010-009-8866-7

Wang, X., Ding, S., Song, W., Li, H., Zhang, Y., Ren, W., Li, M., Lu, J., Ding, J., 2021. A collaborative effect of algae-bacteria symbiotic and biological activated carbon system on black odorous water pretreated by UV photolysis. Biochem Eng J 169, 107983. https://doi.org/10.1016/J.BEJ.2021.107983

Wang, Y., Guo, W., Yen, H.W., Ho, S.H., Lo, Y.C., Cheng, C.L., Ren, N., Chang, J.S., 2015. Cultivation of Chlorella vulgaris JSC-6 with swine wastewater for simultaneous nutrient/COD removal and carbohydrate production. Bioresour Technol 198, 619–625. https://doi.org/10.1016/j.biortech.2015.09.067

Wei, L., Huang, X., Huang, Z., 2014. Temperature effects on lipid properties of microalgae Tetraselmis subcordiformis and Nannochloropsis oculata as biofuel resources. Chinese Journal of Oceanology and Limnology 33, 99–106. https://doi.org/10.1007/s00343-015-3346-0

Wijeyekoon, S., Mino, T., Satoh, H., Matsuo, T., 2004. Effects of substrate loading rate on biofilm structure. Water Res 38, 2479–2488. https://doi.org/10.1016/j.watres.2004.03.005

Wu, L.F., Chen, P.C., Lee, C.M., 2013. The effects of nitrogen sources and temperature on cell growth and lipid accumulation of microalgae. Int Biodeterior Biodegradation 85, 506–510. https://doi.org/10.1016/J.IBIOD.2013.05.016

Xia, A., Murphy, J.D., 2016. Microalgal Cultivation in Treating Liquid Digestate from Biogas Systems. Trends Biotechnol 34, 264–275. https://doi.org/10.1016/j.tibtech.2015.12.010

Xia, L., Rong, J., Yang, H., He, Q., Zhang, D., Hu, C., 2014. NaCl as an effective inducer for lipid accumulation in freshwater microalgae Desmodesmus abundans. Bioresour Technol 161, 402–409. https://doi.org/10.1016/j.biortech.2014.03.063

Xiao, R., Zheng, Y., 2016. Overview of microalgal extracellular polymeric substances (EPS) and their applications. Biotechnol Adv 34, 1225-1244. https://doi.org/10.1016/j.biotechadv.2016.08.004

Xie, S., Sun, S., Dai, S.Y., S.Yuan, J., 2013. Efficient coagulation of microalgae in cultures with filamentous fungi. Algal Res 2, 28–33. https://doi.org/10.1016/j.algal.2012.11.004

Xin, L., Hong-ying, H., Ke, G., Jia, Y., 2010. Growth and nutrient removal properties of a freshwater microalga Scenedesmus sp. LX1 under different kinds of nitrogen sources. Ecol Eng 36, 379–381. https://doi.org/10.1016/j.ecoleng.2009.11.003

Xiong, W., Li, X., Xiang, J., Wu, Q., 2008. High-density fermentation of microalga Chlorella protothecoides in bioreactor for microbio-diesel production. Appl Microbiol Biotechnol 78, 29–36. https://doi.org/10.1007/s00253-007-1285-1

Xu, X., Gu, X., Wang, Zhongyang, Shatner, W., Wang, Zhenjun, 2019. Progress, challenges and solutions of research on photosynthetic carbon sequestration efficiency of microalgae. Renewable and Sustainable Energy Reviews 110, 65–82. https://doi.org/10.1016/j.rser.2019.04.050

Yen, H.W., Ho, S.H., Chen, C.Y., Chang, J.S., 2015. CO2, NOx and SOx removal from flue gas via microalgae cultivation: A critical review. Biotechnol J 10, 829–839. https://doi.org/10.1002/biot.201400707

Yuan, H., Zhang, Xinru, Jiang, Z., Chen, X., Zhang, Xinxin, 2019. Quantitative Criterion to Predict Cell Adhesion by Identifying Dominant Interaction between Microorganisms and Abiotic Surfaces. Langmuir 35, 3524–3533. https://doi.org/10.1021/acs.langmuir.8b03465

Zhang, M., Leung, K.T., Lin, H., Liao, B., 2020. The biological performance of a novel microalgal-bacterial membrane photobioreactor: Effects of HRT and N/P ratio. Chemosphere 261, 128199. https://doi.org/10.1016/j.chemosphere.2020.128199

Zhang, Q., Yu, Z., Jin, S., Liu, C., Li, Y., Guo, D., Hu, M., Ruan, R., Liu, Y., 2020. Role of surface roughness in the algal short-term cell adhesion and long-term biofilm cultivation under dynamic flow condition. Algal Res 46, 101787. https://doi.org/10.1016/j.algal.2019.101787

Zhang, X., Yuan, H., Jiang, Z., Lin, D., & Zhang, X., 2018. Impact of surface tension of wastewater on biofilm formation of microalgae Chlorella sp. Bioresource technology, 266, 498-506. https://doi.org/10.1016/j.biortech.2018.06.082

Zhang, Y., Li, H., 2019. Energy recovery from wastewater treatment plants through sludge anaerobic digestion: effect of low-organic-content sludge. Environmental Science and Pollution Research, 26, 30544-30553. https://doi.org/10.1007/s11356-017-0184-y

Zhang, Y., Wu, H., Yuan, C., Li, T., & Li, A., 2019. Growth, biochemical composition, and photosynthetic performance of Scenedesmus acuminatus during nitrogen starvation and resupply. Journal of Applied Phycology, 31, 2797-2809. https://doi.org/10.1007/s10811-019-01783-z

Zhang, Y, Ren, L., Chu, H., Zhou, X., Yao, T., Zhang, Yalei, 2019. Optimization for Scenedesmus obliquus Cultivation: The effects of temperature, light intensity and pH on growth and biochemical composition. Microbiology and Biotechnology Letters 47, 614–620. https://doi.org/10.4014/mbl.1906.06005

Zhang, Z., Chen, Y.H., Wang, C.M., 2021. Can CO2 Emission Reduction and Economic Growth Be Compatible? Evidence From China. Front Energy Res 9. https://doi.org/10.3389/fenrg.2021.693767

Zhao, J., Tang, J., Dang, T., 2022. Influence of extracellular polymeric substances on the heteroaggregation between CeO2 nanoparticles and soil mineral particles. Science of The Total Environment 806, 150358. https://doi.org/10.1016/j.scitotenv.2021.150358

Zhou, W., Min, M., Hu, B., Ma, X., Liu, Y., Wang, Q., Shi, J., Chen, P., Ruan, R., 2013. Filamentous fungi assisted bio-flocculation: A novel alternative technique for harvesting heterotrophic and autotrophic microalgal cells. Sep Purif Technol 107, 158–165. https://doi.org/10.1016/j.seppur.2013.01.030

Zhu, L., Wang, Z., Shu, Q., Takala, J., Hiltunen, E., Feng, P., Yuan, Z., 2013. Nutrient removal and biodiesel production by integration of freshwater algae cultivation with piggery wastewater treatment. Water Res 47, 4294–4302. https://doi.org/10.1016/j.watres.2013.05.004

Zhu, S., Wang, Y., Xu, Jin, Shang, C., Wang, Z., Xu, Jingliang, Yuan, Z., 2015. Luxury uptake of phosphorus changes the accumulation of starch and lipid in Chlorella sp. under nitrogen depletion. Bioresour Technol 198, 165–171. https://doi.org/10.1016/j.biortech.2015.08.142

Appendix

Appendix

For preparation of the micronutrient stock solution.

- The components in Table A1 are added in the order to ~ 800 mL of dH_2O while stirring continuously.
- The total volume was made up to 1 L with dH_2O.

From this concentrated micronutrient stock solution, 1 mL was used in 1 L of BG 11 medium.

Table A1: Micro-nutrients composition of BG 11 media.

Micro-nutrients	Amount (g/L)	Final Concentrations (mM)
$MnCl_2.4H_2O$	1.81	9
$CuSO_4.5H_2O$	0.079	0.3
$Co\ (NO_3)_2.6H_2O$	0.0494	0.17
H_3BO_3	2.86	46
$ZnSO_4.7H_2O$	0.22	0.77

Table A2: FTIR spectra and functional type of the EPS extracted by three different methods.

Wavenumber (cm^{-1})	Vibration type	Functional type
3750-3747	Stretching vibrations of OH- and NH-	Polymeric compounds
3290-3288	Stretching vibrations of NH-	Amide and amine of proteins
2977-2950	Asymmetrical stretching vibrations of CH_2	Lipids and proteins
2877-2870	Asymmetrical stretching of CH_3	Lipids
2378-2301	Asymmetrical stretching vibration of C=O and C=N	Stretching from cellulose
1760-1746	Stretching vibration of C=O	Esters
1680-1670	Stretching vibration of C-N and deformation vibration of N-H	Amide
1540-1523	NH- bend, C-H stretching	Amide

1377	Stretching vibrations of NH- and C-H	Phosphorylated proteins
1236	Stretching of C- O-C, and C-O	Carbohydrates
1125-1000	Stretching of vibration of C-O and OH fingerprints zone	Ester linkage of uronic acid, polysaccharides
1000-600	Several visible bands	Phosphate, sulfur functional groups

(continued)

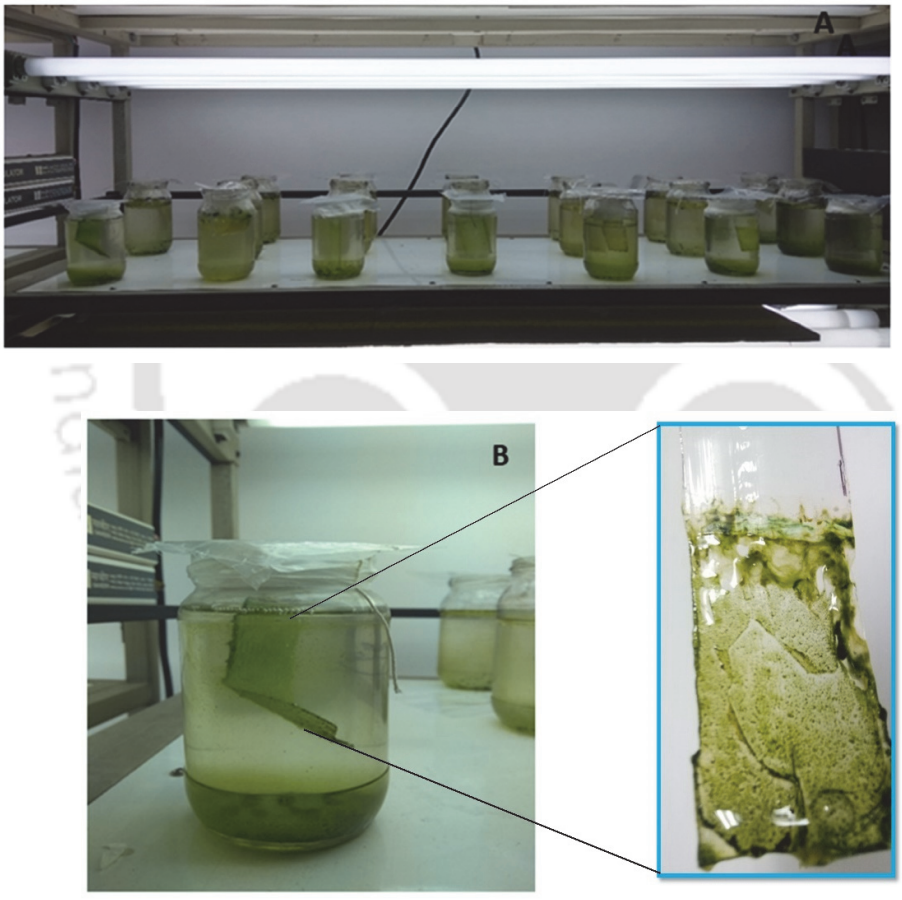

Figure A1: (A) Experimental set up for 500 mL Jam bottle for *Scenedesmus* DDVG I growth on different EPS-attached substrata. B) development of microalgal biomass as a thin green film on the substratum [inset: biofilm of *Scenedesmus* cells over EPS coated substrata].

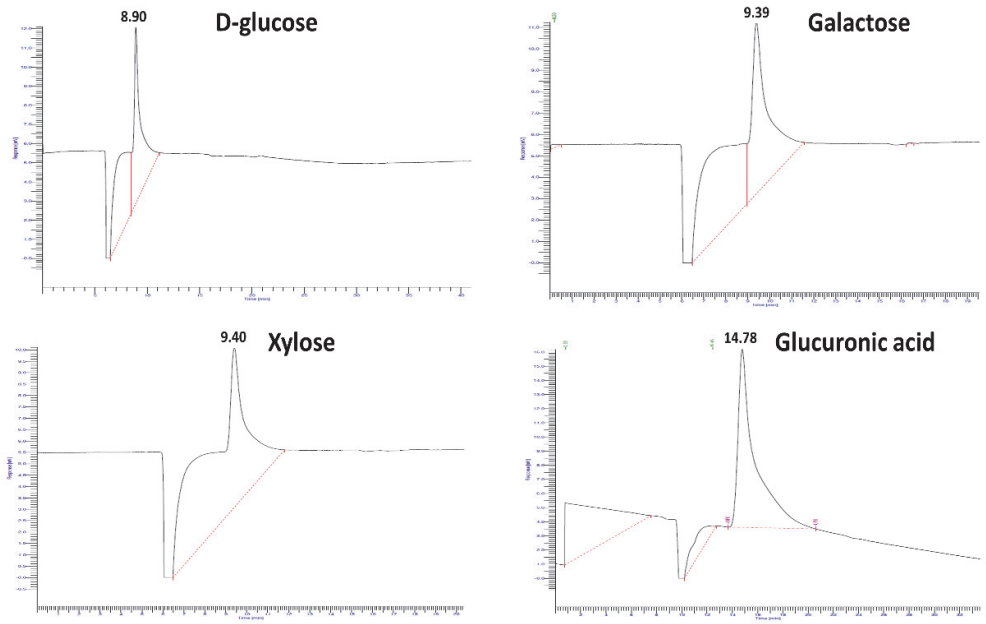

Figure A2: HPLC chromatograph of standard D-glucose, Galactose, Xylose, Glucuronic acid for estimation of monosaccharides of sugar.

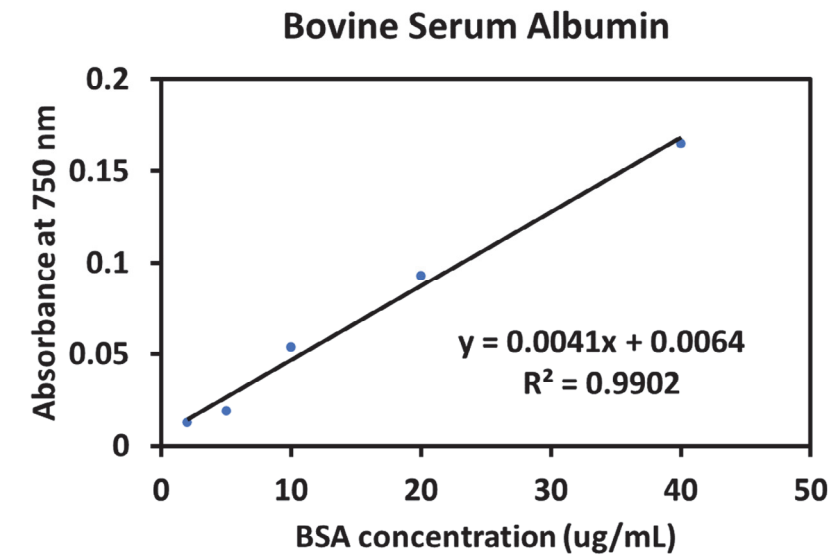

Figure A3: Calibration curve of Bovine Serum Albumin for estimation of protein.

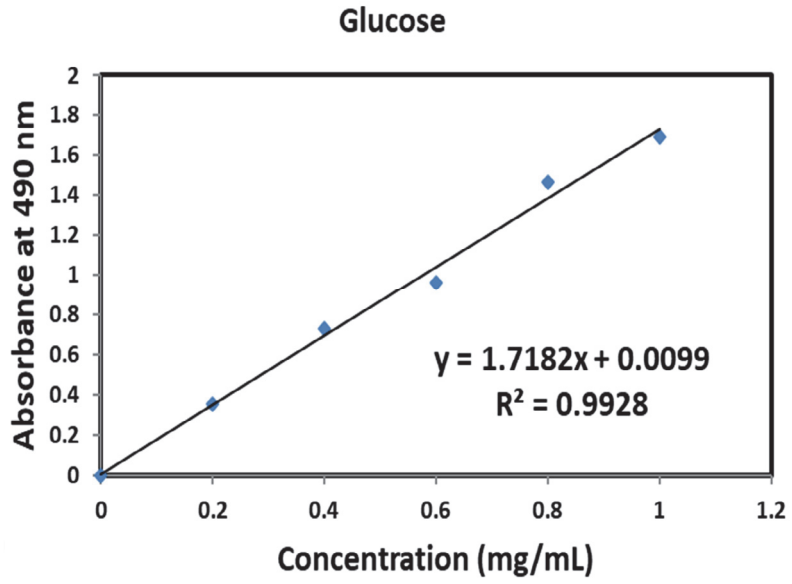

Figure A4: Calibration curve of D-glucose for estimation of carbohydrates and glucose.

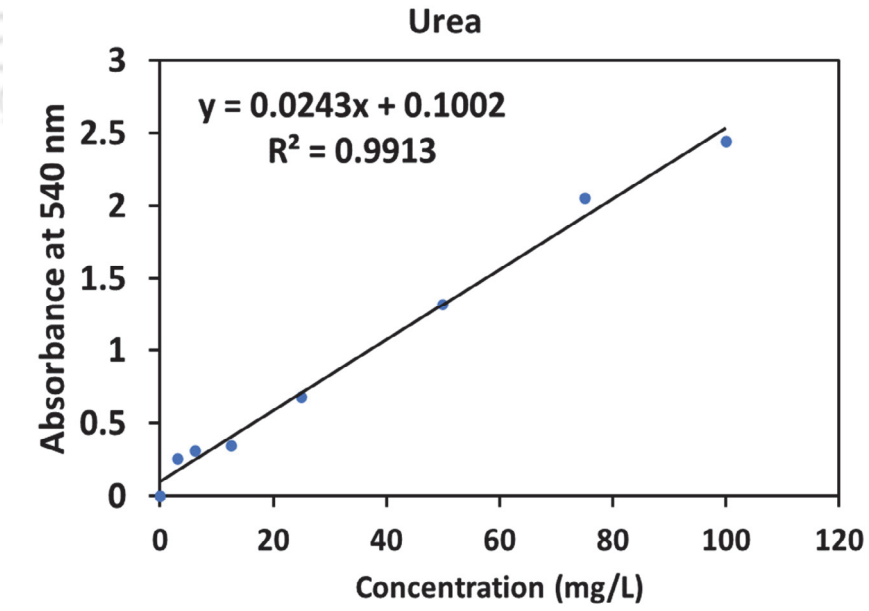

Figure A5: Calibration curve of urea for estimation of urea concentration.

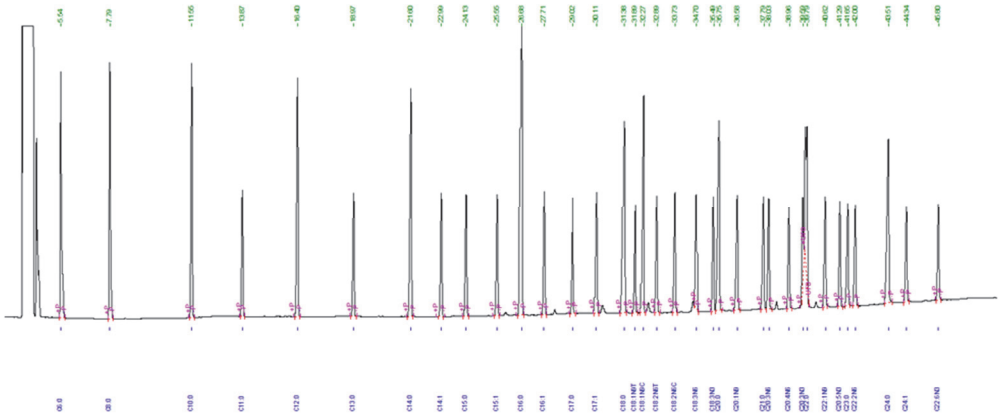

Figure A6: GC chromatograph of FAME standard (Supelco 37 component FAME mix).

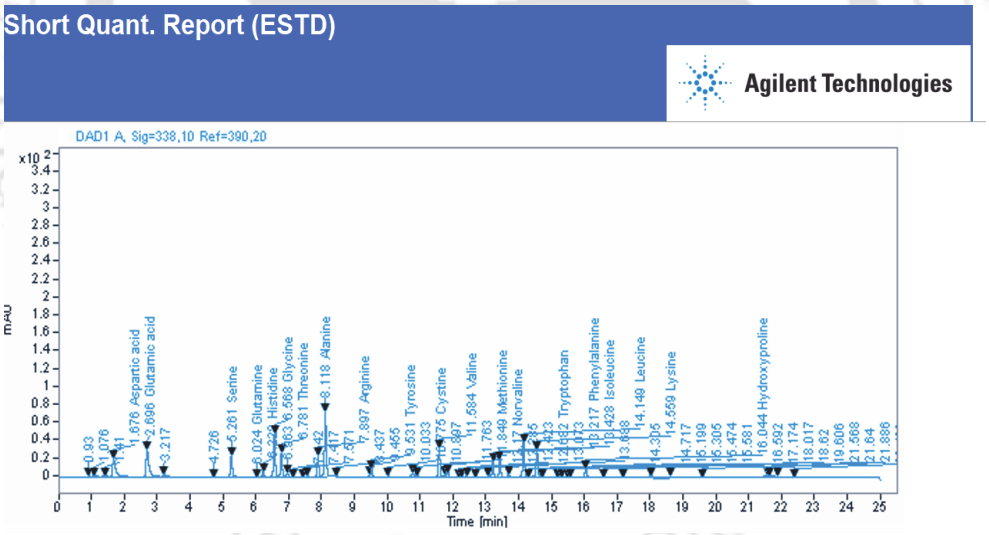

Figure A7: HPLC-DAAD chromatograph of standard amino acid for estimation of amino acid profile.

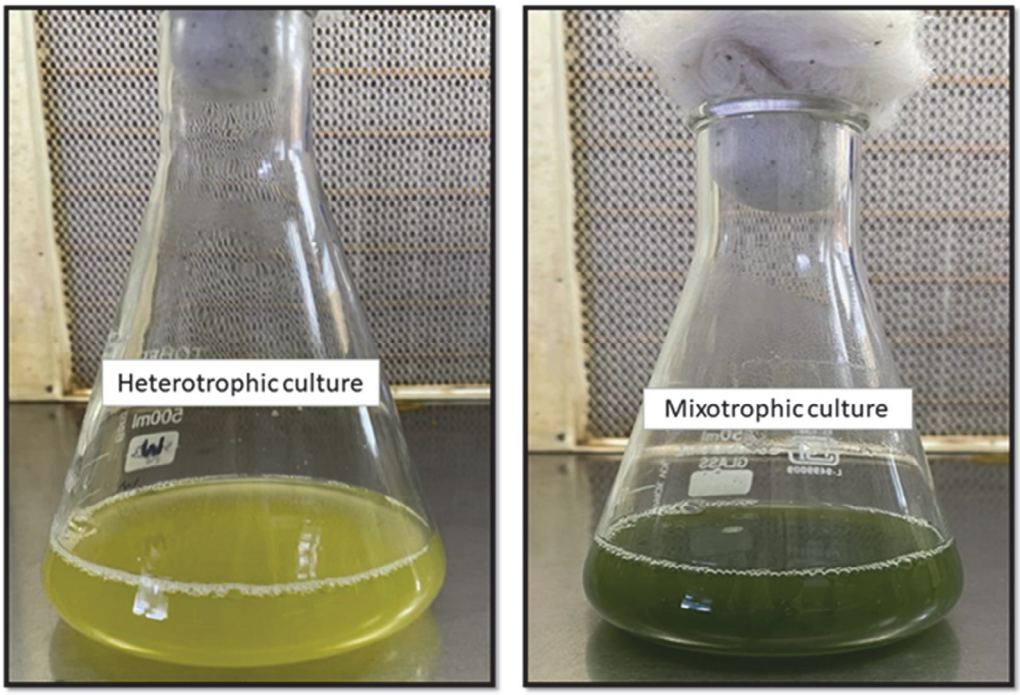

Figure A8: Heterotrophic and mixotrophic growth of *Scenedesmus* sp. DDVG I in PMWW.

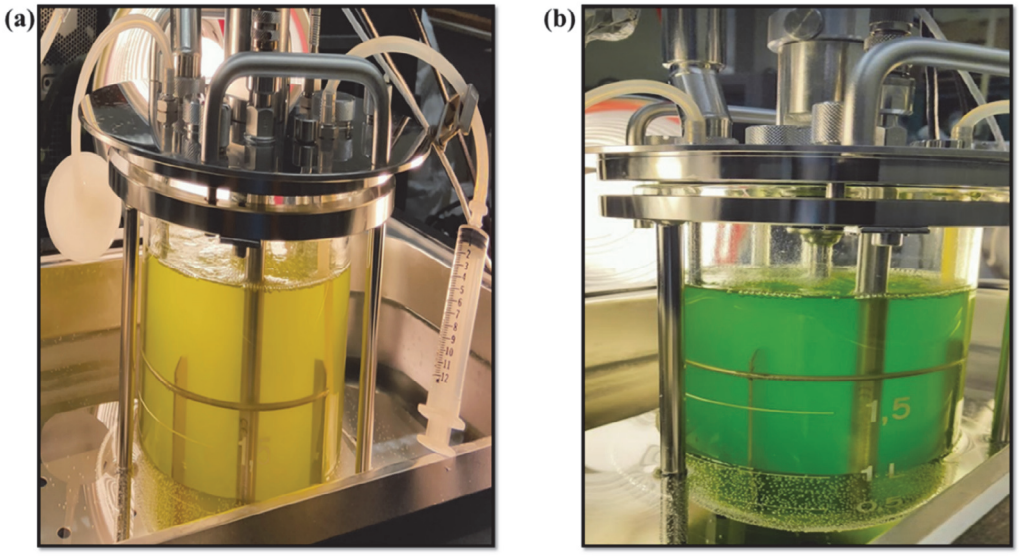

Figure A9: Mixotrophic cultivation of microalgae, *Scenedesmus* DDVG I in PMWW, (a) 1-day, the initial day of inoculation, (b) 10-day (at the end of culture period).

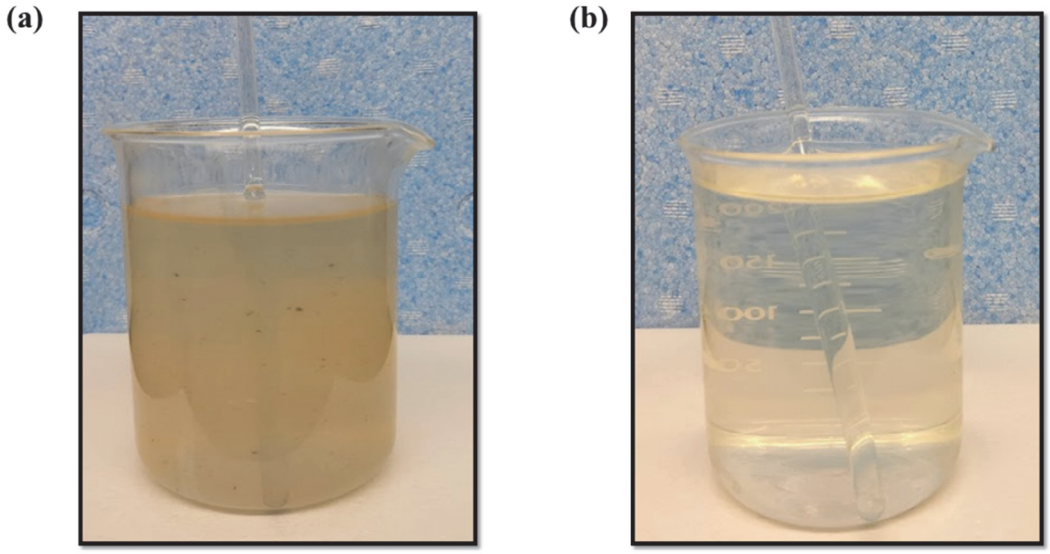

Figure A10: (a) untreated primary municipal wastewater, and (b) treated primary municipal wastewater by *Scenedesmus* sp. DDVG I after 10 days in mixotrophic growth.

Research outputs

Research outputs

Journal Publications

1. **Nongmaithem Debeni Devi,** Rahul Tiwari, Vaibhav. V. Goud, (2021). Cultivating Scenedesmus sp. on substrata coated with cyanobacterial-derived extracellular polymeric substances for enhanced biomass productivity: a novel harvesting approach. *Biomass Conversion and Biorefinery*, 1-13. https://doi.org/10.1007/s13399-021-01432-x.

2. **Nongmaithem Debeni Devi**, Xiao Sun, Lingkan Ding, Vaibhav V. Goud Bo Hu, (2022). Mixotrophic growth regime of novel strain Scenedesmus sp. DDVG I in municipal wastewater for concomitant bioremediation and valorization of biomass. *Journal of Cleaner Production*. 365, 132834. https://doi.org/10.1016/j.jclepro.2022.132834.

3. **Nongmaithem Debeni Devi**, Angana Chaudhuri, Vaibhav V. Goud (2022). Algae biofilm as a renewable resource for production of biofuel and value-added products: A review. *Sustainable Energy Technologies and Assessments*, 53, 102749. https://doi.org/10.1016/j.seta.2022.102749.

4. **Nongmaithem Debeni Devi**, Chandan Mukherjee, Gaurav Bhatt, Lata Rangan, Vaibhav. V. Goud (2022). Co-cultivation of microalgae-cyanobacterium under various nitrogen and phosphorus regimes to concurrently improve biomass, lipid accumulation and easy harvesting. *Biochemical Engineering Journal*, 108706. https://doi.org/10.1016/j.bej.2022.108706.

5. **Nongmaithem Debeni Devi**, Xiao Sun, Bo Hu, Vaibhav V. Goud, (2022). Bioremediation of domestic wastewater with microalgae-cyanobacteria co-culture by nutritional balance approach and its feasibility for biodiesel and animal feed production. *Chemical Engineering Journal*, 140197. https://doi.org/10.1016/j.cej.2022.140197.

Book Chapter

1. **Nongmaithem Debeni Devi**, Vaibhav V. Goud, Bo Hu (2021). Algal cultivation systems and photobioreactor designs. In: Dalai AK, Goud VV, Nanda S, Borugadda VB, editors. Algal Biorefinery: Developments, Challenges and Opportunities: Routledge; p 24. https://doi.org/10.4324/9781003100317.

2. **Nongmaithem Debeni Devi,** Sutapa Das, Angana Chaudhuri, Vaibhav V. Goud, (2022). Renewable fuels recovery from anaerobic digestate. In: V.K. Tyagi, K. Aboudi, C. Eskicioglu: Anaerobic digestate management. IWA Publishing, United Kingdom; p 171. https://doi.org/10.2166/9781789062755_0171.

Publication from other collaborative research work

1. Sun, Xiao, **Nongmaithem Debeni Devi**, Pedro E. Urriola, Douglas G. Tiffany, Jae-Cheol Jang, Gerald G. Shurson, and Bo Hu, (2021). Feeding value improvement of corn-ethanol co-product and soybean hull by fungal fermentation: Fiber degradation and digestibility improvement. *Food and Bioproducts Processing* 130, 143-153.

2. Angana Chaudhuri, **Nongmaithem Debeni Devi**, Dipesh Kumar, Surajit Das, Vaibhav V. Goud (2022) Enhancement of biomass and lipid production via algal-bacteria consortia by treating rubber wastewater. *Sustainable Environment: Proceedings of NERC-2022*, Springer Nature Singapore, 85-103. https://doi.org/10.1007/978-981-19-8464-8_5

Achievements

1. **Bioenergy Award for Cutting Edge Research [(B-ACER) 2019 Internship/5/Nongmaithem Debeni Devi]** under the Indo-US Science and Technology Forum (IUSSTF) and Department of Biotechnology with financial support for Internship at the University of Minnesota, USA (14th January 2020 to 14th July 2020).

2. **Visiting scholar at Departments of Bioproducts and Biosystem Engineering, University of Minnesota** with financial aid from University of Minnesota, USA (14th July 2020 to 14th January 2021).

Conference

1. **Nongmaithem Debeni Devi**, V. V. Goud, A novel co-association of microalga, Scenedesmus sp. DDVG I with cyanobacterium, Limnothrix sp. DDVG II for cost-effective harvesting of biomass. FAST, 11 – 12 Nov, 2019, CIT, Kokrajhar.

2. **Nongmaithem Debeni Devi**, V. V. Goud, Sustainable feedstock Scenedesmus sp. DDVG I and Chloromonas sp. ADIITEC-III: Effect of initial pH and nutrient starvation on growth and lipid yield. "Third ISEES International Conference on Sustainable Energy and Environmental Challenges (III SEEC-2018)" 18th-21st Dec, IIT Roorkee and NIT Uttarakhand, Uttarakhand, India.

3. **Nongmaithem Debeni Devi**, V. V. Goud, Effect of temperature and pH on lipid productivity of microalgae. "International Conference on Renewable & Alternate Energy (ICRAE-2018)" 6th-8th Dec, Assam Science and Technology University (ASTU), Guwahati, Assam, India.